

Determining patterns of post-stroke motor recovery through longitudinal multimodal MRI: A step towards patient stratification

Présentée le 26 août 2022

Faculté des sciences de la vie
Unité du Prof. Hummel
Programme doctoral en neurosciences

pour l'obtention du grade de Docteur ès Sciences

par

Julia BRÜGGER

Acceptée sur proposition du jury

Prof. K. Hess Bellwald, présidente du jury
Prof. F. C. Hummel, directeur de thèse
Prof. A. Luft, rapporteur
Prof. C. Grefkes, rapporteur
Prof. N. Wenderoth, rapporteuse

Acknowledgements

First of all, I would like to thank my thesis supervisor Prof. Friedhelm Hummel for hosting me in his lab and for the opportunity to work on the TiMeS project. The experience I gained in the lab during these past four years is very precious and I appreciated being able to work on such an amazing project.

I am also very grateful to Chang-Hyun and especially Lisa and who spent countless hours reading the different chapters of this thesis, providing me with very valuable feedback and always some words of encouragement which were very much needed in this very intense last phase of the PhD.

Through the TiMeS project I had the opportunity to work with many amazing and bright minds, notably Philipp, Lisa, Andéol, Martino, Silvia, Nathalie, Iris, Aurélie, Valérie, Adrien and Diego who were/are part of the Hummel Lab. A particular thanks goes to Martino and Silvia for hosting many nice dinners and to Martino for showing us how one makes proper pumpkin gnocchi! In addition, I was very lucky to be able to work with the MRI technicians Nathalie, Dorothée, Céline, Laetitia, Christelle and Marie at the cantonal hospital in Sion. Their ability to adapt fast to different situations and to solve a huge amount of unforeseeable problems related to the scanner made the MRI part of this study possible. In addition, a smile was never missing on their faces and exchanging with them made the countless hours spent at the MRI so much nicer.

Another big thanks goes to my fellow PhD colleagues. Despite being located at two different sites we always managed to stay in touch and the “PhD retreat” we had a few months ago was a personal highlight for me. A special thanks goes to the Bikers: Claudia, Pablo, Elena, Andéol and Una. Even if I wanted, I don’t think I could list all the trips, dinners, excursions, climbing hours, coffee breaks and even dance classes that we shared together! Thanks to all of you my life is so much richer and I am deeply grateful for your friendship.

I would also like to thank Pavo, for the many good moments spent together, be it skiing, climbing mountains or travelling. I am especially grateful for your amazing support over these last couple of months of my PhD. Without you, this thesis wouldn’t be what it is today.

No matter how stressed or worn out by the PhD I was, thankfully the get-togethers with “les copines”, Lynn, Tanya, Lauren, Mylène, Joséphine and Eugénie could always cheer me up. To you goes the thanks for the biggest laughs and the most amazing complicity we’ve shared throughout many years now. When going somewhere with you, we somehow never go unnoticed and all the sorrows are forgotten. With you, I just feel home.

I would also like to thank my mum, Therese, and my brother, Lukas, for their unconditional support, the great laughs, flower watering and cooking skills, as well as for their great advice. I truly don’t know what I would do without you. The same goes for Quentin, my best friend, whom I consider family after all these years. Listening to your endless speeches about how to build a dam out of concrete in your aquarium, about how you need six pairs of army shoes just because they last a lifetime, and about how to camp on our balcony in Fribourg in the middle of winter – just to give a few examples – have been life lessons for me! Way to go dipl. Arzt!

Acknowledgements

Finally, the biggest thanks goes to Andéol for sharing all the ups and downs of TiMeS and the PhD in general with me and especially for being such a great friend, in and out of the lab. Through your friendship, your great humor and your marinated mushrooms you truly made this thesis (and the PhD overall) possible, and for that I cannot thank you enough. May we lift many more weights and take many more jumps together in the future!

Abstract

Motivated by the need for a better understanding of post-stroke recovery and new biomarkers to improve stroke patient stratification and outcomes, this thesis investigated structure-function coupling and its role in post-stroke recovery. Furthermore, in order to increase data comparability between sessions and centers (a critical challenge in contemporary clinical research), this thesis assessed the reproducibility of microstructure-informed structural connectivity measures in a multi-center dataset.

Stroke is one of the major sources of permanent impairment, frequently of motor origin. However the clinical picture is very heterogeneous: patients show divergent courses of recovery and the underlying mechanisms are still unclear. In addition, current treatments still have limited success and are restricted to a ‘one-fits-all’ approach, not considering the individual patient’s phenotype. As efforts to stratify patients based on structural or functional biomarkers are still needed, we chose to investigate the potential of a multimodal biomarker, the *Structural Decoupling Index* (SDI) (Preti & Van De Ville, 2019), a new metric assessing the structure-function coupling strength in the brain.

The first part (Studies 1 and 2) of this thesis investigates the potential of the SDI as a biomarker. In **Study 1**, the goals were to evaluate the feasibility of applying the *SDI* on an individual level in healthy older adults and to investigate the effect of an acute stroke on it. Consistent with the literature, we found a network gradient of SDI in healthy older adults, from high coupling in lower-level sensory areas, to low coupling in higher-level cognitive areas. This confirmed the applicability of SDI on an individual level. Furthermore, we showed that stroke impacts the SDI, with a higher decoupling on the ipsi- compared to the contralesional side, and with network-specific effects in RH stroke patients. In **Study 2**, the goal was to see whether the SDI evolved over time post-stroke and whether it links to behavior. The longitudinal analysis revealed differential network effects of stroke at T1 and T3. Furthermore, we showed that impairment in cognitive and psychological behavioral domains significantly correlates with variations in SDI in a number of key areas including motor regions (e.g., primary motor cortex) and that the brain pattern associated to behavior changes between T1 and T2. Surprisingly, motor performance did not explain variability in key motor areas (e.g., primary motor cortex). The link between post-stroke behavioral performance and SDI underlines its potential clinical relevance.

Driven by the quest for more reproducible analysis pipelines in the context of longitudinal and clinical studies, the second part of this thesis (**Study 3**) addressed the subject-specific reproducibility and repeatability of microstructure-informed tractography. Through a multi-center study, we demonstrated its high reproducibility and subject-specificity, and we found evidence for increased biological accuracy.

My thesis made a contribution by showing that the SDI is sensitive to pathophysiological changes that occur following a stroke and that it links to clinically relevant behavioral measures. In addition, it confirms the reproducibility and subject-specificity of microstructure-informed tractography. Together, my findings pave the way towards patient stratification and more personalized treatments in stroke rehabilitation.

Keywords

stroke, motor network, motor function, cognition, functional MRI, Diffusion Weighted Imaging, structure-function coupling, microstructure informed tractography, reproducibility

Résumé

Motivée par le besoin d'une meilleure compréhension de la récupération post-AVC et des nouveaux biomarqueurs pour améliorer la stratification et les résultats des patients victimes d'un accident vasculaire cérébral (AVC), cette thèse a étudié le couplage structure-fonction ainsi son rôle dans la récupération post-AVC. De plus, afin d'augmenter les possibilités de comparaison des données entre les sessions et les centres (défi critique dans la recherche clinique contemporaine), cette thèse a en outre eu pour but d'évaluer la reproductibilité des mesures de connectivité structurelle basées sur la microstructure dans le cadre d'un ensemble de données multicentriques.

L'accident vasculaire cérébral est l'une des principales sources de déficience fonctionnelle permanente, cette dernière étant souvent d'origine motrice. Cependant, la présentation clinique est habituellement très hétérogène: les patients présentent une évolution divergente dans la récupération et les mécanismes sous-jacents impliqués ne sont actuellement toujours pas clairement définis. En outre, les traitements actuels n'ont qu'un succès limité et se réduisent à une approche "générale" ou "universelle", sans tenir compte du phénotype individuel de chaque patient. Comme les efforts pour stratifier les patients sur la base de biomarqueurs structurels ou fonctionnels sont encore nécessaires, nous avons choisi d'étudier le potentiel d'un biomarqueur multimodal, à savoir l'indice de découplage structurel (SDI) (Preti & Van De Ville, 2019b), une nouvelle mesure évaluant la force du couplage structure-fonction dans le cerveau.

La première partie (études 1 et 2) de la thèse étudie le potentiel du SDI en tant que biomarqueur. Dans l'étude 1, les objectifs étaient d'évaluer la faisabilité de l'application du SDI à un niveau individuel chez des adultes âgés en bonne santé et d'étudier l'effet d'un accident vasculaire cérébral aigu sur celui-ci. Conformément à la littérature, nous avons trouvé un gradient dans le SDI chez les adultes âgés en bonne santé, allant d'un couplage élevé dans les zones sensorielles de niveau inférieur à un couplage faible dans les zones cognitives de niveau supérieur, ce qui confirme la possibilité de l'application du SDI à un niveau individuel. En outre, nous avons montré que l'AVC a un impact sur le SDI, avec un découplage plus élevé du côté ipsilésionnel que du côté controlésionnel, et ce avec des effets spécifiques au réseau chez les patients ayant subi un AVC. Dans l'étude 2, l'objectif était de voir si le SDI évoluait dans le temps après l'AVC et s'il était lié au comportement. L'analyse longitudinale a révélé des effets différentiels de l'AVC sur le réseau à T1 et T3. Par ailleurs, nous avons montré que l'altération des domaines du comportement cognitif et psychologique corrèle significativement avec les variations du SDI dans un certain nombre de zones clés, y compris dans les régions motrices (par exemple, le cortex moteur primaire) et que le schéma cérébral associé au comportement change entre T1 et T2. De manière surprenante, la performance motrice n'explique pas la variabilité dans les zones motrices clés comme le cortex moteur primaire. Le lien entre la performance comportementale post-AVC et le SDI souligne sa potentielle relevance clinique.

Poussée par la quête d'un modèle d'analyse plus reproductibles dans le contexte d'études longitudinales et cliniques, la deuxième partie de cette thèse (étude 3) s'est penchée sur la reproductibilité et la répétabilité spécifiques au sujet dans la tractographie basée sur la microstructure. Grâce à une étude multicentrique, nous avons démontré sa reproductibilité élevée et sa spécificité par rapport au sujet, et nous avons trouvé des preuves d'une précision biologique accrue.

Ma thèse a apporté une contribution dans ce domaine en montrant que le SDI est sensible aux changements physiopathologiques qui se produisent après un AVC et qu'il est lié à des mesures comportementales cliniquement pertinentes. De plus, elle confirme la reproductibilité ainsi que la spécificité liée au sujet de la tractographie basée sur la microstructure. Ensemble, mes résultats ouvrent la voie à la stratification des patients et à des traitements plus personnalisés dans la réadaptation post-AVC.

Mots-clés

AVC, réseau moteur, fonction motrice, cognition, IRM fonctionnelle, imagerie pondérée par diffusion, couplage structure-fonction, microstructure informée, tractographie, reproductibilité

Contents

Acknowledgements.....	i
Abstract	iii
Keywords	iv
Résumé.....	v
Mots-clés	vi
List of Figures.....	ix
List of Tables	x
Introduction.....	11
1.1 Stroke pathophysiology	12
1.1.1 Stroke types and acute management.....	12
1.1.2 Symptoms and disabilities	13
1.1.3 Neurobiological mechanisms.....	13
1.2 Post-stroke recovery and rehabilitation	15
1.2.1 Proportional recovery model.....	15
1.2.2 Rehabilitation therapies	17
1.3 Magnetic Resonance Imaging (MRI) in stroke	18
1.3.1 Structural MRI.....	18
1.3.2 Functional MRI.....	20
1.3.3 Understanding of motor recovery and outcome through MRI	22
1.3.4 Multimodal MRI	26
1.4 Framework and purpose of the thesis.....	29
1.4.1 Challenges for research in a clinical environment.....	29
1.4.2 Context of the thesis: Towards Individualized Medicine in Stroke (TiMeS).....	30
1.4.3 Thesis at a glance	32
1.5 Overview and personal contributions.....	34
PART I	37
2.1 Study 1: Acute changes in the coupling strength between brain structure and function following a stroke	39
2.1.1 Abstract.....	40
2.1.2 Introduction	41
2.1.3 Methods.....	42
2.1.4 Results.....	45
2.1.5 Discussion	51
2.1.6 Supplementary Information	55
2.2 Study 2: Post-stroke structure-function coupling relates to cognitive impairments in the acute and early subacute phase.....	59
2.2.1 Abstract.....	60
2.2.2 Introduction	61
2.2.3 Methods.....	62

2.2.4 Results.....	65
2.2.5 Discussion	73
2.2.6 Supplementary Information	80
PART II	97
3.1 Study 3: Evaluating reproducibility and subject-specificity of microstructure-informed connectivity.....	99
3.1.1 Abstract.....	100
3.1.2 Introduction	101
3.1.3 Material and methods	102
3.1.4 Results.....	105
3.1.5 Discussion	109
3.1.6 Conclusion	112
3.1.7 Supplementary Information	114
General Discussion	115
4.1 Evaluating structure-function coupling in a stroke population	115
4.1.1 The impact of stroke on SDI.....	115
4.1.2 The link between SDI and post-stroke clinical measures	117
4.1.3 SDI changes over time post stroke	118
4.2 Methodological considerations	120
4.2.1 Individual-level implementation of the SDI.....	120
4.2.2 The definition of brain networks	121
4.3 Translational aspects	122
4.3.1 Considerations regarding research using MRI	122
4.3.2 Research in a clinical environment.....	123
4.3.3 A step towards patient stratification?	125
References	127
Appendix	153
5.1 Supplementary Study 1: Towards individualized Medicine in Stroke – the TiMeS project: protocol of longitudinal, multi-modal, multi-domain study in stroke	153
5.2 Supplementary Study 2: Differential impact of brain network efficiency on post-stroke motor and attentional deficits	190
Curriculum Vitae	206

List of Figures

Figure 1. Types of stroke and penumbra.	12
Figure 2. Proportional motor recovery in the upper limb.	16
Figure 3. Whole-brain tractogram.	19
Figure 4. Measuring structural and functional connectivity.	21
Figure 5. Motor areas.	23
Figure 6. Functionnectome and Structural Decoupling Index (SDI).	28
Figure 7. Towards Individualized Medicine in Stroke (TiMeS) project.	31
Figure 8. Experimental design of the test-retest reproducibility study.	32
Figure 9. Mean Structural Decoupling Index (SDI) in healthy older adults (HOA).	46
Figure 10. Mean Structural Decoupling Index (SDI) in stroke patients.	47
Figure 11. Mean Structural Decoupling Index (SDI) in the visual and somatomotor networks in stroke patients.	47
Figure 12. Mean Structural Decoupling Index (SDI) left-hemispheric (LH) stroke patients vs healthy older adults (HOA).	48
Figure 13. Mean Structural Decoupling Index (SDI) right-hemispheric (RH) stroke patients vs healthy older adults (HOA).	49
Figure 14. Mean Structural Decoupling Index (SDI) in RH stroke patients vs healthy older adults (HOA).	50
Figure 15. Mean SDI at T1 and T3.	66
Figure 16. Mean SDI in left-hemispheric stroke patients.	69
Figure 17. Multivariate correlation patterns between the SDI and behavioral traits.	71
Figure 18. Contributions of regions of interests (ROIs) across networks to the multivariate correlation pattern.	72
Figure 19. Bray-Curtis dissimilarities.	105
Figure 20. Subject specificity in PCA reduced connectomes for the raw tractogram, the SIFT2 and COMMIT methods.	108
Figure 21. Comparison of group mean weighted TDI maps of microstructure- informed tractography methods.	109

List of Tables

Table 1. Behavioral impairments at T1.....	63
Table 2. List of behavioral tests and sub-scores for all behavioral domains.....	64
Table 3. Summary of cross-sectional effects on SDI at each timepoint.	68
Table 4. Summary of the hemispheric effects in left-hemispheric stroke patients.....	70
Table 5. Inter- and intraindividual dissimilarities.	106
Table 6. Repeated-measure ANOVA comparing mean intra and interindividual dissimilarities.....	107
Table 7. Intra- and interindividual comparison of average Bray-Curtis dissimilarity Index.....	107

Introduction

Understanding how the brain is structured and functions has always been a fascinating challenge for scientists. It has been more than 120 years since the anatomist Brodmann published maps of cortical areas in humans, monkeys and other species, which laid the foundation of today's understanding of brain areas. Back then, a very localizationist view was commonly accepted when defining the function of brain areas: a specific function was regularly attributed to one or several specific brain areas. Several case studies influenced and supported this view, such as the one of Phineas Gage in the middle of the 19th century, whose orbitofrontal and prefrontal cortex was lesioned in an accident and who developed drastic personality changes, or the discovery of Broca's area based on a post-mortem identification of the region in a patient suffering from aphasia, as well as the description of Wernicke's area about 20 years later. All of these examples tie specific functions to specific locations in the brain, which marked the field and were probably part of the reason why researchers continuously tried to connect a function to a specific brain area.

In the past century, advances in brain imaging methods provided opportunities to investigate the brain as a whole entity whose areas are interconnected and function together rather than in an isolated manner. However, in MRI-based research, the concept of functional connectivity only emerged in the 1990s (B. B. Biswal et al., 1997) as the coordinated activity between two brain regions. Even more recently, the structural connectivity in humans as we know it today was introduced in 2007 (Hagmann et al., 2007), as an indirect measure of the underlying number and strength of physical connections between a given pair of brain areas. These relatively young fields have, however, quickly gained in importance and the consensus has now shifted from a localizationist view towards a network approach, which suggests that functions are the result of a set of areas communicating within a network, rather than the activity of an isolated area. However, brain structure and function are still commonly studied one apart from the other.

Analogously, it has been shown that a focal lesion, such as it is caused through a stroke, has widespread consequences within the brain and concerned networks (Guggisberg et al., 2019). Stroke is therefore a network disease and one of the major causes for impairment across the globe. Nevertheless, every stroke is specific with its own structural and functional consequences, which will also be reflected on behavioral level through a variety of impairments, ranging from the motor domain to cognition. Similarly, recovery from stroke is also heterogeneous and the underlying mechanisms are still unclear. Particularly, the link between structure and function is poorly studied during recovery, even though it has been shown that the stroke, as a structural lesion, also impacts functional connectivity.

My thesis fits in this framework as it investigates the link between structural and functional connectivity, an emerging field which stands methodologically and conceptually still in the very beginning. The main aim of this thesis was to investigate the link between structure and function on an individual level, i.e. by using individual functional and structural connectomes instead of group averages, in stroke patients. Therefore, this work aspires to propose a new perspective of how to look at the impact a stroke has on the brain as well as at post-stroke neural reorganization.

In the next sections, I will introduce the general background needed for a good understanding of the present thesis. I will start by defining stroke and its underlying neurobiological mechanisms. Then I will focus on post-stroke recovery and current rehabilitation therapies, before moving on to providing an overview of the state-

of-the-art and challenges in Magnetic Resonance Imaging related to stroke. Finally, I will finish by presenting the theoretical and clinical framework of my thesis.

1.1 Stroke pathophysiology

1.1.1 Stroke types and acute management

The diagnosis of stroke is based on neuroimaging, neuropathology and/or clinical evidence of permanent ischemic or hemorrhagic injury. There are two main types of stroke, ischemic (87% of cases) and hemorrhagic (13%) (Virani et al., 2021).

Ischemic stroke, also called central nervous system (CNS) infarction, is usually caused by an arterial thrombotic or stenotic blockage, which deprives the supplied areas of oxygen (**Figure 1**) (Sacco et al., 2013). Clinically, an ischemic stroke causes an episode of neurological dysfunctions, such as paresis of the arm and/or leg or the inability to comprehend or produce speech. In most cases, the stroke lesion is composed of an irreversibly infarcted core as well as a certain amount of underperfused tissue that can still be salvaged, called the ‘penumbra’ (**Figure 1**). If treatments in the form of thrombolysis – intended to dissolve the blood clot – or thrombectomy – a mechanical excision of the thrombus – are administered rapidly (within a few hours), blood flow is restored and the cells within the penumbra tend to survive (Murphy & Corbett, 2009). However, if the blood flow is not restored, the penumbra will also perish, which is often associated to a negative clinical outcome (Sacco et al., 2013). Moreover, it is well known that “time is brain”, i.e., that administering the appropriate acute care treatment is usually a race against the clock, as 1.9 million neurons die each minute in which the typical patient is not treated for stroke (Saver, 2006). Despite the efficacy of these treatments, only a minority of patients are eligible to receive them, which is why developing adequate rehabilitation therapies is of outmost importance.

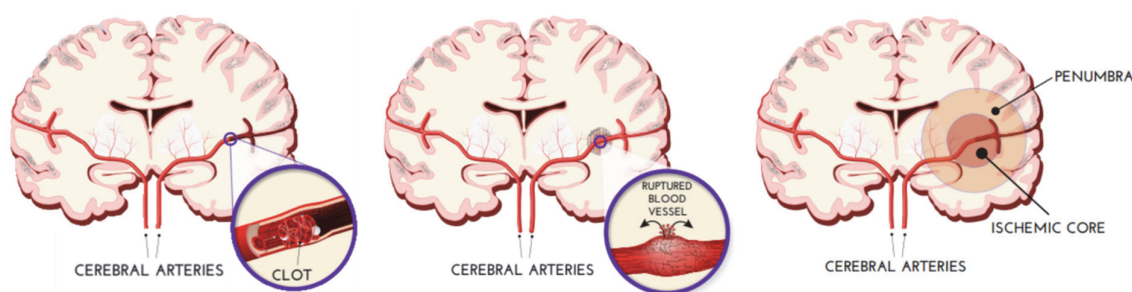


Figure 1. Types of stroke and penumbra.

Left: Ischemic stroke, where a blood clot is obstructing an artery in the brain causing the downstream areas to be deprived of oxygen. Middle: Hemorrhagic stroke, where a blood vessel ruptures and causes a focal collection of blood within the brain tissue or ventricular system. Right: Penumbra. Underperfused tissue surrounding the ischemic core (after an ischemic stroke). Image adapted from <https://www.dana.org/article/stroke/> (consulted on 29.03.2022).

Compared to ischemic stroke, a hemorrhagic stroke (also called parenchymal hemorrhage) is caused by a focal collection of blood within the brain tissue or ventricular system that is not caused by trauma (**Figure 1**). It is usually accompanied by rapidly developing signs of neurological dysfunction and/or headache due to the mass effect (i.e. blood is accumulating and pushing on or displacing surrounding tissue, causing secondary

pathological effects) (Sacco et al., 2013). Compared to ischemic stroke, morbidity and mortality are higher in hemorrhagic stroke patients and early diagnosis and treatment to manage the intracranial pressure are thus crucial (S. Chen et al., 2014). Treatments range from osmotherapy, blood pressure control and reversal of anticoagulant therapy to surgical interventions (S. Chen et al., 2014).

In summary, after an ischemic infarct, the goal of the acute treatment is to restore blood flow as rapidly as possible, whereas after a hemorrhagic stroke, the first priority is to stop further bleeding. Both types of stroke translate to behavioral dysfunctions, such as motor or cognitive deficits which will be further elaborated in the next section.

1.1.2 Symptoms and disabilities

Despite improvements in prevention and acute treatment, which have led to a significant decrease in the burden of stroke over the past decades, stroke remains a major cause of long-term disability (Katan & Luft, 2018). Most frequent symptoms at stroke onset include upper and/or lower limb motor deficits (80-85% of patients), somatosensory deficits (40-50%), language deficit or aphasia (20-25%), visual deficits (15-20%), memory deficits (15-25%), and attention deficits or neglect (25-30%), amongst others (Appelros et al., 2002; Buxbaum et al., 2004; Lawrence et al., 2001; Nys et al., 2007; Ramsey et al., 2017; Rathore et al., 2002; Ringman et al., 2004). Frequently, patients experience more than one symptom and most patients retain functional disabilities after the acute stage. In the case of paralysis, for example, only 15% of patients recover fully (Hendricks et al., 2002). Loss of motor function, particularly of the arm and hand, significantly decreases patients' quality of life as well as devaluates their independence in performing even the simplest everyday tasks, rendering it a key challenge in post-stroke recovery (Stinear, 2017; Stinear et al., 2020). Despite opposed interventions in the hyperacute phase, motor recovery and outcome seem to be independent of the type of stroke (Boyd et al., 2017; Nouri & Cramer, 2011; Stinear et al., 2020), suggesting that these behavioral deficits – and their evolution over time – are the consequence of common underlying neurobiological mechanisms which take place following a stroke.

1.1.3 Neurobiological mechanisms

1.1.3.1 Stroke

The neurobiological mechanisms underlying the behavioral improvements in the first weeks and months post-stroke are still not fully understood (Stinear et al., 2020). Evidence from animal studies suggests that stroke triggers a cascade of hemodynamic and neuroinflammatory reactions within minutes to hours after stroke onset (Murphy & Corbett, 2009). Indeed, neurons stop functioning within seconds of oxygen deprivation and signs of structural damage can be observed already after two minutes (Murphy et al., 2008). Due to a lack of energy, the normal transmembrane ionic gradients cannot be further maintained and the resulting water and ion imbalance initiates apoptotic and necrotic cell death cascades (Besancon et al., 2008; Hossmann, 2006), which lie at the origin of motor and sensory impairments for example (Hossmann, 2006; Murphy & Corbett, 2009; S. Zhang & Murphy, 2007). Following a stroke, structural and functional reorganization takes place thanks to neural plasticity.

1.1.3.2 Spontaneous neural plasticity

A majority of patients will display post-stroke functional improvements, which can be related to brain plasticity. In this regard, both structural and functional changes are involved in stroke recovery, especially in areas and networks that have a close functional link with the lesioned area (Murphy & Corbett, 2009).

1.1.3.2.1 Structural plasticity

In the case of an ischemic stroke, the first main mechanism of repair consists of the salvation through reperfusion of the neurons contained in the penumbra (Murphy & Corbett, 2009). Tissue in the penumbra is also supplied by a parallel artery system, which allows neurons in this area to survive for a few hours, even if the main blood supply is interrupted. Once reperfusion is in place, some damages to the dendritic structure can be reversed and this perilesional area becomes one of the main locations where neural reorganization occurs (Murphy & Corbett, 2009).

In animal studies, structural neural plasticity following a stroke has been shown to involve processes such as axonal sprouting, dendritic branching, synaptogenesis, neurogenesis, as well as gliogenesis, and is observed to be clinically beneficial in areas connected to the damaged area, such as the peri-infarct region, ipsi- and contralesional brain and spinal cord networks (Ward, 2017).

1.1.3.2.2 Functional plasticity

In addition to the aforementioned structural plasticity, a stroke also induces functional plasticity in the form of alterations in neuronal excitability (Carmichael, 2012; Murphy & Corbett, 2009; Ward, 2017). In the first phase after stroke, the neurotransmitter glutamate is excitotoxic and contributes to cell death, which can be counteracted by the inhibitory neurotransmitter GABA through cell hyperpolarization (Lai et al., 2014). In mice, this phase where inhibition in the perilesional area is beneficial, lasts approximately 3 days (Clarkson et al., 2010), while its duration in humans remains unknown (Ward, 2017). Subsequently, the effects reverse and a shift in the cortical excitatory-inhibitory balance towards excitation becomes beneficial for plasticity (Bavelier et al., 2010). Indeed, an increase in excitability at this point has been associated to a re-opening of critical periods of plasticity in the adult brain. Through epigenetics, increased neuronal activity is thought to be at the origin of neurogenesis as well as of an increase in growth factors such as brain-derived neurotrophic factor (BDNF) (Felling & Song, 2015). Hence, functional changes in turn activate further structural plasticity. Furthermore, decreased inhibition has also been linked to expanded receptive fields (Alia et al., 2016; Winship & Murphy, 2008), increased long-term potentiation (Hagemann et al., 1998), as well as remapping of sensorimotor functions to intact cortex in the ipsi- and contralesional hemispheres (Que et al., 1999; Takatsuru et al., 2009). All these effects are thought to be supportive of post-stroke reorganization. Hence, it is believed that a change in balance between GABA- and glutamatergic signaling could be a pivotal event at the origin of neural plasticity (Liuzzi et al., 2014; Ward, 2017).

In addition to a change in the GABA-glutamate balance, homeostatic plasticity has been hypothesized to contribute to neural plasticity in a similar manner (Murphy & Corbett, 2009). Due to a decrease in input from adjacent tissue due to infarct, oedema or decreased blood flow, the synaptic activity also decreases in the perilesional area and in related networks in the first days to weeks after stroke (Bolay et al., 2002; Brown et al., 2009; Butefisch, 2003; Winship & Murphy, 2008). Through homeostatic plasticity, the presynaptic neurotransmitter release and the postsynaptic response to the latter are increased, in order to restore pre-stroke levels of synaptic activity (Turrigiano & Nelson, 2004). The resulting increase in excitability has been linked to the transient appearance of low frequency spontaneous activity (0.1-1Hz) (Carmichael & Chesselet, 2002). This spontaneous activity has been associated to the induction of structural plasticity, such as axonal sprouting (Carmichael, 2003; Carmichael et al., 2001; J.-K. Lee, 2004) and dendritic spine production (Brown

et al., 2007, 2009) which might constitute an attempt to compensate for damaged structural circuits (Murphy & Corbett, 2009).

Collectively, this evidence suggests that increased neuronal excitability is at the origin of downstream changes in axonal structure. Moreover, the phenomena surrounding structural and functional plasticity which are described above exist during a limited amount of time after stroke.

1.1.3.3 Window of opportunity

Recent work has shown that there is a restricted time window of neuroplasticity that opens following a stroke, during which the greatest functional gains are possible, called “window of opportunity” (Biernaskie, 2004; Zeiler et al., 2016). These processes of neuronal recovery are related to the increased gene expression of growth promoting factors (e.g., brain-derived neurotrophic factor (BDNF)) (Chopp et al., 2007; Murphy & Corbett, 2009; Wieloch & Nikolich, 2006). In animal models, the window of plasticity has been shown to close in the first weeks post-stroke with the increase in growth inhibiting factors (e.g., NOGO-A) (Murphy & Corbett, 2009). In addition, the necessity of training in the beginning of this window, within the first days after a stroke, has shown to be crucial. This is nicely illustrated in an experiment by (Zeiler et al., 2016) where a seven-day delay in post-stroke training led to an incomplete recovery of task performance. However, through the induction of a second stroke in the same hemisphere combined with training starting the following day, the mouse was able to fully recover from both events. This shows that there might be a short period of time in which function can be regained through training in addition to a favorable biological environment, which is engendered by the stroke.

Even though molecular and cellular mechanisms of neural plasticity have been well studied in pre-clinical settings, most findings have failed to translate to the clinical environment. Thus, future work in humans should address the open questions related to various aspects of this critical window, such as timing, quantity, intensity, and type of physical training in order to support neurorehabilitation (Ward, 2017). In the next section, I will briefly review the current state of knowledge surrounding recovery and rehabilitation strategies after a stroke.

1.2 Post-stroke recovery and rehabilitation

1.2.1 Proportional recovery model

In parallel to neural plasticity, behavioral changes can be observed. For instance, a majority of patients are expected to spontaneously recover about 70% of their initial impairment within the first 3-6 months (Prabhakaran et al., 2008). These patients are said to follow the so-called ‘proportional recovery rule’ (**Figure 2**) according to which the impairment is defined as the difference between a maximal and an initial score of a behavioral assessment, e.g., a motor test (Grefkes & Fink, 2020; Prabhakaran et al., 2008; Winters et al., 2015). As an example, if a patient initially (shortly after stroke onset) scores 16 out of 66 points on the Fugl-Meyer motor assessment of the upper extremity (UE-FM), his impairment is $66 \text{ (maximal UE-FM score)} - 16 \text{ (initial score)} = 50$ points. The patient is then expected to recover 70% of this initial impairment, i.e., $50 * 0.7 = 35$ points, with a final score of $16 \text{ (initial score)} + 35 \text{ (expected recovery)} = 51$ points. Severely affected patients are thus expected to recover more in absolute numbers than moderate-to-mildly affected patients.

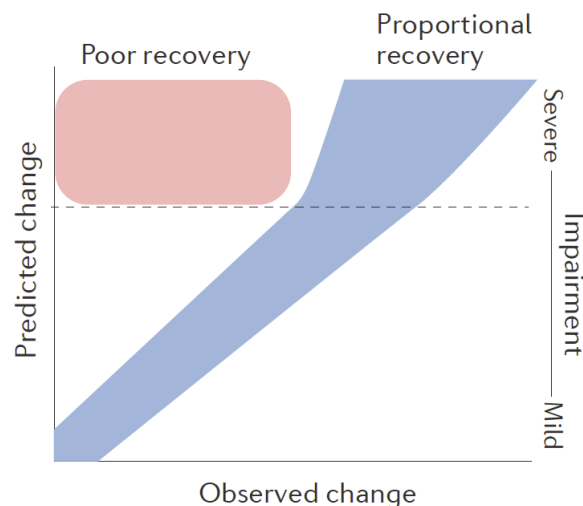


Figure 2. Proportional motor recovery in the upper limb.

Two popular ways of plotting data to investigate proportional recovery. a) Predicted change in a behavioral score vs. observed change. Patients falling in the blue range show proportional recovery, whereas patients falling in the red range recovery poorly. b) Motor function is plotted vs time post-stroke. Patients falling on the blue range recover well, whereas patients falling in the red range do not show proportional recovery. In this example, the recovery curves of patients suggest that the recovery does not depend on initial impairment. Image adapted from Ward (2017).

Proportional recovery was first demonstrated for the upper limb (Prabhakaran et al., 2008) and subsequently extended to other domains such as the lower limb (M.-C. Smith et al., 2017; Veerbeek et al., 2018), visual spatial neglect (Marchi et al., 2017; Winters et al., 2017), aphasia (Lazar et al., 2010; Marchi et al., 2017) and other cognitive domains (Ramsey et al., 2017).

Outcome predictions based on the proportional recovery model have shown to be very accurate for mildly and moderately impaired patients as well as for a part of the severely impaired patients ('fitters', 2/3 of patients), whereas the remaining part of severely impaired patients shows little-to-no spontaneous recovery and hence does not fit the model ('non-fitters', 1/3 of patients) (P. J. Koch et al., 2021). The incomplete understanding of the limited recovery for 'non-fitters' has puzzled the field in the last couple of years and underlines the heterogeneity and unpredictability associated to stroke recovery (Stinear, 2017; Ward, 2017).

Even though proportional recovery has been demonstrated in various studies involving hundreds of stroke patients, recently, criticism has been voiced regarding heavily inflated effect sizes (Bonkhoff et al., 2020) arising from ceiling effects and mathematical coupling (Hawe et al., 2019; Hope et al., 2019). In addition, the model assumes that the type and intensity of physical therapy, e.g., cannot substantially impact the outcome and that recovery is mainly driven by a fundamental neurobiological process ('spontaneous recovery') (Grefkes & Fink, 2020). Indeed, correlations tend to be very high when outcomes are significantly less variable than baselines (Hope et al., 2019). In addition, given that recovery cannot exceed 100% and scores rarely decrease over time post-stroke, the datapoints can only fall within a very restricted area (**Figure 2**), which biases the goodness of fit. In other words, mathematical coupling occurs when "one variable directly or indirectly contains the whole or part of another", which is the case of proportional recovery, where the initial score is part of both the independent (maximum score – initial score) and dependent variable (final score – initial score). The null hypothesis (i.e., no relationship) is thus void (Hawe et al., 2019; Hope et al., 2019). Taking this into account, the authors refute the assumption that fitters' outcomes are largely independent of therapeutic interventions, however, they do not contest the existence of non-fitters, i.e., patients who do

not recover as predicted (Hawe et al., 2019; Hope et al., 2019). In line with this, alternatives to the classical proportional recovery model have recently been proposed (Bonkhoff et al., 2022; Vliet et al., 2020) and they confirmed that the distinction between ‘fitters’ and ‘non-fitters’ was not an artefact of previous confounds. Furthermore, a recent study showed that whole brain connectomics could be a promising new way of distinguishing ‘fitters’ from ‘non-fitters’ more accurately (P. J. Koch et al., 2021).

Therefore, the understanding and prediction of post-stroke recovery and outcome, in particular the non-recovery of a sub-group of patients, remains a challenge and should be further addressed in the future, ideally to predict outcomes for individual patients in order to allow for a better personalization of treatments.

1.2.2 Rehabilitation therapies

Rehabilitation therapies aim at supporting the spontaneous biological recovery in the various behavioral domains. Depending on the impairment, current interventions include physical, occupational and language therapies in addition to more recent multimodal treatments (e.g., music-based or mirror therapy). With regard to motor impairment, usual care therapies seem to benefit the general stroke population, especially in terms of activity capacity, which can increase independence and quality of life and decrease caregiver burden and institutionalization (Stinear et al., 2020; Winstein et al., 2016). However, they mainly follow a ‘one-fits-all’ approach and are not tailored to the individual patient’s needs, especially the needs of patients who belong to ‘non-fitter’ groups, i.e., who show little to no spontaneous recovery.

In response to this need for more individualized therapies, the quest for new appropriate and more personalized therapeutical targets to improve motor outcome is ongoing. However, to this day, clinical trials have been rather unsuccessful (Stinear et al., 2020) which can be accounted for due to several reasons. First, usual care therapies which are ongoing in parallel to clinical trials are often not routinely monitored, hence disentangling the effect of the clinical trial from the usual care effect can be challenging (Stinear et al., 2020). In addition, most motor recovery takes place in acute and early subacute phases after a stroke (i.e., in the first 3 months) (Duncan et al., 2000; Krakauer et al., 2012; Zeiler & Krakauer, 2013) which makes it the ideal moment to further support behavioral improvements (Biernaskie, 2004; Overman & Carmichael, 2014). However, if the clinical trials take place during this period, they are further confounded by spontaneous recovery, whose peak occurs simultaneously (Stinear et al., 2013). Second, the interventions tested in clinical trials might have been too similar to current therapy practices, rendering it difficult to differentiate the two (Jolkkonen, 2016; M.-C. Smith et al., 2017). Third, only few studies (Stinear et al., 2017) selected biomarkers of corticomotor function or structure as inclusion criteria. Therefore, the capacity of patients to respond to treatment (i.e., to the underlying biological mode of action of the intervention) might have differed significantly between control and treatment groups, even if the groups were matched on baseline clinical scores. However, selecting patients based on biomarkers which reflect their capacity to respond to the intervention, could increase the statistical power of a clinical trial and detect effects that are only present in a specific sub-group of the stroke population (Stinear, 2017).

The biggest and foremost challenge of the current time, however, is to have a better understanding of stroke recovery, especially with regard to ‘non-fitters’, which could potentially lead us to identify biomarkers that are more suitable for patient stratification in the context of clinical intervention trials that shape recovery and behavioral outcomes, two common indicators of post-stroke recovery (Guggisberg et al., 2019; Stinear, 2017). To this end, large-scale longitudinal studies including both ischemic and hemorrhagic stroke patients are needed in order to represent the entirety of the stroke population and to draw appropriate conclusions (Guggisberg et al., 2019; Stinear, 2017). Furthermore, in addition to tracking the physical and cognitive

improvements, it is crucial to couple the behavioral observations with neuroimaging, such as Magnetic Resonance Imaging (MRI), in order to relate the recovery to the underlying neural mechanisms.

1.3 Magnetic Resonance Imaging (MRI) in stroke

There are various ways to investigate neural correlates underlying stroke recovery in humans. Here, I will focus on one of the most prominent neuroimaging techniques – Magnetic Resonance Imaging (MRI) – and briefly review the main applications of structural as well as functional MRI, thereby summarizing the main insights they provided related to stroke recovery and outcome over the last decades.

MRI is a non-invasive brain imaging technique, which can inform us about in-vivo brain structure and function in humans. It has been widely used in research to cross-sectionally and longitudinally investigate neural correlates underlying stroke and its recovery (Crofts et al., 2020; Moura & Conforto, 2019). Two of the most frequently used modalities are Diffusion-Weighted Imaging (DWI) and BOLD imaging for structural and functional imaging, respectively. In radiology, the term structural MRI refers to classical T1- and T2-weighted imaging sequences, which provide high resolution images with good contrast between different tissues in the brain (Carneiro et al., 2006). However, for the sake of simplicity and given that DWI provides structural information regarding fiber tracts in the brain (see section 1.3.1 here below), in this thesis, I will use the term “structural MRI” to relate to DWI.

1.3.1 Structural MRI

Through DWI, it has become possible to study fiber tracts and their associated microstructure as well as their changes over time. This makes this method crucial for translational research and for studying the neural reorganization after cerebrovascular accidents. (Guggisberg et al., 2019).

1.3.1.1 Microstructural imaging

Values derived from diffusion imaging, such as the Fractional Anisotropy (FA) or Mean Diffusivity (MD) are often used to describe the integrity of neural tissue (Beaulieu, 2014). FA describes the directionality of diffusion and can take a value between zero and one. A value of zero indicates that diffusion is isotropic (i.e., equal in all directions), whereas a value of one means that the diffusion is oriented along one axis and non-existent in all other directions. FA is typically high in voxels that contain a big amount of highly aligned fibers, because water molecules diffuse mainly along the direction of these fibers. FA can be related to fiber density, axonal diameter and myelination in white matter and tends to be low in grey matter and high in white matter. MD, on the other hand, provides information about the average diffusivity of water in the brain (Beaulieu, 2014) and is similar in gray and white matter.

In theory, in white matter, a stroke would cause a decrease in FA and an increase in MD, due to the loss of directionality of diffusion. Following grey matter damage, MD would also increase, but FA could either increase or decrease depending on the biological process that is triggered (Beaulieu, 2014). However, to this day, the interpretation of changes in diffusion parameters and their implication for tissue (micro-)structure is not fully understood. This is in particular due to limitations related to tractography and essentially its angular resolution (Maier-Hein et al., 2017), which is the capability to distinguish between two distinct fiber tracts that cross at a certain angle. The smaller the angle at which the two fiber tracts are still distinguished by the algorithm, the higher is its angular resolution (Seunarine & Alexander, 2014). Depending on the angular resolution, it can thus be difficult to disentangle a lesion from a simple fiber crossing, as both cause

a decrease in FA in a given voxel (Assaf et al., 2017; Chu et al., 2015; Descoteaux et al., 2009; Jensen et al., 2005; Malcolm et al., 2010). Despite efforts in the achievement of higher angular estimation, which would allow for better results in locations of fiber crossings (Descoteaux et al., 2009; J.-D. Tournier et al., 2004), as well as in the development in higher and more complex models (Alexander et al., 2017; Assaf et al., 2017), the problem is still not fully resolved (Maier-Hein et al., 2017).

1.3.1.2 Tractography

The diffusion signal can also be used to reconstruct fiber tracts. In both healthy and pathological brains, tractography offers a unique opportunity to non-invasively delineate white matter pathways. This makes it suitable to study fiber bundles and structural brain connectivity in vivo in humans (Jeurissen et al., 2017).

Tractograms (**Figure 3**) are constructed based on a tensor or on the orientation distribution of fibers (ODF), which are estimated for every voxel (Jeurissen et al., 2017; O'Donnell et al., 2017). From the latter, tracts can be reconstructed using either deterministic or probabilistic tractography. In deterministic tractography, at every voxel, the direction is given by the major eigenvector of the diffusion tensor or the peak orientation of the ODF (Blyth et al., 2003; Hagmann et al., 2007). As a consequence, for every seed there is a unique streamline and the streamline is fully determined by its seed point (Seunarine & Alexander, 2014). Probabilistic algorithms, in addition to using fiber directions, also use a model of the uncertainty of each fiber orientation estimate, thereby selecting the direction associated to the highest probability (Seunarine & Alexander, 2014).

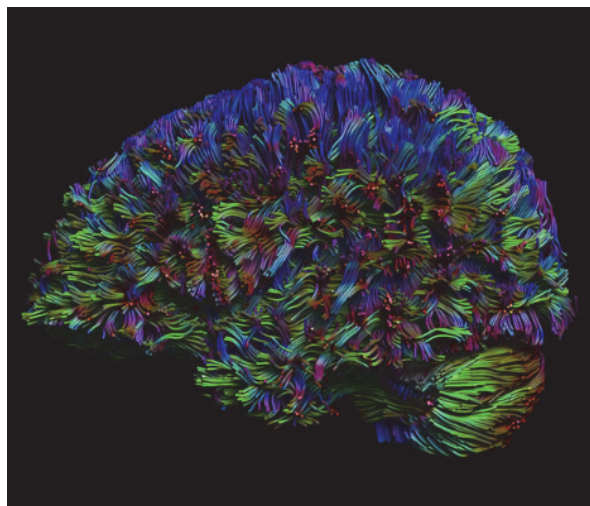


Figure 3. Whole-brain tractogram.

Left: Whole-brain tractogram. Right: A selection of fiber bundle trajectories are virtually dissected. Image adapted from Jeurissen et al. (2017)

A main application derived from tractography is the measure of *structural connectivity*, where the number of 'connections' (i.e., streamlines) between a pair of cortical and/or subcortical grey matter areas reflects their connection strength (Hagmann et al., 2008; Sporns, 2011). Furthermore, a *structural connectome* is a n-by-n matrix in which the structural connectivity of each pair of regions of interest (ROIs) is summarized (n reflects the number of ROIs in the cortical and/or subcortical grey matter parcellation) (**Figure 4**) (Sporns et al., 2005).

Tractography is, however, facing certain reproducibility issues (Brumer et al., 2021), which can mainly be related to the use of different MRI scanners, but also to inter-run variability (Bonilha et al., 2015). In addition, tractography is also subject to considerable variations which depend on the algorithm that is used for fiber tracking. (Maier-Hein et al., 2017). Indeed, tractograms obtained through most algorithms contain approximately 90% of the ground truth bundles, however, they also contain many more valid compared to invalid fiber bundles. Of these false-positive fiber bundles, more than half are systematically reproduced across research groups. Often times, these are considerably dense bundles of plausible looking streamlines in places where they should not actually exist. As for microstructural imaging, the main limitation is related to angular resolution (Maier-Hein et al., 2017). One proposed optimization are streamline filtering techniques, such as Spherical-deconvolution Informed Filtering of Tractograms (SIFT) (R. E. Smith et al., 2013, 2015b) or Convex Optimization Modeling for Microstructure Informed Tractography (COMMIT) (Daducci et al., 2015; Schiavi et al., 2020), which could help reduce tractography biases (Maier-Hein et al., 2017). The underlying idea is to integrate non-local information (R. E. Smith et al., 2013, 2015b) as well as to inform the tractogram with microstructure and anatomical priors (Daducci et al., 2015; Schiavi et al., 2020). To this day it has however not been investigated to what extent these filtering techniques influence reproducibility and repeatability. Despite its limitations, DWI is currently the only method that allows to investigate white matter pathways in humans in vivo and as such remains one of the essential tools used in neuroscience research (Maier-Hein et al., 2017).

In conclusion, DWI greatly facilitated the understanding of the brain's in vivo circuits and the mapping of white matter in healthy and pathological populations. Furthermore, despite its limitations related to reproducibility and the presence of false-positive fiber bundles, it remains the gold standard for the investigation of fiber tracts in humans. However, little can be inferred about the function of the tracts that were discovered through diffusion-weighted imaging, motivating the need for another, functionally-oriented MRI technique.

1.3.2 Functional MRI

Blood flow in the brain is highly locally controlled in accordance to the oxygen demands required by the different brain areas. If a brain area increases its activity, its oxygen requirements increase, which leads to a brief drop in oxygenated hemoglobin as well as an increase in carbon dioxide and deoxygenated hemoglobin. In response to this, blood flow to this area will be increased, which leads to a surplus of oxygenated hemoglobin. It is this peak in local tissue oxygenation which can be captured by functional MRI sequences, rendering BOLD signal an indirect measure of brain activity. The activity of the brain can be observed either during a task or during rest, called task-based or resting-state functional MRI (fMRI), respectively (Belliveau et al., 1991; B. Biswal et al., 1995; Ogawa et al., 1990). fMRI was the first imaging method to offer high spatial resolution, however this comes at the cost of a low temporal resolution, making this method complementary to electroencephalography (EEG), which has a high temporal and low spatial resolution (Filippi, 2015).

1.3.2.1 Task-based fMRI

Task-based fMRI offers unique possibilities to investigate sources of brain activation related to behavior, assessed by tailored experimental paradigms performed in MRI scanners (Ogawa et al., 1990). Through a targeted motor task this allows, for example, to study differences in brain activations occurring in a given movement in time in healthy participants vs. stroke patients with motor deficits (Hannanu et al., 2017; Rehme et al., 2015). In the context of clinical studies, one of the main limitations of this method is the level of impairment of patients. Indeed, patients with strong deficits might not be able to perform the task, which

limits the interpretability of the results (Guggisberg et al., 2019). In the framework of task-based fMRI, the goal is usually to relate the activity of brain areas to a specific function. Lately, the field has moved away from this view towards a more interactive network approach, where a function is related to the interplay between different grey matter areas within a network rather than to the activity in one or several isolated brain regions (Liu & Duyn, 2013). Recent studies started to investigate dynamic co-activation patterns to task-based fMRI, which allows to capture dynamic behavior of networks involved in a given task (Dhanis et al., 2022).

1.3.2.2 Resting-state fMRI

Interactions of neural networks can also be observed through resting-state fMRI without any explicit task. Here, synchronization of hemodynamic fluctuations between brain regions or voxels of interest are studied and the strength of interregional interactions are estimated (B. Biswal et al., 1995; Fries, 2005; Varela et al., 2001). In this context, *functional connectivity* reflects the statistical dependency between two brain regions (or voxels) and is used to describe the coordinated activity between the latter (Friston, 1994; Nozais et al., 2021). Analogously to the structural connectome, a *functional connectome* is a n-by-n matrix in which the functional connectivity of each pair of regions of interest (ROIs) is displayed (n reflects the number of ROIs in the cortical and/or subcortical grey matter parcellation) (Figure 4).

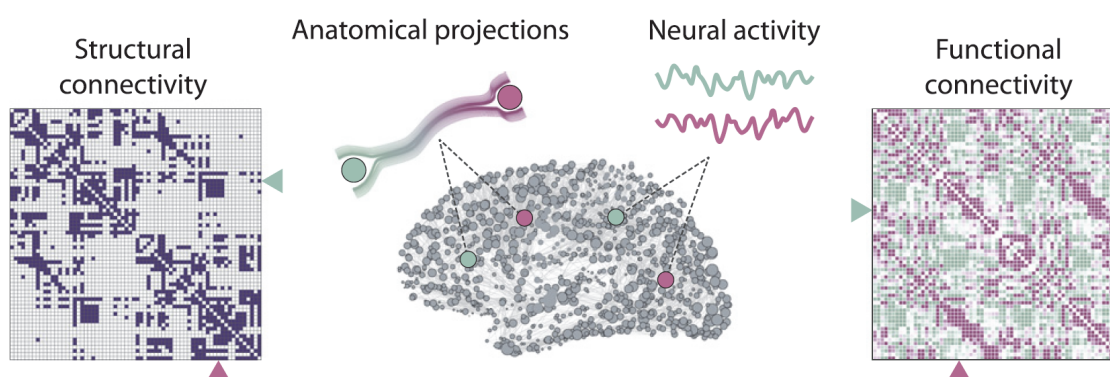


Figure 4. Measuring structural and functional connectivity.

For both structural and functional connectivity, it is necessary to first parcellate the cortex in regions of interest (ROIs) or nodes, displayed as grey dots. Structural connectivity is based by counting, e.g., the number of streamlines – which represent the underlying anatomical projections – between each pair nodes (often times this value is normalized by the total amount of streamlines in the tractogram or by ROI size). The matrix on the left, called structural connectome, summarizes these connectivity values and high connectivity is reflected in blue. To obtain the functional connectome (on the right), the correlation between the averaged neural activity of each pair of ROIs is plotted. Image adapted from Suárez et al (2020).

Resting-state fMRI bears the advantage of being independent of a person's ability to perform a task, which is often restricted after a stroke. Therefore, resting-state fMRI offers a great opportunity to follow post-stroke neural reorganization in patients with all degrees of impairment. In addition, it allows to study several networks and their interactions simultaneously and on whole-brain level (Guggisberg et al., 2019; Karahanoğlu & Van De Ville, 2015). Templates for resting-state networks as published by Yeo et al. (2011) or (S. M. Smith et al., 2009) are frequently used in research and offer various levels of resolution (e.g. Yeo et al. propose a 7-network as well as a 17-network estimate). A limitation of this method is that it is not possible to infer conclusions about the anatomical connections that underlie this functional activation or connectivity.

1.3.3 Understanding of motor recovery and outcome through MRI

As mentioned previously (see section 1.2), there is a need to further improve outcome and prediction accuracy of recovery, as well as to personalize treatment in order to move a step forward in stroke rehabilitation. A better prediction of long-term outcomes after stroke would benefit patients, caregivers and clinicians likewise. It would allow to better define clinical pathways and goal setting and it could potentially help determine type and dose of intervention to promote stroke recovery (Boyd et al., 2017; Cramer et al., 2007). A particular challenge in terms of prediction remain patients with severe initial motor impairments. Some have good natural recovery, whereas others do not and clinical scores at this stage cannot distinguish between the two sub-groups. Therefore, the use of biomarkers based on neuroimaging for patient stratification has been a high priority challenge in clinical research over the past years (P. J. Koch et al., 2021; Stinear, 2017; Ward, 2017).

MRI is a widely used technique for both clinical applications and research related to stroke. In the past two decades, a particular focus has been laid on the understanding and prediction of motor recovery and outcome. Recovery is understood as the improvement over time (e.g., a patient improved 12 points on the UE-FM scale between the acute and chronic phase), whereas the outcome, or residual function, reflects a specific score at a certain point in time (e.g., a UE-FM score of 52 after one year).

In the next sections, I will give an overview of the cortical motor network as well as the main structural and functional neuroimaging biomarkers for patient stratification in the context of motor recovery after stroke.

1.3.3.1 Cortical motor areas

In 1870, Fritsch and Hitzig (Fritsch & Hitzig, 1870) provided the first clear demonstration through electrical stimulation that some areas of the cerebral cortex of dogs were involved in motor function. In non-human primates, Leyton and Sherrington (Leyton & Sherrington, 1917) later applied electrical stimulation at different locations of the precentral cortex and reported that they could induce movements of specific parts of the body. In 1909 Brodmann (Brodmann, 1909) demonstrated differences in the cytoarchitecture between agranular cortex with large pyramidal cells in the anterior bank of the precentral sulcus (Brodmann area 4) and the agranular cortex in the precentral gyrus and the posterior portion of the superior frontal gyrus on both the lateral and medial surfaces of the brain (Brodmann area 6). These findings, along with converging lines of evidence from clinical observations and cortical ablation experiments performed in monkeys, led Fulton (Fulton & Sheehan, 1935) to propose that the motor cortex of human is divided into a primary motor area (M1, corresponding to Brodmann area 4) and a premotor area (PM, corresponding to Brodmann area 6). Today, several distinct nonprimary motor areas have been identified: the PM located on the lateral part of Brodmann area 6 (Picard & Strick, 2001) and the supplementary motor areas (SMA) located on the medial part of Brodmann area 6 (Penfield & Welch, 1951; Picard & Strick, 1996).

M1 hosts the upper motor neurons and is the origin of the majority of descending fiber pathways to the lower motor neurons located in the ventral horn of the spinal cord (Porter & Lemon, 1993). PM has been shown to be activated when a new motor program is established or when the motor program is changed on the basis of sensory information (Roland et al., 1980). Regarding the secondary motor areas, the dorsal part of PM is involved in reaching movements, whereas the ventral part is responsible for hand and finger movements (Hoshi & Tanji, 2007). Additionally, the supplementary motor areas (SMA) have been shown to play an important role in the preparation and organization of voluntary movement, notably in the performance of sequential movements (Nachev et al., 2008). Anatomically, the SMA comprised at least two subareas, the rostral pre-SMA, which is heavily interconnected with prefrontal areas, and the caudal SMA-proper, which is closely interconnected with M1 and PM (Miall, 2016). Both PM and SMA have direct

anatomical projections to spinal motor neurons allowing them to directly influence the motor output (Dum & Strick, 1996; He et al., 1993).

Further areas that are less directly involved comprise 1) the cingulate motor area located along the dorsal and ventral banks of the cingulate sulcus which is involved in the execution of movements (Paus et al., 1993) 2) the posterior parietal cortex (areas 5 and 7) which provides information to the other motor areas regarding the spatial position of the body with respect to the external world as well as the spatial relationship between objects (Whitlock, 2017) 3) the somatosensory cortex (S1, areas 1,2,3), which provides detailed sensory information regarding proprioceptors in muscles and joint as well as from cutaneous receptors and 4) the frontal eye fields and supplementary eye fields (within area 8) which are involved in voluntary control of the eyes (Miall, 2016). For a visual illustration of the motor areas, see **Figure 5**.

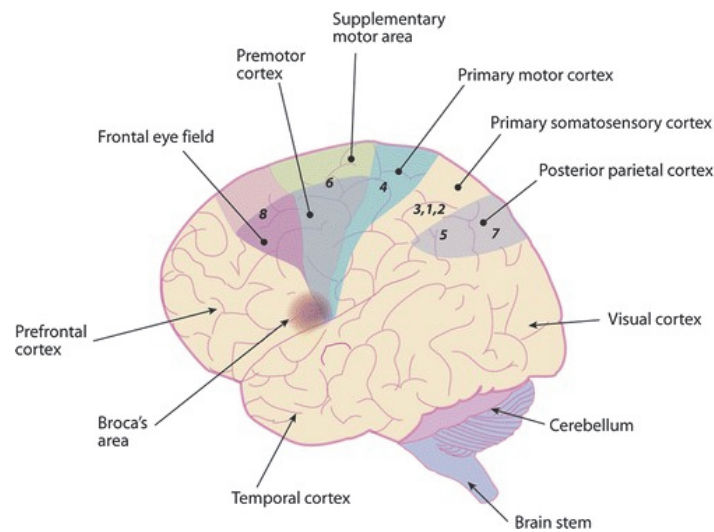


Figure 5. Motor areas.

Illustration of the motor areas of the cerebral cortex. The numbers represent the Brodmann's area. E.g., the primary motor cortex corresponds to Brodmann's area 4. Image adapted from Miall, (2016)

The main inputs to M1 come from PM, SMA, the posterior parietal cortex and S1. In addition, there is further input from the cerebellum via the thalamus and visual information is relayed via PM as well as via the cerebellum to M1. Lastly, the motor cortex receives inputs from the locus coeruleus, the reticular system, and the interthalamic nuclei which adjust the level of motivation or arousal within the voluntary motor system. The main output from the motor cortex are projections belonging to the pyramidal tract, or corticospinal tract (CST), which pass through the internal capsule to the brainstem and the spinal cord (Miall, 2016). Finally, there is also evidence for connections to the contralateral motor cortex through homotopic direct transcallosal projections between M1, PMC and SMA (Boussaoud et al., 2005; Luppino et al., 1993; Rouiller et al., 1994)

In summary, M1, PM and SMA are the central motor areas involved in the planning and execution of a movement. Further information which is relevant for motor control is relayed to them via the cingulate motor area, the posterior parietal cortex, S1, and the frontal eye fields. Therefore, these areas are likely to be affected by a stroke and to play a pivotal role during post-stroke cortical reorganization, which I will address in the next sections.

1.3.3.2 Structural MRI in stroke

Following a stroke, studying microstructure and reconstructing major fiber bundles, e.g. the corticospinal tract (CST), or bundles that connect specific regions of interest, is a promising approach to better understand the impact of a stroke on the brain as well as on motor functions and recovery (Jeurissen et al., 2017; Thiel & Vahdat, 2015). Notably, integrity of the CST is associated with less severe motor impairment in acute and chronic phases, as well as with better recovery (Buch et al., 2016; Byblow et al., 2015; Doughty et al., 2016; Feng et al., 2015; Guggisberg et al., 2017; Kim et al., 2015; Peters et al., 2018; Puig et al., 2011, 2013; Ramsey et al., 2017; Stinear, 2017; Stinear et al., 2007).

Residual motor function is associated with measures such as FA asymmetry of the CST (i.e. the difference between ipsi- and contralesional FA values of the CST divided by the sum of said values) at the level of the pons (Puig et al., 2013), acute lesion load on the ipsilateral CST (i.e. the extent of damage caused by the lesion to the CST) (Buch et al., 2016; Byblow et al., 2015; Doughty et al., 2016; Feng et al., 2015; Lim et al., 2020; Pennati et al., 2020), as well as damage to the posterior limb of the internal capsule (Puig et al., 2011). Indeed, greater FA asymmetry measured 30 days post-stroke predicted worse motor outcomes at two years (Puig et al., 2013) and there was a negative linear relationship between acute lesion load on the ipsilesional CST and UE-FM score three months after stroke (Doughty et al., 2016; Feng et al., 2015). In particular, acute CST damage at the level of the posterior limb of the internal capsule predicted the motor outcome the best (Puig et al., 2011). Interestingly, damage to the white matter was a better indicator of motor outcome than lesion volume (Egger et al., 2021; Puig et al., 2017; Stinear, 2017). One study even found a lesion-cutoff value which identified patients who would have a poor motor outcome with a positive predictive value at 100%. In other words, if the lesion to the CST surpassed a certain size, the patient had a 100% chance to have a poor motor outcome (Feng et al., 2015).

These studies highlight the importance of the ipsilesional hemisphere and CST in motor outcome and recovery after stroke and it has been suggested that FA and lesion load might have cutoff values which could potentially be used as predictors for individual patients (Stinear, 2017). The results of these studies are encouraging, however, the ability to distinguish patients who will have spontaneous recovery ('fitters') from patients who will likely not ('non-fitters'), remains insufficient. In addition, only focal brain areas and pathways related to sensorimotor function were taken into account for the prediction, while it is the current view that stroke is in fact a large-scale network disorder and properties of affected networks could further refine the prediction of motor recovery and outcome (Egger et al., 2021; Guggisberg et al., 2019; P. J. Koch et al., 2021).

In line with this, a study showed that a decrease in FA of remote white matter pathways in the affected hemisphere was linked to improved recovery (Pinter et al., 2020). Furthermore, recent work has identified beneficial effects of including whole-brain connectivity data in prediction for motor recovery (P. J. Koch et al., 2021). Indeed, instead of considering only a selected fiber bundle, in the study of (P. J. Koch et al., 2021), a whole-brain FA connectome was used for each patient. Using support vector machine classifiers, the authors managed to separate 'fitters' from 'non-fitters' with an accuracy of 92% and a precision of 93% in severely affected patients. This underscores the potential of whole-brain measurements for the understanding and prediction of motor recovery. However, the external validation dataset in this study had a small sample size and an inhomogeneous patient distribution in terms of degree of impairment, hence the results will need to be replicated in studies with larger cohorts of patients to appropriately assess the clinical usability (P. J. Koch et al., 2021). Meanwhile, whole-brain measurements can also be explored in the context of fMRI, which could be another, complementary, approach to measures derived from structural MRI.

1.3.3.3 Functional MRI in stroke

In terms of functional measures, it is commonly assumed that patterns of activity more resemblant to those observed in healthy controls are associated to better motor performance at the time of scanning for both resting-state (Siegel et al., 2016; Thiel & Vahdat, 2015) and task-based fMRI (Buma et al., 2010; Favre et al., 2014; Grefkes & Ward, 2014).

Regarding resting-state fMRI, there is ample evidence demonstrating that interhemispheric functional connectivity between homologous sensorimotor areas is decreased in the acute phase of stroke and related to behavioral impairments (Baldassarre et al., 2016; Carter et al., 2010; Golestani et al., 2013; Park et al., 2011; van Meer et al., 2010; L. Wang et al., 2010). It has further been shown to be predictive of better motor recovery (Fan et al., 2015; Park et al., 2011) and able to distinguish between ‘fitters’ and ‘non-fitters’ (Jung et al., 2013). This suggests that a balance between inhibitory and excitatory interhemispheric connections is crucial for intact sensorimotor functions (Grefkes & Fink, 2014; Thiel & Vahdat, 2015). In addition, a decrease in ipsilesional and an increase in contralesional connectivity within the sensorimotor cortex has been described in the subacute stage, however these changes were not related to functional outcome, suggesting a minor role of these mechanisms (Thiel & Vahdat, 2015; Xu et al., 2014). Over time, interhemispheric connectivity between homologous areas increases along with functional recovery. Although it fails to match that of healthy control subjects at the subacute stage (L. Wang et al., 2010; Xu et al., 2014), it tends to gradually normalize towards pre-stroke connectivity in the chronic phase in patients with good recovery. In patients who recover poorly, however, the decrease in interhemispheric connectivity correlates with motor function (J. L. Chen & Schlaug, 2013; Min et al., 2020; Urbin et al., 2014; Xu et al., 2014).

Such reorganization of resting-state connectivity seems to extend to networks which are not directly implicated in sensorimotor processing (Guggisberg et al., 2019; Thiel & Vahdat, 2015). Indeed, in the acute phase, elevated intra-network connectivity was found in different sensory, motor and default mode networks, whereas connectivity was decreased within associative frontoparietal networks and between networks (C. Wang et al., 2014). Furthermore, there have been attempts to use the whole-brain functional connectome to improve functional predictions using measures derived from functional network topology (J. Lee et al., 2015; Olafson et al., 2021).

There were several efforts of predicting motor outcome with task-based fMRI as well. For example, in the study of (Rehme et al., 2015), functional activity related to an active hand-grip task revealed higher activity in the ipsilesional primary motor cortex (M1) and premotor cortex as well as in the contralesional cerebellum in patients with good motor outcomes compared to patients with poor outcome. The authors further report that functional activity predicted the motor outcome better (86%) compared to behavior only (76%). It should however be noted that no severely impaired patients were included in this study as they would not have been able to perform the motor task. Using a passive flexion-extension task of the paretic wrist, similar work of (Hannanu et al., 2017) has also shown lower task-related activity in M1, supplementary motor area (SMA) as well as the contralesional cerebellum compared to healthy controls. Furthermore, the authors observed higher activity in the contralesional primary motor cortex, superior temporal gyrus and the parietal operculum. Task-related activity alone had an increased explained variance (96%) compared to a combination of functional activity and total FM score (87%) (Hannanu et al., 2017). Results of these two studies suggest that motor outcome can potentially be better predicted using task-related functional activity compared to behavioral data alone. However, these findings need to be corroborated in larger cohorts (Stinear, 2017).

In summary, both structural and functional biomarkers have shown promising results in terms of prediction of motor outcome and recovery after a stroke. However, their applicability in clinics is still very limited, either

due to the lack of large-scale evidence, or due to the inability to predict the outcome or the recovery for individual patients (Stinear, 2017). Combining biomarkers has been proposed to address this issue (Boyd et al., 2017) and will be presented hereafter.

1.3.3.4 Combining biomarkers

In an attempt to explain variance in motor recovery or outcome, studies frequently combined clinical, demographic and biomarker information in multivariable regression models. However, the resulting equations are limited in making predictions for individual stroke survivors in clinical settings (Stinear, 2017), as they predict recovery or outcome for groups of patients. Recently, however, combining several biomarkers sequentially instead of using multiple biomarkers simultaneously has shown promising results in addressing the aforementioned gap (Stinear et al., 2017). For instance, the Predict Recovery Potential 2 (PREP2) algorithm sequentially combines a measure of upper limb impairment, age, the presence or absence of upper limb motor evoked potentials elicited with transcranial magnetic stimulation (TMS) as well as either stroke lesion load obtained from MRI or stroke severity assessed with the NIHSS score. The biomarker obtained through TMS is indicated for one third of the patients and if associated with the NIHSS score, the prediction can be made as accurately and without costly MRI. The algorithm has a prediction accuracy of 75% and has been successfully implemented in clinical practice, paving the way for other centers to a more personalized treatment of stroke patients (Connell et al., 2021; Stinear et al., 2017). Consequently, assessment of clinical implications showed that the duration of upper limb therapy was not altered, as opposed to the content. In addition, inpatient length of stay was reduced by approximately one week (Stinear et al., 2017). This pioneering clinical implementation of PREP2 demonstrates the potential of individualized care and has shown to optimize treatment strategies and decreased costs related to hospitalization, paving the way towards new clinical intervention trials that can appropriately stratify patients prior to inclusion. Potential for improvement lies in the quantity of biomarkers needed for PREP2, as they can be costly and time-consuming, especially for severely impaired patients. Instead of achieving multimodality by combining unimodal biomarkers sequentially, a new approach could thus be to probe multimodal biomarkers instead. Hence, the following section will address multimodal MRI approaches and their potential for understanding and prediction of stroke recovery.

1.3.4 Multimodal MRI

Structural and functional MRI are inherently complementary (Thiel & Vahdat, 2015) and serve as remarkable tools enabling us to investigate neural correlates at rest or during a task as well as their underlying anatomical substrates. Even though it is well known that brain activity is biologically constrained by the underlying anatomy (i.e., structure), the mechanisms enabling functional activity in neuroimaging to be shaped by the underlying anatomical backbone, that is structural connectivity, remain poorly understood (Preti & Van De Ville, 2019; Stiso & Bassett, 2018; Suárez et al., 2020).

In a pathology such as stroke, a structural damage necessarily evokes functional changes. Establishing and predicting the consequences of a brain lesion on the functional activity and connectivity, however, still poses a significant challenge (Silasi & Murphy, 2014). Given the complementarity between DWI and fMRI, there have been several attempts of enhancing the functional data with structural information, with the aim of obtaining a clearer idea of the interplay between brain structure and functional activity, as well as understanding how pathology can affect it (Preti & Van De Ville, 2019; Suárez et al., 2020).

The first attempts involved the simple correlation of functional connectivity with the corresponding structural connectivity (Hagmann et al., 2008; Honey et al., 2009). The authors found structural connectivity

to be highly predictive of functional connectivity, but less reliably so vice versa. Namely, due to numerous indirect connections between regions, the authors hypothesized that functional connectivity could remain strong without a direct structural connection.

Another attempt of including structural information in a functional analysis involved using anatomical priors gained from DWI measurements to estimate effective connectivity using dynamic causal modelling (DCM) (Friston et al., 2003; Stephan et al., 2009). In this case, the changes in coupling among brain regions are evaluated depending on the underlying structural connectivity. After assessing several models relating the two, the authors report that the anatomical and effective connectivity are best related in a monotonic and nonlinear (sigmoidal) fashion, implying that the increase in structural connectivity leads to the (nonlinear) increase in effective connectivity. However, similar to previous work, these authors also stressed that effective connectivity was constrained, but not determined by anatomical connectivity. Specifically, they argue that the existence of an anatomical connection did not imply its involvement in a particular process, meaning that even if a synaptic connection is there, it can remain inactive (Stephan et al., 2009).

Recently, several more sophisticated methods linking brain structure and function emerged: First, a recent study (Sarwar et al., 2021) successfully used deep learning to predict an individual's brain function from their structural connectome, and additionally showed that the inter-individual variation in predicted functional connectivity was related to cognitive performance.

Second, the *Functionnectome* introduced a new concept – the study of the function of white matter pathways (Nozais et al., 2021) performed through the combination of task-related fMRI and anatomical priors for brain circuits, where a prior reflects a voxel and its probability of structural connectivity with all other brain voxels. To obtain a Functionnectome, the functional signal of two areas which are linked by a white matter pathway is combined, thereby penalizing the statistical activation if only one region is significantly activated by the investigated function. The end result is a white matter activation map which reflects the associated pathway's significant involvement during a task (**Figure 6**). The downside of this method is that it needs powerful computational resources due to a sizeable number of priors (one for every voxel in the brain). In addition, priors are based on 100 healthy young participants and the method can thus not readily be adapted to other populations such as healthy older adults or stroke patients.

Third, the emergence of network neuroscience enabled the extraction of system-level network properties. Organizational principles of structural and functional connectivity can be summarized and compared, or be used to inform one with the other (Suárez et al., 2020). Two recent studies (Medaglia et al., 2018; Preti & Van De Ville, 2019) explored this framework using resting-state fMRI as well as diffusion spectrum imaging (DSI) (Medaglia et al., 2018) and DWI (Preti & Van De Ville, 2019), respectively. Both studies used the eigenspectrum of the structural connectome to measure the distance of framewise regional BOLD activity from the underlying white matter. Through graph signal filtering, the functional signal was split into two parts based on the quality of coupling with structure – coupled and decoupled. (Preti & Van De Ville, 2019) named the ratio between the decoupled and coupled portions of the signal the *Structural Decoupling Index* (SDI). The first study (Medaglia et al., 2018) related functional alignment with the underlying structure to cognitive flexibility. The second study (Preti & Van De Ville, 2019) went a step further and demonstrated the existence of a gradient ranging from high structure-function coupling (i.e., low SDI) in areas involved in lower-level sensory functions (e.g., somatomotor or visual areas) to high structure-function decoupling (i.e. high SDI) in regions involved in higher-level cognitive functions (e.g., memory or emotions) (**Figure 6**).

Recently, this method was further extended to task-based MRI (Griffa et al., 2022), where structure-function coupling was shown to be task-dependent and SDI-related measures managed to identify an individual within a group with near-perfect accuracy. This suggests that the structure-function coupling might serve as a

fingerprint – or an intrinsic feature – of an individual’s brain organization. The ability of SDI to characterize an individual renders it particularly interesting and promising for clinical studies, where the understanding of individual patients’ features and pathological traits is a top priority, as it would allow for more patient-tailored approaches with respect to acute treatment and rehabilitation.

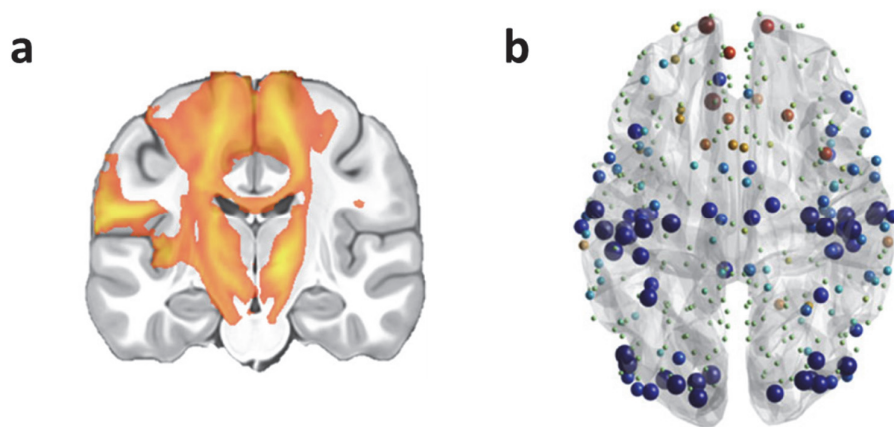


Figure 6. Functionnectome and Structural Decoupling Index (SDI).

Outputs of the Functionnectome (a) and SDI (b) analysis pipelines. a) Functionnectome: a white matter activation map which reflects the associated pathway’s significant involvement during a task. b) The colored nodes represent the SDI values. The bigger and the more blue, the lower the SDI (i.e. the higher the coupling), the smaller and the more red, the higher the SDI. Image adapted from Nozais et al.(2021); Preti & Van De Ville (2019).

1.3.4.1 Multimodal approaches in stroke research

In addition to the above-described methods which integrate structural with functional information and which were conceptualized based on healthy individuals, it is also possible to study the structure-function association by combining information about a (structural) lesion in the functional connectome. Lesion network mapping (Boes et al., 2015) offers such a possibility and it is based on the principle that lesions of different locations can cause the same symptoms. In this framework, the lesion location of patients who share similar symptoms is determined by means of MRI or Computed Tomography (CT) and traced onto a common brain atlas. Subsequently, the functional connectivity between each patient’s lesion location and the rest of the brain is computed using the human connectome – a normative map of anatomical and functional brain connections which is based on thousands of healthy people. This results in an individual lesion-function network map for each patient, which can then be overlapped with the maps from patients who are sharing similar symptoms, in order to identify common locations between the network maps.

Furthermore, DCM has also been successfully applied to stroke, shedding light onto how the interactions of cortical motor areas change after a stroke and throughout recovery. A stroke with an associated motor deficit has been shown to lead to disturbances in the communication between key motor areas, such as M1, SMA and PM. Indeed, previous studies demonstrated that early after stroke the contralesional M1 had a supportive influence on ipsilesional M1 (Rehme et al., 2011). However, subsequently there was a shift towards enhanced inhibitory coupling between the contralesional M1 and the ipsilesional M1, which correlated with the degree of motor impairment (Grefkes et al., 2008; Rehme et al., 2011), suggesting that increased interhemispheric inhibition from the contra- to the ipsilesional M1 is a maladaptive process. These results were further supported by a evidence from Grefkes et al. (2010) who showed that inhibition of the contralesional M1 resulted in a transiently decreased interhemispheric inhibition from the contra- onto the ipsilesional M1 which correlated with behavioral improvements. In addition, initially reduced positive

coupling between ipsilesional SMA and PM with ipsilesional M1 has been shown to increase with recovery and associated with better outcome (Grefkes et al., 2010).

Even though these findings shed some light onto the link between structure and function in stroke, DCM does not fully integrate function and structure, as the model is simply based on anatomical priors. While lesion network mapping is a fascinating approach, it does not take into account the individual functional data and is thought to work rather on group level. There is therefore still a need for a better understanding of the relationship between structure and function and how it is impacted by a stroke, especially on individual level.

As discussed above, recent studies (Griffa et al., 2022; Nozais et al., 2021; Preti & Van De Ville, 2019; Sarwar et al., 2021) have made a tremendous progress in the understanding of the structure-function relationship through multimodal approaches. So far, however, the population samples of these studies have been limited to group-level analyses in healthy young adults, and the role of age and focal brain lesions as well as its relationship to behavioral changes remains unknown. These steps should be investigated before probing these measures for patient stratification in the context of clinical trials. Particularly the SDI seems to be promising for future implementation in stroke research, as it offers the possibility to obtain results based on the individual structural and functional connectome and it can be run very fast and on a regular computer, as opposed to, e.g., the Functionnectome.

1.4 Framework and purpose of the thesis

1.4.1 Challenges for research in a clinical environment

As indicated above, in order to gain a better understanding of stroke rehabilitation, especially with regard to ‘non-fitters’ there is a strong need for large-scale longitudinal studies with big sample sizes which could deepen the understanding of underlying neural mechanisms and help identify interventional targets. Furthermore, there is a need for the inclusion of both ischemic and hemorrhagic stroke patients in clinical studies, as there isn’t any strong evidence indicating differences in terms of recovery (Jang et al., 2013) or outcome (Favre et al., 2014) between the two types of stroke. In addition, recent advances in network imaging have proposed new multimodal techniques (Griffa et al., 2022; Nozais et al., 2021; Preti & Van De Ville, 2019; Sarwar et al., 2021), notably the SDI (Preti & Van De Ville, 2019), which could serve as a promising tool for identifying novel biomarkers aimed at ‘patient phenotyping’ (Griffa et al., 2022), an inevitable step towards more patient-tailored treatment approaches (Guggisberg et al., 2019).

Moreover, in order to have interpretable and clinically relevant results, it is important that the acquired data and applied analysis pipelines have been optimized and show a high test-retest reliability within and across centers and time in a healthy population. There are several reasons for this: First, to ensure that potentially observed differences across timepoints in patients (i.e. longitudinally) actually reflect changes related to the recovery and not intraindividual variance related to the method or equipment. Second, conclusions derived from a given dataset should be valid for the whole stroke population, independent of the center where the data was acquired. Third, despite its high relevance for clinical research, access to patients remains one of the biggest challenges that contemporary research groups face. One approach is to run multi-center clinical studies, as they can help to increase sample size and accordingly statistical power of the findings. Multi-center studies still remain quite scarce, potentially due to the potential variance between the data acquired at two different sites (which could occur even with very similar equipment used at each recording site) (Bonilha et al., 2015). However, there are some initiatives such as ENIGMA (Liew et al., 2020), the largest

multisite retrospective stroke data collaboration to date, which illustrate the abundant possibilities of a large-scale collaboration, but which also reveals the need for data stability (in a healthy population) and robust analysis pipelines across centers in order to be able to validate, compare and combine results.

Therefore, intraindividual stability for a given neuroimaging method first needs to be demonstrated in healthy participants, before being applied in clinics or clinical research. The goal is that both data and results withstand any analytical bias and, moreover, that they are independent of the type of analytical pipeline employed. However, tractography results in particular remain subject to considerable variability arising from the algorithm used (see section 1.3.1.2)(Maier-Hein et al., 2017). It has been proposed that the stability of tractography results could be improved through filtering of the tractogram with SIFT (R. E. Smith et al., 2013, 2015b) or COMMIT (Daducci et al., 2015; Schiavi et al., 2020), but so far no study has systematically compared the two filtering options nor assessed their stability across sessions and centers. Identifying the best filtering method could thus lead to an improvement of analytical pipelines and to better data comparability across different sessions and centers, thereby facilitating the increase in multicenter clinical studies as well as cross-center clinical data analyses in translational neuroscience.

The purpose of this thesis is to address the above-mentioned challenges in three studies – two multimodal imaging studies investigating the structure-function in stroke patients using SDI, as well as a reproducibility study assessing the stability of different filtering methods in a test-retest setting. In the final sections of this introduction, the context, outline, as well as the main aims and hypotheses of this thesis will be elaborated.

1.4.2 Context of the thesis: Towards Individualized Medicine in Stroke (TiMeS)

The present thesis was realized in the context of a larger, longitudinal project entitled *“Towards Individualized Medicine in Stroke”* (TiMeS) with the aim to address aforementioned challenges and to pave the way for personalized precision medicine through a multimodal approach. In TiMeS, we collected an extensive multidimensional and longitudinal dataset representative for a stroke population in Switzerland with the aim of identifying new biomarkers for patient stratification. More precisely, through multimodal analyses, we intended to achieve a better understanding of post-stroke recovery and to bring about potential new biomarkers which could eventually lead to the end goal of TiMeS, which is the personalization of new therapeutical approaches, such as the individualization of non-invasive brain stimulation (NIBS) protocols, thanks to a better stratification of patients.

TiMeS targets patients with upper-limb motor deficits at stroke onset and comprises measurements coming from synergistic state-of-the-art systems neuroscience methods, such as structural and functional MRI, combined transcranial magnetic stimulation and electroencephalography (TMS-EEG), and electromyography (EMG). Furthermore, it contains an evaluation of behavioral outcomes such as motor function, but also of all other cognitive domains, in an attempt to have a complete overview of a patients' deficits and recovery. The assessment is longitudinal over the course of recovery, spread over four timepoints (one week (T1), three weeks (T2), three months (T3), and one year (T4)), until one year post-stroke. The project was implemented in collaboration with several clinical partners at the Clinique Romande de Réadaptation (CRR) in Sion, Switzerland. Patient recruitment, behavioral assessment at T1 as well as MRI acquisitions for all timepoints takes place at the Cantonal Hospital in Sion (HVS). After inpatient treatment at HVS, patients either go into rehabilitation at the CRR or at the Berner Klinik (BK) in Crans-Montana, or they return to their homes, depending on their degree of impairment. Behavioral follow-ups take place at either of the rehabilitation

clinics (CRR or BK) for T2 and at the CRR for T3 and T4, whereas MRI and TMS-EEG measurements for all timepoints are conducted at HVS and the CRR, respectively. For an illustration, see **Figure 7**.

This thesis focused on the MRI part of TiMeS as well as the relationship of neural correlates with behavior. In total 86 patients were included in the study and I acquired 200 timepoints in total (T1: 67, T2: 54, T3: 47, T4: 32 datasets, see **Figure 7B**).

The MRI protocol consists of several structural sequences, DWI, as well as a resting-state fMRI sequence:

- For structural imaging T1-weighted magnetization-prepared, rapid acquisition gradient-echo sequence (MPRAGE) is being acquired. Additionally, we acquire sequences for quantitative maps (MP2RAGE and multi-echo T2 GRASE) to gain a deeper insight in the microstructure in gray and white matter regions, by modeling, for example, the myelin water fraction. Finally, susceptibility-weighted images (SWI) is used to detect and quantify hemorrhagic processes in the brain.
- For DWI, we use a multishell approach with high gradient strength and large number of gradient directions. This data allows to model more advanced fiber tract distributions as compared to conventional diffusion tensor imaging.
- For resting-state functional imaging (fMRI), a multiband gradient echo-planar imaging (EPI) sequence is deployed and participants are instructed to fix a cross on the screen.

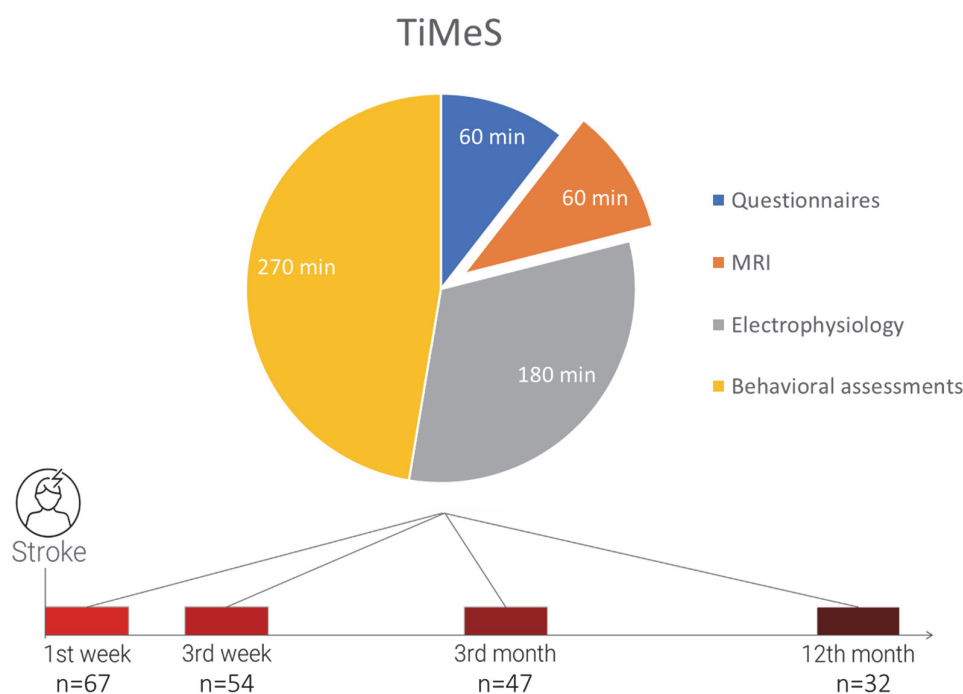


Figure 7. Towards Individualized Medicine in Stroke (TiMeS) project.

Composition in terms of duration of every timepoint in TiMeS. *n* reflects the number of patients who completed the MRI part of the project at each timepoint.

1.4.3 Thesis at a glance

The general purpose of the present thesis is to better understand the neural correlates of post-stroke recovery through multimodal imaging, with the primary goal to identify potential biomarkers that could be probed for patient stratification in the future. The secondary goal is to optimize a DWI analysis pipeline in terms of test-retest reproducibility, in order to obtain higher stability in the analysis of patient data.

Hence, the first part of this thesis revolves around the investigation of the structure-function relationship using SDI in the data acquired through DWI and resting-state sequences within the TiMeS framework. The gathered data allowed me to assess the complex interactions of structural and functional connectivity parameters within certain domain-specific networks, as well as within the whole brain (**Chapter 2**). Moreover, to the best of my knowledge, I was the first one to run such analyses in a stroke population. Given that a deficit of the upper limb at stroke onset was a common denominator for all included patients, a particular interest lied on identifying structure-function changes in the motor network. Structure-function coupling has been shown to be high in low-level sensorimotor areas (Preti & Van De Ville, 2019), which is why we hypothesized that a stroke, through the structural disruption and the functional changes this engenders, would lead to an increase in SDI in areas related to the lesion and notably in the motor network. Furthermore, in a second step, I extended the work previously done on recovery of one particular function after stroke, i.e., motor function, to a longitudinal multi- and inter-domain assessment of recovery and related the performance at different timepoints to variations in structure-function coupling (**Chapter 3**). From a clinical point of view, it becomes increasingly clear that often times a stroke does not affect only one domain, but multiple domains simultaneously. This is further supported by evidence that recovery of one function, such as motor function, is also dependent on the status of various other cognitive functions, such as attention (Ramsey et al., 2017). Thus, we hypothesized that worse performance in the motor, but also in cognitive domains, would be associated with changes in SDI not only in the motor network, but also in brain areas associated to other domains, such as cognition.

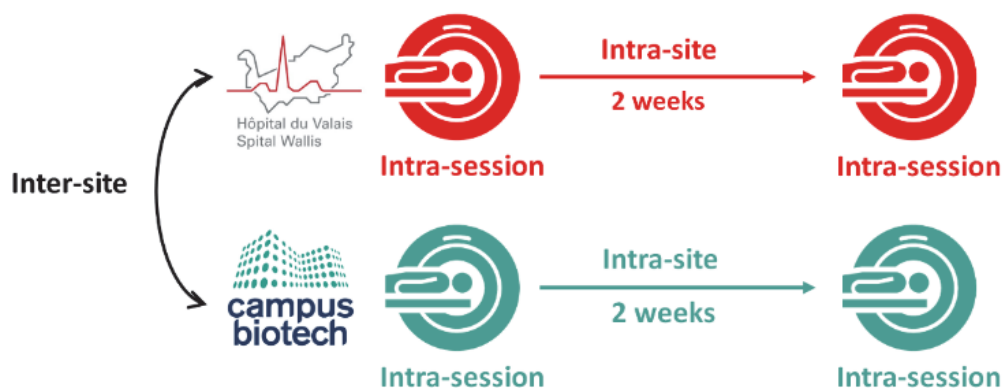


Figure 8. Experimental design of the test-retest reproducibility study.

20 healthy young participants were tested twice at Campus Biotech (Geneva) and twice at the Cantonal Hospital in Sion (HVS) at two weeks interval. During every session, the protocol was repeated twice in order to assess intra-session repeatability.

The second part of this thesis aims at improving analytical pipelines and increasing data comparability between sessions and centers, as this could benefit future clinical studies, especially in a multi-center setting. By performing microstructure-informed tractography through the use of filtering methods such as SIFT (R. E. Smith et al., 2013, 2015b) and COMMIT (Daducci et al., 2015; Schiavi et al., 2020), it is hypothesized that false-positive estimation biases can be reduced while increasing true-positive connections. Therefore,

Chapter 4 of this thesis revolves around the assessment of the stability of structural connectivity measures with and without COMMIT and SIFT in a multi-center dataset. In the lack of ground truth data, one promising way to validate technical improvements is by assessing the subject specificity and reproducibility of connectomes across sessions and locations. In the study presented in Chapter 4, 20 healthy young participants underwent four sessions of MRI, two of which took place at Campus Biotech Geneva and two at HVS in Sion (**Figure 8**). In addition, during every session, the protocol was run twice, in order to test repeatability, resulting in 8 datasets per participant and 160 datasets in total. We hypothesized that repeatability and reproducibility can be increased by including information derived from microstructure in the tractogram (i.e. through filtering), while we estimated that the most important portion of intra-subject variability would be associated to the use of different MRI scanners.

1.5 Overview and personal contributions

Personal contributions are labelled with the taxonomy coming from CRediT (*CRediT Author Statement*, 2022).

PART I

For both articles included in Part I, my contribution included conceptualization of the analysis (applying the Structural Decoupling Index developed by a collaborating lab to a stroke population), investigation (MRI data collection), data curation, formal analysis, visualization, writing – original draft and writing - review & editing

Study 1: *Structure-function coupling following an acute stroke.* **Brügger, J.**, Koch, P.J., Preti, M.G., Fleury, L., Park, C.H., Cadic-Melchior, A., Schmidt, L., Ceroni, M., Avanzi, S., Wessel, M., Maceira, P., Popa T., Meyer N.H., Blanke, O., Adolphsen, J., Jagella, C., Micera, S., Constantin, C., Vincent, A., Ghika, J., Vuadens, P., Turlan, J.L., Mühl, A., San Millán, D., Bonvin, C., Van de Ville, D., Hummel, F.C. *In preparation.*

Study 2: *Post-stroke structure-function coupling relates to cognitive impairments in the acute and early subacute phase.* **Brügger, J.**, Koch, P.J., Preti, M.G., Fleury, L., Park, C.H., Cadic-Melchior, A., Ceroni, M., Avanzi, S., Wessel, M., Meyer N.H., Blanke, O., Adolphsen, J., Jagella, C., Micera, S., Constantin, C., Vincent, A., Ghika, J., Vuadens, P., Turlan, J.L., Mühl, A., San Millán, D., Bonvin, C., Van de Ville, D., Hummel, F.C. *In preparation.*

PART II

For the article included in Part II, my contribution included conceptualization (participation in study design), investigation (MRI data collection), data curation, formal analysis, writing - review & editing

Study 3: *Evaluating reproducibility and subject-specificity of microstructure-informed connectivity.* Koch, P. J.*, Girard, G.*, **Brügger, J.**, Cadic-Melchior, A., Beanato, E., Park, C.H., Morishita, T., Pizzolato, M., Canales-Rodríguez, E.J., Fisch-Gomez, E., Schiavi, S., Daducci, A., Piredda, G.F., Hilbert, T., Kober, T., Thiran, J.P. §, Hummel, F.C. § *Under revision. NeuroImage.*

*, § authors contributed equally

APPENDIX

Supplementary study 1:

Towards individualized Medicine in Stroke – the TiMeS project: protocol of longitudinal, multi-modal, multi-domain study in stroke

Fleury, L.*, Koch, P.J.*, Wessel, M.J.*, Bonvin, C., San Millan, D., Ghika, J., Constantin, C., Vuadens, P., Adolphsen, J., Cadic-Melchior, A., **Brügger, J.**, Beanato, E., Ceroni, M., Menoud, P., de Leon Rodriguez, D., Zufferey, V., Meyer, N., Egger, P., Harquel, S., Popa, T., Raffin, E., Girard, G., Thiran, J.P., Vaney, C., Alvarez, V., Turlan, J.-P., Mühl, A., Leger, B., Morishita, T., Micera, S., Blanke, O., Van de Ville, D., Hummel, F.C. *In preparation.*

Personal contribution: writing – original draft (methods related to MRI), writing – review & editing (methods related to MRI).

Supplementary study 2:

Efficiency of unaffected parts of the brain network differentially impacts motor and attentional impairment after stroke. Evangelista, G.G.*, Egger, P.*, **Brügger, J.**, Beanato, E., Koch, P.J., Ceroni, M., Fleury, L., Cadic, A., Meyer, N.H., Avanzi, S., de León Rodriguez, D., Girard, G., Turlan, J.L., Mühl, A., Vuadens, P., Adolphsen, J., Jagella, C., Constantin, C., Alvarez, V., Ghika, J.A., San Millán, D., Bonvin, C., Morishita, T., Wessel, M.J., Van de Ville, D., Hummel, F.C. *Under review. Brain.*

Personal contribution: Investigation (data collection), data curation, formal analysis, writing – original draft (MRI methods), writing – review & editing (MRI methods).

IN ADDITION: IN PREPARATION

Supplementary study 3:

Variability and reproducibility in multi-echo T2 relaxometry: Insights from multi-site, multi-session and multi-subject MRI acquisitions

Fischi-Gomez, E.*, Girard, G.*, Koch P.J., Pizzolato, M., **Brügger, J.**, Piredda, G.F., Hilbert, T., Yu, T., Cadic-Melchior, A., Beanato, E., Park, C.H., Morishita, T., Schiavi, S., Daducci, A., Kober, T., Canales-Rodríguez, E.J., Hummel, F.C.[§] & Thiran, J.P.[§] *In preparation.*

Personal contribution: Investigation (data collection), data curation

Supplementary study 4:

Longitudinal evaluation of microcircuits' dynamical properties of the lesioned motor cortex in stroke: towards new readouts of motor deficit and recovery. Cadic-Melchior, A.*, Harquel, S.*, Morishita, T., Fleury, L., Ceroni, M., **Brügger, J.**, Meyer, N., Adolphsen, J., Jagella, C., Vaney, C., Alvarez, V., Ghika, J., Vuadens, P., Léger, B., Turlan, J.L., Mühl, A., Bonvin, C., Van De Ville, D., Koch, P.J., Wessel, M.J. & Hummel, F.C. *In preparation.*

Supplementary study 5:

Longitudinal evaluation of spontaneous and induced brain oscillations in stroke. Harquel, S.* , Cadic-Melchior, A.* , Morishita, T., Fleury, L., Ceroni, M., **Brügger, J.**, Meyer, N., Adolphsen, J., Jagella, C., Vaney, C., Alvarez, V., Ghika, J., Vuadens, P., Léger, B., Turlan, J.L., Mühl, A., Bonvin, C., Van De Ville, D., Koch, P.J., Wessel, M.J. & Hummel, F.C. *In preparation*.

*,^{\$} authors contributed equally

PART I

2.1 Study 1: Acute changes in the coupling strength between brain structure and function following a stroke

Brügger Julia^{1,2}, Koch Philipp Johannes^{1,2,3,4}, Preti Maria Giulia^{5,6}, Park Chang-Hyun^{1,2}, Cadic-Melchior Andéol^{1,2}, Ceroni Martino^{1,2}, Fleury Lisa^{1,2}, Wessel Maximilian Jonas^{1,2,7}, Maceira Elvira Pablo^{1,2}, Popa Traian^{1,2}, Beanato Elena^{1,2}, Nathalie Meyer⁸, Blanke Olaf^{8,9}, Adolphsen Jan¹⁰, Jagella Caroline¹⁰, Constantin Christophe¹¹, Alvarez Vincent¹², Ghika Joseph-André¹², Léger Bertrand¹³, Vuadens Philippe¹³, Turlan Jean-Luc¹³, Mühl Andreas¹³, San Millán Diego¹¹, Bonvin Christophe¹², Van de Ville Dimitri^{5,6}, Hummel Friedhelm Christoph^{1,2,9}

¹ Defitech Chair of Clinical Neuroengineering, Center for Neuroprosthetics and Brain Mind Institute, Swiss Federal Institute of Technology (EPFL), Geneva, Switzerland.

² Defitech Chair of Clinical Neuroengineering, Clinique Romande de Réadaptation, Center for Neuroprosthetics and Brain Mind Institute, Swiss Federal Institute of Technology (EPFL Valais), Sion, Switzerland.

³ Department of Neurology, University of Lübeck, Lübeck, Germany.

⁴ Center of Brain, Behavior and Metabolism (CBBM), University of Lübeck, Lübeck, Germany.

⁵ Medical Image Processing Laboratory, Institute of Bioengineering, Swiss Federal Institute of Technology (EPFL), Geneva, Switzerland.

⁶ Department of Radiology and Medical Informatics, University of Geneva, Geneva, Switzerland.

⁷ Department of Neurology, University Hospital Würzburg, Würzburg, Germany.

⁸ Laboratory of Cognitive Neuroscience, Center for Neuroprosthetics and Brain Mind Institute, Swiss Federal Institute of Technology (EPFL), Geneva, Switzerland.

⁹ Department of Neurology, Geneva University Hospitals, Geneva, Switzerland.

¹⁰ Berner Klinik Montana, Crans-Montana, Switzerland.

¹¹ Department of Radiology, Hôpital du Valais, Sion, Switzerland.

¹² Department of Neurology, Hôpital du Valais, Sion, Switzerland.

¹³ Clinique Romande de Réadaptation, Sion, Switzerland.

2.1.1 Abstract

In MRI-based neuroimaging research, functional (fMRI) and diffusion-weighted MRI (DWI) are widespread, but evaluated largely independently with a lack of knowledge about the link between both. Recent methodological advancements allow to quantify the coupling strength between them through the Structural Decoupling Index (SDI) (Preti & Van De Ville, 2019). Such metric could be of great interest in the understanding of post-stroke brain states. The aim of this study was to determine the influence of a lesion on the structure-function interaction and to contrast it to results obtained from age-matched healthy older adults (HOA). DWI and resting-state fMRI was acquired in 44 stroke patients with motor deficits (65.4 ± 14.4 y) and 33 HOA (62.4 ± 7.6 y). Patients were scanned in the first week after stroke. The SDI was calculated for every participant/patient and for every cortical region defined in the Glasser atlas. In HOA, results indicated a network gradient of SDI (visual << limbic network) consistent with previous findings in healthy young and we showed a significantly higher SDI in the left compared to the right hemisphere (LH/RH) in the somatomotor, dorsal attention, limbic and default mode networks. The same pattern was observed in LH stroke patients. In RH stroke patients, stroke-related effects could be observed in the somatomotor, ventral attention, limbic and default mode networks, suggesting that structure-function coupling is more vulnerable to RH compared to LH stroke. We show that the SDI applied at the level of an individual in HOA shows comparable results in to previous studies where the SDI analysis was performed on group-level. In addition, a stroke in the acute phase impacts on the coupling strength between brain structure and function in several brain networks with a potential importance of lesion site. The present study further confirmed the feasibility of applying SDI on the individual level. A crucial next step will be to see how these findings relate to recovery and the underlying functional and structural neural reorganization, in order to evaluate the potential of SDI as a biomarker to stratify stroke patients.

2.1.2 Introduction

Classical understanding of brain structure and function through Magnetic Resonance Imaging (MRI) were for a long time two separate fields, used to investigate both healthy and pathological brains. Through functional MRI (fMRI) it was possible for the first time to relate activity of brain regions to a specific task (Ogawa et al., 1990), giving a better understanding of the role of these areas and the functioning of the brain as a whole. In this localizationist framework, the goal was thus to relate the activity of brain regions to a specific function. Lately, the field has moved forward towards a more interactive network approach, where a function is related to the interplay between different grey matter areas within a network rather than to the activity in one or several isolated brain regions (Nozais et al., 2021). In this context, *functional connectivity* reflects the statistical dependency between two brain regions and is used to describe the coordinated activity between the latter (Friston, 1994; Nozais et al., 2021). However, a limitation of this method is that it is not possible to draw conclusions about the anatomical connections that underlie this functional connectivity. This is why, in parallel, attempts to re-construct the anatomical backbone of the brain in vivo resulted in the development of diffusion-weighted imaging (DWI) methods, where the diffusion of water molecules along axons is measured and then serves to reconstruct the brain's white matter pathways (i.e. tracts) (Jeurissen et al., 2019; Stejskal & Tanner, 1965). By counting the number of 'connections' (i.e. streamlines) between a pair of cortical and/or subcortical grey matter areas, their connection strength can be established, commonly referred to as *structural connectivity* (Hagmann et al., 2008; Sporns, 2011). This method greatly facilitated the understanding of the brain's in vivo circuits and the mapping of white matter in healthy and pathological populations. However, nothing can be inferred about the function of the tracts that were discovered through DWI.

Functional and structural connectivity are thus highly complementary. Studying only one of the two at a time paints an incomplete picture of the brain about, rendering the need to combine these two modalities (Nozais et al., 2021; Preti & Van De Ville, 2019). The first attempts were based on correlational approaches (Hagmann et al., 2008; Honey et al., 2009), followed by increasingly complex brain computational and communication models (Bassett & Sporns, 2017; Bullmore & Sporns, 2009; Deco et al., 2009, 2011, 2012; Fornito et al., 2013; Ghosh et al., 2008; S. Gu et al., 2015; Honey et al., 2007; Ritter et al., 2013; Sporns, 2010, 2018; Stephan et al., 2009). Recently, a new and more integrative approach was developed, the Structural Decoupling Index (SDI), which focuses on the structural connectivity between gray matter areas at rest (Preti & Van De Ville, 2019) or during a task (Griffa et al., 2022). This nodal metric quantifies the coupling strength between brain structure and function, i.e., the extent to which the function relies on the underlying anatomical backbone in a specific brain area. In healthy young, previous work identified a gradient ranging from high structure-function coupling (i.e., low SDI) in areas involved in lower-level sensory functions (e.g. somatomotor or visual areas) to high structure-function decoupling (i.e., high SDI) in regions involved in higher-level cognitive functions (e.g., memory or emotions) (Preti & Van De Ville, 2019). This finding was supported by other reports of such gradients for functional activity (Margulies et al., 2016), cortical microstructure (Huntenburg et al., 2017), as well as gene expression (Cioli et al., 2014; Hawrylycz et al., 2012). Namely, lower-level areas have been related to faster processing and the expression of genes favoring temporal precision, whereas higher-level areas were characterized by slower processing and the expression of genes supporting slower and rhythmic activation (Cioli et al., 2014). It is believed that the less the brain structure and function are coupled, the less efficient the brain is (Suárez et al., 2020). A higher coupling strength for lower-level sensory areas could thus be useful for fast and reliable reactions to external input, whereas more decoupled areas would be involved in cognitive processes that need to be more flexible and which are less predictable (Preti & Van De Ville, 2019).

An aspect which has not been studied so far is the potential lateralization of the SDI. Given that a number of brain networks are known to be lateralized (e.g., somatomotor (Lubben et al., 2021), limbic (Jamieson et al., 2021; Tippet et al., 2018), ventral attention networks (Barrett et al., 2019; Bartolomeo & Seidel Malkinson, 2019; Bernard et al., 2020)), it could be expected that the SDI follows this pattern.

So far, structure-function coupling has been studied only in the healthy brain and it is unclear how it is impacted by pathology, such as stroke. However, investigating the relationship between structure and function in the stroke population has been suggested as an improvement to current analysis methods, as it could unveil new aspects to post-stroke recovery (Silasi & Murphy, 2014). There is growing evidence suggesting that stroke does not affect just one function, but rather is a veritable network disease (Carrera & Tononi, 2014; Guggisberg et al., 2019), resulting in important network-wide alterations in neural activity (Alstott et al., 2009; Honey & Sporns, 2008). Therefore, one could hypothesize that a stroke would render the brain less efficient and consequently would cause increases in SDI (i.e., higher decoupling) in areas affected directly by the stroke, but, also in areas more distant to the lesion and their related networks, through the respective network effects or diaschisis (Carmichael et al., 2004; Carrera & Tononi, 2014),

In the present work, we investigated structure-function coupling in stroke. For this aim, we first attempted to extend findings from healthy young (Griffa et al., 2022; Preti & Van De Ville, 2019) to the age-matched control group composed of healthy older adults (HOA). Given that previous analyses were done on averaged group functional and structural connectomes, investigating the structure-function coupling in HOA also allowed us to assess the feasibility of computing the SDI based on individual structural and functional connectomes and with shorter resting-state Magnetic Resonance Imaging (MRI) sequences. Based on previous work (Preti & Van De Ville, 2019), we expected high structure-function coupling (i.e., low SDI) in low-level networks such as the somatomotor or visual networks and high decoupling (i.e., high SDI) in higher-level networks, such as the limbic network. Given the known lateralization of the somatomotor (Lubben et al., 2021), limbic (Jamieson et al., 2021; Tippet et al., 2018) and ventral attention networks (Barrett et al., 2019; Bartolomeo & Seidel Malkinson, 2019; Bernard et al., 2020), we also expected to see hemispheric differences in SDI in these networks. Subsequently, studying the SDI within a stroke population and comparing it to a control group offers a unique insight into changes of structure-function interactions within a network following a structural lesion. We thus investigated how a stroke leading to a motor impairment in the acute phase impacts on the SDI within the main brain networks and notably within the somatomotor network. Finally, we compared the SDI of the stroke population to the HOA. Given that the stroke leads to lesioning of the brain tissue, and that the function is lost or cannot rely on the usual anatomical connections, we expected a higher SDI in the ipsi- compared to the contralesional hemisphere. Correspondingly, we expected an increased SDI in the ipsilesional hemisphere compared to HOA, especially in the somatomotor network, since all included patients had a motor deficit of the upper limb at stroke onset.

2.1.3 Methods

2.1.3.1 Participants

Forty-four stroke patients (Age: 65.4 ± 14.4 y, 12 females) were enrolled in the study after being admitted at the Regional Hospital of Sion (HVS), Switzerland. Patients underwent scanning during the first week post-stroke (5.2 ± 2.6 days). Inclusion criteria for the study included being older than 18 years of age, having motor deficits of the upper limb and absence of contraindications for MRI. Exclusion criteria were requests not to be informed in case of incidental findings, inability to provide informed consent, history of seizures, pregnancy, severe neuropsychiatric or medical diseases, regular use of narcotic drugs as well as implanted

medical electronic devices or ferromagnetic metal implants which are not MRI compatible. Patients with either first-ever or recurrent stroke were included in the study. Twenty-one patients had a left-hemispheric (LH) stroke, 23 a right-hemispheric (RH) stroke. Of the patients with LH stroke, 16 were right-handed, 2 left-handed and 3 ambidextrous. Of the RH stroke patients, 19 were right handed, 2 left-handed and 2 were ambidextrous.

The control group comprised 33 participants (Age: 62.4 ± 7.6 , 17 females). The inclusion criteria comprised being older than 50 years old and in good health as well as the absence of contraindication for MRI.

Written informed consent was obtained from each participant following the Declaration of Helsinki and the study was authorized by the local ethical committee (Swissethics approval number 2018-01355 for the patients and 2017-00301 for the control group).

2.1.3.2 Magnetic Resonance Imaging Data Acquisition

Structural, functional and diffusion-weighted MRI data were acquired using a 3T Magnetom Prisma scanner (Siemens, Erlangen, Germany) with a 64-channel head and neck coil. Images were acquired 5 days post stroke on average (± 2.6 days).

Diffusion-weighted images were acquired using pulsed gradient spin echo technique (TR = 5000 ms; TE = 77 ms; slices = 84; field of view = 234 mm; voxel resolution = $1.6 \times 1.6 \times 1.6$ mm; readout bandwidth = 1630 Hz/pixels; 64-channel head coil; SENSE acceleration factor = 3). Seven T2-weighted images without diffusion weighting ($b = 0$ s/mm²) were acquired, including one in opposite phase encoded direction. Further, 101 images with noncollinear diffusion gradient directions distributed equally over the half-sphere covering 5 diffusion gradient strengths were obtained (b -values = [300, 700, 1000, 2000, 3000] s/mm²; shell-samples = [3, 7, 16, 29, 46]). In addition, T1-weighted images were acquired using 3D MPRAGE (TR = 2300 ms; TE = 2.96 ms; flip angle = 9°; slices = 192; voxel size = $1 \times 1 \times 1$ mm, FOV 256 × 256 mm). Finally, resting-state BOLD data (with fixation cross) was acquired using a multi-band echo-planar imaging (EPI) sequence. In total, 385 functional volumes were acquired and every volume comprised 75 axial slices covering the whole brain (in-plane resolution 2 × 2mm; slice thickness 2 mm; no gap, FOV = 224mm, TE = 32ms, TR=1s, flip angle=58°, Accel. Factor slice = 5).

2.1.3.3 Image Analysis

2.1.3.3.1 Lesion segmentation

All the lesion masks were hand-drawn using mrview from MRtrix3 (J.-D. Tournier et al., 2019) and subsequently verified by a neurological clinician.

2.1.3.3.2 Processing of diffusion-weighted images

For the cortical parcellation, the Glasser atlas (180 per hemisphere) (Glasser et al., 2016) was used. The parcellation was performed on the T1 mprage image using Freesurfer (Destrieux et al., 2010; Fischl, 2004, 2012). For stroke patients, the voxels corresponding to the lesion were stamped out and replaced by the mirrored voxels of the contralateral side.

The diffusion-weighted images were preprocessed using, MRtrix3, FSL topup and eddy (Andersson et al., 2003; Andersson & Sotiropoulos, 2016; S. M. Smith et al., 2004; J.-D. Tournier et al., 2019). First, Gibbs ringing artefacts were removed from the data (Kellner et al., 2016; J.-D. Tournier et al., 2019), then motion artefact reduction, as well as field inhomogeneity, susceptibility-induced off-resonance field and eddy currents correction was performed. Multi-shell multi-tissue constrained spherical deconvolution (Jeurissen et al.,

2014) was used to estimate the fibre orientation distributions within each voxel. Whole-brain probabilistic tractography was performed using the second-order integration over fibre orientation distribution (iFOD2) (J.-D. Tournier et al., 2019), initiating 1 million streamlines in all voxels of the white matter. For each dataset, 1 million streamlines were selected with both endpoints in the individual cortical or subcortical mask using the Dipy software package (Garyfallidis et al., 2014). The obtained tractograms were filtered based on underlying white matter fiber densities using SIFT2 (R. E. Smith et al., 2015b). Tissue partial volume estimates were obtained from the T1-weighted image using the FSL Fast (Y. Zhang et al., 2001) and BET (S. M. Smith, 2002) methods. The T1-weighted image was registered to the average b0 image using FSL FLIRT (Jenkinson & Smith, 2001) and FNIRT (Andersson et al., 2010) methods.

For each participant, a structural connectome (SC) was built with 360 pairs of areas obtained through the parcellation. The number of streamlines connecting each pair of areas was normalized by the sum of the size of the two areas.

2.1.3.3.3 Processing of functional images

All preprocessing and statistical analyses were conducted using the SPM12 package (*SPM - Statistical Parametric Mapping*, SPM12) running on Matlab (*MathWorks - MATLAB and Simulink Conferences*, v2019b). Functional images were realigned to the mean functional image. Then, the anatomical image was co-registered to the mean functional image. The anatomical image was segmented into tissue maps based on tissue probability maps of SPM12 (for patients, voxels corresponding to the lesion were not considered). The resulting forward deformation field was used to warp both the anatomical and functional images into MNI space. Finally, the functional images were smoothed using a Gaussian kernel (FWHM = 6mm). The first 10 volumes were discarded so that the fMRI signal achieves steady-state magnetization, resulting in 375 functional volumes.

Using the conn toolbox (Whitfield-Gabrieli & Nieto-Castanon, 2012), voxel fMRI time courses were detrended and nuisance variables were regressed out (6 head motion parameters, average cerebrospinal fluid and white matter signal). Finally, to reduce effects of very low and high frequency physiological noise, a band-pass filter was applied (0.01-0.15Hz). The average time course was then extracted for every ROI of the Glasser parcellation and functional connectomes were computed as Pearson correlation between time courses.

2.1.3.4 Estimation of structure-function coupling

The functional and structural connectomes of every patient were then fed to the SDI pipeline as described in (Preti & Van De Ville, 2019) in order to calculate the coupling strength between brain structure and function (i.e., SDI) for every area in the Glasser atlas and every patient. The SDI is obtained by decomposing the structural connectome into harmonics in the graph frequency domain and by subsequently representing the spatial pattern of functional activation as a weighted linear combination of these structural harmonic components. The functional activity is then filtered into two parts, a low frequency component, which is coupled with the SC, as well as a high frequency component which is decoupled from the SC. Finally, the ratio between these two components represents the SDI of a brain region.

2.1.3.5 Statistical Analysis

Linear mixed effects models were used for statistical analysis. First, we evaluated the variation of the SDI within the 7 yeo networks (Thomas Yeo et al., 2011) in the control group (HOA population), considering the hemisphere side. Using R (R Core Team, 2017) and lme4 (Bates et al., 2014), we performed a linear mixed effects analysis with Network (Visual, Somatomotor, Dorsal attention, Ventral attention, Limbic, Frontoparietal, Default mode) and Hemisphere (Left, Right) as fixed effects (with interaction term). As

random effect, we had intercepts for subjects. Secondly, an analogous model was built for the stroke population, taking into account whether the considered areas were located ipsi- or contralesionally and whether it was a RH or LH stroke. The factor Hemisphere was thus replaced by factors Side (Ipsilesional, Contralesional) and Lesion Site (Left, Right).

Subsequently, in order to directly compare the healthy controls with two sub-groups of the stroke population (i.e., LH stroke and RH stroke), we performed a linear mixed effects analysis of the relationship between the mean SDI and the seven Yeo networks (Thomas Yeo et al., 2011), the group (i.e., HOA vs stroke) as well as the brain hemisphere. Network (Visual, Somatomotor, Dorsal attention, Ventral attention, Limbic, Frontoparietal, Default Mode), Group (Patients, HOA) and Hemisphere (Left, Right) were entered into the model as fixed effects (with interaction term). As random effect, we had intercepts for subjects. Random effects for all linear mixed effects models were added based on a model selection with Bayesian information criterion (BIC). For fixed effects, p-values were obtained by likelihood ratio tests, and degrees of freedom were approximated using the Kenward-Roger method (R Core Team, 2017).

To assess post-hoc differences for significant Network effects, we used Tukey's Honestly Significant Difference (HSD) test. SDI outliers were excluded based on the interquartile range method. For the healthy older adults, 3.3% of the data needed to be discarded and for the stroke patients 3.4%.

2.1.4 Results

2.1.4.1 Healthy older adults

Mixed-effects linear regression on structure-function coupling, with Mean SDI as dependent variable and Hemisphere as well as Network as fixed effects revealed a main effect of Hemisphere ($F(1,11449)=13.76$, $p<0.001$), indicating that the SDI is globally higher in the left compared to the right hemisphere in HOA (**Figure 9A**). We also report a main effect of Network ($F(6,11449)=193.08$, $p<0.001$) (**Figure 9B**). A post hoc Tukey test showed that all networks significantly differed from each other at $p<0.05$, except from the somatomotor and frontoparietal networks as well as the dorsal attention and default mode networks. Hence, we observed the following SDI gradient (from low to high decoupling): 1) Visual network 2) Somatomotor & Frontoparietal networks 3) Dorsal attention & Default mode networks 4) Ventral attention network 5) Limbic network. In addition, there was a significant interaction between the two fixed effects ($F(6,11449)=2.60$, $p=0.016$).

Following the visual inspection of the results, we performed the same mixed effects linear regression for each Network level. Results showed that the SDI was significantly higher in the left compared to the right hemisphere for the somatomotor ($F(1,1632.6)=4.18$, $p=0.041$), dorsal attention ($F(1,1123)=4.66$, $p=0.032$), limbic ($F(1,769.34)=8.86$, $p=0.003$) and default mode network ($F(1,2773.2)=5.17$, $p=0.023$). No hemispheric differences were observed for the visual ($F(1,2121.2)=0.04$, $p=0.836$), ventral attention ($F(1,1413.5)=0.15$, $p=0.698$) and frontoparietal networks ($F(1,1423)=1.52$, $p=0.219$).

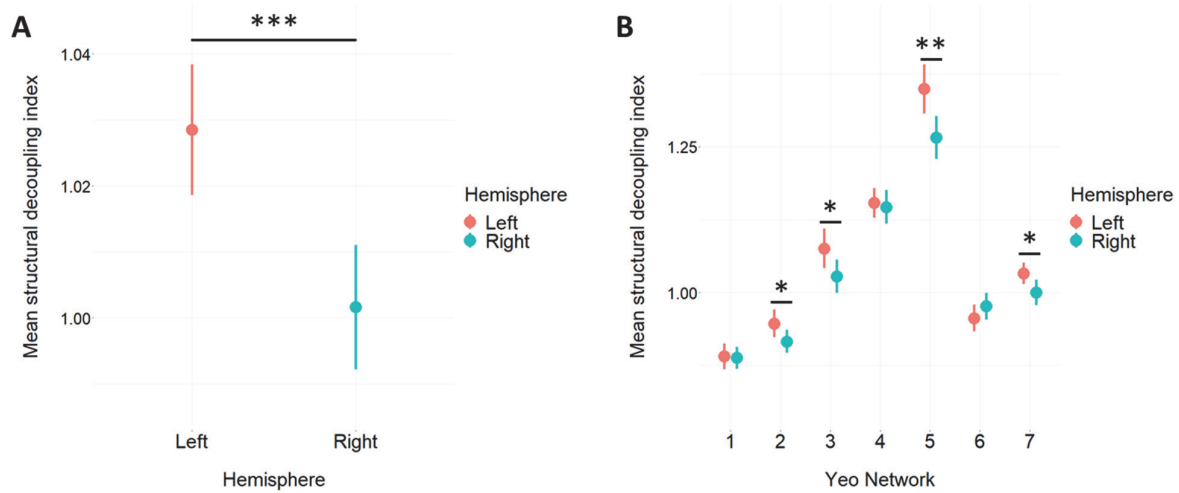


Figure 9. Mean Structural Decoupling Index (SDI) in healthy older adults (HOA).

(A) Mean SDI per hemisphere. The SDI in the left hemisphere was significantly higher in the left compared to the right hemisphere. (B) Mean SDI per Yeo network (1: Visual network, 2: Somatomotor network, 3: Dorsal attention network, 4: Ventral attention network, 5: Limbic network, 6: Frontoparietal network, 7: Default mode network) and hemisphere. A gradient of SDI can be depicted across networks, the visual network having the lowest SDI and the limbic network the highest. SDI of networks were significantly different from each other, except from the somatomotor (2) and frontoparietal (6) as well as the dorsal attention (3) and default mode networks (7). In all plots, error bars show the standard error of the mean (SEM). *: $p < 0.05$, **: $p < 0.01$, ***: $p < 0.001$

2.1.4.2 Stroke patients

In stroke patients, a mixed-effects linear model with Side (Ipsilesional, Contralesional), Network (Visual, Somatomotor, Dorsal attention, Ventral attention, Limbic, Frontoparietal, Default Mode) and Lesion site (Left, Right) as fixed effects and Mean SDI as dependent variable indicated a main effect of Side, with a higher SDI in the ipsi- compared to the contralesional hemisphere ($F(1,15265.3)=4.84$, $p=0.028$) (**Figure 10A**) and Network ($F(6,15265.3)=292.43$, $p < 0.001$) (**Figure 10B**). A post hoc Tukey test showed that all networks significantly differed from each other at $p < 0.05$, except from the dorsal attention and default mode networks. We thus see the following SDI gradient (from low to high decoupling): 1) Visual network 2) Somatomotor network 3) Frontoparietal network 4) Dorsal attention & Default mode networks 5) Ventral attention network 6) Limbic network. Furthermore, Lesion site interacted significantly with Network ($F(6,15265.3)=4.70$, $p < 0.001$). There was no significant main effect of Lesion site ($F(1,15265.3)=0.0034$, $p=0.954$), no two-way interaction between Side and Network ($F(6,15265.3)=0.56$, $p=0.762$) or Side and Lesion site ($F(1,15265.3)=0.45$, $p=0.50$), nor a three-way interaction between Side, Network and Lesion site ($F(6,15265.3)=1.63$, $p=0.13$).

Analogously to the healthy older adults, we performed the same mixed effects linear regression for each Network level. In the visual network, we found a significant interaction between Side and Lesion site ($F(1,2813.33)=5.59$, $p=0.018$) and the SDI was higher in the right hemisphere both for patients with LH ($F(1,1040.4)=5.19$, $p=0.023$) and RH stroke ($F(1,1473.2)=4.92$, $p=0.027$) (**Figure 11A**), however, there were no main effects of Side ($F(1,2813.33)=0.50$, $p=0.480$) and Lesion site ($F(1,44.13)=1.99$, $p=0.165$). For the somatomotor network, we found a main effect of Lesion site (i.e. higher SDI in patients who had a right-hemispheric stroke compared to patients who had a left-hemispheric stroke) ($F(1,44.03)=4.68$, $p=0.036$), a tendency for a main effect of Side ($F(1,2173.35)=2.75$, $p=0.097$) and for an interaction between Side and Lesion site ($F(1,2173.35)=2.53$, $p=0.10$) (**Figure 11B**). For all other networks (dorsal attention, ventral

attention, limbic, frontoparietal and default mode), there were no significant main effects or interactions (for an overview, see Supplementary Table S1).

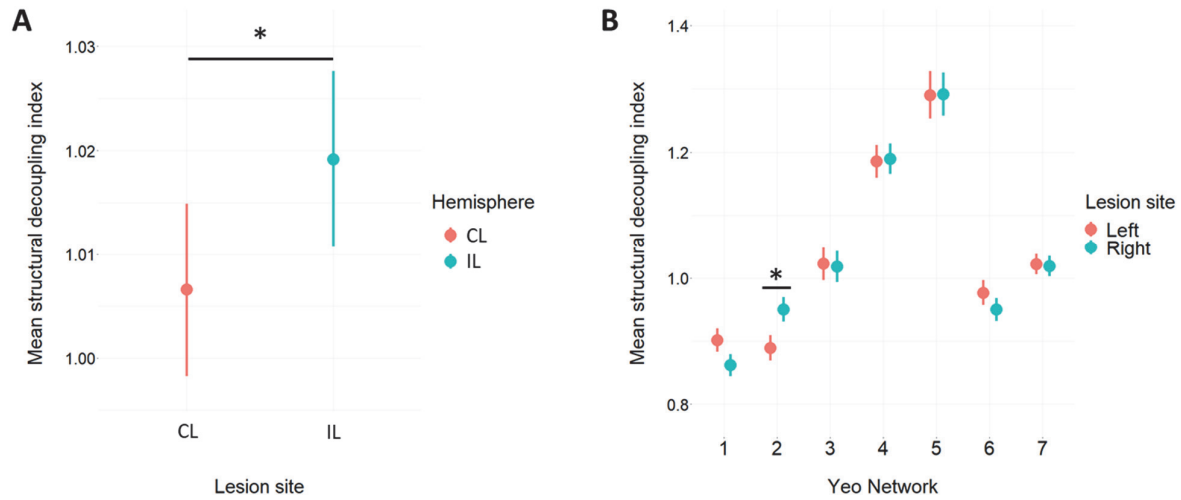


Figure 10. Mean Structural Decoupling Index (SDI) in stroke patients.

(A) Mean SDI per hemisphere. The SDI in the ipsilesional hemisphere was significantly higher compared to the contralesional hemisphere. (B) Mean SDI per Yeo network (1: Visual network, 2: Somatomotor network, 3: Dorsal attention network, 4: Ventral attention network, 5: Limbic network, 6: Frontoparietal network, 7: Default mode network) and lesion site . A gradient of SDI can be depicted across networks, the visual network having the lowest SDI and the limbic network the highest. All networks were significantly different from each other, except from the dorsal attention (3) and default mode networks (7). In all plots, error bars show the standard error of the mean (SEM). *:p<0.05, **:p<0.01, ***:p<0.001

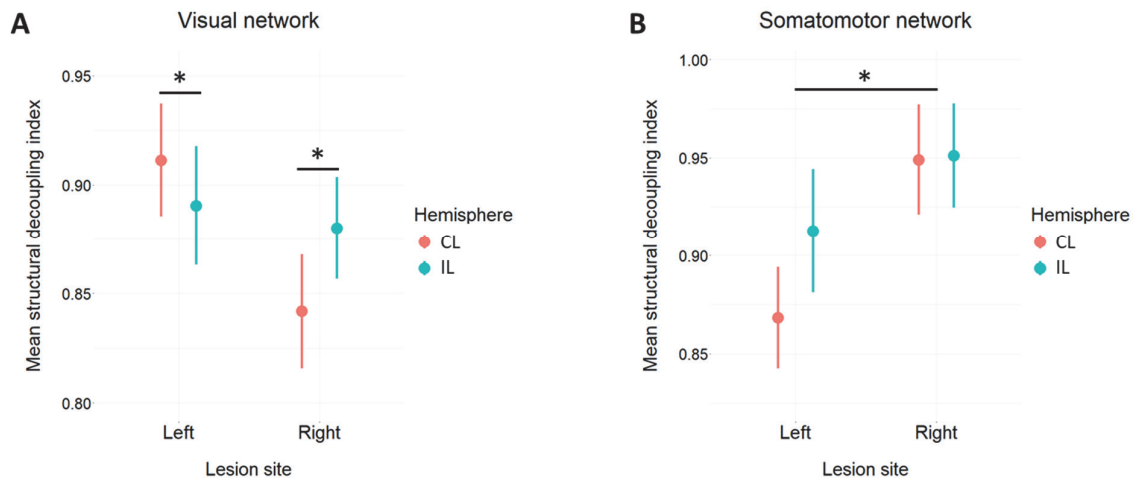


Figure 11. Mean Structural Decoupling Index (SDI) in the visual and somatomotor networks in stroke patients.

(A) Mean SDI per lesion site and hemisphere in the visual network. The SDI was significantly higher in the right hemisphere for both LH and RH stroke. (B) Mean SDI per lesion site and hemisphere in the somatomotor network. The SDI was higher in RH stroke patients compared to LH stroke patients. In all plots, error bars show the standard error of the mean (SEM). *:p<0.05, **:p<0.01, ***:p<0.001

2.1.4.3 Stroke patients vs healthy older adults

Finally, we directly compared stroke patients to healthy older adults by splitting the stroke patients into two groups, namely left-hemispheric stroke and right-hemispheric stroke. The data was analyzed using a mixed-effects linear regression with Group (Healthy older adults, Patients), Hemisphere (Left, Right) and Network (Visual, Somatomotor, Dorsal attention, Ventral attention, Limbic, Frontoparietal, Default Mode) as fixed effects and Mean SDI as dependent variable.

2.1.4.3.1 Left-hemispheric stroke patients vs healthy older adults

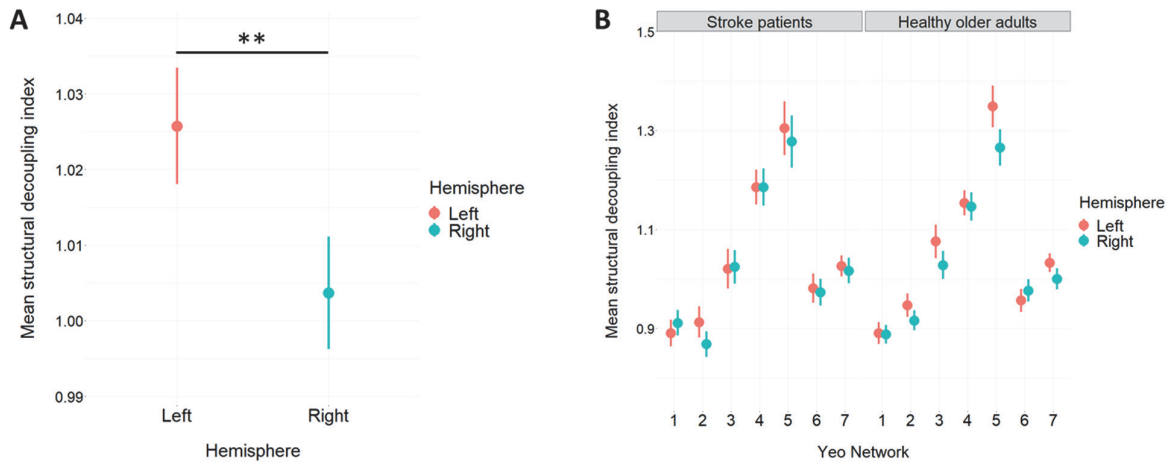


Figure 12. Mean Structural Decoupling Index (SDI) left-hemispheric (LH) stroke patients vs healthy older adults (HOA).

(A) Mean SDI per hemisphere in LH stroke patients and HOA (pooled). The SDI in the left hemisphere is significantly higher compared to the right hemisphere. (B) Mean SDI per Yeo network (1: Visual network, 2: Somatomotor network, 3: Dorsal attention network, 4: Ventral attention network, 5: Limbic network, 6: Frontoparietal network, 7: Default mode network), hemisphere and group. A gradient of SDI can be depicted across networks, the visual network having the lowest SDI and the limbic network the highest. In all plots, error bars show the standard error of the mean (SEM). *: $p < 0.05$, **: $p < 0.01$, ***: $p < 0.001$

The regression revealed a main effect of Network ($F(6,18730.4)=311.85$, $p < 0.001$) (Figure 12B) and Hemisphere ($F(1,18730.3)=9.84$, $p=0.002$), with a higher SDI in the left, compared to the right hemisphere (Figure 12A). There were also a significant two-way interactions between Network and Hemisphere ($F(6,18730.4)=2.29$, $p=0.032$) as well as between Network and Group ($F(6,18730.4)=3.26$, $p=0.003$). There was no main effect of Group ($F(1,56.4)=0.06$, $p=0.82$), no interaction between Group and Hemisphere ($F(1,18730.3)=2.24$, $p=0.135$), nor between Network, Group and Hemisphere ($F(6,18730.4)=0.96$, $p=0.448$). On network-level, we observed a main effect of Hemisphere for the somatomotor ($F(1,2673.12)=9.47$, $p=0.002$) and limbic networks ($F(1,1258.25)=6.31$, $p=0.012$), with a higher SDI in the left hemisphere. There was no main effect of Group for either of the networks (somatomotor: $F(1,54.09)=2.73$, $p=0.104$; limbic: $F(1,54.42)=0.192$, $p=0.662$) nor interaction between the fixed effects (somatomotor: $F(1,2673.12)=0.32$, $p=0.571$; limbic: $F(1,1258.25)=1.34$, $p=0.25$). There were no other network effects or network-specific differences between groups (for an overview, see Supplementary Table S2).

2.1.4.3.2 Right-hemispheric stroke patients vs healthy older adults

There was a significant main effect of Network ($F(6,19433.32)=346.32$, $p < 0.001$) (**Figure 13B**), as well as two-way interactions between Network and Group ($F(6,19433.4)=3.72$, $p=0.001$) (**Figure 13A**), Network and Hemisphere ($F(6,19433.4)=2.50$, $p=0.02$), as well as between Group and Hemisphere ($F(1,19433.4)=15.88$, $p < 0.001$). We observed no main effects of Group ($F(1,58.7)=0.11$, $p=0.75$) or Hemisphere ($F(1,19433.4)=0.65$, $p=0.421$), nor was there a three-way interaction between Network, Group and Hemisphere ($F(6,19433.4)=1.04$, $p=0.394$).

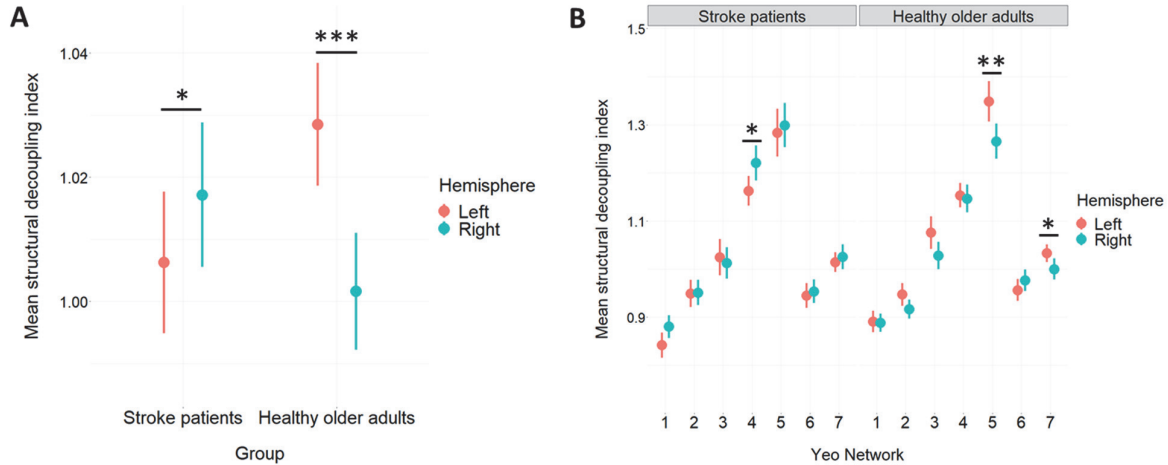


Figure 13. Mean Structural Decoupling Index (SDI) right-hemispheric (RH) stroke patients vs healthy older adults (HOA).

(A) Mean SDI per group and hemisphere. The SDI is significantly higher in the ipsilesional (i.e., right) hemisphere for stroke patients and significantly higher in the left hemisphere for healthy controls. (B) Mean SDI per Yeo network (1: Visual network, 2: Somatomotor network, 3: Dorsal attention network, 4: Ventral attention network, 5: Limbic network, 6: Frontoparietal network, 7: Default mode network), hemisphere (left = red, right = green) and group. A gradient of SDI can be depicted across networks, the visual network having the lowest SDI and the limbic network the highest. In all plots, error bars show the standard error of the mean (SEM). *: $p < 0.05$, **: $p < 0.01$, ***: $p < 0.001$

Subsequently, we ran a separate analysis for each Network. For the ventral attention network (**Figure 14A**), results revealed an interaction between Group and Hemisphere ($F(1,2400.01)=4.68$, $p=0.031$), showing that the SDI was higher in the right compared to the left hemisphere for RH stroke patients ($F(1,986.3)=5.97$, $p=0.015$), a difference which was absent in healthy controls ($F(1,1413.5)=0.151$, $p=0.698$). There were tendencies for a main effect of Group ($F(1,56.45)=2.83$, $p=0.098$) and of Hemisphere ($F(1,2400.01)=2.80$, $p=0.094$). In the limbic network (**Figure 14B**), there was also an interaction between Group and Hemisphere ($F(1,1312.44)=5.22$, $p=0.022$), but , there was no hemispheric difference for stroke patients ($F(1,543.33)=0.23$, $p=0.630$), whereas the SDI was higher in the left compared to the right hemisphere for healthy older adults ($F(1,769.34)=8.86$, $p=0.003$). There were no main effects of Group ($F(1,56.65)=0.26$, $p=0.614$) or Hemisphere ($F(1,1312.44)=2.40$, $p=0.121$). Analogously to the limbic network, the default mode network shows an interaction between Group and Hemisphere ($F(1,4706.6)=3.93$, $p=0.047$), with a hemispheric difference for healthy

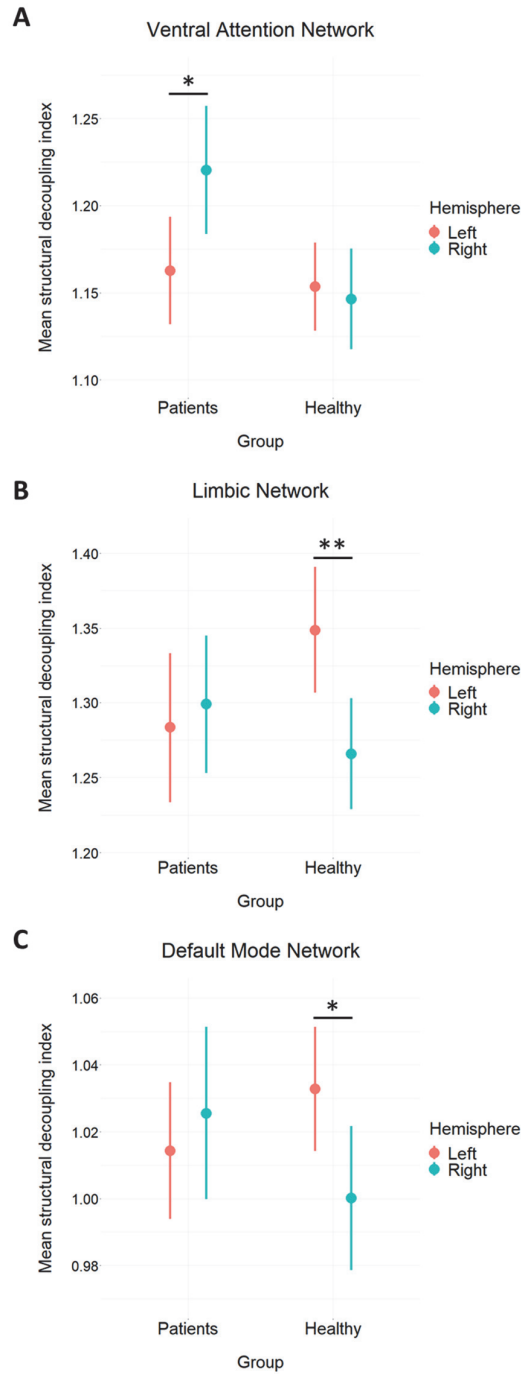


Figure 14. Mean Structural Decoupling Index (SDI) in RH stroke patients vs healthy older adults (HOA).

(A) Mean SDI per group and hemisphere in the ventral attention network. The SDI was higher in the right (ipsilesional) compared to the left hemisphere. There was no left-right difference in HOA. (B) Mean SDI per group and hemisphere in the limbic network. The SDI is higher in the left compared to the right hemisphere in healthy controls, a difference which is absent in stroke patients. (C) Mean SDI per group and hemisphere in the default mode network. The SDI is higher in the left hemisphere compared to the right in healthy controls and there is no hemispheric difference in RH stroke patients. In all plots, error bars show the standard error of the mean (SEM). *: $p < 0.05$, **: $p < 0.01$, ***: $p < 0.001$

controls (SDI higher in the left compared to the right hemisphere; $F(1,2773.2)=5.17$, $p=0.023$) which is absent in the patient group ($F(1,1933.3)=0.44$, $p=0.507$) (**Figure 14C**). There were no main effects of Group ($F(1,56.7)=0.03$, $p=0.861$) or Hemisphere ($F(1,4706.6)=0.99$, $p=0.320$). There were no other network effects or network-specific differences between groups (for an overview, see Supplementary Table S3).

2.1.5 Discussion

2.1.5.1 SDI varies between networks in HOA and stroke patients

The present work aimed at investigating for the first time the structure-function coupling in HOA and stroke patients. We expected high coupling for low-level networks and lower coupling for high-level networks. Our results showed that the SDI varied between networks in all our analyses and the effect was robust enough to remain highly significant even following a stroke. Notably, both in HOA and stroke patients, we observed lower decoupling for lower-level sensory networks, such as the visual and somatomotor networks, and higher decoupling in the limbic, ventral, dorsal attention, and default mode networks, consistently with previous results (Preti & Van De Ville, 2019). Surprisingly, the frontoparietal network was not more decoupled than the somatomotor network in HOA. This could arise from age-related changes previously demonstrated in this network (Campbell et al., 2012; Malagurski et al., 2020; Zanchi et al., 2017). A higher SDI is associated with cognitive processes that require more flexibility, therefore a decrease in SDI in this network could be associated to decreased cognitive performances. Namely, age-related functional changes in the frontoparietal network have been associated with a decrease in cognitive performance (Campbell et al., 2012; Zanchi et al., 2017). Moreover, as age-related changes have been observed for both structural and functional connectivity (Damoiseaux, 2017). Thus, it is likely that these changes in connectivity are also reflected in changes in structure-function coupling. Therefore, future work will need to investigate the effect of ageing on the SDI more closely. Particularly network effects as well as their behavioral relevance should be further studied.

2.1.5.2 Hemispheric lateralization in HOA

Due to the known lateralization of certain brain networks (e.g., somatomotor, limbic, ventral attention networks), we anticipated hemispheric differences in SDI for these networks in HOA. Indeed, we observed a higher SDI in the left (dominant) hemisphere for the somatomotor, dorsal attention, limbic and default mode networks, compared to the right hemisphere. No lateralization was observed for the visual, ventral attention and frontoparietal networks.

Hemispheric left-lateralization in the somatomotor network has been previously related to the hemispheric asymmetry for motor performance (Triggs et al., 1997) and the typical preference for one side of the body over the other, most prominently observed in the handedness (Lubben et al., 2021). For the limbic network, a right-lateralization has been previously shown, especially with regard to the processing of faces (Jamieson et al., 2021; Tippet et al., 2018). The default mode network is known to be rather left-lateralized (Banks et al., 2018; Nielsen et al., 2013). Finally, lateralization of the dorsal attention network has not been reported. As the relationship between the dorsal attention network and aging remains poorly investigated, the lateralization of this network might in fact reflect an adaptation to old age (Nielsen et al., 2013).

In summary, the somatomotor and default mode networks are both left-lateralized and show a higher SDI in the left hemisphere. The limbic network is right-lateralized and the dorsal attention network is not known to be lateralized, however, both display a higher SDI in the left hemisphere. It is thus difficult to generalize SDI patterns based on these results. However, given that the SDI was also overall significantly higher in the left

compared to the right hemisphere in HOA, we hypothesize that this could indicate a “special role” of the left (dominant) hemisphere, as decoupling is thought to facilitate regional and individual specialization of behavior (Z. Gu et al., 2021; Preti & Van De Ville, 2019; Sarwar et al., 2021). This general lateralization is possibly related to the fact that all HOA are right-handed, meaning that the left hemisphere is their dominant one. This effect could be further investigated, e.g., by performing the same experiment in a group of left-handed people.

2.1.5.3 Impact of stroke on structure-function coupling

The stroke population provided us with a unique opportunity to study changes in coupling strength in brain networks following a structural lesion. We hypothesized that, as a consequence of the acute stroke and the structural damage it causes, the function(s) related to the affected area cannot rely on the usual anatomical backbone anymore, resulting in an increase in structure-function decoupling (i.e., higher SDI) in the ipsi- compared to the contralesional hemisphere. Moreover, we also expected a heightened SDI ipsilesionally in the somatomotor network of stroke patients compared to HOA, given that all included patients had a motor deficit at stroke onset. As anticipated, the SDI was generally higher in the ipsi- compared to the contralesional hemisphere. On network level we observed, on one hand, effects independent of lesion site (i.e., the same SDI change occurs, independently of whether the left or right hemisphere is affected by the stroke), such as for the visual network. On the other hand, we observed lesion-site-dependent effects, such as for the somatomotor network, in which the SDI was higher in RH compared to LH stroke patients. Though there was only a trend for an interaction, it could be observed that the pattern of SDI in LH stroke patients resembles that of HOA adults more (SDI left > right hemisphere) than the pattern in RH stroke patients (SDI left = right hemisphere), suggesting that the somatomotor network might be more severely impacted after a RH stroke. This should, however, be corroborated in a larger cohort of patients, as the lack of a significant effect might simply be related to a lack of statistical power.

This lesion site dependency became even more evident in a direct comparison between stroke patients (split in RH and LH stroke groups) and healthy older adults, as network-specific differences between stroke patients and healthy older adults were only present in RH stroke patients. For instance, in the limbic and default mode networks, the higher decoupling between structure and function (higher SDI) in the left compared to the right hemisphere is present equally in healthy older adults and LH stroke patients, but not in RH stroke patients. In addition, there was no hemispheric effect in the ventral attention network in the control group, but a stroke in the RH led to a significant increase in SDI in the ipsilesional hemisphere compared to the contralesional side, causing a hemispheric imbalance.

Overall, based on these findings, the structure-function coupling seems to be more affected by a RH stroke. This indicates a potentially higher vulnerability of the right and higher resilience of the left hemisphere to a structure-function coupling change after stroke in some of the major brain networks, such as the somatomotor, limbic, default mode and ventral attention networks. Previous work has associated RH stroke with poor functional outcome (Kwakkel et al., 2003; Ward, 2017). Hence, a perturbed SDI in RH stroke patients could potentially be related to higher functional impairment. However, this should be assessed in future studies by relating it to behavioral measures which are relevant for the impacted networks.

For example, for the limbic network, the vulnerability of the RH might be explained by previous findings that indicated a high right-lateralization of the limbic network, with regard to the processing of faces and negative emotions, as well as non-verbal communication (Jamieson et al., 2021; Tippet et al., 2018). Indeed, a damage to the right hemisphere has been associated to impairments in emotion identification (Sheppard et al., 2020). Similarly, the ventral attention network is also right-lateralized (Barrett et al., 2019; Bartolomeo & Seidel

Malkinson, 2019; Bernard et al., 2020) and RH stroke is associated with visuospatial neglect due to deficits in ventral attention (Lunven & Bartolomeo, 2017; Rode et al., 2017). Future investigations should more closely address the relationship between changes in SDI in the limbic or ventral attention network following RH stroke and impairments in the processing of emotions and spatial neglect, respectively.

Finally, the somatomotor and default mode networks are known to be rather left-lateralized and changes in SDI related to stroke in the non-dominant hemisphere cannot be fully explained along the same lines. It is nevertheless noteworthy, that three out of the four networks which are altered only in RH stroke patients (somatomotor, limbic and default mode networks) were the same networks that exhibited a left-lateralization in HOA.

In the motor network, previous studies showed an increased motor-related neural activation post-stroke in contralesional primary motor cortex as well as in bilateral premotor areas compared to healthy controls (i.e. a loss of the usual lateralization pattern) (Rehme et al., 2012). Good functional outcome was associated with a return to the recruitment of the original functional network. It is difficult to predict how this changed activation pattern would translate to changes in SDI in the involved areas (primary motor and premotor areas), especially given that a change in SDI does not just depend on how either functional or structural connectivity change, but how one changes with respect to the other. However, one could speculate that a return to the normal state of lateralization, i.e. a higher SDI in the left compared to the right hemisphere in the somatomotor, limbic and default mode networks, would be associated with an improved functional outcome for RH stroke patients, as it has been shown repeatedly for motor function (Boyd et al., 2017; Guggisberg et al., 2019; Hummel et al., 2008; Rehme et al., 2012)

Future studies should investigate i) the role of the hemispheric lateralization in HOA and ii) the effect of the RH-stroke-related changes in above-mentioned networks, especially with regard to lateralization, on the degree of impairment and the individual recovery process of stroke patients.

2.1.5.4 Conclusion and future perspectives

In conclusion, this work shows the existence of a structure-function gradient in HOA similar to healthy young. Additionally, we demonstrate hemispheric coupling differences in specific brain networks, thereby initiating a new line of investigation for network changes related to healthy aging. Finally, we highlight the importance of lesion site for stroke-induced network alterations. This work contributes to a better understanding of the impact a stroke has on the brain and its networks. Our results further suggest that the SDI represents a promising new approach to study the impact of stroke on structure-function coupling in the brain as well as its changes related to reorganization thereafter. In order to further validate the SDI as a potential biomarker for patient stratification, follow-up work should include an in-depth longitudinal analysis of the structure-function coupling during post-stroke recovery and an understanding of the relationship between the SDI and behavior. Ideally, this would be done on individual level. Indeed, the information contained in the “decoupled” portion of the SDI has been shown to distinguish very well among individuals (Griffa et al., 2022). This could eventually help characterize stroke patients and their specific pathological traits (Griffa et al., 2022), thereby paving the way to a more personalized understanding of and treatment for stroke.

Acknowledgements

We thank Silvia Avanzi for her excellent work during the recruitment and organization of timepoints.

Funding

Partially supported by #2017-205 'Personalized Health and Related Technologies (PHRT-205)' of the ETH Domain, Defitech Foundation (Strike-the-Stroke project, Morges, Switzerland), Bertarelli Foundation (Catalyst Deep-MCI-T project), FreeNovation Program of the Novartis Research Foundation and the Wyss Center for Bio and Neuroengineering.

2.1.6 Supplementary Information

Table S1. Mean Structural Decoupling Index (SDI) in stroke patients.

An overview of the ANOVA for the linear mixed-effects regression assessing mean SDI, for timepoint T1. No variables were significant with $p < 0.05$

Network	Variable	Numerator df	Denominator df	F value	p value
Dorsal attention	Side	1	1503.35	0.19	0.65
	Lesion site	1	44.11	0.02	0.88
	Side * Lesion site	1	1503.35	0.06	0.81
Ventral attention	Side	1	1894.14	2.61	0.11
	Lesion site	1	44.17	0.05	0.83
	Side * Lesion site	1	1894.14	2.90	0.09
Limbic	Side	1	1032.57	0.93	0.34
	Lesion site	1	44.25	0.00	0.99
	Side * Lesion site	1	1032.57	0.10	0.76
Frontoparietal	Side	1	1905.34	0.47	0.50
	Lesion site	1	44.29	1.33	0.26
	Side * Lesion site	1	1905.34	0.003	0.96
Default mode	Side	1	3684.5	0.74	0.38
	Lesion site	1	44.7	0.004	0.95
	Side * Lesion site	1	3684.5	0.0042	0.95

PART I

Table S2. Mean Structural Decoupling Index (SDI) left-hemispheric (LH) stroke patients vs healthy older adults (HOA). An overview of the ANOVA for the linear mixed-effects regression assessing mean SDI, for timepoint T1. No variables were significant with $p < 0.05$.

Network	Variable	Numerator df	Denominator df	F value	p value
Visual	Group	1	54.1	0.19	0.66
	Hemisphere	1	3461.4	0.60	0.44
	Group * Hemisphere	1	3461.4	1.07	0.30
Dorsal attention	Group	1	54.85	1.64	0.21
	Hemisphere	1	1836.4	1.60	0.21
	Group * Hemisphere	1	1836.4	2.18	0.14
Ventral attention	Group	1	54.41	1.92	0.17
	Hemisphere	1	2321.38	0.04	0.85
	Group * Hemisphere	1	2321.38	0.08	0.78
Frontoparietal	Group	1	54.62	0.23	0.63
	Hemisphere	1	2338.59	0.21	0.65
	Group * Hemisphere	1	2338.59	1.19	0.28
Default mode	Group	1	54.8	0.07	0.80
	Hemisphere	1	4524.4	3.5	0.06
	Group * Hemisphere	1	4524.4	1.08	0.30

PART I

Table S3. Mean Structural Decoupling Index (SDI) right-hemispheric (RH) stroke patients vs healthy older adults (HOA). An overview of the ANOVA for the linear mixed-effects regression assessing mean SDI, for timepoint T1. No variables were significant with $p < 0.05$.

Network	Variable	Numerator df	Denominator df	F value	p value
Visual	Group	1	56.1	1.70	0.20
	Hemisphere	1	3594.4	2.54	0.11
	Group * Hemisphere	1	3594.4	3.45	0.06
Somatomotor	Group	1	56.16	0.65	0.43
	Hemisphere	1	2765.78	1.60	0.21
	Group * Hemisphere	1	2765.78	1.71	0.19
Dorsal attention	Group	1	56.64	1.75	0.07
	Hemisphere	1	1912.81	3.22	0.29
	Group * Hemisphere	1	1912.81	1.11	0.78
Frontoparietal	Group	1	56.43	0.62	0.44
	Hemisphere	1	2413.68	1.46	0.23
	Group * Hemisphere	1	2413.68	0.18	0.67

2.2 Study 2: Post-stroke structure-function coupling relates to cognitive impairments in the acute and early subacute phase

Brügger Julia^{1,2}, Koch Philipp Johannes^{1,2,3,4}, Fleury Lisa^{1,2}, Preti Maria Giulia^{5,6}, Park Chang-Hyun^{1,2}, Cadic-Melchior Andéol^{1,2}, Ceroni Martino^{1,2}, Wessel Maximilian Jonas^{1,2,7}, Beanato Elena^{1,2}, Nathalie Meyer⁸, Blanke Olaf^{8,9}, Micera Silvestro^{14,15}, Adolphsen Jan¹⁰, Jagella Caroline¹⁰, Constantin Christophe¹¹, Alvarez Vincent¹², Ghika Joseph-André¹², Léger Bertrand¹³, Vuadens Philippe¹³, Turlan Jean-Luc¹³, Mühl Andreas¹³, San Millán Diego¹¹, Bonvin Christophe¹², Van de Ville Dimitri^{5,6}, Hummel Friedhelm Christoph^{1,2,9}

¹ Defitech Chair of Clinical Neuroengineering, Center for Neuroprosthetics and Brain Mind Institute, Swiss Federal Institute of Technology (EPFL), Geneva, Switzerland.

² Defitech Chair of Clinical Neuroengineering, Clinique Romande de Réadaptation, Center for Neuroprosthetics and Brain Mind Institute, Swiss Federal Institute of Technology (EPFL Valais), Sion, Switzerland.

³ Department of Neurology, University of Lübeck, Lübeck, Germany.

⁴ Center of Brain, Behavior and Metabolism (CBBM), University of Lübeck, Lübeck, Germany.

⁵ Medical Image Processing Laboratory, Institute of Bioengineering, Swiss Federal Institute of Technology (EPFL), Geneva, Switzerland.

⁶ Department of Radiology and Medical Informatics, University of Geneva, Geneva, Switzerland.

⁷ Department of Neurology, University Hospital Würzburg, Würzburg, Germany.

⁸ Laboratory of Cognitive Neuroscience, Center for Neuroprosthetics and Brain Mind Institute, Swiss Federal Institute of Technology (EPFL), Geneva, Switzerland.

⁹ Department of Neurology, Geneva University Hospitals, Geneva, Switzerland.

¹⁰ Berner Klinik Montana, Crans-Montana, Switzerland.

¹¹ Department of Radiology, Hôpital du Valais, Sion, Switzerland.

¹² Department of Neurology, Hôpital du Valais, Sion, Switzerland.

¹³ Clinique Romande de Réadaptation, Sion, Switzerland.

¹⁴ Bertarelli Foundation Chair in Translational Neuroengineering, Center for Neuroprosthetics, Institute of Bioengineering, Swiss Federal Institute of Technology (EPFL), Geneva, Switzerland

¹⁵ Translational Neural Engineering Area, The Biorobotics Institute, Scuola Superiore Sant'Anna, Pisa, Italy

2.2.1 Abstract

Stroke is one of the main causes of death and a major source of permanent impairment, frequently of motor origin. However, the clinical picture is very heterogeneous and the understanding of the mechanisms underlying the divergent courses of recovery is still incomplete. Personalization of treatment has been suggested to improve outcome, however it requires efficient biomarkers for patient stratification. Current structural and functional biomarkers based on Magnetic Resonance Imaging (MRI) still lacks clinical application, due to missing large-scale evidence or due to the inability to predict outcomes on an individual basis. This study aimed at achieving a better understanding of post-stroke recovery by studying the structure-function coupling (through the *Structural Decoupling Index*) longitudinally as well as by evaluating its links with functional impairments. Diffusion-Weighted Imaging (DWI) and resting-state functional MRI were acquired in 62 stroke patients with motor deficits (66.4 ± 14.1 y) in the first week after stroke (T1), after three weeks (T2) and three months (T3). The SDI was calculated for every patient, every timepoint and for every cortical region of the Glasser atlas. Behavioral domains consisted of Motor, Language, Memory, Attention, Executive Functions, General Cognitive Screening (MoCA), Anxiety&Depression and Fatigue. Multivariate correlation patterns (PLSC) associating behavior to SDI variability were performed for every timepoint. Results indicated network-specific effects of stroke on SDI at T1 (ventral attention) and T3 (somatomotor and limbic) in right-hemispheric (RH), but not left-hemispheric (LH) stroke patients. Variations in SDI in a number of identified key areas correlated significantly with cognitive and psychological scores (CPS). At T1, the SDI in the frontoparietal and default mode network correlated the most with CPS, whereas at T2 the contribution of each network was more balanced. At both T1 and T2, the SDI in several key motor areas (e.g. primary motor cortex) correlated significantly with CPS, but not with motor performance. This suggests that variability in SDI in key motor areas is behaviorally relevant for cognitive, but not motor functions. Future directions include a longitudinal and individualized assessment of key areas identified in this study and an evaluation of the importance of stroke side to further demonstrate the clinical relevance of SDI.

2.2.2 Introduction

Stroke is one of the leading causes for death and long-term disability world-wide (Katan & Luft, 2018). The most frequent symptoms at stroke onset are upper and/or lower limb motor deficits (80-85%), somatosensory deficits (40-50%), attention deficits or neglect (25-30%) and language deficits or aphasia (20-25%) amongst others (Appelros et al., 2002; Buxbaum et al., 2004; Lawrence et al., 2001; Nys et al., 2007; Ramsey et al., 2017; Rathore et al., 2002; Ringman et al., 2004). Although many patients experience a combination of symptoms, restoration of motor function has become a priority in post-stroke rehabilitation, as motor deficits, in addition to being the most common type, tend to be very debilitating in everyday life and thus cause loss of independence. However, motor recovery is heterogeneous, with two thirds of patients ('fitters' to the proportional motor recovery) showing natural recovery, which represents approximately 70% of the initial deficit, and the remaining third showing very limited to no recovery ('non-fitters') (Prabhakaran et al., 2008). In spite of the heterogeneity of recovery, the current therapies mostly follow a 'one-fits-all' approach and are not adapted to the individual needs of patients. Especially for 'non-fitters', finding optimal treatment strategies remains a significant clinical challenge. Thus, there is a strong need for research oriented towards personalized therapy. However, due to incomplete understanding of the neuronal mechanisms underlying recovery, the predictability of individual recovery and outcomes, as well as patient stratification, remain challenging (Stinear, 2017).

Recently, studies using Magnetic Resonance Imaging (MRI) have shed some light onto the mechanisms underlying post-stroke recovery, mainly by investigating structural white matter changes (through Diffusion-Weighted Imaging (DWI)) and functional grey matter activity (through functional MRI (fMRI)) (Boyd et al., 2017; Grefkes & Fink, 2020; Guggisberg et al., 2019; P. J. Koch & Hummel, 2017). In particular, many studies have described potential biomarkers which could serve as predictors for post-stroke recovery. Notably, the integrity of the corticospinal tract (CST) is among the most commonly researched structural biomarkers which could predict recovery (Stinear, 2017) and also predictions based on the whole-brain structural connectome have shown promising results (P. J. Koch et al., 2021). In addition, measures related to fMRI, such as intra-, interhemispheric connectivity (Fan et al., 2015; Park et al., 2011; Siegel et al., 2016) or task-related activity in M1 (Hannanu et al., 2017; Rehme et al., 2015, for review see previous references) have also provided valuable insights into the prediction of motor recovery. However, the applicability of these biomarkers in clinics remains limited. This is mainly due to lack of large-scale evidence, insufficient prediction accuracy, and the inability to predict outcomes for individual patients, rendering a need for novel and better predictive biomarkers (Boyd et al., 2017).

Above-mentioned biomarkers are all based on either brain structure or function, but it remains unclear whether their relationship could also serve as a predictor for post-stroke recovery. The *Structural Decoupling Index (SDI)* is a new tool which enables to quantify the degree of coupling between structure and function in each grey matter area (Preti & Van De Ville, 2019). The work done in healthy young adults has shown that function closely relies on structure in areas related to low-level sensorimotor functions (e.g., primary somatomotor areas), whereas it is much more detached from its underlying anatomical backbone in areas involved in higher level cognitive functions (e.g., prefrontal cortex) (Preti & Van De Ville, 2019). Our previous work has extended these results from a healthy population to stroke, and demonstrated a higher decoupling in the ipsilesional hemisphere, as well as alterations in hemispheric coupling differences in specific brain networks, namely in the somatomotor, limbic, ventral attention, visual network and default mode networks (Brügger et al., in preparation, see Study 1). In addition, we showed that these changes were observed only in right-, but not left-hemispheric stroke patients. However, despite observing alterations in structure-function coupling following a stroke, its clinical relevance and link to behavior remain unknown. Elucidating

the relationship between structure-function coupling and functional impairments, as well as the evolution of this relationship over time post-stroke, will add to a better understanding of stroke-related deficits and the underlying mechanisms of recovery. In addition, it is a necessary next step in the evaluation of structure-function coupling as a potential future biomarker for post-stroke recovery, before it can be explored for patient stratification.

In order to investigate the potential of structure-function coupling in regard of the above-mentioned points, we addressed two related research questions. (i) We investigated the evolution of structure-function coupling (by using the SDI) in the first 3 months post-stroke. (ii) We evaluated the behavioral relevance of inter-individual differences in coupling after a stroke through multivariate correlation patterns. The evolution of the structure-function coupling over time, as determined here, has not yet been investigated in a stroke population. One might assume that, e.g., the structural disruption caused by the stroke lesion would lead to a higher decoupling between brain structure and function (especially ipsilesionally) in the acute phase, as the function is unable to rely on the underlying structure anymore. This assumption is supported by our previous work, where we showed a higher decoupling in the ipsilesional, compared to the contralesional hemisphere (Brügger et al., in preparation, see Study 1). The evolution of the SDI over time post-stroke could take various courses, and can be influenced by changes in either brain structure or function or through a combination of both. Regarding our second research question, we hypothesized that changes in coupling in areas closely related to the lesion – hence mainly ipsilesionally – would be associated to worse performance in the behavioral domains, and especially in the motor domain, in the acute stage. We expected this pattern to become more spatially distributed over time, with involvement of various areas in both the ipsi- and contralesional hemispheres at the early subacute stage.

2.2.3 Methods

2.2.3.1 Participants

Sixty-two stroke patients (Age: $66.4y \pm 14.1y$, 17 females) were enrolled in the study following admission at the Cantonal Hospital in Sion (HVS), Switzerland. 52 patients were right-handed, 4 were left-handed and 6 were ambidextrous. The patient cohort of this study largely overlaps with the cohort of Brügger et al. (in preparation, see Study 1), as the patients included in Study 1 are also included for Study 2. Patients underwent scanning at three timepoints, hereafter referred to as T1 (first week), T2 (3 weeks) and T3 (3 months). On average, T1 took place 5.1 ± 2.6 days post-stroke, T2 after 25.6 ± 4.5 days and T3 after 97.1 ± 11.9 days. Inclusion criteria for the study included being older than 18 years of age, having motor deficits of the upper limb and absence of contraindications for MRI. Exclusion criteria were requests not to be informed in case of incidental findings, inability to provide informed consent, history of seizures, pregnancy, severe neuropsychiatric or medical diseases, regular use of narcotic drugs, as well as implanted medical electronic devices or ferromagnetic metal implants which are not MRI compatible. Patients with either first-ever or recurrent stroke were included in the study. Thirty-one patients had a left-hemispheric (LH) stroke, thirty-one a right-hemispheric (RH) stroke. A summary of the behavioral deficits of the cohort can be found in **Table 1**. Written informed consent was obtained from each participant following the Declaration of Helsinki and the study was authorized by the local ethical committee (Swissethics approval number 2018-01355).

2.2.3.2 MRI Data Acquisition and Image Analysis

For the analysis of both fMRI and DWI data we used the same preprocessing and processing pipeline as outlined in our previous work Brügger et al. (in preparation, see Study 1). The resulting individual structural

and functional connectomes had 360 regions of interests (ROIs) (Glasser et al., 2016). For post-hoc analyses, each ROI was attributed to one of the 7 Yeo networks (Thomas Yeo et al., 2011) through majority voting.

Table 1. Behavioral impairments at T1

Average impairment taking into account all included sub-scores (see Table 2).

Behavioral domain	Percentage of patients who have an impairment at T1
Motor	100%
Language	19%
Memory	19.9%
Attention	35.9%
Executive functions	31.9%
General cognitive screening	79.4%
Anxiety & Depression	18.5%
Fatigue	28%

2.2.3.3 Structure-function coupling

In an equivalent manner detailed in our previous work (Brügger et al., in preparation, see Study 1), to determine structure-function coupling for every ROI of the Glasser parcellation (180 areas per hemisphere) (Glasser et al., 2016), we applied the Structural Decoupling Index (SDI) pipeline described in (Preti & Van De Ville, 2019). In brief, to obtain the SDI, the functional signals at each point in time are first decomposed onto the underlying structural backbone and subsequently filtered into low-frequency (coupled) and high-frequency (decoupled) portions. The SDI is the ratio of the decoupled and the coupled portion in every ROI. We used the individual structural and functional connectomes for each patient and timepoint, as described in Brügger et al. (in preparation).

2.2.3.4 Longitudinal effects of stroke on structure-function coupling

To assess the longitudinal effects related to structure-function coupling between the acute and early subacute phase, we ran two separate mixed-effects linear regressions – comparing the acute (T1) with different levels of subacute stages (T2/T3). For completeness, we also assessed changes between T2 and T3, which yielded no significant differences (Table S4). Both regressions contained Mean SDI as dependent variable and Hemisphere (Ipsilesional (IL), Contralesional (CL)), Lesion side (Left, Right), Network (Visual, Somatomotor, Dorsal attention, Ventral attention, Limbic, Frontoparietal, Default Mode), and Timepoint (T1 and T2 for the first model; T1 and T3 for the second model) as fixed effects. Random effects for all linear mixed effects models were added based on a model selection with Bayesian information criterion (BIC). For fixed effects, p-values were obtained by likelihood ratio tests, and degrees of freedom were approximated using the Kenward-Roger method (R Core Team, 2017). To assess post-hoc differences for significant Network effects, we used Tukey's Honestly Significant Difference (HSD) test. Outliers were excluded based on the interquartile range, which concerned 3.4% of datapoints.

2.2.3.5 Behavioral data

In the context of this study, we acquired motor and neuropsychological data spanning all cognitive domains at each of the three timepoints. Indeed, the behavioral data was divided in 8 domains: Motor, Language, Memory, Attention, Executive functions, MoCA, Anxiety & Depression and Fatigue. A list of tests and sub-scores included in each behavioral domain can be found in **Table 2**. For all motor scores, the ratio between the score related to the affected and the unaffected side was used. In order to have the same interpretation for the 9 Hole Peg Test as for the others contained in the motor domain (i.e., higher score corresponds to

PART I

better performance), we subtracted the raw score from the maximum score (i.e., 180). Whenever more than one score was available per domain, we applied Principal Component Analysis (PCA) and used the projection onto the first component as behavioral score for the domain.

Table 2. List of behavioral tests and sub-scores for all behavioral domains.

Domain	Test	Sub-score used
<i>Motor</i>	Fugl-Meyer Upper Limb (Fugl-Meyer, 1980)	Total score
	Pinch & Grip (Mathiowetz et al., 1984)	Pinch
		Fist
		Key
	Medical Research Council muscle strength testing (MRC) (Ciesla et al., 2011; Montgomery et al., 2007)	Total
	Nine-Hole Peg Test (9HPT) (Mathiowetz et al., 1985)	Total
<i>Language</i>	Phonological verbal fluency (Godefroy et al., 2012)	Final score
	Semantic verbal fluency (Godefroy et al., 2012)	Final score
<i>Memory</i>	Digit span (Wechsler, 2008)	Forward span score
	Corsi-Kessels (Kessels et al., 2000)	Forward span score
	Consortium to Establish a Registry for Alzheimer's Disease (CERAD) (Morris et al., 1989)	Delayed copy recall total
<i>Attention</i>	Test of Attention Performance (TAP) (Zimmermann & Fimm, 2002)	Alert with warning Reaction Time (RT)
		Alert without warning RT
		Divided attention (single condition: visual) RT
		Divided attention (single condition: auditive) RT
		Divided attention (both conditions) - total omissions
		Divided attention (both conditions) - total errors
	Bells cancellation test (Gauthier et al., 1989)	Total omissions
		Time
	Color Trail Test (D'Elia et al., 1996)	Subtest A - time
		Subtest B - time
<i>Executive functions</i>	Digit span (Wechsler, 2008)	Backward span score
		Sequencing span score
	Bimanual coordination (Dolivo & Assal, 1985)	Total
	Consortium to Establish a Registry for Alzheimer's Disease (CERAD) (Morris et al., 1989)	Copy total – score
<i>MoCA</i>	Montreal Cognitive Assessment (MoCA) (Nasreddine et al., 2005)	Total score
<i>Depression & Anxiety</i>	Hospital Anxiety and Depression Scale (HADS) (Snaith, 2003)	Depression total score
	State/Trait Anxiety Inventory for adults (STAI) (Spielberger, 1983, 2010)	Anxiety trait total score
	Fear And Stress scale (FAS) (Sandi, 2013)	Total
<i>Fatigue</i>	Multidimensional Fatigue Inventory (MFI) (Smets et al., 1995)	Physical
		Motivation
		General
		Activities
		Mental

2.2.3.6 Multivariate brain-behavior correlation patterns

We used Partial Least Square Correlation (PLSC) analyses (Krishnan et al., 2011; McIntosh et al., 1996) to identify multivariate correlation patterns between patient-specific nodal SDI measures and the eight behavioral domains mentioned in 2.2.3.5. Given that patients needed to have all sub-scores to be included for a given timepoint, due to the inability of PCA to deal with missing values, out of the 62 patients included in the study, we could only include 32 patients for T1, 34 patients for T2 and 31 patients for T3 for the PLSC analysis. PLSC identifies linear combinations of SDI measures that maximally covary with linear combinations of behavioral scores (Griffa et al., 2022; Krishnan et al., 2011). Here, hemispheres were flipped for patients with a RH stroke, so that all lesions were located on the left side of the brain in order to allow for a comparison between the ipsi- and contralesional side. For the analysis, we used the pipeline provided in (Griffa et al., 2022) and outputs include: 8 sets of brain-behavior saliences, which correspond to the left and right singular vectors of the data covariance matrix; 8 sets of singular values, which represent the explained covariance; as well as 8 pairs of behavioral and brain latent scores, which are the data projections onto the behavioral and brain saliences.

The statistical significance of each multivariate correlation pattern was evaluated with permutation testing (1000 permutations) (McIntosh et al., 2004; McIntosh & Lobaugh, 2004). For significant multivariate correlation patterns, the reliability of corresponding nonzero behavioral and brain saliences was assessed through a bootstrapping procedure (1000 random samples) (Efron & Tibshirani, 1986; McIntosh et al., 2004) and the construction of standard scores based on the bootstrap distributions. Values of an absolute standard score >2 were considered reliable (Krishnan et al., 2011). Finally, the amount of variance explained by the multivariate correlation pattern was obtained through R-squared (squared Pearson's correlation) between the brain and behavioral latent scores.

2.2.4 Results

2.2.4.1 Longitudinal effects on the Structural decoupling index (SDI)

Between T1 and T2, mixed-effects linear regressions with mean SDI as dependent variable showed no main effect of Timepoint ($F(1,14003.4)=0.07$, $p=0.796$) nor was there a significant interaction between Timepoint and any of the other fixed effects (for an overview, see Supplementary Table S5).

When comparing T1 with T3 with an analogous mixed-effects linear regression, again, we did not observe a main effect of Timepoint ($F(1,10389)=0.016$, $p=0.90$). However, Timepoint interacted with Lesion side ($F(1,10389)=4.80$, $p=0.0285$) and we observed a main effect of Network ($F(6,29505)=527.64$, $p < 0.001$). A post hoc Tukey test revealed differences in SDI between some of the networks at $p < 0.05$, and thus the following SDI gradient (from low to high decoupling): 1) Visual, Somatomotor & Frontoparietal networks 2) Dorsolateral & Default Mode networks 3) Ventral attention & Limbic networks. The networks within each of the three "gradient groups" are not significantly different from each other. Network also significantly interacted with Lesion side ($F(6,29505)=7.12$, $p < 0.001$) as well as with Lesion side and Hemisphere in a three-way interaction ($F(6,29505)=3.60$, $p=0.001$). No other main effects or interactions were significant (Supplementary Table S6). To further investigate the nature of interactions with the Network variable, we ran equivalent mixed-effects regressions for each timepoint (section 4.1.1) and for each lesion side (section 4.1.2).

2.2.4.1.1 SDI at individual timepoints

Acute phase (T1)

For T1, we observed a significant effect of Hemisphere ($F(1,17327.4)=6.16$, $p=0.013$), with a higher SDI in the IL compared to the CL hemisphere, as well as a significant effect of Network ($F(6,17327.3)=310.57$, $p<0.001$), with the same SDI gradient as previously shown in (Brügger et al., in preparation, see Study 1). In addition, the analysis revealed a significant two-way interaction between Network and Lesion side ($F(6,17327.3)=3.88$, $p<0.001$) as well as a strong trend for a three-way interaction between Network, Hemisphere and Lesion side ($F(6,17327.3)=2.07$, $p=0.054$). The remaining main effect of Lesion side ($F(1,17327.3)=0.0007$, $p=0.978$) as well as the two-way interactions between Network and Hemisphere ($F(6,17327)=0.55$, $p=0.767$) and between Hemisphere and Lesion side ($F(1,17327)=0.36$, $p=0.55$) did not reach significance. To investigate the nature of the significant interactions involving the Network variable, we performed equivalent mixed effects linear regression for each Network level.

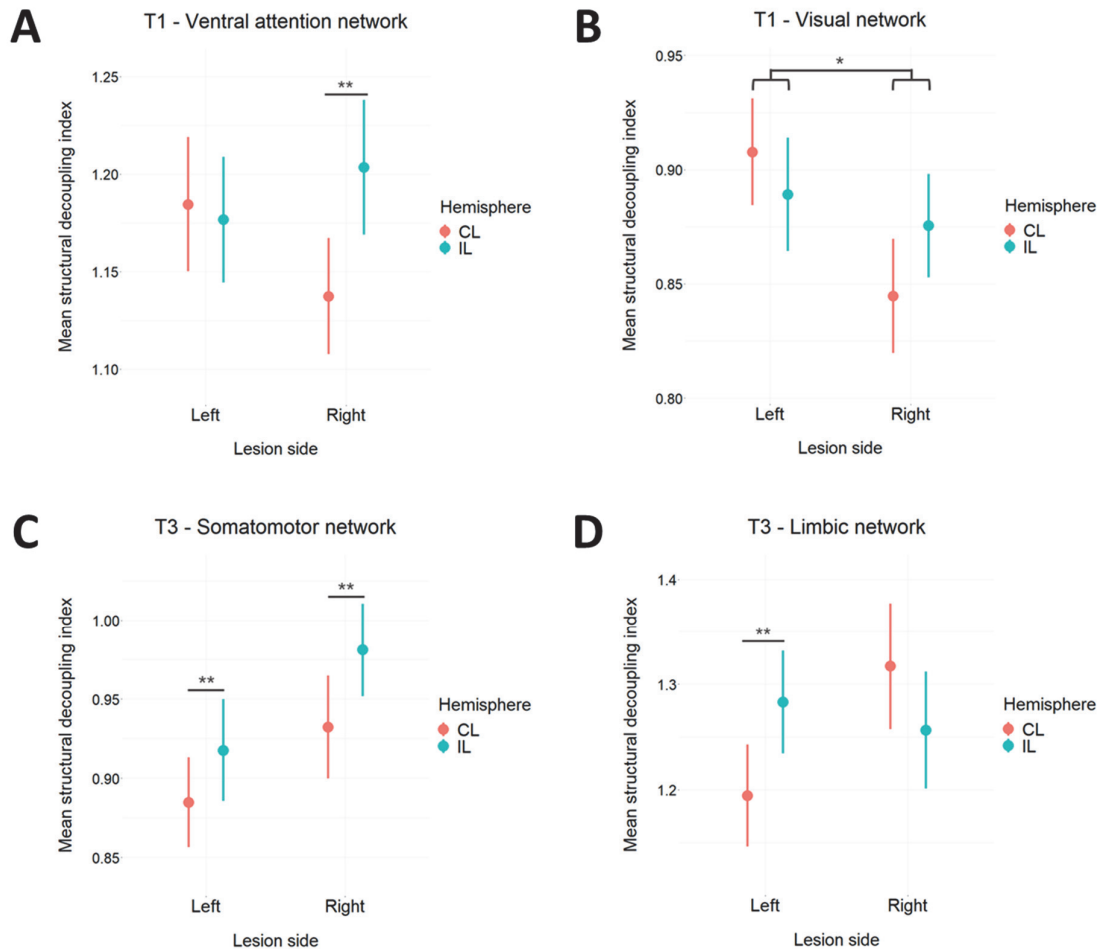


Figure 15. Mean SDI at T1 and T3.

Mean SDI in left- (LH) ($N=31$) and right-hemispheric (RH) ($N=31$) stroke patients for significant networks in timepoints T1 (A, B) and T3 (C, D). The SDI in the ipsilesional hemisphere (IL) is depicted in cyan and the SDI in the contralesional hemisphere (CL) in coral. A) Ventral attention network at T1. While there was no difference between RH and LH stroke patients, only in RH patients the SDI is higher in IL compared to CL. B) Visual network at T1. Lesion side significantly interacts with Hemisphere, the opposite pattern is observed between sub-groups. C) Somatomotor network at T3. The SDI is higher in IL compared to CL, both in LH and RH patients. D) Limbic network at T3. Mean SDI is higher in IL compared to the CL, but only in LH patients. *: $p < 0.05$, **: $p < 0.01$

In the ventral attention network (**Figure 15A**), the regression revealed a significant interaction between Hemisphere and Lesion Side ($F(1,2154.12)=5.42$, $p=0.019$), but no main effects (Hemisphere: $F(1,2154.12)=3.12$, $p=0.078$; Lesion side: $F(1,50.21)=0.12$, $p=0.729$). Post-hoc analysis of the interaction showed a significantly higher SDI in the IL compared to the CL hemisphere for RH stroke patients only ($F(1,1068.2)=8.70$, $p=0.003$), with no hemispheric differences for LH stroke patients ($F(1,1085.9)=0.15$, $p=0.695$).

For the visual network (**Figure 15B**), we similarly found a significant interaction between Hemisphere and Lesion side ($F(1,3197.2)=4.44$, $p=0.035$). However, post-hoc analysis revealed no significant hemispheric differences in either LH or RH stroke patients (RH stroke patients: $F(1,1598)=3.42$, $p=0.065$; LH stroke patients: $F(1,1599.2)=1.27$, $p=0.26$). As for the ventral attention network, no main effects were significant (Hemisphere: $F(1,3197.2)=0.26$, $p=0.607$; Lesion side: $F(1,50)=1.98$, $p=0.166$).

For the remaining investigated networks (i.e., somatomotor, dorsal attention, limbic, frontoparietal and default mode networks) no main effects nor interactions were significant (for an overview, see Supplementary Table S7).

Late subacute phase (T3)

At T3, we observed a significant main effect of Network ($F(6,12154.5)=235.07$, $p<0.001$), as well as significant two-way interactions between Hemisphere and Network ($F(6,12154.3)=2.70$, $p=0.013$), and Network and Lesion side ($F(6,12154.5)=3.82$, $p<0.001$). A post hoc Tukey test for Network variable revealed significant differences in SDI between some of the networks at $p<0.05$ and therefore the following network gradient can be observed (from low to high decoupling): 1) Visual & Somatomotor networks 2) Dorsolateral & Frontoparietal & Default Mode networks 3) Ventral attention & Limbic networks. The networks within each of the three “gradient groups” are not significantly different from each other.

In addition, there was also a significant three-way interaction between Hemisphere, Network and Lesion side ($F(6,12154.3)=2.80$, $p=0.010$). However, there were no hemispheric differences ($F(1,12154.2)=0.001$, $p=0.967$), nor differences in SDI between LH and RH stroke patients ($F(1,37.6)=0.67$, $p=0.417$) overall in the brain. Finally, there was also no interaction between Hemisphere and Lesion side ($F(1,12154.2)=0.04$, $p=0.847$). Subsequently, given the presence of significant interactions with Network, we performed the same mixed effects linear regression for each Network level.

For the somatomotor network (**Figure 15C**), we found a main effect of Hemisphere ($F(1,1739.28)=7.02$, $p=0.008$), with a higher SDI in the IL compared to the CL side in addition to a tendency for a difference in SDI between LH and RH stroke patients ($F(1,34.95)=3.97$, $p=0.054$), suggesting a higher SDI in RH stroke patients. There was no interaction between Hemisphere and Lesion side ($F(1,1739.28)=0.23$, $p=0.628$).

In the limbic network (**Figure 15D**), the regression revealed a significant interaction between Hemisphere and Lesion side ($F(1,815.88)=8.24$, $p=0.004$), but no significant main effects (Hemisphere: $F(1,815.88)=0.29$, $p=0.592$; Lesion side: $F(35.33)=1.59$, $p=0.216$). Post-hoc testing indicated a higher ipsilesional (i.e., left-hemispheric) SDI in LH stroke patients ($F(1,443.4)=6.88$, $p=0.009$), whereas there was no significant hemispheric difference in RH stroke patients ($F(1,372.49)=2.30$, $p=0.130$).

There were no significant main effects or interactions in the remaining networks (i.e., visual, dorsal attention, ventral attention, frontoparietal and default mode networks) (Supplementary Table S8).

In summary (**Table 3**), we observed distinct network effects at T1 and T3. At T1, the SDI was higher in the ipsi- compared to the contralesional hemisphere on whole-brain level. More precisely, in the ventral

attention network, this hemispheric difference was present only in RH stroke patients. The same pattern could be observed for the visual network, however, only with a trend towards significance. Contrary to T1, at T3 there was no overall difference in SDI between the ipsi- and contralateral hemisphere (whole-brain), however, in the somatomotor network, the SDI was higher ipsi- compared to contralesionally. Finally, in the limbic network at T3, the same pattern could be observed in LH, but not in RH stroke patients. For completeness, all effects were compared to those observed in the control population (i.e., healthy older adults) reported in (Brügger et al., in preparation, see Study 1).

Table 3. Summary of cross-sectional effects on SDI at each timepoint.

T1 = Timepoint 1; T3 = Timepoint 3; LH = left-hemispheric stroke patients; RH = right-hemispheric stroke patients; IL = Structural Decoupling Index (SDI) in the ipsilesional hemisphere; CL = SDI in the contralesional hemisphere.

<i>Timepoint (T)</i>	<i>Population</i>	<i>Network</i>	<i>Hemispheric comparison</i>	<i>Effect similar to control group as reported in Brügger et al. (in preparation, see Study 1)</i>
<i>T1</i>	LH	Visual	IL = CL	Yes
	RH	Visual	IL > CL (trend only)	No
	LH	Ventral attention	IL = CL	Yes
	RH	Ventral attention	IL > CL	No
<i>T3</i>	RH + LH	Somatomotor	IL > CL	Yes for LH
	LH	Limbic	IL > CL	Yes
	RH	Limbic	IL = CL	No

2.2.4.1.2 Left-hemispheric vs. right-hemispheric stroke patients

Based on our previous work (Brügger et al., in preparation, see Study 1) where we showed that stroke differently impacted LH and RH stroke patients, and given that here we observed significant interactions with Lesion side variable (see above), we ran a separate linear mixed effects analysis for each of the two lesion sides (LH and RH).

LH stroke patients

In LH stroke patients, results show a main effect of Network ($F(6,15289)=264.52$, $p<0.001$) as well as an interaction between Hemisphere and Network ($F(6,15289.8)=4.10$, $p<0.001$). Through post-hoc analysis (Tukey) we identified differences between some of the networks at $p<0.05$ and we thus observe the following network gradient (from low to high decoupling, networks do not differ from each other within groups): 1) Visual, Somatomotor & Frontoparietal networks 2) Dorsolateral & Default Mode networks 3) Ventral attention & Limbic networks.

There were no changes over timepoints ($F(1,5548.2)=2.28$, $p=0.131$), and also no other significant main effects or interactions (see Table S9). Given the significant interaction between Hemisphere and Network, we subsequently ran a separate analysis for each network. We observed a significant hemispheric difference in the somatomotor (IL > CL, $F(1,2190.0)=7.48$, $p=0.006$) (**Figure 16A**), ventral attention (CL > IL, $F(1,1925.52)=5.58$, $p=0.018$) (**Figure 16B**), and limbic (IL > CL, $F(1,1033.81)=6.41$, $p=0.012$) networks (**Figure 16C**). These effects were independent of timepoint. In addition, a higher contralesional SDI was observed in

the frontoparietal network (**Figure 16D**), however only at T3 (Interaction Hemisphere and Timepoint: $F(1,1899.56)=5.75$, $p=0.012$; Post-hoc: Main effect of Hemisphere: T1 – $F(1,1089.2)=0.37$, $p=0.542$), T3 – $F(1,810.15)=7.72$, $p=0.006$). We found no significant main effects or interactions for the visual, dorsal attention and default mode networks (see Supplementary Table S10 for details). An overview of the LH effects is given in **Table 4**, together with their comparison with the effects observed in the control group in our previous work (Brügger et al., in preparation, see Study 1).

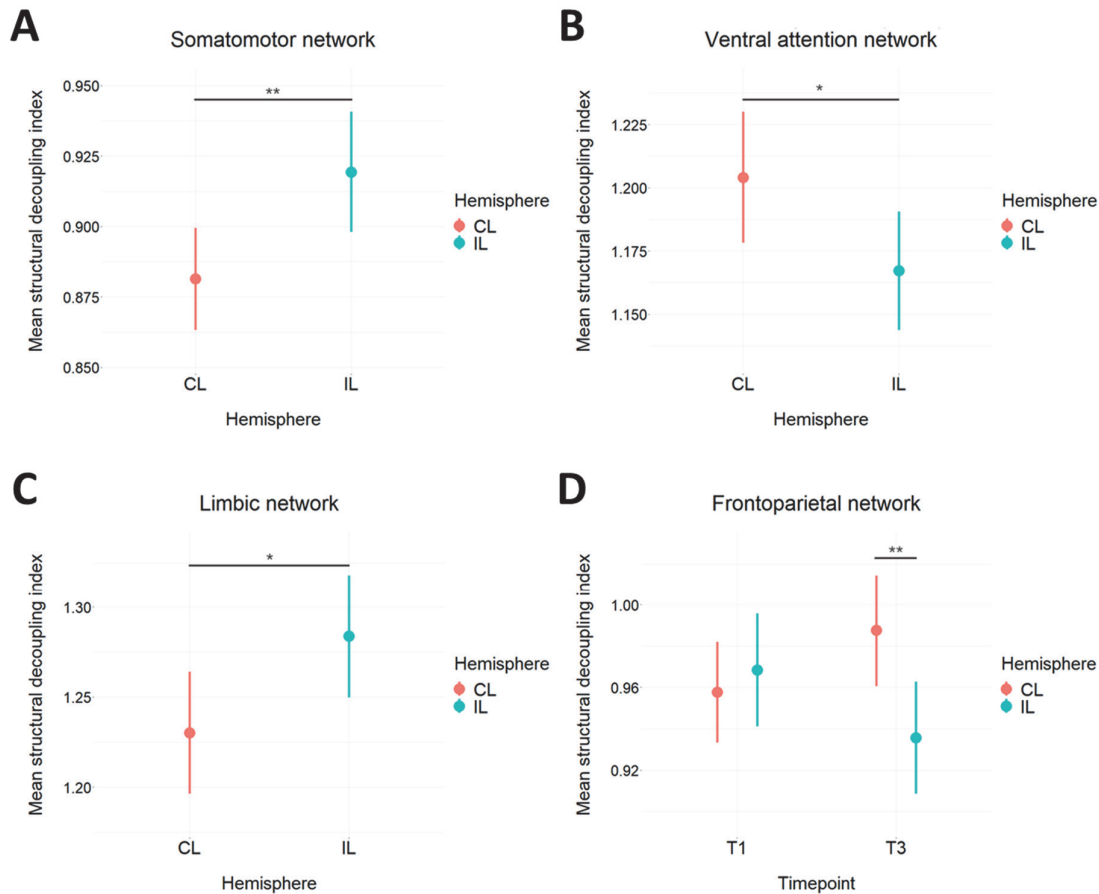


Figure 16. Mean SDI in left-hemispheric stroke patients.

Mean SDI in the ipsi- (IL) and contralesional (CL) hemispheres of left-hemispheric (LH) stroke patients. SDI was higher in IL compared to CL in somatomotor (A) and limbic (C) networks, whereas the opposite pattern was observed in ventral attention (B) and Frontoparietal network at T3 (D). *: $p<0.05$; **: $p<0.01$

RH stroke patients

In RH stroke patients, we found no significant main effects or interactions except from a significant main effect of Network ($F(6,14182.8)=270.05$, $p<0.001$) (Supplementary Table S11). Post-hoc analysis of Network (using Tukey) identified a more segregated gradient between the networks than for LH stroke patients: 1) Visual network 2) Somatomotor & Frontoparietal networks 3) Dorsal attention & Default mode network 4) Ventral attention network 5) Limbic network.

In summary although we observed no main effect of Timepoint, analysis for individual timepoints separately revealed changes in SDI in specific networks across time. In LH stroke patients, the SDI was higher in the IL compared to the CL hemisphere in the somatomotor and limbic networks. The opposite was observed in the ventral attention network (independent of timepoint) as well as in the frontoparietal network at T3. There were no significant effects/interactions for RH stroke patients other than the main effect of Network.

Table 4. Summary of the hemispheric effects in left-hemispheric stroke patients.

LH = left-hemispheric; IL = Structural Decoupling Index (SDI) in the ipsilesional hemisphere; CL = SDI in the contralesional hemisphere

Group	Networks	Hemispheric comparison	Effect similar to control group as reported in Brügger et al. (in preparation, see Study 2)
LH stroke patients	Whole brain	IL > CL	Yes
	Somatomotor & limbic	IL > CL	Yes
	Ventral attention & frontoparietal (T3 only)	CL > IL	No

2.2.4.2 SDI in the primary motor cortex (M1) and motor score

Given that all included patients had a motor deficit at stroke onset, we were particularly interested in the evolution of the SDI in the primary motor cortex (M1). Mixed-effects linear regression with Mean SDI in M1 as dependent variable and Lesion side (Left, Right) as well as Timepoint (T1, T3) revealed a higher SDI in RH compared to LH stroke patients ($F(1,61.89)=4.11$, $p=0.047$). There was no significant effect of Timepoint ($F(1,38.43)=0.27$, $p=0.604$), nor did it significantly interact with Lesion side ($F(1,38.43)=0.17$, $p=0.679$).

2.2.4.3 Multivariate brain-behavior correlation patterns at each timepoint

In the second part of our analyses, we applied PLSC to investigate the inter-individual relationship between variations in structure-function coupling (i.e., the SDI) and the performance in 8 behavioral domains (Motor, Language, Memory, Attention, Executive functions, MoCA, Anxiety & Depression, and Fatigue). We performed one PLSC per timepoint and found significant brain-behavior multivariate correlations for T1 ($p=0.021$) and T2 ($p=0.033$), but not for T3 ($p=0.19$). At all timepoints, positive weights for all behavioral domains except MoCA reflect worse performance in the corresponding scores (**Figure 17A,C**). For MoCA, a negative weight represents worse performance.

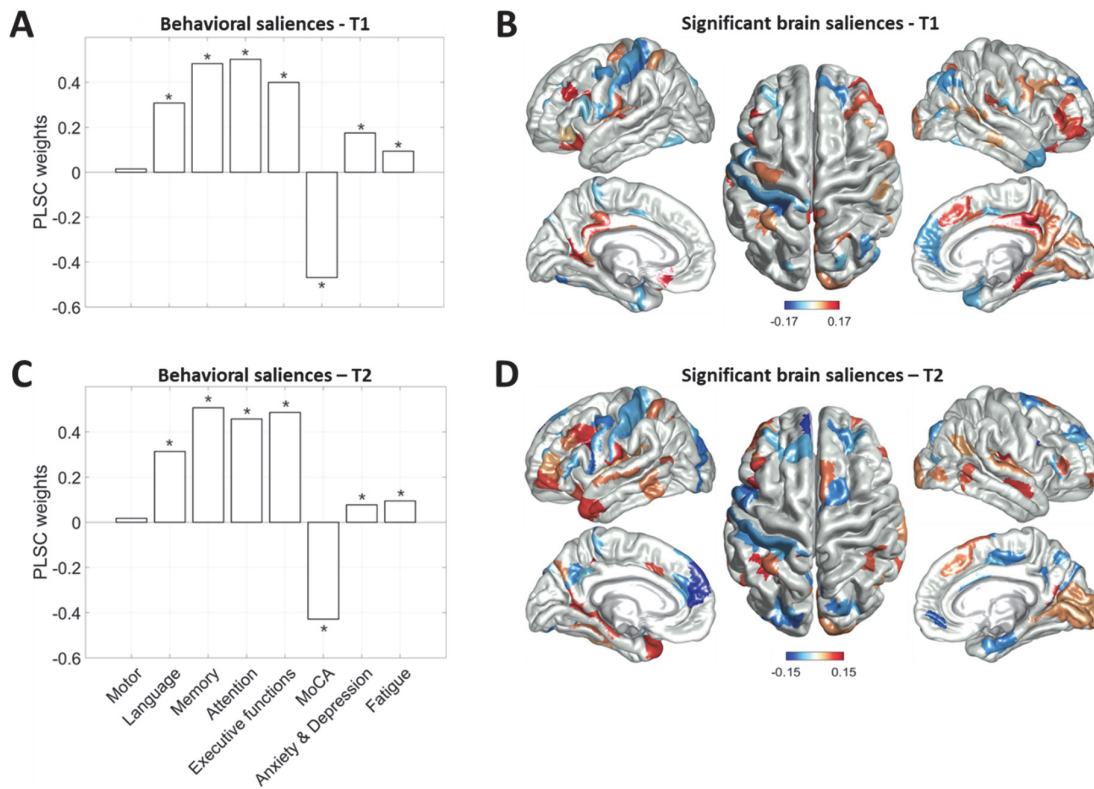


Figure 17. Multivariate correlation patterns between the SDI and behavioral traits.

Significant partial least square correlation (PLSC) patterns between behavioral scores (A and C) and SDI (B and D, significant weights only) at T1 (A, B) and T2 (C, D). A, C: Behavioral saliences (weights) are plotted for each score. Positive weights represent worse performance for all domains except MoCA. Domains that have a contribution significantly different from zero are marked with a star. B, D: Brain saliences (weights) for significant areas are displayed, ranging from negative (blue) to positive (orange-red), representing lower and higher SDI, respectively. E.g., in B, there is a significant positive relationship between worse performance (in all behavioral domains except motor) and the SDI in the ipsilesional (left) hand knob.

2.2.4.3.1 Acute phase (T1)

Having indicated a relationship between behavioural variables and individual ROIs (**Figure 17**), we further investigated the contribution of the networks to which those ROIs belong (**Figure 18**). To that aim, we associated ROIs to their corresponding Yeo network (Thomas Yeo et al., 2011) and assessed 1) how many ROIs in each network exhibited significant weights (**Figure 18A** T1 and **Figure 18C** for T2) and 2) what was the average weight across significant ROIs per network (**Figure 18B** for T1 and **Figure 18D** for T2). To illustrate

this, we will focus on the somatomotor network, as it was of particular interest for this study. At T1, compared to the other networks, the somatomotor network had the biggest portion of its ROIs (40%) significantly accounting for variations in the behavior (**Figure 18A**). In other words, this means that worse performance in all behavioral domains except motor was related to changes in SDI in 40% of the areas belonging to the somatomotor network. Interestingly, regardless of the substantial involvement of somatomotor network as a whole, the average weight of its individual ROIs was rather low, compared to, e.g., the frontoparietal and default mode networks, whose average weight was significantly different from zero (**Figure 18B**). Similarly, a higher SDI in the ventral attention and visual network was also correlated to worse performance in all behavioral domains except motor, but less so than in the frontoparietal and default mode networks. On average, the dorsal attention and limbic network did not contribute substantially to the observed brain pattern.

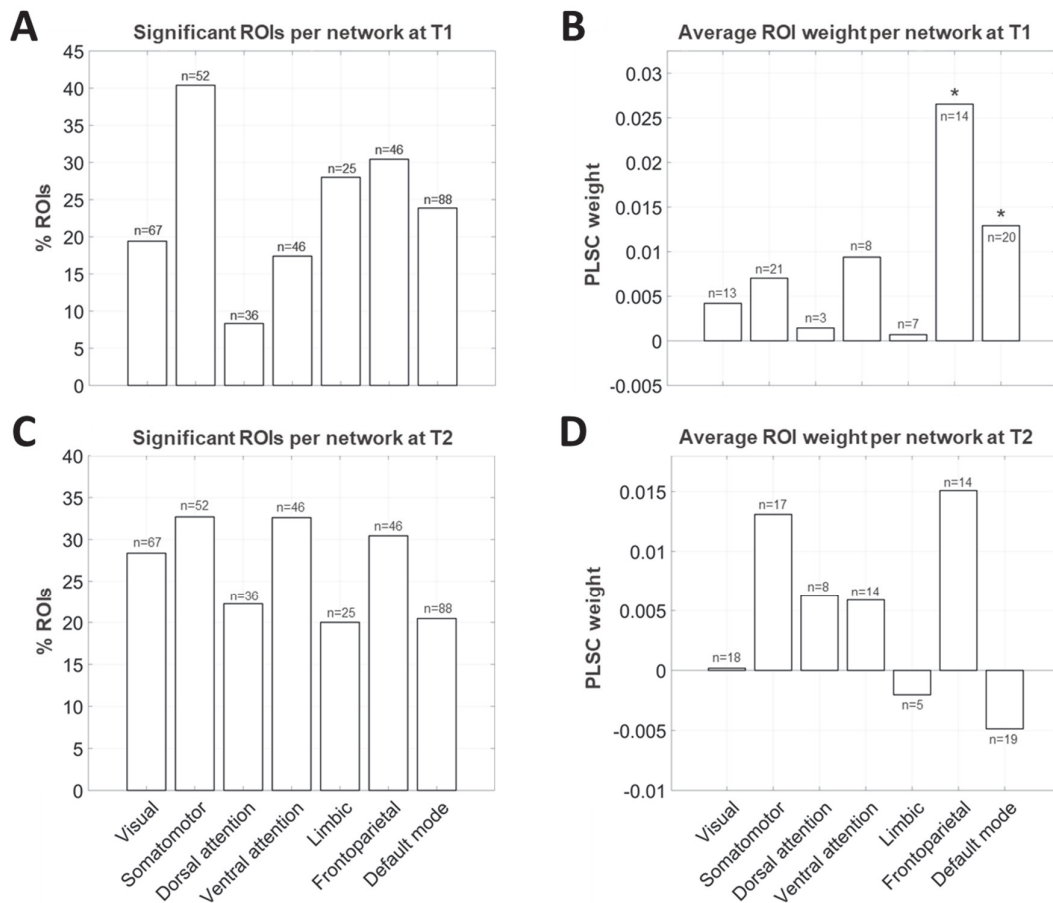


Figure 18. Contributions of regions of interests (ROIs) across networks to the multivariate correlation pattern.

Percentage of ROIs with significant weights by network at T1 (A) and T2 (C). The total number (n) of ROIs per network is indicated on the top of each bar. Average weights across significant ROIs at T1 (B) and T2 (D). The total number (n) of significant ROIs per network is indicated on the top of each bar. Weights significantly different from zero are indicated with stars. While at T1 the Frontoparietal and Default mode networks indicated average ROI weights different from zero (B), at T2, average ROI weights of all networks were indistinguishable from zero (D). Note the difference in scales of y axis in B compared to D.

2.2.4.3.2 Early subacute phase (T2)

At T2, the behavioral saliences were similar to T1, with all domains contributing significantly to the multivariate correlation pattern, except from the motor domain (**Figure 17B**). As in T1, positive weights for all the behavioral domains except MoCA indicate worse performance in the associated score. For MoCA, negative weights reflect worse performance. The brain pattern associated to behavior at T2 was also similar to the pattern observed at T1 – e.g., a lower SDI in the ipsilesional S1 and the more lateral portion of the ipsilesional M1. However, there were also some differences in the T2 brain pattern, notably in secondary and associative motor areas. Indeed, we observed a higher SDI in the ipsilesional premotor area and dorsolateral prefrontal cortex, as well as variations in SDI in the contralesional supplementary motor area (SMA), with one sub-part of the SMA correlating with a higher SDI and the other with a lower SDI. Changes in the degree of correlation to behavior of some ROIs resulted in a different distribution of network contributions in T2 (**Figure 18C**) compared to T1 (**Figure 18A**). Furthermore, in T2, a similar percentage of each network was significantly involved in the correlation with the behavior (**Figure 18C**), indicating a more balanced distribution of contributions across networks. Contrary to T1, however, none of the average network contributions remained significantly different from zero (**Figure 18D**). Interestingly, despite its similar overall contribution at T1 (24%) and T2 (22%), the average ROI of the default mode network contributed significantly and positively at T1 (weight 0.0129), however at T2 the contribution did not remain significant and, in addition, it changed polarity (weight -0.0055). This suggests that a lower SDI in the default mode network at T2 was associated to worse performance in the significant behavioral domains. Furthermore, the average ROI of the frontoparietal network also contributed significantly at T1 (weight 0.0265), but not anymore at T2 (weight 0.0151).

As mentioned previously, the multivariate correlation pattern was not significant at T3 ($p=0.19$), indicating that the behavior could explain variations in SDI less reliably, however results resembled those obtained at T2 (Supplementary Figure S1, Figure S2, Table S13).

In summary, we found significant multivariate correlation patterns at T1, T2, but not at T3. The behavioral motor scores do not contribute significantly to the multivariate correlation pattern at any of the timepoints, notwithstanding all patients having a motor deficit at stroke onset. Despite this, at T1, we see significant involvement of key primary somatomotor as well as of some associative motor areas (mainly ipsilesionally) whereas at T2, there is a shift from primary to secondary motor areas in terms of correlation with behavior (e.g., involvement of the ipsilesional premotor and dorsolateral prefrontal cortex, as well as of the contralesional SMA). Finally, at T1, the ROIs belonging to the frontoparietal and default mode networks were correlating the most (on average) and positively with worse performance in behavior. At T2, their average contribution is decreased (not significantly different from zero anymore) and the polarity of the default mode network is reversed.

2.2.5 Discussion

2.2.5.1 Limited longitudinal changes in structure-function coupling on whole-brain and network levels

In the first part of our study, we addressed the longitudinal evolution of SDI between the first week and the third month post-stroke. When investigating a larger cohort of the TiMeS study longitudinally, we further substantiated the previous findings (Brügger et al., in preparation, see Study 1) related to hemispheric differences and lesion side. This was expected, as the cohorts of Study 1 and Study 2 largely overlap. Analysis for individual timepoints separately revealed changes in SDI in specific networks across time on group-level.

Indeed, in the acute phase (T1), we observed whole-brain (higher SDI ipsi- vs contralesional) and network effects (ventral attention) which were in concordance with findings from our previous work (Brügger et al., in preparation, see Study 1). In the late subacute phase (T3), we also found timepoint-specific effects, notably in the somatomotor, limbic and frontoparietal networks.

For LH stroke patients, almost all observed hemispheric effects (T1 and T3), i.e. in the ventral attention, somatomotor, visual and limbic networks, were consistent with previous findings in the acute phase where the SDI pattern was identical that of healthy controls (Brügger et al., in preparation, see Study 1). In RH stroke patients, however, the hemispheric SDI pattern was disturbed in all these network, suggesting that the absence (limbic network) or presence (somatomotor, ventral attention networks) of hemispheric difference in RH stroke patients could be pathological and that RH stroke patients are more vulnerable to changes in SDI compared to LH stroke patients. Consistent with these results, previous research has linked RH stroke to more severe impairment (Kwakkel et al., 2003; Ward, 2017), suggesting that the RH tends to be more affected by a stroke than the LH. Moreover, the limbic and ventral attention networks – two out of the three networks which displayed an altered SDI pattern in RH stroke patients – are known to be right dominant and have been shown to be more affected by a RH stroke in the past. Indeed, RH stroke can lead to the disturbance of the ventral attention network, which behaviorally expresses under the form of visuospatial neglect (Lunven & Bartolomeo, 2017; Rode et al., 2017). Similarly, RH stroke has been shown to impact the limbic network, resulting in impairment of emotion identification (Sheppard et al., 2020). It is thus a possibility that a higher vulnerability of these networks to RH stroke is underlying the observed changes in SDI. However, out of the 62 patients included in this study, only 13 (9 RH stroke patients) were affected by neglect, suggesting that this might not be the sole explanation for alterations in the ventral attention network on group level (in total 31 RH stroke patients). The relationship between RH stroke and behavior should nevertheless be further investigated, as a disturbed SDI pattern in the ventral attention network might not always lead to neglect, but rather depend on the level of perturbation of the network. Regarding the remaining network which was disturbed in RH stroke patients at T3, i.e. the somatomotor network, the interpretation is more challenging, as it is known to be left-lateralized/dominant in right handers (52/62 patients were right-handed) (Lubben et al., 2021; Triggs et al., 1997), but its SDI pattern is altered only after a RH stroke. The same goes for the frontoparietal network in LH stroke patients at T3, where no evidence points towards hemispheric lateralization. The explanation for this finding remains an open question for future research and an important next step will be to establish whether these network alterations in RH stroke patients are behaviorally relevant, i.e. whether they occur concomitantly to changes in behavioral outcomes which are associated to these networks (e.g., motor function for the somatomotor network, emotion recognition for the limbic network, executive functions for the frontoparietal network and neglect for the ventral attention network).

Interestingly, in our previous analysis (Brügger et al., in preparation, see Study 1), the somatomotor and the limbic networks already showed alterations in the acute phase, whereas this was not the case in the present study, where we found significant effects in these networks only in the late subacute phase (T3). Compared to our previous work, 18 patients were added (i.e. a 40% increase), of which half had a RH stroke. Stroke side is thus likely not the reason why we see slightly different results compared to the analysis in a smaller cohort. Given that the power is increased in the present compared to our previous work, one would assume that the results found in the present study are more reliable. However, further analysis should determine whether this difference in findings can be explained by, e.g., different levels of impairment or patient heterogeneity in the added sub-cohort.

Finally, one more point which should be given consideration is the absence of a main effect of Timepoint on both whole-brain and network level, which was contrary to our hypothesis. Indeed, we presumed that the structural and functional changes underlying post-stroke reorganization over time would be reflected in the

SDI and point towards brain networks which were involved in this reorganization. One possibility for the absence of change over time could be that the SDI is affected by a stroke, but that it is not sensitive enough to capture the subsequent functional and structural reorganization. However, given the large body of evidence describing post-stroke structural and functional changes (Boyd et al., 2017; Grefkes & Fink, 2020; Guggisberg et al., 2019; P. J. Koch & Hummel, 2017), it seems more likely that we did not see intra-network changes over time because the changes in SDI of the individual ROIs belonging to a network are averaged-out on whole-brain and on network level, due to the fact that some areas might show an increase in coupling over time, whereas others could experience a decrease (depending on the underlying structural and functional changes). In addition, the networks we selected were rather broad (Yeo et al., 2011) and it might be beneficial to perform a more fine-grained longitudinal SDI analysis by considering only key areas involved in post-stroke reorganization. Furthermore, the heterogeneous patient population might also cause some patient-specific effects to be averaged out on group-level, which is why analyses assessing inter-individual differences might be more helpful to understand the evolution of structure-function coupling after a stroke.

2.2.5.2 Changes in the SDI pattern at different timepoints account for variability in cognitive and psychological scores

In the second part of our study, we investigated the behavioral relevance of the SDI by investigating the link between performance in eight behavioral domains and SDI through inter-individual multivariate correlation patterns. Globally, the observed brain-behavior multivariate correlation patterns had a very high explained variance (ranging from 78.3% to 87% between timepoints), which was considerably higher than in healthy young (18%) (Griffa et al., 2022), suggesting that the SDI captures inter-individual variations in behavior following a stroke particularly well. These correlation patterns were significant at T1 and T2, but not at T3. Contrary to our expectations, variations in structure-function coupling in the brain are not contributing to performance in the motor domain, despite all patients having a motor deficit at stroke onset. However, particularly the cognitive (Language, Memory, Attention, Executive functions and General Cognitive Assessment – MocA) and psychological scores (Anxiety&Depression, Fatigue) have shown to substantially explain variations in coupling in widespread areas of the brain.

2.2.5.2.1 Somatomotor areas

In the acute (T1) phase, multiple primary somatomotor areas, such as the ipsilesional M1 (notably the hand-knob) and S1, the contralesional M1, as well as some secondary motor areas (mainly ipsilesionally) significantly correlated with performance in cognitive and psychological domains, but not with the motor domain. Given that all patients had a motor impairment of the upper limb at stroke onset, we expected to observe changes in SDI in areas closely connected to the lesion, i.e., notably in primary and secondary motor areas, such as it could be depicted in this study. Indeed, we assume that the structural disruption induced by the lesion results in the inability of the function to rely on the underlying anatomical backbone, implying that function is more decoupled from structure, translating into a higher SDI. However, we also expected the behavioral pattern, which is associated to SDI variability, to involve motor performance, which was not the case. Indeed, at T1, worse performance in all domains except motor was associated to variation of structure-function coupling in numerous key sensorimotor areas.

At T2, we observed a shift from primary to higher-level motor areas, as indicated by significant correlations between the ipsilesional premotor area, the dorsolateral prefrontal cortex and the contralesional SMA, and the cognitive and psychological (but not motor) domains. This shift from primary to higher level somatomotor areas can potentially be explained by cortical reorganization, which has been associated to the recruitment of secondary motor areas two weeks post-stroke (Quandt et al., 2019; Rehme et al., 2011; Schulz, Koch, et al., 2015; Ward et al., 2006). Indeed, a change in structure-function coupling in these areas could reflect the

structural (P. J. Koch et al., 2021; Schulz, Braass, et al., 2015; Schulz et al., 2017; Schulz, Koch, et al., 2015) and/or functional reorganization (Grefkes et al., 2008, 2010; Rehme et al., 2011, 2012; Ward et al., 2006) that these regions undergo during motor recovery. Hence, to observe the involvement of the motor network as a whole during the first weeks of post-stroke recovery is to be expected. What is curious, however, is that changes in structure-function coupling in these key motor areas could not be explained by motor performance, but by performance in cognitive and psychological domains. In addition to these key areas, the somatomotor network as a whole also exhibited a considerable contribution, with 40% of its ROIs at T1 (the most of all networks) and 35% at T2 significantly correlating with performance in all behavioral domains except motor.

Even though some cognitive tests also contain a motor component, such as, e.g., the Color Trail Test and the Test of Attention Performance (TAP) (Zimmermann & Fimm, 2002) (both “Attention” domain), as well as the Bimanual coordination test (“Executive functions” domain) (Dolivo & Assal, 1985), it is unlikely that a motor action required to complete those tests could fully account for the correlation between motor areas and the cognitive domains. First, because we expect the motor deficits to be reflected in the certified motor tests used in this study (see list in section 2.2.3.5) and second, because we cannot assess the extent to which the motor impairment would lead to a worse performance in these cognitive tests, as this depends on the hand the patients used to perform the test – i.e., affected or unaffected, dominant or non-dominant.

In addition, recent evidence suggest that both motor and e.g. attentional deficits are the result of a common, abnormal network state, implying that they are correlated and show a similar recovery over time (Corbetta et al., 2015; Ramsey et al., 2017). This finding suggests common underlying reorganization processes related to motor and cognitive functions, as well as an overlap of involved networks. This could explain in parts the fact that the SDI pattern in the motor areas correlates with cognitive performance. However, on the basis of this hypothesis, we would have expected correlations between the motor and cognitive domains, which was not the case in our cohort (see Supplementary Table S14) and which is inconsistent with above-mentioned findings (Ramsey et al., 2017). Therefore, it would be interesting for future analyses to investigate specific sub-domains related to the behavioral domains studied here, in order to have a more fine-grained analysis (e.g., specific motor functions (e.g., force, dexterity) or attentional sub-functions (e.g., divided/sustained attention)).

The correlation between key motor areas and the cognitive and psychological scores could also be explained by the involvement of these secondary and associative areas in other networks. For instance, the dorsolateral prefrontal cortex is part of the frontoparietal network and the sub-parts of the SMA also belong to the frontoparietal, dorsal or ventral attention networks, respectively (Thomas Yeo et al., 2011). Variability in SDI in these secondary and associative areas could thus be behaviorally relevant for cognition, but not necessarily for motor function. In addition, a recent study has shown that motor network connectivity is also relevant for functional impairment in spatial neglect following right brain stroke (Barrett et al., 2019). More precisely, the authors related spatial neglect to a decrease in connectivity between the ventral attention network and M1. Hence, this could indicate that changes in functional (and/or structural) connectivity between lower-level somatomotor and higher-level cognitive areas could lead to changes in structure-function coupling in both of these areas. This could thus indicate that the variability in SDI, which we observe in the primary somatomotor cortices, is behaviorally relevant for cognitive, but not necessarily motor functions. Nevertheless, these interpretations should be taken with caution, as the evidence is limited and, in the study of (Barrett et al., 2019), it is based on small sample-sizes.

2.2.5.2.2 Frontoparietal & default mode networks

In the acute stage (T1), worse performance in Language, Memory, Attention, Executive functions and MoCA as well as to a lesser extent Anxiety&Depression and Fatigue were also associated to a higher structure-function decoupling in the frontoparietal and default mode networks. The average contribution (weight) of these networks – i.e., of the ROIs belonging to these networks - to the multivariate correlation pattern was significantly different from zero, which was not the case for other networks, suggesting a more prominent role of these two networks in the correlation. In other words, worse performance in behavior (in all domains except motor) was more strongly reflected in increases in SDI in these two networks compared to other networks. In line with these results, worse performance in functions associated to the frontoparietal network, such as executive functions, have previously been associated to higher structure-function decoupling in healthy young (Griffa et al., 2022). In addition, behavioral impairment has been strongly associated with stroke lesions in the “rich club” (Egger et al., 2021), a group of areas that are both highly connected to each other and the rest of the brain, and that largely overlap with the default mode network (Choi & Jezzard, 2021). Hence, structural lesions might account for the strong correlation between worse performance and high decoupling within the default mode network in the acute phase – thereby resulting in an increase in SDI - in “rich club” areas.

When comparing T1 to T2, we observed considerable changes in the correlation between behavior and areas belonging to the default mode and frontoparietal networks. Both average weights were not significantly different from zero anymore at T2, potentially indicating a more balanced contribution of networks across the brain. In addition, the polarity of the average weight related to the default mode network is reversed. In other words, in the acute phase, a higher coupling in the default mode network is related to better cognitive function, whereas in the early subacute phase a lower coupling represents an advantage. Behaviorally, cognitive processes such as episodic memory or self-referential thoughts – which are attributed to the default mode network – are thought to benefit from a lower structure-function coupling (Preti & Van De Ville, 2019). Therefore, a link between better cognitive performance and decreased coupling in the early subacute phase could represent a shift towards a normal functioning of the default mode network, which is accompanied by better behavioral performance. This is in line with previous literature which showed that a return to a more “normal” brain state is associated to recovery and better functional outcome (Grefkes et al., 2010; Rehme et al., 2011, 2012).

Taken together, between the acute (T1) and early subacute phase (T2), we observed a change in the pattern of regions that show correlations with behavioral performance and, in the case of the default mode network, also a reversal of sign. This indicates that ROIs, which are significantly contributing to the brain-behavior pattern, could reflect key areas where behaviorally relevant reorganization takes place after a stroke. However, understanding why worse performance is positively correlated to the SDI in, e.g., one motor area, but negatively in another, requires a thorough understanding of the mechanisms underlying changes in SDI in these areas. Indeed, several mechanisms could account for a change in SDI, which we will address in the next section.

2.2.5.3 Potential mechanisms underlying changes in structure-function coupling after a stroke

It is difficult to predict or explain how processes taking place following a stroke, such as structural and functional plasticity, impact the SDI in a given area, as a change in SDI can reflect various underlying mechanisms. To illustrate this, we can base ourselves on the following (simplified) example: It has been shown that loss of motor-related fMRI activity in ipsilesional M1 in acute phase is correlated with more severe motor impairment (Rehme et al., 2012). In other words, based on this example, one could assume that

patients who have a severe impairment are distinguishable from those with a mild impairment, based on the motor-related fMRI activity in the acute stage. However, it is unclear how these differences in function relate to the underlying structure. We hypothesize that the structural disruption caused by the stroke lesion leads to a higher decoupling between brain structure and function (especially ipsilesionally) in the acute phase, as the function is detached from the anatomical backbone. This assumption is supported by a finding of this work where we showed that the decoupling is higher in the ipsi- compared to the contralesional hemisphere.

If (hypothetically), in the early subacute phase, activity were to increase also in patients with severe deficits, this would result in a similar activation pattern for all patients and the inability to distinguish patients based on motor-related fMRI activity in M1. However, how these findings would translate to changes in structure-function coupling within the motor network, but also in more remote areas, remains an open question, as there could be several different underlying mechanisms. For instance, functional activity could have increased in severely affected patients by means of the already existing structural connectivity. These connections would relay more information (i.e. functional signal), which would then lead to a tighter coupling between function and structure. Another possibility is that this increased activity is related to increased input from a more distributed network of areas, relying less on the underlying direct structural connections, causing thus a higher decoupling between function and structure. Finally, the coupling could also change depending on structural changes, either through an increase of (new) connections through plasticity (Ward, 2017) or a decrease (loss) of existing connections, through Wallerian degeneration (Koeppen, 2004), for example.

Hence, even though research into structure-function coupling stands only at the very beginning, understanding post-stroke changes in structure-function coupling could offer tremendous potential for the understanding of post-stroke reorganization. Perhaps, it could even help disentangle adaptive from maladaptive processes, when, e.g., the apparent activity is the same between ‘fitters’ and ‘non-fitters’ in a given area (as described in this example), but the structure-function coupling is different, due to distinct underlying mechanisms.

The body of evidence illustrating the advantages of taking into account both structural and functional information when analyzing MRI data is growing by the day. For instance, taking into account tractography measures when performing DCM has been shown to improve models of functional integration (Stephan et al., 2009). Furthermore lesion network mapping has gained popularity in the past years, enabling the identification of a network of brain areas likely to be involved in a given symptomatology by taking into account patients’ individual lesion mask (Boes et al., 2015; Fox, 2018). The SDI now offers a new descriptive measure of the brain, describing how much the functional activity in one node is globally relying on the underlying structure, i.e. whether the functional activity in this node is rather constrained by anatomy or rather liberal, taking into account all the connections with the other ROIs. The advantage of this approach is that it is fully personalized (relying on the individual patients’ data) and data-driven, which stands in contrast with other methods that take into account anatomical priors, such as DCM (Gandolla et al., 2021; Grefkes et al., 2008, 2010; Rehme et al., 2011), where a set of areas of interest need to be defined beforehand. Given that stroke has been shown to cause structural (P. J. Koch et al., 2021; Schulz, Braass, et al., 2015; Schulz et al., 2017; Schulz, Koch, et al., 2015) and functional (Grefkes et al., 2008, 2010; Rehme et al., 2011, 2012; Ward et al., 2006) changes in widespread brain areas and networks (Guggisberg et al., 2019; P. J. Koch et al., 2021), the SDI is potentially a more appropriate measure to capture these brain-wide changes than DCM, for example.

2.2.5.4 Summary and outlook

In the present work, we extend previous findings which showed that RH stroke patients are more prone to changes in coupling between brain structure and function than LH stroke patients. In addition, we show for the first time that inter-individual patterns of behavior related to cognitive and psychological domains can be explained to a great extent through variations in SDI in areas belonging to several widespread networks. Notably, we show that the performance in cognitive and psychological (but not motor) domains is dependent on variability in structure-function coupling in numerous somatomotor areas. In addition, we demonstrate that the brain pattern associated to behavior to changes from one timepoint to another, which could be reflective of underlying cortical reorganization. Given that the key areas identified in this study might be driving recovery, a longitudinal evaluation of the structure-function coupling within these regions might be more fruitful in identifying time-related changes in coupling compared to whole brain and network-based analyses, as performed in the first part of this study. Finally, this study showed that the SDI can capture behaviorally relevant post-stroke differences in structure-function coupling, thereby further supporting its potential to become a biomarker for patient stratification in the future. The next step in this direction will therefore be the investigation of the brain-behavior relationship in individual patients. Given that the key areas identified in this study best reflect inter-individual variance, investigating the brain-behavior relationship in these regions in individual patients could shed new light on their individual post-stroke recovery. Patient stratification based on new biomarkers, could eventually lead to more personalized choices of treatment and a better functional outcome.

Acknowledgements

We thank Silvia Avanzi for her excellent work during the recruitment and organization of timepoints.

Funding

Partially supported by #2017-205 'Personalized Health and Related Technologies (PHRT-205)' of the ETH Domain, Defitech Foundation (Strike-the-Stroke project, Morges, Switzerland), Bertarelli Foundation (Catalyst Deep-MCI-T project), FreeNovation Program of the Novartis Research Foundation and the Wyss Center for Bio and Neuroengineering.

2.2.6 Supplementary Information

Table S4. Longitudinal effects related to structure-function coupling between the third week (T2) and the third month (T3).

An overview of the ANOVA for the linear mixed-effects regression assessing mean SDI, reported in the main text. Variables indicated in green were significant with $p < 0.05$.

Variable	Numerator df	Denominator df	F value	p value
Network	6	26406	481.3784	< 2.2e-16
Hemisphere	1	26406	0.0134	0.907861
Lesion side	1	51	0.1382	0.711629
Timepoint	1	4832	0.0704	0.790742
Network * Hemisphere	6	26406	2.6432	0.014548
Network * Lesion side	6	26406	5.7150	5.966e-06
Hemisphere * Lesion side	1	26406	0.2287	0.632510
Network * Timepoint	6	26406	1.4982	0.174243
Hemisphere * Timepoint	1	26406	0.0257	0.872651
Lesion side * Timepoint	1	4832	0.4235	0.515224
Network * Hemisphere * Lesion side	6	26406	3.4060	0.002321
Network * Hemisphere * Timepoint	6	26406	0.8966	0.496152
Network * Lesion side * Timepoint	6	26406	0.4742	0.827971
Hemisphere * Lesion side * Timepoint	1	26406	0.0403	0.840843
Network * Hemisphere * Lesion side * Timepoint	6	26406	0.9300	0.471856

PART I

Table S5. Longitudinal effects related to structure-function coupling between the first week (T1) and the third week (T2). An overview of the ANOVA for the linear mixed-effects regression assessing mean SDI, reported in the main text. Variables indicated in green were significant with $p < 0.05$.

Variable	Numerator df	Denominator df	F value	p value
Network	6	31581.6	552.42	< 0.001
Hemisphere	1	31581.6	2.22	0.136
Lesion side	1	58.3	0.14	0.704
Timepoint	1	14003.4	0.07	0.796
Network * Hemisphere	6	31581.5	0.49	0.819
Network * Lesion side	6	31581.6	4.99	< 0.001
Hemisphere * Lesion side	1	31581.6	0	0.986
Network * Timepoint	6	31581.5	1.35	0.232
Hemisphere * Timepoint	1	31581.4	3.24	0.072
Lesion side * Timepoint	1	14003.4	0.01	0.937
Network * Hemisphere * Lesion side	6	31581.5	3.31	0.003
Network * Hemisphere * Timepoint	6	31581.4	0.82	0.556
Network * Lesion side * Timepoint	6	31581.5	1	0.421
Hemisphere * Lesion side * Timepoint	1	31581.4	0.59	0.442
Network * Hemisphere * Lesion side * Timepoint	6	31581.4	0.16	0.986

PART I

Table S6. Longitudinal effects related to structure-function coupling between the first week (T1) and the third month (T3). An overview of the ANOVA for the linear mixed-effects regression assessing mean SDI, reported in the main text. Variables indicated in green were significant with $p < 0.05$.

Variable	Numerator df	Denominator df	F value	p value
Network	6	29505	527.64	< 0.001
Hemisphere	1	29505	2.63	0.105
Lesion side	1	59	0.26	0.613
Timepoint	1	10389	0.02	0.901
Network * Hemisphere	6	29505	1.62	0.136
Network * Lesion side	6	29505	7.12	< 0.001
Hemisphere * Lesion side	1	29505	2.43	0.119
Network * Timepoint	6	29505	1.43	0.198
Hemisphere * Timepoint	1	29505	2.43	0.119
Lesion side * Timepoint	1	10389	4.8	0.029
Network * Hemisphere * Lesion side	6	29505	3.6	0.001
Network * Hemisphere * Timepoint	6	29505	1.94	0.071
Network * Lesion side * Timepoint	6	29505	0.52	0.793
Hemisphere * Lesion side * Timepoint	1	29505	0.28	0.6
Network * Hemisphere * Lesion side * Timepoint	6	29505	1.32	0.242

PART I

Table S7. Mean SDI in networks at T1.

An overview of the ANOVA for the linear mixed-effects regression assessing mean SDI, for timepoint T1. No variables were significant with $p < 0.05$.

Network	Variable	Numerator df	Denominator df	F value	p value
Somatomotor	Hemisphere	1	2463.5	3.13	0.077
	Lesion side	1	50.1	3.07	0.086
	Hemisphere * Lesion side	1	2463.5	2.41	0.12
Dorsal attention	Hemisphere	1	1706.72	0.03	0.87
	Lesion side	1	50.27	0.37	0.545
	Hemisphere * Lesion side	1	1706.72	0.77	0.38
Limbic	Hemisphere	1	1166.78	1	0.317
	Lesion side	1	50.25	0.13	0.718
	Hemisphere * Lesion side	1	1166.78	0.16	0.693
Frontoparietal	Hemisphere	1	2164.59	1.47	0.225
	Lesion side	1	50.44	0.12	0.734
	Hemisphere * Lesion side	1	2164.59	0.12	0.731
Default mode	Hemisphere	1	4180.6	0.53	0.466
	Lesion side	1	50.6	0.39	0.535
	Hemisphere * Lesion side	1	4180.6	0.01	0.914

PART I

Table S8. Mean SDI in networks at T3.

An overview of the ANOVA for the linear mixed-effects regression assessing mean SDI, for timepoint T3. No variables were significant with $p < 0.05$.

Network	Variable	Numerator df	Denominator df	F value	p value
Visual	Hemisphere	1	2246.11	0.02	0.9
	Lesion side	1	34.99	1.25	0.271
	Hemisphere * Lesion side	1	2246.11	0.19	0.663
Dorsal attention	Hemisphere	1	1186.07	0.13	0.723
	Lesion side	1	35.52	0.55	0.463
	Hemisphere * Lesion side	1	1186.07	0.67	0.412
Ventral attention	Hemisphere	1	1522.04	3.81	0.051
	Lesion side	1	34.84	0.46	0.504
	Hemisphere * Lesion side	1	1522.04	3.35	0.068
Frontoparietal	Hemisphere	1	1498.32	3.56	0.06
	Lesion side	1	35.28	0.28	0.603
	Hemisphere * Lesion side	1	1498.32	3.14	0.077
Default mode	Hemisphere	1	2940.81	2.67	0.103
	Lesion side	1	35.92	0	0.96
	Hemisphere * Lesion side	1	2940.81	0.14	0.71

PART I

Table S9. Mean SDI in left-hemispheric stroke patients.

An overview of the ANOVA for the linear mixed-effects regression assessing mean SDI, reported in the main text. Variables indicated in green were significant with $p < 0.05$.

Variable	Numerator df	Denominator df	F value	p value
Network	6	15289.9	264.5423	<2.2e-16
Hemisphere	1	15289.8	1.0300	0.3101641
Timepoint	1	5548.2	2.2757	0.1314692
Network * Hemisphere	6	15289.8	4.1040	0.0004036
Network * Timepoint	6	15289.8	0.7133	0.6388776
Hemisphere * Timepoint	1	15289.7	0.5675	0.4512740
Network * Hemisphere * Timepoint	6	15289.7	1.6354	0.1328688

PART I

Table S10. Mean SDI by network in left-hemispheric stroke patients.

An overview of the ANOVA for the linear mixed-effects regression assessing mean SDI, for left hemisphere lesions. No variables were significant with $p < 0.05$.

Network	Variable	Numerator df	Denominator df	F value	p value
Visual	Hemisphere	1	2816.25	1.11	0.292
	Timepoint	1	21.79	0.11	0.747
	Hemisphere * Timepoint	1	2816.35	0.19	0.665
Dorsal attention	Hemisphere	1	1510.05	0.35	0.555
	Timepoint	1	634.93	1.14	0.285
	Hemisphere * Timepoint	1	1509.76	0.01	0.93
Default mode	Hemisphere	1	3707.1	1.23	0.268
	Timepoint	1	998.6	0.28	0.597
	Hemisphere * Timepoint	1	3707	0.09	0.761

PART I

Table S11. Mean SDI in right-hemispheric stroke patients.

An overview of the ANOVA for the linear mixed-effects regression assessing mean SDI, for right hemisphere lesions. Variables indicated in green were significant with $p < 0.05$.

Variable	Numerator df	Denominator df	F value	p value
Network	6	14182.8	270.05	< 0.001
Hemisphere	1	29.3	1.84	0.185
Timepoint	1	4671.5	2.31	0.128
Network * Hemisphere	6	14183	1.28	0.262
Network * Timepoint	6	14182.6	1.21	0.298
Hemisphere * Timepoint	1	467.9	1.08	0.298
Network * Hemisphere * Timepoint	6	14182.9	1.63	0.134

Table S12. Significant regions of interest (ROIs) at T1 and T2.

Significant brain saliences					
T1			T2		
Glasser ROI	Hemisphere	Weight	Glasser ROI	Hemisphere	Weight
L_RSC	Left	0.0714	L_POS2	Left	0.0661
L_POS1	Left	0.1297	L_POS1	Left	0.0864
L_d23ab	Left	0.1048	L_23c	Left	0.1454
L_31pv	Left	0.0823	L_7PC	Left	0.0755
L_7PC	Left	0.0698	L_MIP	Left	0.0711
L_6d	Left	0.0791	L_p32pr	Left	0.0879
L_47l	Left	0.0474	L_8C	Left	0.098
L_IFJa	Left	0.1019	L_a47r	Left	0.0922
L_IFJp	Left	0.0717	L_IFJa	Left	0.1335
L_p9-46v	Left	0.126	L_p9-46v	Left	0.072
L_13l	Left	0.0967	L_47s	Left	0.0874
L_47s	Left	0.1067	L_OP4	Left	0.1028
L_OP4	Left	0.0863	L_OP1	Left	0.0679
L_OP2-3	Left	0.0788	L_PFcml	Left	0.0582
L_52	Left	0.0774	L_Pol2	Left	0.0511
L_Pol2	Left	0.0799	L_PreS	Left	0.0886
L_ProS	Left	0.115	L_ProS	Left	0.1105
L_PBelt	Left	0.1172	L_A5	Left	0.0732
L_IP2	Left	0.0775	L_PHA3	Left	0.0766
L_PHA2	Left	0.0804	L_TGd	Left	0.0968
L_31a	Left	0.0905	L_TE1p	Left	0.074
L_25	Left	0.1308	L_TE2p	Left	0.0604
L_Pol1	Left	0.1254	L_TPOJ2	Left	0.0851
L_Ig	Left	0.0694	L_IP2	Left	0.1184
L_MBelt	Left	0.0692	L_VMV3	Left	0.0719
L_LBelt	Left	0.0987	L_PHA2	Left	0.0797
R_V2	Right	0.0746	L_Pol1	Left	0.1086
R_RSC	Right	0.0687	L_Ig	Left	0.0837
R_PCV	Right	0.0844	L_p47r	Left	0.0706
R_7m	Right	0.084	R_V2	Right	0.0665
R_POS1	Right	0.086	R_LO2	Right	0.0662
R_23d	Right	0.1114	R_A1	Right	0.0762
R_v23ab	Right	0.0756	R_SFL	Right	0.0789
R_d23ab	Right	0.1209	R_POS1	Right	0.1139
R_31pv	Right	0.1653	R_8BM	Right	0.0733
R_23c	Right	0.0807	R_IFSa	Right	0.0848
R_MIP	Right	0.0844	R_a10p	Right	0.0838
R_6v	Right	0.0791	R_OP1	Right	0.093
R_p32pr	Right	0.0866	R_OP2-3	Right	0.1526
R_8BM	Right	0.0988	R_52	Right	0.0691

PART I

R_8C	Right	0.0661	R_RI	Right	0.0602
R_a47r	Right	0.1053	R_Pol2	Right	0.0735
R_IFSa	Right	0.1087	R_PBelt	Right	0.0846
R_46	Right	0.0899	R_PHA3	Right	0.0562
R_11l	Right	0.0747	R_STSda	Right	0.0961
R_13l	Right	0.1115	R_PHT	Right	0.086
R_RI	Right	0.0969	R_IP2	Right	0.0858
R_PFcM	Right	0.0946	R_PGi	Right	0.0582
R_PFt	Right	0.0617	R_V4t	Right	0.072
R_PHA1	Right	0.1276	R_Pol1	Right	0.052
R_PHA3	Right	0.1155	R_lg	Right	0.1468
R_TPOJ1	Right	0.0683	R_MBelt	Right	0.0763
R_TPOJ3	Right	0.0585	R_A4	Right	0.0658
R_PHA2	Right	0.1041	R_PI	Right	0.0813
R_31a	Right	0.1213	L_V4	Left	-0.0912
R_Pol1	Right	0.091	L_55b	Left	-0.0945
R_lg	Right	0.076	L_V3A	Left	-0.1006
R_p47r	Right	0.0929	L_V7	Left	-0.0814
R_TE1m	Right	0.0616	L_V3B	Left	-0.0796
R_PI	Right	0.088	L_7m	Left	-0.0853
L_V8	Left	-0.1023	L_5m	Left	-0.0706
L_PEF	Left	-0.0654	L_1	Left	-0.0722
L_55b	Left	-0.0853	L_2	Left	-0.067
L_FFC	Left	-0.059	L_6v	Left	-0.0769
L_5m	Left	-0.0634	L_d32	Left	-0.0841
L_24dv	Left	-0.0636	L_9m	Left	-0.1335
L_1	Left	-0.0766	L_8BL	Left	-0.0699
L_2	Left	-0.1023	L_45	Left	-0.0738
L_3a	Left	-0.0616	L_6r	Left	-0.1037
L_44	Left	-0.0554	L_9-46d	Left	-0.0649
L_9-46d	Left	-0.0566	L_FOP4	Left	-0.0651
L_43	Left	-0.0829	L_Pir	Left	-0.0628
L_Pir	Left	-0.1065	L_PFt	Left	-0.0834
L_FOP2	Left	-0.0986	L_V6A	Left	-0.062
L_PeEc	Left	-0.0688	L_31pd	Left	-0.0535
L_V6A	Left	-0.0484	L_p24	Left	-0.0667
R_FFC	Right	-0.0511	R_V6	Right	-0.0915
R_24dv	Right	-0.0631	R_V7	Right	-0.0844
R_p32	Right	-0.0886	R_7Pm	Right	-0.0847
R_9m	Right	-0.0771	R_v23ab	Right	-0.0578
R_9p	Right	-0.0915	R_24dd	Right	-0.0892
R_6r	Right	-0.0538	R_24dv	Right	-0.0656
R_OP4	Right	-0.0606	R_6ma	Right	-0.0885
R_Pir	Right	-0.0761	R_33pr	Right	-0.0784
R_TGd	Right	-0.0703	R_10r	Right	-0.1054
R_PGs	Right	-0.0854	R_9p	Right	-0.087
R_V6A	Right	-0.0652	R_45	Right	-0.069

PART I

R_LO3	Right	-0.0685	R_IFJp	Right	-0.1441
			R_9-46d	Right	-0.0671
			R_EC	Right	-0.09
			R_H	Right	-0.0578
			R_PeEc	Right	-0.0786
			R_V6A	Right	-0.0759
			R_V3CD	Right	-0.0681
			R_31pd	Right	-0.0912
			R_p24	Right	-0.056

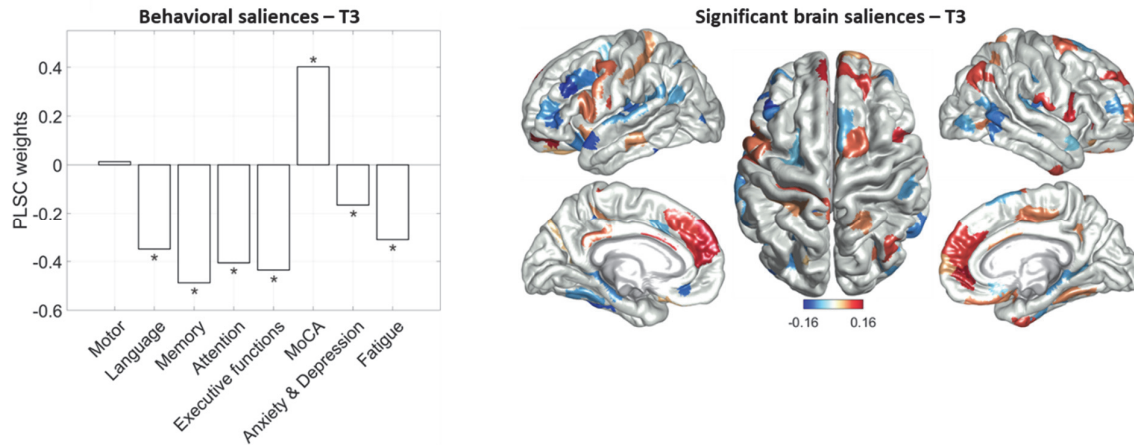


Figure S1. Multivariate correlation pattern between SDI and behavioral traits at T3.

Non-significant partial least square correlation (PLSC) pattern between behavioral scores (left) and SDI (right, significant weights only) at T3. First column: Behavioral saliences (weights) are plotted. Positive weights for all scores except motor represent worse performance and vice-versa. Domains that have a contribution that is significantly different from zero are marked with a star. Second column: Brain saliences (weights) for significant areas are displayed. The weights ranged from negative (blue) to positive (orange-red) areas.

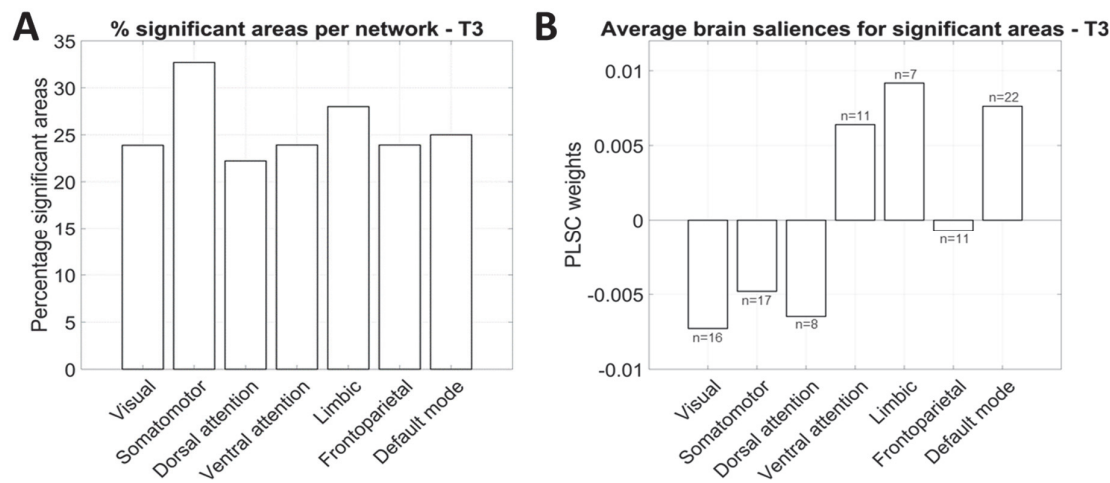


Figure S2. Contributions of brain networks to the multivariate correlation pattern at T3.
(A) Percentage of regions of interests (ROIs) with significant weights by network at T3. (B) Average brain saliences for significant ROIs at T3. None of the networks' average weights is significantly different from zero.

Table S13. Significant regions of interest (ROIs) at T3.

Significant brain saliences					
T3					
Glasser ROI	Hemisphere	Weight	Glasser ROI	Hemisphere	Weight
L_55b	Left	0.082	L_V3B	Left	-0.084
L_d23ab	Left	0.0843	L_LO1	Left	-0.1005
L_5mv	Left	0.0672	L_A1	Left	-0.1019
L_2	Left	0.067	L_PSL	Left	-0.0722
L_3a	Left	0.0911	L_23c	Left	-0.1061
L_6v	Left	0.0792	L_MIP	Left	-0.0768
L_33pr	Left	0.1033	L_8C	Left	-0.0906
L_d32	Left	0.1076	L_p9-46v	Left	-0.1262
L_8BM	Left	0.0977	L_a9-46v	Left	-0.0775
L_9m	Left	0.1322	L_47s	Left	-0.088
L_44	Left	0.0773	L_6a	Left	-0.0576
L_6r	Left	0.0781	L_OP1	Left	-0.0699
L_11l	Left	0.1546	L_RI	Left	-0.0665
L_OFC	Left	0.0533	L_PreS	Left	-0.0855
L_AAIC	Left	0.0696	L_STGa	Left	-0.1193
L_DVT	Left	0.0489	L_PBelt	Left	-0.0957
L_FOP5	Left	0.1104	L_TE2p	Left	-0.1185
L_TE1m	Left	0.0663	L_PGi	Left	-0.0708
R_V3B	Right	0.0813	L_VVC	Left	-0.0753
R_24dd	Right	0.0731	L_s32	Left	-0.1007
R_24dv	Right	0.0786	L_Ig	Left	-0.1048
R_7AL	Right	0.0721	L_p47r	Left	-0.102
R_6ma	Right	0.0846	L_A4	Left	-0.0749
R_LIPv	Right	0.0707	R_LO1	Right	-0.0737
R_33pr	Right	0.0717	R_LO2	Right	-0.0775
R_d32	Right	0.1089	R_A1	Right	-0.0716
R_p32	Right	0.1559	R_SFL	Right	-0.0701
R_10r	Right	0.1132	R_a9-46v	Right	-0.0812
R_47m	Right	0.0609	R_RI	Right	-0.0782
R_9m	Right	0.0985	R_PFt	Right	-0.0745
R_9p	Right	0.1	R_PreS	Right	-0.0778
R_10d	Right	0.0592	R_ProS	Right	-0.0667
R_6r	Right	0.1231	R_PHT	Right	-0.0988
R_OFC	Right	0.0763	R_TPOJ2	Right	-0.0912
R_OP4	Right	0.1014	R_TPOJ3	Right	-0.0746
R_Pir	Right	0.0746	R_IP0	Right	-0.0656
R_PGs	Right	0.0937	R_V4t	Right	-0.0646
R_FST	Right	0.0722	R_25	Right	-0.0623
R_VMV2	Right	0.0861	R_Ig	Right	-0.0996
R_31pd	Right	0.0683	R_MBelt	Right	-0.0707

PART I

R_VVC	Right	0.0694	R_LBelt	Right	-0.057
R_pOFC	Right	0.0682	R_STSva	Right	-0.0779
R_FOP5	Right	0.1229	R_PI	Right	-0.1044
R_p10p	Right	0.0789			
R_TGv	Right	0.093			

PART I

Table S14. Pearson's correlation of Principal Component (PC) 1 with PC1 of the other domains.
No correlations were significant with $p < 0.05$.

Variable 1	Variable 2	Pearson's correlation	Statistic	p value
Motor	Motor	1	Inf	0
Motor	Language	0.19	1.084295	0.287
Motor	Memory	-0.14	-0.75064	0.459
Motor	Attention	0.14	0.781935	0.44
Motor	Executive_fct	0.16	0.873149	0.39
Motor	MoCA	-0.018	-0.10092	0.92
Motor	PsychTests	0.23	1.294061	0.206
Motor	Fatigue	0.2	1.134321	0.266

PART I

PART II

PART II

3.1 Study 3: Evaluating reproducibility and subject-specificity of microstructure-informed connectivity

Philipp J. Koch^{1,2,3, a}, Gabriel Girard^{4,5,6,a,*}, **Julia Brügger**^{1,2}, Andéol Cadic-Melchior^{1,2}, Elena Beanato^{1,2}, Chang-Hyun Park^{1,2}, Takuya Morishita^{1,2}, Maximilian J. Wessel^{1,2, 7}, Marco Pizzolato^{6,8}, Erick J. Canales-Rodríguez⁶, Elda Fisch-Gomez^{6,9}, Simona Schiavi^{10, 11}, Alessandro Daducci¹⁰, Gian Franco Piredda^{5,6,12}, Tom Hilbert^{5,6,12}, Tobias Kober^{5,6,12}, Jean-Philippe Thiran^{4,5,6,b}, Friedhelm C. Hummel^{1,2,13,b}

¹ Defitech Chair of Clinical Neuroengineering, Center for Neuroprosthetics (CNP) and Brain Mind Institute (BMI), Swiss Federal Institute of Technology, 1202 Geneva, Switzerland

² Defitech Chair of Clinical Neuroengineering, Center for Neuroprosthetics (CNP) and Brain Mind Institute (BMI), Swiss Federal Institute of Technology (EPFL Valais), Clinique Romande de Réadaptation, 1951 Sion, Switzerland

³ Department of Neurology, University of Lübeck, 23562 Lübeck, Germany

⁴ CIBM Center for Biomedical Imaging, Switzerland

⁵ Radiology Department, Centre Hospitalier Universitaire Vaudois and University of Lausanne, Lausanne, Switzerland

⁶ Signal Processing Laboratory (LTS5), École Polytechnique Fédérale de Lausanne (EPFL), Switzerland

⁷ Department of Neurology, Julius-Maximilians-University Würzburg, Würzburg, Germany

⁸ Department of Applied Mathematics and Computer Science, Technical University of Denmark, Kgs. Lyngby, Denmark

⁹ Translational Machine Learning Lab, Radiology Department, Centre Hospitalier Universitaire Vaudois and University of Lausanne, Lausanne, Switzerland

¹⁰ Diffusion Imaging and Connectivity Estimation (DICE) Lab, Department of Computer Science, University of Verona, Verona, Italy

¹¹ Department of Neuroscience, Rehabilitation, Ophthalmology, Genetics, Maternal and Child Health (DINO GMI), University of Genoa, Genoa, Italy

¹² Advanced Clinical Imaging Technology, Siemens Healthcare AG, Lausanne, Switzerland

¹³ Clinical Neuroscience, University Hospital of Geneva (HUG), Geneva, Switzerland

a, b These authors contributed equally

*Corresponding author

Gabriel Girard, PhD

gabriel.girard@epfl.ch

EPFL-STI-IEM-LTS5

Station 11

CH-1015 Lausanne, Switzerland

3.1.1 Abstract

Tractography enables identifying and evaluating the healthy and diseased brain's white matter pathways from diffusion-weighted magnetic resonance imaging data. As previous evaluation studies have reported significant false-positive estimation biases, recent microstructure-informed tractography algorithms have been introduced to improve the trade-off between specificity and sensitivity. However, a major limitation for characterizing the performance of these techniques is the lack of ground truth brain data. In this study, we compared the performance of two relevant microstructure-informed tractography methods, *SIFT2* and *COMMIT*, by assessing the subject specificity and reproducibility of their derived white matter pathways. Specifically, twenty healthy young subjects were scanned at eight different time points at two different sites. Subject specificity and reproducibility were evaluated using the whole-brain connectomes and a subset of 29 white matter bundles. Our results indicate that although the raw tractograms are more vulnerable to the presence of false-positive connections, they are highly reproducible, suggesting that the estimation bias is subject-specific. This high reproducibility was preserved when microstructure-informed tractography algorithms were used to filter the raw tractograms. Moreover, the resulting track-density images depicted a more uniform coverage of streamlines throughout the white matter, suggesting that these techniques could increase the biological accuracy of the estimated fascicles. Notably, we observed an increased subject specificity by employing pre-processing techniques to reduce the underlying noise and the data dimensionality (using principal component analysis), highlighting the importance of these tools for future studies. Finally, no strong bias from the scanner site or time between measurements was found. The largest intra-individual variance originated from the sole repetition of data measurements (inter-run).

Keywords

diffusion-weighted MRI, microstructure informed tractography, reproducibility, structural connectome, white matter fascicles

Abbreviations

MD: Mean Diffusivity; COMMIT: convex optimization modelling for microstructure-informed tractography; FA: Fractional Anisotropy; MRI: Magnetic resonance imaging; PCA: principal component analysis; SIFT2: spherical-deconvolution informed filtering of tractograms; TDI: track-density imaging.

Highlights

- Raw whole-brain tractograms are highly reproducible, and erroneous estimations are subject-specific.
- Microstructure-informed connectivity methods maintain high reproducibility as well as subject specificity.
- TDI maps reveal a reduction of high-density biases in deep white matter regions using microstructure-informed tractography.
- Tractography is reproducible in time and site, and most of the variance comes from the measurements repetition itself.

3.1.2 Introduction

Diffusion-weighted magnetic resonance imaging (DW-MRI) and tractography algorithms enable the indirect, in-vivo assessment of white matter fascicles' trajectories and properties in the human brain. This has revolutionized neuroscience, allowing researchers to move away from post mortem analysis and perform their studies non-invasively (Assaf et al., 2017). These techniques have become a fundamental part of systems and translational neuroscience. From the measurements of the displacement of water molecules for specific gradient directions, it is possible to obtain the 3-dimensional (3D) reconstruction of white matter fascicles' trajectories and the description of whole-brain connectomes. Moreover, the local qualitative and quantitative examination of microstructure offers unique possibilities to address various questions in clinics and research. For instance, the study of temporal changes of white matter structures allows the assessment of plastic changes and factors like degeneration persistent in healthy and neurological disease (Sagi et al., 2012). Longitudinal evaluations of the white matter hereby reveal insights into, e.g., learning processes (Scholz et al., 2009) or white matter reorganization after focal brain lesions, such as stroke (P. J. Koch et al., 2021; P. J. Koch & Hummel, 2017). Still, those techniques encompass multiple steps vulnerable to noise, uncertainties, and approximations that affect the interpretation of findings.

The main critical drawback of fibre tracking techniques is the reconstruction of a significant number of invalid tracts, i.e., false positives. Interestingly, a recent international tractography challenge revealed that a high percentage of false positives could be obtained even when the ground truth fibre orientational distribution functions (ODFs) are used (Maier-Hein et al., 2017). Thus, new innovative methods to improve the trade-off between sensitivity and specificity are needed (Schilling et al., 2019) by identifying and filtering out the spurious streamlines. Another important limitation is that the structural connectivity matrix estimated by commonly used tractography algorithms remains qualitative, with an unknown biological meaning, because the density of reconstructed connections does not reflect the underlying white matter fibre density (R. E. Smith et al., 2015b). To address the limitations, microstructure-informed tractography methods were introduced, where each generated streamline is evaluated by its consistency in relation to the whole tractogram and the measured DW-MRI data. Two state-of-the-art methods are the spherical-deconvolution informed filtering of tractograms (R. E. Smith et al., 2013, 2015b) and convex optimization modelling for microstructure-informed tractography (Daducci et al., 2015). Both approaches differ on how the consistency of each streamline is measured. In *SIFT2*, the optimal weighted set of streamlines is determined so that the resulting weighted local orientation density of streamlines is as close as possible to the fibre ODFs estimated using spherical deconvolution (J. D. Tournier et al., 2007). The authors hypothesized that this postprocessing step permits using the sum of streamline weights as a biological marker of connection density (R. E. Smith et al., 2015a). Similarly, *COMMIT* solves a global inverse problem to estimate a weight for each streamline by assuming a generative multi-compartment microstructure model for the measured data, which usually includes the intra- and extra-axonal spaces and free water. The global optimization problem is solved by using constant microstructure properties throughout each streamline trajectory (Barakovic et al., 2016; Barakovic, Girard, et al., 2021; Barakovic, Tax, et al., 2021; Daducci et al., 2013, 2015; Ocampo-Pineda et al., 2021; Sherbondy et al., 2010; R. E. Smith et al., 2013, 2015b). The generated signals are projected to the 3D voxel-space by considering the length of their segments crossing each voxel, which is assumed to be proportional to the local volume fraction (Daducci et al., 2013; 2015). A linear regression model is then designed to decompose the measured data as a linear combination of the generated signals. The estimated weights, thus, quantify the signal fraction of each streamline in the measured data and assign a biological meaning to each connection as a surrogate of the axonal cross-sectional area (Daducci et al., 2015). Those streamlines with trajectories not supported by the measured data have weights close to zero and thus are considered false positives. Like *SIFT2*, *COMMIT* can correct for overrepresented or underrepresented streamlines (due to

tractography biases) by adjusting their weights (Ocampo-Pineda et al., 2021; Schiavi et al., 2020). Although previous studies found that these microstructure-informed tractography algorithms can significantly alter the estimated white matter network topology (Frigo et al., 2020; R. E. Smith et al., 2015b), their stability, reproducibility, and accuracy have not been compared. This is a crucial step before its use for answering neuroscientific and clinical questions. Thus, this study evaluates the reproducibility and repeatability of microstructure-informed tractography methods considering the site, session, and run effects. This was done by collecting DW-MRI data from 20 healthy participants in two scanners located at different sites during two consecutive scanning sessions and two distinct time points, for a total of 160 datasets (eight per participant).

3.1.3 Material and methods

3.1.3.1 Participants

Twenty healthy subjects (Age: 27 (24 – 33 years old, +/- 3 years SEOM), nine female) were enrolled in the study. Magnetic resonance imaging (MRI) was performed at two sites (Geneva: G, Sion: S) at two different time points (sessions). At each session, two independent repetitions of the neuroimaging protocols were acquired (run), ending up in 8 datasets per participant. Between the runs, subjects exited the scanner and were then repositioned, followed by a new shimming. For each session, a single 3D MPAGE was acquired. The mean elapsed time between intra-site and inter-site repetitions was 16 days (+/- 10 days) and 29 days (+/- 17 days), respectively. All subjects were right-handed and had no neuropsychiatric diseases or contraindications for MRI. Written informed consent was obtained from each participant following the Declaration of Helsinki. The ethical approval was obtained from the cantonal ethics committee Vaud, Switzerland (project number: 2018-01355).

3.1.3.2 Magnetic resonance imaging data acquisition

At both sites (G and S), structural T1-weighted and diffusion-weighted MRI data were acquired at 3T (MAGNETOM Prisma scanner, Siemens Healthcare, Erlangen, Germany) and employed the same acquisition protocol. DW-MRI data were acquired using a pulsed gradient spin echo sequence with the following parameters: TR = 5000 ms; TE = 77 ms; slices = 84; field of view = $234 \times 234 \text{ mm}^2$; voxel resolution = $1.6 \times 1.6 \times 1.6 \text{ mm}^3$; slice thickness of 1.6 mm; readout bandwidth = 1630 Hz/pixels; 64-channel head coil; GRAPPA acceleration factor = 3. Seven T2-weighted images without diffusion weighting (b_0 ; $b = 0 \text{ s/mm}^2$) were acquired, including one in opposite phase encoding direction. A total of 101 images with noncollinear diffusion gradient directions distributed equidistantly over the half-sphere and covering 5 diffusion-weighting gradient strengths were obtained (b -values = [300, 700, 1000, 2000, 3000] s/mm^2 ; shell-samples = [3, 7, 16, 29, 46]). In addition, T1-weighted images were acquired using a 3D MPAGE sequence with the following acquisition parameters: TR = 2300 ms; Inversion Time = 7.1 ms; TE = 2.96 ms; flip angle = 9° ; slices = 192; voxel size = $1 \times 1 \times 1 \text{ mm}^3$, field of view = $256 \times 256 \text{ mm}^2$.

3.1.3.3 Image analysis

The DW-MRI images were corrected for Gibbs ringing artefacts using *MRtrix3* (Kellner et al., 2016; J.-D. Tournier et al., 2019) and for motion, field inhomogeneity, susceptibility-induced off-resonance field, and eddy currents using the *FSL topup* and *eddy* (Andersson et al., 2003; Andersson & Sotiropoulos, 2016; S. M. Smith et al., 2004). Subsequently, the images were corrected for spatial intensity variations using *FSL FAST* (Y. Zhang et al., 2001). Multi-shell multi-tissue constrained spherical deconvolution (Jeurissen et al., 2014) was used to estimate the fibre ODF within each voxel. Whole-brain probabilistic tractography was performed using the second-order integration over fibre orientation distribution (iFOD2)(J.-D. Tournier et al., 2019),

initiating streamlines in all voxels of the white matter. For each dataset, 5 million streamlines were generated, from which 1 million were randomly selected with both endpoints in the individual cortical or subcortical brain masks using the *Dipy* software package (Garyfallidis et al., 2014). Moreover, the diffusion tensors and corresponding Mean Diffusivity (MD) and Fractional Anisotropy (FA) maps were estimated using *MRtrix3* (J.-D. Tournier et al., 2019). Tissue partial volume estimates were obtained from the T1-weighted image using the *FSL FAST* (Y. Zhang et al., 2001) and *BET* (S. M. Smith, 2002) methods. The T1-weighted image was registered to the average b0 image using *FSL FLIRT* (Jenkinson et al., 2002) and *FNIRT* (Andersson et al., 2010).

3.1.3.4 Whole-brain connectome estimation

For the cortical parcellation, the Destrieux atlas (74 areas per hemisphere) was used, available in FreeSurfer (Destrieux et al., 2010; Fischl et al., 2002, 2004; Iglesias et al., 2015). Additionally, subcortical areas (thalamus, caudate, putamen, hippocampus, amygdala), the cerebellum, and a subdivision of the brainstem (midbrain, pons, medulla) were added, yielding 163 cortical and subcortical areas. This resulted in a structural connectivity analysis of 13,203 pairs of areas. Connectomes were generated in three different fashions. First, we estimated the fraction of streamlines connecting two regions of interest (i.e., the number of streamlines between all pairs of regions divided by the total number of streamlines). Second, tractograms were filtered based on the underlying white matter fibre densities using *SIFT2* (R. E. Smith et al., 2015b). Third, each streamline was weighted by using *COMMIT* (Daducci et al., 2015) with a Stick-Ball-Zeppelin diffusion model using. The stick compartment models the intra-axonal water with parallel diffusivity fixed to $1.7 \mu\text{m}^2/\text{ms}$ and no perpendicular diffusivity. The Ball compartment accounts for the isotropic extra-axonal water having a diffusivity of $1.7 \mu\text{m}^2/\text{ms}$ and the free water with diffusivity of $3.0 \mu\text{m}^2/\text{ms}$ (Alexander, 2008; Scholz et al., 2009). The Zeppelin compartment models the anisotropic extra-axonal water with parallel and perpendicular diffusivities fixed to $1.7 \mu\text{m}^2/\text{ms}$ and $0.51 \mu\text{m}^2/\text{ms}$ (Alexander, 2008), respectively.

3.1.3.5 Principal component analysis of whole-brain connectomes

Principal Component Analysis (PCA) was employed to reduce the dimensionality of the connectomes. The eigenvectors and eigenvalues were chosen to account for 10% - 100% of the variance explained. This was performed for the three connectome constructions (i.e., raw and filtered tractograms using *SIFT2* and *COMMIT*). Afterward, principal components were applied to reconstruct the connectomes in the original space. These analyses were performed to keep the individual connectomes in the native space while reducing their intrinsic dimensionality.

3.1.3.6 Bundle connectivity vector estimation

Twenty-nine white matter fascicles of the human brain were automatically segmented using a white matter query language (Wassermann et al., 2016). See the supplementary material for more details about the selected white matter fascicle definition (queries). The areas used for the anatomical definition of the white matter bundles were obtained from *FreeSurfer* (Fischl et al., 2002). The following white matter fascicles were reconstructed: right and left Arcuate Fasciculus (frontotemporal, frontoparietal, parietotemporal), right and left Cingulum, right and left Fornix, right and left Inferior Fronto-Occipital Fasciculus, right and left Optic Radiation, right and left Pyramidal Tract, right and left Superior Longitudinal Fasciculus (I, II, III), right and left Uncinate Fasciculus, Corpus Callosum (anterior, mid anterior, central, mid posterior, posterior). The connectivity of the 29 white matter fascicles was represented as a vector, termed bundle connectivity vector, which was created for the raw and filtered tractograms (using *SIFT2* and *COMMIT* methods), respectively.

3.1.3.7 Diffusion Tensor Imaging

The white matter parcellation of every individual dataset was obtained using FreeSurfer (Fischl et al., 2002). For each region of interest, the mean values of the orientationally invariant scalar maps (MD and FA) were estimated for every subject, resulting in a vector with 148 values, representing the areas of white matter parcellation for each subject.

3.1.3.8 Tract-density imaging maps

Track-density imaging (TDI; Calamante et al., 2010) maps were created using *MRtrix3* (J.-D. Tournier et al., 2019) for the three evaluated tractograms (raw and filtered streamlines). TDI maps are built by counting the number of streamlines intersecting each voxel. For *SIFT2* and *COMMIT* methods, the maps were created by summing the weights of the streamlines intersecting each voxel. The maps of all the participants were registered to the MNI standard space. Subsequently, the average map was estimated and voxelwise transformed to z-scores.

3.1.3.9 Connectome reproducibility and subject-specificity

3.1.3.9.1 Dissimilarity measure

To compare connectomes, bundle connectivity vectors and tensor map vectors, we used the Bray–Curtis dissimilarity index (Bray & Curtis, 1957), defined as:

$$\frac{\sum |C1_{ij} - C2_{ij}|}{\sum |C1_{ij} + C2_{ij}|},$$

where C1 and C2 are two non-zero connectomes or bundle connectivity vectors, i and j are the line and column index, respectively. The Bray–Curtis dissimilarity index value ranges between 0 and 1.

3.1.3.9.2 Seven-nearest-neighbour clustering

There are eight datasets for each of the 20 participants of the study. For each dataset and connectivity metric (connectomes, bundle connectivity vectors, tensor map vectors), the seven datasets with the lowest Bray–Curtis dissimilarity were selected. Among them, we identified how many datasets match that participant, producing a score between 0 and 7. This was repeated for all 160 datasets, resulting in a clustering score between 0 and 1120 for each connectivity method. A good performing algorithm should separate participants (producing high inter-individual Bray–Curtis dissimilarity values) and be reproducible for datasets acquired from the same participant (with low intraindividual Bray–Curtis dissimilarity values).

3.1.3.9.3 Distribution of fascicle connectivity

For every dataset and each of the 29 white matter fascicles, the distribution of structural connectivity estimates within the 20 subjects was estimated and analysed with the Shapiro–Wilk test for evaluating whether the estimates deviate from the normal distribution. This was performed for the raw and filtered tractograms. The percentage of datasets following a normal distribution was compared.

3.1.3.10 Data availability statement

Data can be made available upon reasonable request.

3.1.4 Results

3.1.4.1 Dissimilarity between connectomes and connectivity vectors

We have acquired 8 datasets of 20 individuals over a short period using the same acquisition parameters (160 datasets). The structural connectivity estimated from these datasets for one individual should show strong similarity as no major changes should have taken place among scans. Moreover, the structural connectivity should show subject-specificity and thus an increased dissimilarity among subjects. **Figure 19** shows the Bray-Curtis dissimilarity index between all pairs of connectomes and bundle connectivity vectors. The Bray-Curtis dissimilarity index for the diffusion tensor map is shown in the supplementary material (Figure S3). The structural connectivity values were computed from the raw tractogram (first column), *COMMIT* weights (second column), and *SIFT2* weights (third column). Datasets are ordered by subjects, sites (site G, then site S), sessions, and runs. The colours codify the Bray-Curtis dissimilarity among all datasets and methods. The 8x8 squares visible around the diagonal (blue) show the intra-subject dissimilarities, and the off-diagonal values show the inter-subject dissimilarities.

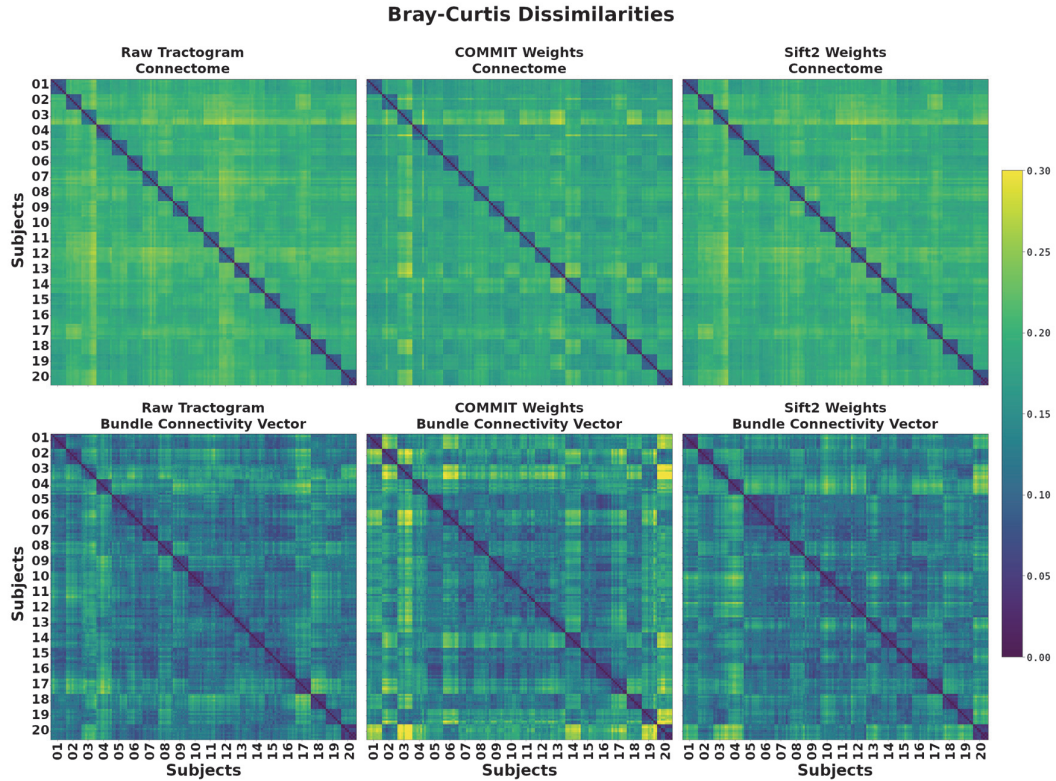


Figure 19. Bray-Curtis dissimilarities.

Bray-Curtis dissimilarities between connectomes (first row) and bundle connectivity vectors (second row) computed from the raw tractograms (first column), and tractograms filtered by *COMMIT* (second column) and *SIFT2* (third column). Each subject has eight MRI datasets (two sites, two sessions per site, and two runs per session). The colours indicate the Bray-Curtis dissimilarity between all datasets and methods. The 8x8 blue squares around the main diagonal show the intra-subject dissimilarities, and other values depict the inter-subject dissimilarities.

Table 5 reports the corresponding interindividual to intraindividual dissimilarity ratio (mean of the inter-subject dissimilarity over the mean of the intra-subject dissimilarity) and the seven-nearest-neighbour clustering performances of each method. The intraindividual dissimilarity ratio is equal for the whole-brain

connectome using the raw tractogram or the filtered one with *SIFT2* at 2.32 and decreases to 1.96 for the *COMMIT* method. Their corresponding clustering performances are almost perfect for all methods. The *SIFT2* and *COMMIT* methods have an increased intraindividual dissimilarity ratio compared to the raw tractogram when using the bundle connectivity vectors. Although the clustering performance decreases, it remains high, ranging from 82% (*COMMIT*) to 86% (raw tractogram). The tensor map vectors show a lower intraindividual dissimilarity ratio of 2.05 and 1.84 when using the FA and MD, respectively. The clustering performance remains high when utilizing the tensor map vectors with a clustering performance of 95%.

Method	Inter to Intraindividual Dissimilarity Ratio	Clustering Performance (max. 1120)
Whole-brain Connectome	Raw Tractograms	2.32
	COMMIT	1.96
	SIFT2	2.32
Bundle Connectivity Vector	Raw Tractogram	2.32
	COMMIT	2.44
	SIFT2	2.45
Diffusion Tensor Map	Average FA	2.05
	Average MD	1.84

Table 5. Inter- and intraindividual dissimilarities.

The ratio of interindividual to intraindividual dissimilarities measured by Bray-Curtis dissimilarity index and classification performances on the connectome, the bundle connectivity vectors, and the tensor map vectors. The dissimilarity index (between 0 and 1) represents how different two connectivity estimates are from each other. The clustering performance of 1120 indicates that each connectome or vector seventh-nearest-neighbours are from the same subject, i.e., any subject can identify the seven other datasets matching that subject.

Table 6 shows the results of the repeated measure ANOVA analysis comparing the mean intra- and inter-individual dissimilarities between sites, sessions, and runs for the three studied whole-brain connectome methods. The comparison reveals no significant differences between the raw tractograms and COMMIT weights. 7.1% and 2.8% of the data variance were explained by the factors site, session and run for the raw tractogram and COMMIT weights, respectively. Using the SIFT2 weights, the repeated measure ANOVA reveals a significant difference with 11.3 % of variance explained. However, post hoc analysis showed no significant differences between the dissimilarities comparing sites, session and run individually, after correction for multiple comparisons.

Table 7 presents the average Bray-Curtis dissimilarity indices between datasets of different individuals (inter-subject) and between datasets of the same individuals (intra-subject). Moreover, the average dissimilarity indices between datasets of the same individual, acquired at different sites (inter-site), or acquired at the same site but during different sessions (inter-session), or acquired at the same site and session but during different runs (inter-run) are reported. It is important to note that the inter-session dissimilarity also includes the dissimilarity inter-run. Similarly, the inter-site dissimilarity also includes the inter-session dissimilarity. For the whole-brain connectomes, the raw tractogram method depicts higher average interindividual dissimilarity and lower average intraindividual dissimilarity, compared to *SIFT2* and *COMMIT*. The raw tractogram and the SIFT2-filtered one showed similar results regarding the bundle connectivity vectors, while *COMMIT* shows higher values. The average inter-run dissimilarity corresponds to 71.7% of the average inter-

site dissimilarity. On the other hand, the increase in the dissimilarity for the inter-session dataset corresponds to 19.8% of the average inter-site dissimilarity. Finally, the mean increase in the dissimilarity for the inter-site dataset corresponds to 8.5% of the total dissimilarity when comparing datasets of the same subject. Overall, the inter-run dissimilarity (same subject, scanner, and session) shows the highest percentage of dissimilarity when comparing the repeatability of all methods. This result is confirmed when considering only the raw diffusion signal, represented as tensor (FA, MD).

Method	Degrees of freedom	F-value	Uncorrected p-value	Partial eta-square effect size	Greenhouse-Geisser epsilon factor
Raw Tractogram	5	1.462263	0.209474	0.071461	0.329294
COMMIT	5	0.562517	0.728459	0.028755	0.385971
SIFT2	5	2.440955	0.039749	0.113845	0.385287

Table 6. Repeated-measure ANOVA comparing mean intra and interindividual dissimilarities.

Repeated measure ANOVA comparing mean intra and interindividual dissimilarities between site, session and run for the three evaluated whole-brain reconstruction methods.

		Average Bray-Curtis dissimilarity Index				
Method		Inter-Subject	Intra-Subject	Inter-Site	Inter-Session	Inter-Run
Whole-brain Connectome	Raw Tractogram	0.2024	0.0871	0.0927	0.0856	0.0677
	COMMIT	0.1873	0.0956	0.1003	0.0954	0.0770
	SIFT2	0.199	0.0858	0.0916	0.0845	0.0651
Bundle Connectivity Vector	Raw Tractogram	0.1323	0.0570	0.0618	0.0540	0.0438
	COMMIT	0.1506	0.0618	0.0679	0.0577	0.0457
	SIFT2	0.1332	0.0543	0.0576	0.0545	0.0410
Diffusion Tensor	Average FA	0.0456	0.0222	0.0242	0.0216	0.0159
	Average MD	0.0343	0.0186	0.0198	0.0186	0.0136

Table 7. Intra- and interindividual comparison of average Bray-Curtis dissimilarity Index.

Average Bray-Curtis dissimilarity Index comparing interindividual and intraindividual dissimilarities with dissimilarities between sites, sessions and runs for whole-brain connectomes and bundle connectivity vectors using the raw tractograms, SIFT2, and COMMIT. The dissimilarity index of the mean fractional anisotropy (FA) and mean diffusivity (MD) is also reported. Please note that the inter-session dissimilarity also includes the inter-run dissimilarity. Similarly, the inter-site dissimilarity also includes the inter-session dissimilarity.

Figure 20 shows the whole-brain connectome interindividual to intraindividual dissimilarity (left) and clustering performances (right), decreasing the variance explained by the data after PCA filtering. The raw tractograms and SIFT2-filtered ones show similar results with an increase in ratio when decreasing the

percent of variance explained. The maximum dissimilarity ratio is obtained using 80% of the variance and decreases as the percentage decreases further. The COMMIT method shows a different profile with a rapid increase at 80% of the variance, then a further increase as the percentage of the variance is reduced. Although the COMMIT method has a lower maximum ratio, the ratio is higher than that obtained for the raw tractogram and SIFT2 method when using a 30% to 10% of the variance. The whole-brain connectome clustering performance is systematically higher for the raw tractogram, except for the COMMIT method when using 10% of variance explained by the data.

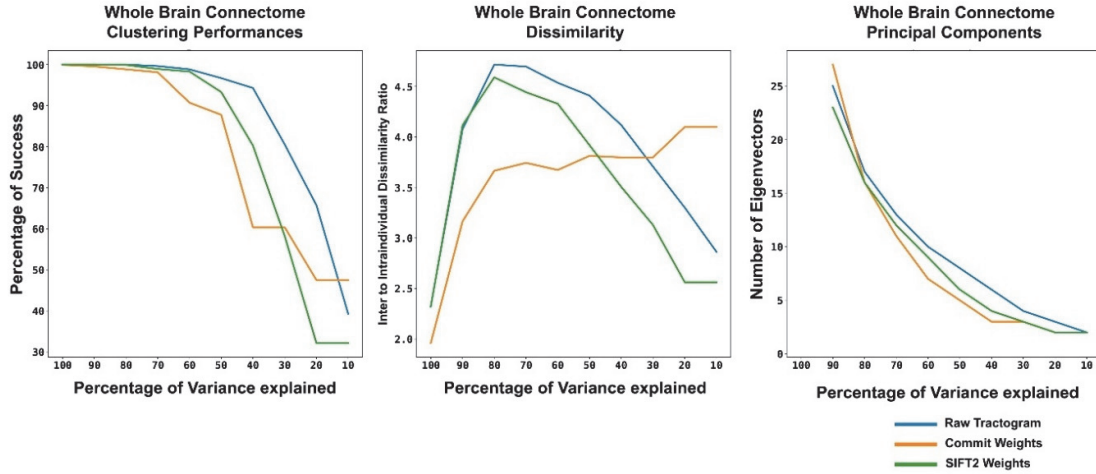


Figure 20. Subject specificity in PCA reduced connectomes for the raw tractogram, the SIFT2 and COMMIT methods. Percentage of successrate in seventh-nearest-neighbours clustering (left) as well as the Interindividual to intraindividual dissimilarity ratio of whole-brain connectomes (middle) are shown accounting for various levels of explained variance by the Principal Component Analysis (PCA). Using PCA the complex dataset of whole brain connectomes was reduced in dimensionality to a certain amount of eigenvectors explaining variance of the data ranging from 10-90% (right). Please note, that for 100% of variance, no PCA was performed, but the raw connectome and filtered connectomes are shown (same data as in e.g. Figure 19, Table 5).

3.1.4.2 Track-density imaging

Figure 21A depicts the z-score map computed from the mean weighted track-density imaging (TDI) map. The distribution of the z-score for the white matter volume is shown in **Figure 21B**. High positive z-score values (red) indicate regions of over-representation of the white matter trajectories, and increased negative z-score values (blue) indicate regions of underrepresentation. Voxel of white matter tissue should ideally show similar values. The raw tractogram and the SIFT2 weighting methods show high z-scores values in the deep white matter. SIFT2 shows a slight reduction in high z-score values compared to the raw tractogram. COMMIT showed a further decrease in high z-score voxels in the deep white matter. However, higher z-score values are noticeable in regions of single fibre populations (e.g., intern capsule, corpus callosum). Interestingly, both SIFT2 and COMMIT showed an increased z-score in the cerebellum (**Figure 21A** bottom row), suggesting an underrepresentation in this region by the raw tractogram. Moreover, the z-scores produced by COMMIT are more equally distributed in this region, which is not the case for other methods, particularly the raw tractogram. **Figure 21B** also shows an increase in high negative z-scores for the COMMIT method. These values are located at the grey matter and white matter boundaries, likely in voxels with partial volume contamination. The raw tractogram and SIFT2 also estimated high negative z-score values in those voxels.

3.1.4.3 Normal distribution of weights

For every white matter fascicle weight estimated at every repetition, the distribution of the structural connectivity estimates was evaluated within the studied cohort using the Shapiro Wilk test (Shapiro and Wilk, 1965). The percentage of normal distribution of the 29 fascicle weights is 10.2%, 55.6%, and 50.0% for the raw tractogram, *SIFT2*, and *COMMIT*, respectively. This suggests that microstructure-informed tractography reduces connectivity weights biases and provides more fascicles with normally distributed weights across the population.

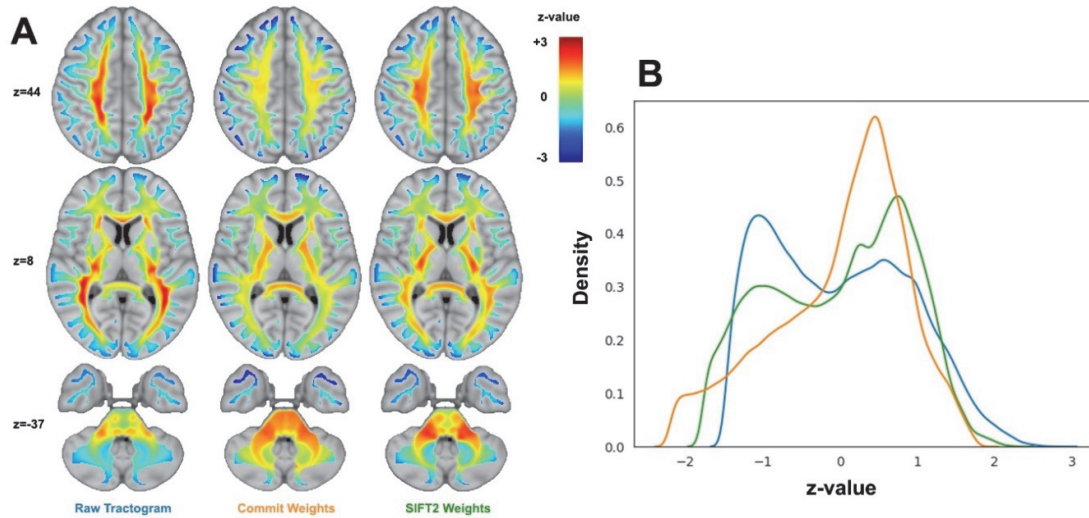


Figure 21. Comparison of group mean weighted TDI maps of microstructure-informed tractography methods.

A: TDI-maps were created using the raw streamline and considering the weighting by the *SIFT2* and *COMMIT* methods. An average map was created over all 160 datasets. All values were z-transformed, indicating the variance of structural connectivity over the whole-brain and presented on MNI standard brain (z-indices of horizontal slices given). B: The density plot shows the frequency of certain z-values.

3.1.5 Discussion

Microstructure-informed tractography methods have been introduced to address the specificity-sensitivity trade-off in tractography by reducing false-positive connections and adding biological meaning to reconstructed streamlines. Analyses in synthetic models of white-matter fascicles have proven high accuracy for *SIFT2* and *COMMIT* (Daducci et al., 2015; R. E. Smith et al., 2015b). Although, the validation is the bottleneck of tractography-based connectivity estimation algorithms. Previous studies used simplified phantoms with connectivity patterns much simpler than those observed in human brains. As an alternative validation approach, some studies focused on studying the reproducibility and repeatability of the estimated connectivity matrices. For example, the reproducibility of white matter reconstruction has been investigated comparing the acquisition and local diffusion models (Dayan et al., 2015; Gigandet et al., 2013; Prčkovska et al., 2016; Roine et al., 2019; Schumacher et al., 2018; Zhao et al., 2015), different tractography methods (Bonilha et al., 2015; Girard et al., 2020; Thomas et al., 2014), thresholding approaches (Colon-Perez et al., 2016; Konopleva et al., 2020; Roine et al., 2019) weighting of white matter pathways (R. E. Smith et al., 2015b), and differences in cortical and subcortical brain parcellations (Besson et al., 2014; F. Zhang et al., 2019). With the lack of ground truth data, the biological accuracy of estimated structural connectivity must be evaluated differently. Firstly, a robust tractography reconstruction must be reproducible. As such, the

connectivity of large white matter bundles of a healthy population is expected to follow a normal distribution. Secondly, it must be biologically meaningful, i.e., representing key aspects of human brain anatomy. Thirdly, a valid reconstruction needs to be sensitive to individual differences, i.e., estimates need subject specificity. Finally, there is a need to investigate the influences on white matter reconstruction caused by differences between runs, sessions, and scanners to characterize the stability of the measurements and analyses. This is especially important when studying structural connectivity alterations in clinical applications, like in longitudinal studies with repetitive measurements, as findings can only be detected (and interpreted) when exceeding the intrinsic variability of the measurement itself, and large multi-centre studies are optimal if the employed methods do not show scanner and location bias.

In neuroimaging, reducing and quantifying variability is a necessity for translational research and for applying potential findings in clinical settings, especially in the view that longitudinal changes are crucially important in the understanding, monitoring and predicting of neurological disorders such as, e.g., stroke (Guggisberg et al., 2019; P. J. Koch et al., 2021; P. J. Koch & Hummel, 2017). Further, being sensitive to individual structural connectivity differences reflects the accuracy of white matter estimates. Evaluating the different impacts on reproducibility by site, time or run offers the possibility to pinpoint the greatest influence to guide further investigations. Finally, the quantification of the degree of uncertainties allows the translation to neuroscientific and clinical questions, expecting a significantly higher effect size than the noise level found in pure intraindividual and interindividual variability. Thus, in this study, we evaluate the reproducibility and repeatability of white matter reconstruction and microstructure-informed tractography methods considering the effects of site, time and run. We evaluated those differences within the whole-brain connectomes and 29 large white matter bundles.

3.1.5.1 Subject-specificity in whole-brain structural connectivity

The whole-brain connectomes constructed by using the raw streamlines were highly subject-specific. High inter-subject and low intra-subject dissimilarities and maximal scores in seven-nearest-neighbours clustering were obtained (see **Figure 19, Table 5**). This surprising result indicates that already the reconstruction of the raw connectome, despite its potentially high incidence of false-positive connections and biases, represents a highly specific individual profile. Tractography is known to be susceptible to false-positive streamlines, but false-positives seem to capture subject specificity. In other words, this suggests that the false-positive streamlines are not random trajectories, but dependent on the subjects' anatomy. When using microstructure-informed tractography methods, the reproducibility of connectomes remains high, as indicated by a high ratio of inter-subject and intra-subject dissimilarity as well as a high score in seven-nearest-neighbours clustering (see **Figure 19, Table 5**).

3.1.5.2 Bundle connectivity vectors

Considering the reconstruction of the 29 bundles, the application of microstructure-informed tractography methods is superior to results from the raw streamline with respect to inter-subject and intra-subject dissimilarity. This implies that adding microstructure information to the estimation of structural connectivity shows high subject specificity while remaining biologically meaningful connectivity estimates. Although, it was not possible to successfully identify every subject using the connectivity of the white matter bundles.

3.1.5.3 PCA-reduced connectomes

Reducing the dimensionality of the whole-brain connectomes increases the inter-subject to intra-subject dissimilarity ratio with an optimum at 80% of the explained variance with approximatively 15 eigenvectors (raw tractogram: 16, *SIFT2*: 15, *COMMIT*: 14) while maintaining a 100% success rate of seven-nearest-

neighbour clustering (for the raw tractogram and *SIFT2*, see **Figure 20**). This implies that not all elements of the whole-brain connectome are needed to identify individuals. Another explanation might be that PCA denoises the connectome elevating the biological meaning. This result withholds novel and exciting possibilities for future connectome analyses. With 15 eigenvectors more complex statistical analyses are possible without losing too many degrees of freedom, while maintaining a high subject specificity. Surprisingly, when reducing the amount of variance explained by the used eigenvectors even further the *COMMIT* filtered connectomes maintain a high interindividual to intraindividual dissimilarity ratio. In contrast, the ratio decreases for the raw tractogram and the *SIFT2* method. This implies that even subcomponents of the connectome obtained using *COMMIT* show high subject specificity.

3.1.5.4 Group-level reproducibility

The standardized mean TDI maps (see **Figure 21**) show the distribution of estimated streamlines density throughout the white matter and reflect key pitfalls in the reconstruction. High positive z-scores in the healthy white matter represent an oversampled density bias estimated from tractography. Areas of convergence of multiple fibre populations are vulnerable to those types of errors, being, e.g., the internal capsule and the corpus callosum. Overall, prominently *COMMIT* reduces quantitatively the number of voxels above 1.0 standard deviation (*COMMIT*: 0.8%, *SIFT2*: 1.2%), whereas the raw tractogram displayed an oversampling density bias (streamline distribution: 1.4%). This reduction of overestimated connectivity by *SIFT2* and *COMMIT* seems especially prominent in the deep white matter (upper row), the internal capsule (middle row). Negative z-scores represent two aspects. One the one hand, voxels containing grey matter are expected to have lower white matter volume and thereby streamline density. On the other hand, low z-values within deep white matter voxels represent an underestimation of streamline density. Areas of high complex fibre architecture including crossing and kissing configurations are vulnerable to these types of errors, i.e., the pons and projection fibres with the cerebellum. Although the microstructure-informed tractography did not alter the overall number of voxels below -1.0 standard deviation (raw tractogram 1.4%, *SIFT2*: 1.6%, *COMMIT* 1.3%), the qualitative inspection of *SIFT2* and *COMMIT* within the pons and the cerebellar white matter clearly shows a dense distribution of white matter fibers. In contrast, there is a bias on the trajectory of the corticospinal pathways and the cerebellar peduncle and a low density within the pons and the cerebellar white matter in the map obtained from the raw tractogram. Using microstructure-informed tractography, most voxels with negative z-scores seem to be on the white matter and grey matter boundary, as expected.

3.1.5.5 Normal distribution of white matter fascicles

We segmented 29 white matter fascicles using anatomical landmarks and the white matter query language. Investigating the structural connectivity within these bundles in the studied cohort suggested a substantial deviation from a normal distribution for most of the fascicles when considering the raw tractogram (10%, normally distributed). After applying microstructure-informed tractography, the connectivity distribution at the group level normalizes up to 50-55%, indicating a higher group level reproducibility, likely by putting high weights on valid fibres.

3.1.5.6 Source of structural connectivity variability

The impact of location, timepoint and run was evaluated. It was hypothesized that the intra-subject dissimilarity between datasets is the most sensitive to potential influences and variability of the acquisition and reconstruction. The repeated measure ANOVA revealed no differences in the dissimilarity scores between the acquisitions. 3%, 7% and 11% of the total variance was attributed to the acquisition when considering *COMMIT*, raw tractogram and *SIFT2*, respectively (**Table 6**). The maximum intraindividual

variance was 0.096 for the whole-brain connectomes and 0.062 for the bundle connectivity vectors. The minimum inter-subject dissimilarity was 0.187 for the whole-brain connectomes and 0.132 for the bundle connectivity vectors. This already implies excellent stability of measurements and reconstructions. More detailed analyses revealed that most of the dissimilarity appears by repeating the measurements, and repeating the measurements at a different scanner does not considerably increase the dissimilarity, thus the greatest amount of the inter-individual variance could be attributed to the inter-run comparison (71.7%). This surprising result underpins the great reproducibility of structural connectivity, especially when considering time and location/scanner. It shows that the acquisition itself induces most of the variance. Still, this raised the question of the source of the variance. Repeating the analysis not using the reconstructed streamlines, but the mean of FA and MD maps derived from the diffusion tensor model confirms that the greatest variance is between runs (**Table 7**). This emphasizes that the measured data (used by the diffusion tensor model) shows the highest variance between runs. The processing algorithms like tractography or microstructure-informed tractography do not add much to the variance. Deviations from this natural variability thus mark a true biological difference, highlighting its meaning for systems neuroscience.

3.1.5.7 The structural connectivity fingerprint

Using the whole-brain connectome, seven-nearest-neighbour successfully clustered all datasets belonging to the same subject, i.e., the whole-brain connectivity profile is unique and reliable to identify an individual subject, such as a fingerprint. This was already shown for functional connectivity (Amico & Goñi, 2018; Finn et al., 2015; Van De Ville et al., 2021), particularly in the frontoparietal network. Moreover, the structural connectome is highly subject-specific (Yeh et al., 2016), with 100% subject classification performances using an alternative structural connectivity pipeline.

3.1.5.8 Limitations

Several aspects have to be mentioned limiting the conclusions of the given analyses. A generalisation of the results on the reproducibility is limited by the assessment in only two sites using the same scanner and acquisition protocol. Showing reproducibility in total independence of the scanner is needed (Kurokawa et al., 2021). In addition, the algorithm for tractography nor the set of streamlines or the cortical parcellation was altered, which can impact the reconstruction of connectomes and white matter bundles. Moreover, all results were based on the multi-tissue constrained spherical deconvolution method, and other alternative techniques are available (e.g., see (Canales-Rodríguez et al., 2015, 2019; Daducci et al., 2014). Finally, the impact of microstructure-informed tractography was analysed solely for *COMMIT* and *SIFT2* with standard parameters and microstructure models.

3.1.6 Conclusion

Surprisingly, the raw tractogram shows high subject specificity at the connectome level, though its biological interpretation is limited. Microstructure-informed tractography shows high subject specificity as well as group reproducibility on connectome level and bundle connectivity vectors. By reducing high fibre density selectively in areas of fibre convergence architecture, microstructure-informed tractography increases the biological meaning of white matter reconstructions. Moreover, reducing the dimensionality of the data through PCA increases the subject specificity and represents a promising analysis step to be included when dealing with whole-brain connectomes. Finally, the largest amount of intraindividual variance arrives from inter-run comparison, most likely by the diffusion signal itself and not by the connectivity analysis. Time and scanner have a small influence on the variance. These results are fundamentally important considering the

design and results of translational neuroscience and patient work and supporting cross-centre clinical data analyses. Findings exceeding the natural intrinsic variability may mark true biological meaning.

Acknowledgements

We acknowledge access to the facilities and expertise of the CIBM Center for Biomedical Imaging, a Swiss research center of excellence founded and supported by Lausanne University Hospital (CHUV), University of Lausanne (UNIL), École polytechnique fédérale de Lausanne (EPFL), University of Geneva (UNIGE) and Geneva University Hospitals (HUG). Marco Pizzolato acknowledges the European Union's Horizon 2020 research and innovation programme under the Marie Skłodowska-Curie grant agreement No 754462. Erick J. Canales-Rodríguez was supported by the Swiss National Science Foundation (SNSF, Ambizione grant PZ00P2_185814). We would like to thank the MRI facilities of the Human Neuroscience Platform of the Fondation Campus Biotech Geneva and the Department of Radiology of the Hôpital Valais de Sion. This study was supported by #2017-205 'Personalized Health and Related Technologies (PHRT-205 to FCH)' of the ETH Domain and by the Defitech Foundation (to FCH).

Conflict of interest

G.F.P., T.H., and T.K. are employees of Siemens Healthcare AG, Switzerland.

3.1.7 Supplementary Information

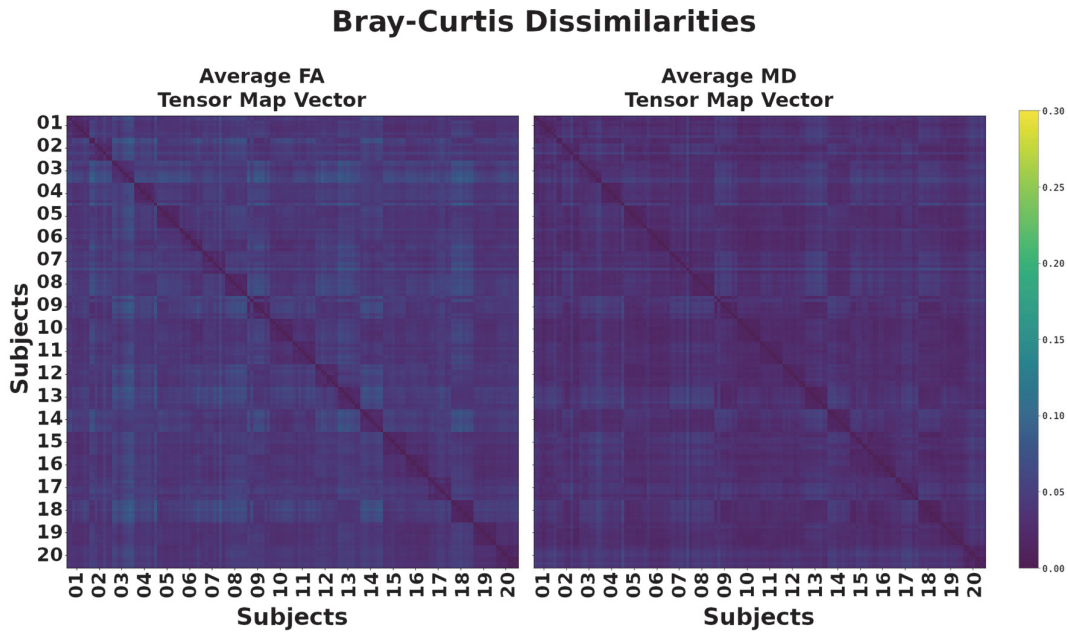


Figure S3. Bray-Curtis dissimilarities between the region-based average fractional anisotropy (left) and mean diffusivity (right) maps (148 region of interest).

Each subject has eight MRI datasets (two sites, two session per site, and two runs per session). The colours indicate the Bray-Curtis dissimilarity between all datasets and methods. The 8x8 blue squares on the diagonal show the intra-subject dissimilarities and other values depicts the inter-subject dissimilarities.

General Discussion

This thesis was motivated by the need for a better understanding of post-stroke recovery in order to pave the way towards the identification of new biomarkers for better patient stratification and in order to improve long-term outcomes after stroke. To that purpose, the present work investigated structure-function coupling as a novel way of understanding the neural mechanisms underlying post-stroke recovery. The second objective of this thesis was to assess the reproducibility of microstructure-informed structural connectivity measures in a multi-center dataset with the goal of increasing data comparability between sessions and centers, as this could highly benefit future clinical studies. In this chapter, I will summarize all the findings and discuss them more broadly, thereby relating the findings of different studies with each other.

I will discuss the impact of stroke on structure-function coupling, its relationship to clinical measures as well as whether and how it changes over time post-stroke. Next, I will review the “network framework” in which the analyses were performed as well as challenges and opportunities related to SDI. Finally, I will consider challenges in MRI (pre-)processing and in clinical research. I will conclude by discussing the extent to which the present thesis contributed towards future patient stratification.

4.1 Evaluating structure-function coupling in a stroke population

4.1.1 The impact of stroke on SDI

In a first step towards determining whether changes in structure-function coupling could give new insights into post-stroke recovery and potentially serve as a biomarker in the future, e.g. for the prediction of recovery or response to treatment, we evaluated whether the SDI – as a way to measure structure-function coupling – was impacted by a stroke. In Study 1, we observed in HOA, a network gradient in line with previous findings (Preti & Van De Ville, 2019) and ranging from low decoupling in the visual and somatomotor networks to high decoupling in the ventral attention and limbic networks. Crucially, this finding persisted following a stroke. However, our results also suggest that a stroke in the acute phase does have an impact on structure-function coupling (i.e., the SDI). Indeed, in stroke patients, we observed globally higher decoupling in the ipsilesional compared to the contralesional hemisphere. This supported our hypothesis that the structural damage induced by a lesion leads to a detachment between structure and function and hence to an increase in SDI. Furthermore, we observed network-specific effects of stroke in RH, but not LH stroke patients in the somatomotor, ventral attention, limbic and default mode networks. This finding was further confirmed in an enlarged cohort in Study 2, except for the default mode network.

When comparing stroke patients to the control group (i.e., HOA, Study 1), results suggest that the “healthy” SDI pattern observed in HOA - namely a higher decoupling in the left compared to the right hemisphere on whole-brain level, as well as in the somatomotor, dorsal attention, limbic and default mode networks - is also present in LH stroke patients and disturbed solely in RH stroke patients. However, the interpretation of why RH stroke patients are more affected by a stroke than LH stroke patients remains an open question. For the ventral attention and limbic networks, an answer might lie in previous studies, which showed that alterations

in these networks due to RH, but not LH stroke, can lead to neglect (Lunven & Bartolomeo, 2017; Rode et al., 2017) and impairments in emotion recognition (Sheppard et al., 2020), respectively. One might thus assume that the higher vulnerability of these networks to RH stroke is at the origin for the change in SDI in the given network. However, out of the 62 patients included in Study 2 only 13 were affected by neglect, of which 9 had a RH stroke, indicating that this is probably not the sole explanation for significant alterations in the ventral attention network on group level (in total 31 RH stroke patients). Further investigations relating behavioral measures for neglect and emotion recognition to the SDI in the ventral attention and limbic networks are however needed to further examine this assumption. For the remaining networks, the interpretation seems more challenging, as both the somatomotor and default mode networks are known to be rather left-lateralized (Banks et al., 2018; Lubben et al., 2021; Nielsen et al., 2013; Triggs et al., 1997), but their SDI patterns are altered only after a RH stroke. The explanation for this finding remains an open question for future research and shows that the investigation of structure-function coupling offers new perspectives into network organization and alterations following a stroke. A crucial next step will be to establish whether these network alterations in RH stroke patients are behaviorally relevant, i.e. whether they occur concomitantly to changes in behavioral outcomes which are associated to these networks (e.g., motor function for the somatomotor network, autobiographic memory for the default mode network, emotion recognition for the limbic network and neglect for the ventral attention network).

Compared to other methods that combine structural with functional measures of brain data to investigate post-stroke recovery, such as DCM or lesion network mapping the SDI offers a different type of information. The SDI allows to investigate how much the functional activity in one node is globally relying on the underlying structure, i.e. whether the functional activity in this node is rather constrained by anatomy or rather liberal, taking into account all the connections with the other ROIs. Changes in SDI after a stroke inform us about global underlying connectivity changes (i.e. of that ROI with all other ROIs). As we show in Study 1, SDI can take into account both the individual structural and functional data (further discussed in section 4.2.1), allowing for a data-driven patient-tailored investigation of post-stroke changes without relying on theoretical priors. In comparison, DCM gives us information about specific (directed) connectivity between areas within a pre-defined network. Even though DCM could also take into account anatomical priors derived from tractography (Stephan et al., 2009), most of the studies are hypothesis-driven and derive the priors from previous studies in animals or humans (Gandolla et al., 2021; Grefkes et al., 2008, 2010; Rehme et al., 2011), thereby ignoring the patients actual structural connectivity. In addition, the number of areas that can be considered for DCM is typically limited to up to 10 areas (Frässle et al., 2017), whereas for the computation of the SDI, information from the whole brain (360 cortical areas in our case) is used, thereby also taking into account changes in structural and/or functional connectivity between certain areas which might not have been foreseen. Even though it is now possible to infer whole-brain connectivity through regression DCM (Frässle et al., 2017), to my knowledge it has not been applied to stroke so far. Furthermore, lesion network mapping offers yet another type of information, identifying brain areas that are likely to be impacted after a stroke given a particular symptom (Boes et al., 2015; Fox, 2018). However, only the lesion is directly derived from the patient, the remaining analysis is based on the Human (functional) Connectome derived from thousands of healthy individuals. In addition, in the case of lesion network mapping, one symptom at a time is usually analyzed. Which method to use eventually depends on the type of information that is sought after. If one is interested in investigating specific connections within a network, DCM is the way to go. If one wants to identify the network which is affected given a specific symptom and lesion location, lesion network mapping is the appropriate approach. While both DCM and lesion network mapping can/do take into account anatomical information, the results do not allow any inference regarding the structure-function relationship, which, however, can be described by means of the SDI.

Finally, a last point to consider is that this thesis also offers new future directions for research in healthy aging, e.g., with respect to the lateralization effect of the dorsal attention network, which we observed in Study 1, and which might be related to age (Nielsen et al., 2013). In a further next step it would thus be of interest to compare structure-function coupling of HOA to that of healthy young, in order to better understand the changes in structure-function coupling related to healthy ageing.

4.1.2 The link between SDI and post-stroke clinical measures

In Study 1, we determined that stroke does have an effect on SDI measures in the acute phase. The next step in probing the SDI as a biomarker was to determine the behavioral relevance of the SDI by relating it to several behavioral domains. In Study 2, we showed that inter-individual patterns of brain structure-function coupling following a stroke could be explained to a great extent (78.3% - 87% of explained variance) through performance in several cognitive and psychological domains. Notably, at T1 (first week post-stroke), the SDI in frontoparietal and default mode networks correlated the most (i.e., with average weights significantly different from zero) and negatively with performance in these domains, whereas the contribution of the different networks was more balanced at T2 (3 weeks post-stroke). The negative correlation between behavior and SDI in the frontoparietal network was in line with previous findings, where worse performance in cognition was associated to a higher SDI in this network (Griffa et al., 2022). In addition, behavioral impairment has been associated with stroke lesions in the “rich club” (Egger et al., 2021; Evangelista et al., under revision, see Appendix), which largely overlaps with the default mode network (Choi & Jezzard, 2021). Hence, we speculated that increases in SDI in “rich club” areas might be at the origin of the strong negative correlation between SDI and behavioral performance (i.e., the higher the SDI, the worse the performance).

Given that almost 80% of patients included in the study had a cognitive impairment according to MoCA, we expected the cognitive domains to be involved in the multivariate brain-behavior correlation pattern and our findings confirmed this. However, all patients also had a motor deficit at stroke onset and we thus presumed the motor domain to correlate with variations in SDI, notably in core motor areas, such as M1, S1, PM and SMA, as they have been previously shown to be involved in both functional (Grefkes et al., 2008, 2010; Rehme et al., 2011, 2012; Ward et al., 2006) and structural (P. J. Koch et al., 2021; Schulz, Braass, et al., 2015; Schulz et al., 2017; Schulz, Koch, et al., 2015) post-stroke cortical reorganization. In line with our hypothesis, we found that variability in structure-function coupling in numerous primary (e.g., M1, S1) and secondary (e.g., PMC, SMA) somatomotor areas as well as in the dorsolateral PFC (involved in cognitive motor control (B.-C. Lee et al., 2020)) was associated to behavior in the first weeks post-stroke. However, surprisingly, the structure-function coupling in these areas was not dependent on the performance in motor function, but on performance in cognitive and psychological domains. In particular, at T1, the brain pattern associated to the performance in cognitive and psychological domains involved multiple primary somatomotor areas (mainly ipsilesionally). Then, from T1 to T2, we observed a shift from primary to secondary motor areas, which could reflect underlying cortical reorganization related to recovery. Indeed post-stroke cortical reorganization has previously been associated to the recruitment of secondary motor areas two weeks post-stroke (Rehme et al., 2011, 2012; Ward et al., 2006). The involvement of areas belonging to the motor network during the first weeks post-stroke, as we observed it in Study 2, could be anticipated based on previous findings related to post-stroke motor recovery (see above), however, it remains puzzling why it was not related to performance in the motor domain. Recent work showed that stroke symptoms, and notably motor and attentional deficits, appear in clusters which are thought to be the behavioral output of a common abnormal network state, implying that they are correlated and show a similar recovery over time (Corbetta et al., 2015; Ramsey et al., 2017). This finding suggests an overlap of networks involved in both functions (motor and attention),

which would mean that they share some of the underlying reorganization processes related to recovery. Even though the motor scores were not correlated to any of the other domains in Study 2, this finding could explain in parts the fact that the SDI pattern in the motor areas correlates with cognitive performance. Furthermore, a recent study established a link between a decrease in connectivity between M1 and the ventral attention network, and spatial neglect (Barrett et al., 2019), suggesting that lower-level somatomotor areas could also be involved in cognitive functions. Assuming that this is the case, changes in said connectivity between M1 and the ventral attention network could lead to changes in the structure-function coupling in the involved areas (i.e., in M1 and areas belonging to the ventral attention network). This change in coupling might then be related to cognitive rather than motor function. Furthermore, the secondary motor areas (e.g., PMC, SMA) and the dorsolateral PFC are also involved in networks other than the somatomotor (e.g. dorsal and ventral attention, and default mode network) (Thomas Yeo et al., 2011). Hence, this could mean that the variability in SDI, which we observe in M1 and higher-level motor areas, is behaviorally relevant for cognitive, but not necessarily for motor functions. Nevertheless, the evidence for this interpretation is limited and should be taken with a grain of salt.

Taken together, the overall change in pattern of regions that show a significant correlation with behavioral performance between the acute (T1) and early subacute phase (T2) is consistent with previous literature and could indicate that the ROIs identified at T2 are key areas where behaviorally relevant reorganization takes place after a stroke and which should thus be further studied, especially in terms of longitudinal SDI changes post-stroke. The extensive cortical patterns (i.e., key areas) which we identified suggest that widespread networks are involved in the recovery process, which is in line with previous literature (P. J. Koch et al., 2021). Studying the evolution of SDI in these key areas in individual patients could offer the possibility of a more in-depth understanding of their personal course of recovery and help explain why some patients recover well while others do not.

There are two more points worth addressing related to our PLSC results: First, the absence of a significant brain-behavior multivariate correlation pattern at T3 could potentially be explained by the fact that most patients have recovered well three months post-stroke and that the variability in the behavioral domains is now too small for the PLSC to detect. Second, the hemispheric effects, as well as the differential impact a stroke has on the RH compared to the LH, which we described in Study 1 and 2, could not be studied in the multivariate correlation analysis, as all lesions were flipped to the left side. Unfortunately, we did not have enough power to analyse the brain-behavior relationship in LH and RH stroke patients separately. It would however be important that future research endeavors study these lateralization and lesion-side specific effect also in the context of the brain-behavior relationship, as brain patterns associated to behavior are likely to differ between RH and LH stroke patients.

4.1.3 SDI changes over time post stroke

If the SDI is reflecting underlying neural reorganization, we would expect to observe longitudinal changes in SDI throughout the course of recovery. In Study 2, we observed this change by revealing distinct hemispheric or network effects at different points in time. However, the main effect of time between T1 and T3 was absent in all our analyses. In the acute stage (T1), decoupling was higher in the ipsi- compared to the contralesional hemisphere, but this effect disappeared in the late subacute phase (T3). In addition, most network-specific SDI patterns in LH stroke patients observed in Study 2 (all timepoints) resembled those of the control group in Study 1, except from the ventral attention network and frontoparietal networks, where the hemispheric differences changed between T1 and T3. This was not the case in RH stroke patients, who showed a deviation from the pattern observed in HOA (in Study 1) in the ventral attention network at T1 as

well as in the somatomotor and limbic networks at T3. This suggests that even though a stroke has a bigger impact on changes in structure-function coupling in RH stroke patients in the acute phase, both LH and RH stroke patients undergo network changes between T1 and T3.

A peculiarity of Study 2 that is also worth discussing is the absence of network-specific main effects of time, i.e., the SDI did not significantly increase or decrease in any of the networks between T1 and T3. This finding was surprising, and one interpretation could be that a lesion impacts the SDI at stroke onset, but that the subsequent reorganization on functional and structural level is not reflected in the SDI. However, given the large body of evidence describing structural and functional changes related to post-stroke reorganization, it seems more likely that the networks we analyzed were simply too broad to capture intra-network changes over time in SDI, which potentially occurred only in a few sub-areas (e.g., key areas identified in Study 2). Another reason could be increases in SDI in some areas and decreases in others, which would result in changes to be averaged out when grouping brain areas by networks. Hence, one possible approach would be to investigate time-related changes in the key areas identified in the brain-behavior correlation analysis in Study 2, as these are areas that are potentially involved in reorganization.

Understanding how the structure-function coupling changes during post-stroke recovery could help disentangling underlying neurobiological mechanisms and potentially distinguish between adaptive and maladaptive processes. For example, if the functional activation in a given area (e.g., M1) is high during a task, the SDI could delineate whether this is due to input from areas which have close anatomical link or from more distant and distributed areas without strong direct anatomical connection. Indeed, if the input stems from an area with close anatomical link, the SDI would be assumed to be low (because the function is closely linked to the underlying anatomy), whereas it would be expected to be higher if the input comes from more a more distributed network. Potentially, we could thus observe differences between patients who show similar activation value, but diverging behavioral performance and make inferences about the underlying neural reorganization based on the amount of decoupling in the brain area in question. Compared to other measures relying on anatomical priors, such as, e.g., DCM, the SDI cannot give us information regarding specific connections within the network, but it can be seen as a “compound” measure, summarizing how much the functional connectivity of a node (with the rest of the brain) globally relies on the underlying structure. It is thus a global characterization of a node, taking into account its relationship with the whole brain. In contrast, DCM is usually restricted to a few pre-defined areas and all connections with other areas are evaluated individually (i.e., it is not a “compound” measure). Given that stroke has been shown to cause changes in widespread brain areas and networks (Guggisberg et al., 2019), the SDI is potentially a more appropriate measure to capture these brain-wide changes than DCM, for example.

In the acute phase, we showed in both Studies 1 and 2 that the SDI is (on whole brain level) higher in the ipsi- compared to the contralesional hemisphere, which is, as we assume, related to the structural disruption through the lesion, rendering the function unable to rely on the underlying anatomical scaffold. This effect disappeared at T3, suggesting that there were changes in SDI in various brain areas between these timepoints which re-balanced the overall intra-hemispheric coupling. It is very challenging to predict how the structure-function coupling would evolve in a specific area after the acute stage of a stroke (and what change would be beneficial), as a change in SDI could have various origins of both functional or structural nature. A change in functional activity could be, for example, the result of either one (anatomical) connection being used more intensively or of an increased amount of functional inputs from distributed areas in the network, relying less on the underlying direct structural connections. In the first case, the SDI would likely decrease, as the function is heavily relying on the structure, whereas in the second case, it might rather increase, because the function is more detached from the structure. The coupling could also change following structural changes, through the formation of new connections through plasticity (Ward, 2017), for example. It is thus to be expected that

the different brain areas (360 cortical areas in total) show a heterogeneous post-stroke longitudinal SDI evolution, depending on their individual functional and structural characteristics. This could be the reason why we did not observe a main effect of time for any of the networks. An evaluation of the longitudinal evolution of the SDI, investigating all 360 brain areas individually, does not seem feasible, however key areas identified in Study 2 offer a good starting point for selecting areas of interest to understand the dynamics of changes in SDI throughout post-stroke recovery.

With the experiments performed in this thesis, it is unfortunately not possible to determine the nature of the underlying mechanisms causing changes in SDI, as a change in SDI does not just depend on how either function or structure changes, but how one changes with respect to the other. However, future studies could use the SDI as a tool to disentangle the underlying neural mechanisms and increase the understanding of cortical reorganization, by applying novel experimental paradigms (such as the one described above) that investigate functional activations concomitantly to structure-function coupling in areas or networks of interests.

4.2 Methodological considerations

4.2.1 Individual-level implementation of the SDI

Having discussed the results related to structure-function coupling in the context of neuroscience and pathophysiology, it is also important to consider challenges and opportunities related to the method itself. The SDI was developed using group functional and structural connectomes derived from data from the Human Connectome Project (HCP) involving healthy young participants (Preti & Van De Ville, 2019). Hence, the first challenge in applying it to our data, was to use the individual instead of the group connectome and we needed to evaluate the feasibility of an intra-individual SDI measure. In this context, an important consideration was also the difference between the resting-state fMRI sequence used in this thesis compared to the one used in Preti & Van De Ville (2019), as this can also have an impact on the feasibility of the SDI analysis, notably in terms of stability of the connectivity strength, accuracy of the estimation of the hemodynamic response function and statistical power (Birn et al., 2013). Indeed, our resting-state fMRI sequence differed considerably from the one used in the HCP, notably in terms of TR (1.25s in our vs 0.72s in the HCP dataset), as well as in terms of length. While our sequence lasted a little more than eight minutes, they used two times fifteen minutes of resting-state acquisitions. Our analysis in HOA (Study 1) demonstrated the existence of a network gradient consistent with previous findings from Preti & Van De Ville (2019), which allowed us to assume that the SDI can be applied on individual data as well as on shorter resting-state fMRI sequences. This is essential to apply the SDI in clinics, where there is a strong need for an individual evaluation for every patient and where patients are not very compliant with long MRI sessions.

After having verified the feasibility of intra-individual SDI measures, we faced some issues specific to the stroke population. Namely, in stroke patients, parcellation errors due to the stroke lesion can sometimes occur, even though we tried to correct for the lesion by applying a “lesion transplantation” procedure, in which the lesioned portion of the brain is replaced by the corresponding portion of the contralesional (i.e., healthy) hemisphere. Especially in patients with large cortical lesions, the transplanted portion did not always align perfectly with the tissue surrounding the lesion, notably due to hemispheric asymmetries. Thus, it could happen that one or several ROIs did not have any streamline starting/ending in them, leading to a “zero-node”, i.e., a node in the structural connectome with a connectivity value of zero. These connectomes could not be processed by the SDI pipeline (due to a division by zero in the computation of the spectral

decomposition), which meant that this session had to be excluded, thus leading to a missing data point for the patient in question. Missing data points were an issue also for other analyses, notably for the PLSC analysis (Study 2). Indeed, we used PCA for the dimensionality reduction within every behavioral domain, however, nor PCA nor PLSC allow missing values. Hence, we could only consider patients who had all sub-scores for all domains, leading to a loss of roughly half the patients for every timepoint (of 62 patients included in the study we could only include 32 patients for T1, 34 patients for T2 and 31 patients for T3). The reason for missing behavioral data were mainly due to patient compliance (i.e., not all tests could be performed due to fatigue or other reasons), which means that this is likely a problem for clinical studies in general. Hence, it would be desirable for methods related to dimensionality reduction (e.g., PCA) and statistical methods (e.g. PLSC) to be mathematically adapted in a way that they are able to deal with missing values in the future, as more meaningful conclusions could be drawn from analyses with higher power.

Finally, methods that fully integrate structural with functional measures are scarce, and the only method that can probably compare with the SDI method on this level is the *Functionnectome* (Nozais et al., 2021). However, while the *Functionnectome* addresses an interesting question, which is the function of white matter tracts in the brain, it presents a considerable amount of methodological disadvantages compared to the SDI. For instance, the *Functionnectome* relies on a substantial amount of priors, that it cannot be individualized and that it needs a considerable amount of processing power (whereas the SDI can be run on a regular computer). Measures derived from the *Functionnectome* would thus be less suitable as biomarkers, as it would be difficult to integrate it in the clinical routine. Thanks to the findings presented in this thesis, I therefore conclude that the SDI is – to the best of my knowledge – the only measure of combined structure-function information that can be applied on an individual level (Study 1) and in a stroke population (Studies 1 and 2) at this moment, making it a promising tool for post-stroke investigation of neural correlates.

4.2.2 The definition of brain networks

Another methodological challenge that is important to address is related to the definition of brain networks. In the last years, neuroscience has moved away from a localizationist approach, where researchers tried to attribute a specific behavioral function to one specific brain area, to a network-based approach, where it is assumed that a behavioral function is the result of the interactions between areas belonging to a network (Guggisberg et al., 2019). Stroke research has accordingly moved in this direction, redefining stroke as a “network disease” – implying that a lesion might have an impact on the entire brain and its network properties (Alstott et al., 2009; Grefkes & Fink, 2014; Guggisberg et al., 2019; Honey & Sporns, 2008; P. Koch et al., 2016; P. J. Koch et al., 2021). Methodologically, this was reflected in a shift in the way neuroimaging data was analyzed, moving away from defining functionally specialized brain areas based on fMRI paradigms towards a within-network analysis of data. When analyzing results on a network level, the definitions of different networks that are used should be universal, in order for results to be comparable across studies. This is, however, not the case. Indeed, there are currently more network labels than there are underlying networks, because visually similar networks are often assigned different labels (Uddin et al., 2019; Witt et al., 2021). This leads to confusion and inconsistencies when relating findings to results from previous studies as well as when designing new experiments based on prior work. To avoid ambiguities, it would be better to use network definitions based on prior template, such as the one from Smith et al. (S. M. Smith et al., 2009) and Yeo et al. (Thomas Yeo et al., 2011) – who derived the networks from large resting-state fMRI datasets – as well as from Witt et al. (Witt et al., 2021) who extended this work by basing the templates on task-based and resting-state fMRI datasets obtained in 69 studies. In this thesis, I used the 7-network solution from Yeo et al. (Thomas Yeo et al., 2011) to subdivide the 360 Glasser ROIs (Glasser et al., 2016) into networks.

However, even when using this template, interpretation is not always straightforward. The somatomotor network from Yeo only includes primary somatomotor areas (motor, sensory, auditory), for example, whereas the common definition of the motor network also includes higher-level areas, such as the premotor cortex, or the SMA (Miall, 2016; Rehme et al., 2011). Hence, one should be aware of what areas are included in a network at hand and be careful with the impact this might have on the interpretation of the results.

An additional point which caught my attention was that most definitions of networks attribute one brain area to one specific brain network, even if it has been shown to be involved in other networks too. This is still a leftover from the localizationist point of view, which attributed one area one specific function (Pessoa, 2014). To illustrate, the SMA is a higher-level motor area, however it is not encompassed in the somatomotor network from Yeo et al. (Thomas Yeo et al., 2011), but its sub-parts belong to the dorsal and ventral attention as well as the frontoparietal networks. Hence, when investigating a specific network, one has to manually verify, based on literature, whether all relevant areas are included in the predefined template, which further adds to the confusion and heterogeneity of network definition. Therefore, the definition of more comprehensive templates in the future (i.e., in which areas can belong to more than one network) would allow us to go towards a more complete and comparable way of analysing brain networks. In the case of analyses presented in this thesis, the 7-network solution might not have been the most appropriate choice for all my research questions, however I decided to abide by it, as it made my results more comparable with existing literature and because it avoids overrepresentation of certain areas in the results. For future analysis in the context of Studies 1 and 2, it could however be of interest to redefine e.g., the somatomotor network towards a more pure motor network, including primary and higher-level motor areas, as motor recovery is one of the main focus of TiMeS.

4.3 Translational aspects

4.3.1 Considerations regarding research using MRI

Another important consideration when performing MRI-based experiments is reproducibility, as increasing data comparability between sessions and centers could benefit future studies. This is especially true in the context of multi-timepoint studies, where one wants to observe the experimental effect and not random variability. In addition, this question is important for longitudinal clinical studies, especially in a multi-center setting. We addressed this challenge in Study 3 of this thesis, where we tackled a particular angle of the reproducibility issue, comparing the performance of two relevant microstructure-informed tractography methods, SIFT2 and COMMIT, by assessing the subject specificity and reproducibility of their derived white matter pathways. We showed that even though raw tractograms are more vulnerable to false-positive connections, they are nevertheless highly reproducible, suggesting that the estimation bias could be subject-specific. The high reproducibility was preserved when filtering the tractograms with SIFT2 and COMMIT, and we observed that the coverage of streamlines throughout the white matter was more uniform, hinting that it could increase the biological accuracy of the estimated fascicles. We further observed that the largest intra-individual variance stems from the repetition of data measurement (inter-run), whereas scanner site or time between measurements were not adding considerably to the bias. In addition, we found that preprocessing techniques to reduce the underlying noise and the data dimensionality using PCA could increase subject specificity.

With regard to preprocessing steps, it seems worthwhile mentioning that there is currently no gold standard in terms of DWI preprocessing and processing (Tax et al., 2022), further impacting the comparability across

analyses and datasets. Indeed, modules from different software packages can be combined, steps can be performed in various orders and many of the preprocessing variables are user-dependent (Tax et al., 2022). This contrasts with (pre-)processing pipelines in fMRI, which are mostly relying on the SPM software (Ashburner et al., 2014) and applying largely identical steps (even though alternatives are available through other software packages such as e.g., FSL or Analysis for Functional NeuroImages (AFNI)). When using SPM12, there is still a certain number of variables to be determined depending on the data (e.g., Gaussian smoothing kernel), however they are limited and well documented. In order for advanced DWI and fMRI analyses to be applied in clinics, it is crucial that these steps are simplified, especially for DWI, where the choice of optimal pipeline can be challenging even for experts (Tax et al., 2022). Indeed, a too complex use of software or application of analysis to a dataset risks to hinder translation of promising research into clinics. Efforts towards the simplification of MRI (pre)processing have been made in the fMRI field, with a promising example of the CONN toolbox (Whitfield-Gabrieli & Nieto-Castanon, 2012), that proposes different automatized preprocessing pipelines for functional data (based on SPM8 or SPM12), and provides an intuitive Graphical User Interface (GUI). In addition, for the SPM alternatives, an automatized preprocessing pipeline named fMRIPrep (Esteban et al., 2019) has recently been published and a similar effort has been made in the DWI field through the publication of toolboxes such as dMRIPrep (*dMRIPrep*, 2019/2022) or MRtrix3_connectome (*Bids-Apps/MRtrix3_connectome*, 2016/2022), amongst others, which intended to make preprocessing more user friendly.

An additional challenge when analyzing data from a stroke population is the performance of additional manual steps, such as lesion segmentation or drawing individualized masks for the CST. Notably, for the SDI analysis applied in this thesis, all lesions needed to be hand drawn prior to preprocessing and processing, as automatized methods are not (yet) as good as humans in performing this task (Maier et al., 2015). Hence, this step requires expert knowledge in the identification of brain lesions and it can also be very time consuming, depending on the extent and location of the lesion. Finally, a considerable potential source of problem could be the use of Linux-based toolboxes and programs for the analysis of DWI data. Indeed, this operating system is not frequently used in clinics and could represent an additional hurdle in the translation of biomarkers to clinics. However, more tools to promote availability of reproducible pipelines have been made available lately through containers (Tax et al., 2022), which can run on both Windows and Linux-based systems, and could be useful for the application of automated processing pipelines in clinics.

4.3.2 Research in a clinical environment

After discussing some considerations related to research using MRI, I will now briefly discuss more general challenges one might encounter when setting up a study in a clinical environment, such as it was the case for TiMeS. Being able to assess stroke patients in a longitudinal study starting from the first week, i.e., the acute phase, post-stroke is a privilege and offers tremendous opportunities for research, as it allows to capture the full picture of post-stroke recovery. However, performing research in a hospital is different from a laboratory environment and one needs to adapt to the ongoing clinical schedule. Nevertheless, through close collaboration with clinical partners for recruitment and data acquisition, even large and time-intensive studies can turn into a success. The TiMeS project is a great example to illustrate this subject, as it includes three different hospitals/rehabilitation clinics in two different locations and assessing several modalities, namely MRI, TMS-EEG as well as neuropsychological and motor tests, with a total assessment time of approximately two days.

By working on this study, I realized that the physical proximity to the hospital (in our case the cantonal hospital of Sion, Switzerland (HVS)) and rehabilitation clinics (in our case the Clinique Romande de

Réadaptation in Sion, Switzerland (CRR) and the Berner Klinik in Crans-Montana, Switzerland (BK)) is essential when acquiring data with stroke patients who are in the acute and early subacute phase. Indeed, performing experiments at these stages would have hardly been possible if the experimental facilities were not located within the partner institutions where patients who were participating in the study were hospitalized.

When conducting a multimodal and longitudinal study, a considerable amount of specialized manpower and a team effort for both the patient recruitment as well as for the organization and execution of the experiments is required. Indeed, efficient exchange within the team and with the clinical partners is also here primordial for the experiments to go ahead as planned. This is especially true when patients are still hospitalized and also have a rehabilitation schedule. In addition, in a bilingual canton such as Valais (Switzerland), where the experiments for this thesis were performed, knowing both French and German is an advantage, as some patients know only one or the other language.

In studies that have long protocols, such as it was the case for TiMeS, patient compliance is another relevant point. Indeed, depression rate and fatigue are high in stroke patients, most notably in the early phases after a stroke (in the TiMeS cohort 11% of patients were scored as clinically depressed and 37% showed general fatigue at T1) and experiment duration can be lengthy, which can impact the patients' motivation in participating in a study and – in the context of MRI – to hold still. As an example, the MRI protocols are rather short (~15 minutes at the cantonal hospital in Sion, Switzerland), whereas our research protocols are lengthy (~1 hour in the studies presented in this thesis). This can be very straining for patients, especially in the acute stage, as they often experience discomfort in this phase. Notably, it is difficult for patients to remain still for an extended period of time, which leads to an increased amount of motion artifacts in MRI acquisitions which can render statistical dependencies spurious. Furthermore, a considerable amount of individuals tend to be claustrophobic, adding on to the challenges of MRI-based research. Nevertheless, my experience is that compliance can be greatly increased by adapting the schedule to the individual patients need and capacity, for example by spreading out the assessments of the different modalities over more than two days, giving the patient additional time to rest in between. Furthermore, my experience was that explaining the individual steps of the MRI protocol and the functioning of the MRI scanner itself (in simple words), in addition of frequent contact during the scanning, could help reassuring patients and ensuring that data could be acquired, even if the patients were reluctant in the beginning.

Naturally, missing timepoints cannot always be avoided, be it due to absolute refusal to enter an MRI scanner (i.e. missing only that part of the study; 7/86 patients in TiMeS) or due to skipping of timepoints. Indeed, in longitudinal studies such as TiMeS, where the participants are enrolled and participating in experiments up to one year post-stroke, one often observes a considerable amount of skipped timepoints and higher drop-out rates than more short-term studies. In the case of TiMeS, this was accentuated by the COVID-19 pandemic, which resulted in an additional amount of omitted timepoints due to stopping of experiments during several months in total, but also due to the reluctance of some patients to come to the laboratory in these circumstances. Hence, given it is quite challenging to have a large and complete dataset, rendering it precious and highlighting the importance of using a maximum of available datapoints in analyses. However, in some cases, parts of the data still had to be excluded for analysis due to technical circumstances, such as methods that cannot deal with missing values, as mentioned in section 4.2.1. Hence, this shows that there is still need for improvement, mainly on the methodological side.

Despite all challenges, the effort is well worth being made, as such clinical studies could offer new insights into post-stroke recovery and the quest for new biomarkers for patient stratification, which could eventually lead to an improved and more personalized course of treatment and better outcomes for stroke patients.

4.3.3 A step towards patient stratification?

This thesis started with a need for a better understanding of post-stroke recovery as well as with a quest for new biomarkers, based on the need for better patient stratification and individualized therapies to improve functional outcome after a stroke. Currently probed biomarkers in the field of MRI are based on either structural or functional MRI and very little is known about the link between structure and function as well as how it is impacted by a stroke. Therefore, in the first part of this thesis I investigated the structure-function relationship in stroke patients, as well as its link to behavior. Furthermore, based on a need for reproducible analysis pipelines, which is especially important in the context of clinical studies, the second part of this thesis addressed the reproducibility of structural connectivity in the context of microstructure-informed tractography.

Collectively, with the work I presented in this thesis, I established that the SDI – a recently introduced method to assess structure-function coupling (Preti & Van De Ville, 2019) – is sensitive to pathophysiological changes that occur following a stroke and the reorganization thereafter. In doing so, I additionally showed that post-stroke changes in SDI link to clinically relevant behavioral measures and that the corresponding brain patterns are associated to behavioral changes over time. Moreover, I complemented these findings with a study evaluating reproducibility and subject-specificity of microstructure-informed connectivity. We showed that microstructure-informed tractography seems to improve biological meaning of white matter reconstructions, while keeping a high subject specificity, suggesting that filtering methods such as SIFT2 and COMMIT can improve current DWI analytical pipelines.

The current evidence presented in this thesis shows that structure-function coupling is a promising new approach to study the impact of stroke on the brain as well as its reorganization thereafter and it portrays the SDI as an auspicious potential candidate to become a predictive biomarker for post-stroke recovery in the future. However, one question remains – did this thesis bring the field a step closer to patient stratification? The present work is merely a first and nevertheless important step in that direction. Indeed, by quantifying the relationship between neuropsychological measures of function and variations in post-stroke structure-function coupling and by adapting the SDI method to be used with individual patient's data, we are moving closer to the main goal, which is to determine whether it can add to the prediction of recovery and response to treatment based on a patient-specific biomarker derived from structure-function coupling. Nevertheless, the clinical relevance and time-specificities of the SDI need to be further confirmed, especially on the level of the individual patient and considering key brain areas identified in this thesis. In this context, it will be important to link intra-individual behavioral scores with intra-individual SDI values in specific areas of interest and understanding their evolution over time, before attempting to stratify patients based on these findings.

Considering clinical relevance, it is important to keep in mind the difference between statistical significance and clinical relevance or importance when performing clinical studies. A significant difference is not always clinically relevant and vice-versa. Taking the example of the SDI as a hypothetical future biomarker, a clinical relevant enhancement could be seen as a higher prediction accuracy compared to existing methods which are already applied in clinics, such as PREP2, which has a prediction accuracy of 75% (Connell et al., 2021; Stinear et al., 2017). However, “higher” doesn't necessarily mean “statistically significantly higher”, meaning that a prediction accuracy of, e.g., 76% would probably not be considered clinically relevant. But what or who determines what is clinically relevant? LeFort (1993) suggests that clinical relevance or significance is dependent on “the extent of change, whether the change makes a real difference to subject lives, how long the effects last, consumer acceptability, cost-effectiveness and ease of implementation”. In contrast to statistical significance testing, there is however no fixed threshold that evaluates clinical

significance/relevance (Fethney, 2010), and frequently it is the judgment of the clinician, and sometimes the patient, that determines whether or not a result is clinically significant/relevant (Ranganathan et al., 2015). It is hence not possible to give a clear answer to what minimum prediction accuracy would be needed for the SDI to represent a clinically significant biomarker, as this would depend on the multiple factors mentioned above. One clear advantage of the SDI as a new biomarker, however, would consist in the fact that most patients undergo a clinical MRI anyhow within the first few days of in-patient care and it would thus be straightforward to integrate the necessary measurements in the already established clinical routine.

In conclusion, by studying the structure-function coupling in stroke patients, this thesis lays at the intersection of clinical translational and basic systems neuroscience and opens a completely new and multimodal perspective of how to look at the lesioned brain. Combined with the rich behavioral dataset collected in the TiMeS project, this innovative metric offers a whole new range of possibilities to investigate the complex mechanisms of post-stroke reorganization, thereby hopefully paving the way towards a better individualized understanding of post-stroke recovery leading to individualized, precision medicine-based treatments. Indeed, future research endeavors have to investigate to what degree the SDI can predict outcome, course of the disorder or treatment responses, such as to non-invasive brain stimulation.

References

- Alexander, D. C. (2008). A general framework for experiment design in diffusion MRI and its application in measuring direct tissue-microstructure features. *Magnetic Resonance in Medicine*, 60(2), 439–448. <https://doi.org/10.1002/mrm.21646>
- Alexander, D. C., Zikic, D., Ghosh, A., Tanno, R., Wotschel, V., Zhang, J., Kaden, E., Dyrby, T. B., Sotiropoulos, S. N., Zhang, H., & Criminisi, A. (2017). Image quality transfer and applications in diffusion MRI. *NeuroImage*, 152, 283–298. <https://doi.org/10.1016/j.neuroimage.2017.02.089>
- Alia, C., Spalletti, C., Lai, S., Panarese, A., Micera, S., & Caleo, M. (2016). Reducing GABAA-mediated inhibition improves forelimb motor function after focal cortical stroke in mice. *Scientific Reports*, 6(1), 37823. <https://doi.org/10.1038/srep37823>
- Alstott, J., Breakspear, M., Hagmann, P., Cammoun, L., & Sporns, O. (2009). Modeling the Impact of Lesions in the Human Brain. *PLoS Computational Biology*, 5(6), e1000408. <https://doi.org/10.1371/journal.pcbi.1000408>
- Amico, E., & Goñi, J. (2018). The quest for identifiability in human functional connectomes. *Scientific Reports* 2018 8:1, 8(1), 1–14. <https://doi.org/10.1038/s41598-018-25089-1>
- Andersson, J. L. R., Jenkinson, M., & Smith, S. (2010). *Non-linear registration aka Spatial normalisation, FMRIB Technial Report TR07JA2*.
- Andersson, J. L. R., Skare, S., & Ashburner, J. (2003). How to correct susceptibility distortions in spin-echo echo-planar images: Application to diffusion tensor imaging. *NeuroImage*, 20(2), 870–888. [https://doi.org/10.1016/S1053-8119\(03\)00336-7](https://doi.org/10.1016/S1053-8119(03)00336-7)
- Andersson, J. L. R., & Sotiropoulos, S. N. (2016). An integrated approach to correction for off-resonance effects and subject movement in diffusion MR imaging. *NeuroImage*, 125, 1063–1078. <https://doi.org/10.1016/j.neuroimage.2015.10.019>
- Appelros, P., Karlsson, G. M., Seiger, A., & Nydevik, I. (2002). Neglect and Anosognosia After First-Ever Stroke: Incidence and Relationship to Disability. *Journal of Rehabilitation Medicine*, 34(5), 215–220. <https://doi.org/10.1080/165019702760279206>
- Ashburner, J., Barnes, G., Chen, C., Daunizeau, J., Flandin, G., Friston, K., Kiebel, S., Kilner, J., Litvak, V., Moran, R., Penny, W., Stephan, K., Gitelman, D., Henson, R., Hutton, C., Glauche, V., & Phillips, C. (2014). *SPM12 Manual The FIL Methods Group (and honorary members)*.
- Assaf, Y., Johansen-Berg, H., & Thiebaut de Schotten, M. (2017). The role of diffusion MRI in neuroscience. *NMR in Biomedicine*, September 2016, 1–16. <https://doi.org/10.1002/nbm.3762>
- Baldassarre, A., Ramsey, L., Rengachary, J., Zinn, K., Siegel, J. S., Metcalf, N. V., Strube, M. J., Snyder, A. Z., Corbetta, M., & Shulman, G. L. (2016). Dissociated functional connectivity profiles for motor and attention deficits in acute right-hemisphere stroke. *Brain*, 139(7), 2024–2038. <https://doi.org/10.1093/brain/aww107>
- Banks, S. J., Zhuang, X., Bayram, E., Bird, C., Cordes, D., Caldwell, J. Z. K., & Cummings, J. L. (2018). Default Mode Network Lateralization and Memory in Healthy Aging and Alzheimer’s Disease. *Journal of Alzheimer’s Disease*, 66(3), 1223–1234. <https://doi.org/10.3233/JAD-180541>

References

- Barakovic, M., Girard, G., Schiavi, S., Romascano, D., Descoteaux, M., Granziera, C., Jones, D. K., Innocenti, G. M., Thiran, J.-P., & Daducci, A. (2021). Bundle-Specific Axon Diameter Index as a New Contrast to Differentiate White Matter Tracts. *Frontiers in Neuroscience*, 0, 687. <https://doi.org/10.3389/FNINS.2021.646034>
- Barakovic, M., Romascano, D., Dyrby, T., Alexander, D., Descoteaux, M., & Jean-Philippe Thiran, A. D. (2016). Assessment of bundle-specific axon diameter distributions using diffusion MRI tractography. *Organization for Human Brain Mapping (HBM'16)*.
- Barakovic, M., Tax, C. M. W., Rudrapatna, U., Chamberland, M., Rafael-Patino, J., Granziera, C., Thiran, J. P., Daducci, A., Canales-Rodríguez, E. J., & Jones, D. K. (2021). Resolving bundle-specific intra-axonal T2 values within a voxel using diffusion-relaxation tract-based estimation. *NeuroImage*, 227, 117617. <https://doi.org/10.1016/j.neuroimage.2020.117617>
- Barrett, A. M., Boukrina, O., & Saleh, S. (2019). Ventral attention and motor network connectivity is relevant to functional impairment in spatial neglect after right brain stroke. *Brain and Cognition*, 129, 16–24. <https://doi.org/10.1016/j.bandc.2018.11.013>
- Bartolomeo, P., & Seidel Malkinson, T. (2019). Hemispheric lateralization of attention processes in the human brain. *Current Opinion in Psychology*, 29, 90–96. <https://doi.org/10.1016/j.copsyc.2018.12.023>
- Bassett, D. S., & Sporns, O. (2017). Network neuroscience. *Nature Neuroscience*, 20(3), 353–364. <https://doi.org/10.1038/nn.4502>
- Bates, D., Mächler, M., Bolker, B., & Walker, S. (2014). Fitting Linear Mixed-Effects Models using lme4. *ArXiv:1406.5823 [Stat]*. <http://arxiv.org/abs/1406.5823>
- Bavelier, D., Levi, D. M., Li, R. W., Dan, Y., & Hensch, T. K. (2010). Removing Brakes on Adult Brain Plasticity: From Molecular to Behavioral Interventions. *Journal of Neuroscience*, 30(45), 14964–14971. <https://doi.org/10.1523/JNEUROSCI.4812-10.2010>
- Beaulieu, C. (2014). The Biological Basis of Diffusion Anisotropy. In *Diffusion MRI* (pp. 155–183). Elsevier. <https://doi.org/10.1016/B978-0-12-396460-1.00008-1>
- Belliveau, J. W., Kennedy, D. N., McKinstry, R. C., Buchbinder, B. R., Weisskoff, R. M., Cohen, M. S., Vevea, J. M., Brady, T. J., & Rosen, B. R. (1991). Functional Mapping of the Human Visual Cortex by Magnetic Resonance Imaging. *Science*, 254(5032), 716–719.
- Bernard, F., Lemee, J., Mazerand, E., Leiber, L., Menei, P., & Ter Minassian, A. (2020). The ventral attention network: The mirror of the language network in the right brain hemisphere. *Journal of Anatomy*, 237(4), 632–642. <https://doi.org/10.1111/joa.13223>
- Besancon, E., Guo, S., Lok, J., Tymianski, M., & Lo, E. H. (2008). Beyond NMDA and AMPA glutamate receptors: Emerging mechanisms for ionic imbalance and cell death in stroke. *Trends in Pharmacological Sciences*, 29(5), 268–275. <https://doi.org/10.1016/j.tips.2008.02.003>
- Besson, P., Lopes, R., Leclerc, X., Derambure, P., & Tyvaert, L. (2014). Intra-subject reliability of the high-resolution whole-brain structural connectome. *NeuroImage*, 102(P2), 283–293. <https://doi.org/10.1016/j.neuroimage.2014.07.064>
- Bids-apps/MRtrix3_connectome*. (2022). [Python]. BIDS Apps. https://github.com/bids-apps/MRtrix3_connectome (Original work published 2016)

References

- Biernaskie, J. (2004). Efficacy of Rehabilitative Experience Declines with Time after Focal Ischemic Brain Injury. *Journal of Neuroscience*, 24(5), 1245–1254. <https://doi.org/10.1523/JNEUROSCI.3834-03.2004>
- Birn, R. M., Molloy, E. K., Patriat, R., Parker, T., Meier, T. B., Kirk, G. R., Nair, V. A., Meyerand, M. E., & Prabhakaran, V. (2013). The effect of scan length on the reliability of resting-state fMRI connectivity estimates. *Neuroimage*, 83, 550–558.
- Biswal, B. B., Kylen, J. V., & Hyde, J. S. (1997). Simultaneous assessment of flow and BOLD signals in resting-state functional connectivity maps. *NMR in Biomedicine: An International Journal Devoted to the Development and Application of Magnetic Resonance In Vivo*, 10(4–5), 165–170.
- Biswal, B., Zerrin Yetkin, F., Haughton, V. M., & Hyde, J. S. (1995). Functional connectivity in the motor cortex of resting human brain using echo-planar mri. *Magnetic Resonance in Medicine*, 34(4), 537–541. <https://doi.org/10.1002/mrm.1910340409>
- Blyth, R., Cook, P., & Alexander, D. (2003). *Tractography with multiple fibre directions*. 1.
- Boes, A. D., Prasad, S., Liu, H., Liu, Q., Pascual-Leone, A., Caviness, V. S., Jr, & Fox, M. D. (2015). Network localization of neurological symptoms from focal brain lesions. *Brain*, 138(10), 3061–3075. <https://doi.org/10.1093/brain/awv228>
- Bolay, H., Gürsoy-Özdemir, Y., Sara, Y., Onur, R., Can, A., & Dalkara, T. (2002). Persistent Defect in Transmitter Release and Synapsin Phosphorylation in Cerebral Cortex After Transient Moderate Ischemic Injury. *Stroke*, 33(5), 1369–1375. <https://doi.org/10.1161/01.STR.0000013708.54623.DE>
- Bonilha, L., Gleichgerrcht, E., Fridriksson, J., Breedlove, J. L., Rorden, C., Nesland, T., Paulus, W., Helms, G., & Focke, N. K. (2015). Reproducibility of the structural brain connectome derived from diffusion tensor imaging. *PLoS ONE*, 10(9), 1–17. <https://doi.org/10.1371/journal.pone.0135247>
- Bonkhoff, A. K., Hope, T., Bzdok, D., Guggisberg, A. G., Hawe, R. L., Dukelow, S. P., Chollet, F., Lin, D. J., Grefkes, C., & Bowman, H. (2022). Recovery after stroke: The severely impaired are a distinct group. *Journal of Neurology, Neurosurgery, and Psychiatry*, 93(4), 369–378. <https://doi.org/10.1136/jnnp-2021-327211>
- Bonkhoff, A. K., Hope, T., Bzdok, D., Guggisberg, A. G., Hawe, R. L., Dukelow, S. P., Rehme, A. K., Fink, G. R., Grefkes, C., & Bowman, H. (2020). Bringing proportional recovery into proportion: Bayesian modelling of post-stroke motor impairment. *Brain: A Journal of Neurology*, 143(7), 2189–2206. <https://doi.org/10.1093/brain/awaa146>
- Boussaoud, D., Tanné-Gariépy, J., Wannier, T., & Rouiller, E. M. (2005). Callosal connections of dorsal versus ventral premotor areas in the macaque monkey: A multiple retrograde tracing study. *BMC Neuroscience*, 6(1), 1–18.
- Boyd, L. A., Hayward, K. S., Ward, N. S., Stinear, C. M., Rosso, C., Fisher, R. J., Carter, A. R., Leff, A. P., Copland, D. A., Carey, L. M., Cohen, L. G., Basso, D. M., Maguire, J. M., & Cramer, S. C. (2017). Biomarkers of stroke recovery: Consensus-based core recommendations from the Stroke Recovery and Rehabilitation Roundtable. *International Journal of Stroke*, 12(5), 480–493. <https://doi.org/10.1177/1747493017714176>
- Bray, J. R., & Curtis, J. T. (1957). An Ordination of the Upland Forest Communities of Southern Wisconsin. *Ecological Monographs*, 27(4), 325–349. <https://doi.org/10.2307/1942268>

References

- Brodmann, K. (1909). *Vergleichende Lokalisationslehre der Grosshirnrinde in ihren Prinzipien dargestellt auf Grund des Zellenbaues*. Barth.
- Brown, C. E., Aminoltejari, K., Erb, H., Winship, I. R., & Murphy, T. H. (2009). In Vivo Voltage-Sensitive Dye Imaging in Adult Mice Reveals That Somatosensory Maps Lost to Stroke Are Replaced over Weeks by New Structural and Functional Circuits with Prolonged Modes of Activation within Both the Peri-Infarct Zone and Distant Sites. *Journal of Neuroscience*, 29(6), 1719–1734. <https://doi.org/10.1523/JNEUROSCI.4249-08.2009>
- Brown, C. E., Li, P., Boyd, J. D., Delaney, K. R., & Murphy, T. H. (2007). Extensive Turnover of Dendritic Spines and Vascular Remodeling in Cortical Tissues Recovering from Stroke. *Journal of Neuroscience*, 27(15), 4101–4109. <https://doi.org/10.1523/JNEUROSCI.4295-06.2007>
- Brügger, J., Koch, P. J., Preti, M. G., Park, C.-H., Cadic-Melchior, A., Ceroni, M., Fleury, L., Wessel, M. J., Maceira-Elvira, P., Popa, T., Beanato, E., Meyer, N., Blanke, O., Adolphsen, J., Jagella, C., Constantin, C., Alvarez, V., Ghika, J.-A., Léger, B., ... Hummel, F. C. (in preparation, see Study 1). *Acute changes in the coupling strength between brain structure and function following a stroke*.
- Brumer, I., De Vita, E., Ashmore, J., Jarosz, J., & Borri, M. (2021). Reproducibility of MRI-based white matter tract estimation using multi-fiber probabilistic tractography: Effect of user-defined parameters and regions. *Magnetic Resonance Materials in Physics, Biology and Medicine*. <https://doi.org/10.1007/s10334-021-00965-6>
- Buch, E. R., Rizk, S., Nicolo, P., Cohen, L. G., Schnider, A., & Guggisberg, A. G. (2016). Predicting motor improvement after stroke with clinical assessment and diffusion tensor imaging. *Neurology*, 86(20), 1924–1925. <https://doi.org/10.1212/WNL.0000000000002675>
- Bullmore, E., & Sporns, O. (2009). Complex brain networks: Graph theoretical analysis of structural and functional systems. *Nature Reviews Neuroscience*, 10(3), 186–198. <https://doi.org/10.1038/nrn2575>
- Buma, F. E., Lindeman, E., Ramsey, N. F., & Kwakkel, G. (2010). Review: Functional Neuroimaging Studies of Early Upper Limb Recovery After Stroke: A Systematic Review of the Literature. *Neurorehabilitation and Neural Repair*, 24(7), 589–608. <https://doi.org/10.1177/1545968310364058>
- Butefisch, C. M. (2003). Remote changes in cortical excitability after stroke. *Brain*, 126(2), 470–481. <https://doi.org/10.1093/brain/awg044>
- Buxbaum, L. J., Ferraro, M. K., Veramonti, T., Farne, A., Whyte, J., Ladavas, E., Frassinetti, F., & Coslett, H. B. (2004). Hemispatial neglect: Subtypes, neuroanatomy, and disability. *Neurology*, 62(5), 749–756. <https://doi.org/10.1212/01.WNL.0000113730.73031.F4>
- Byblow, W. D., Stinear, C. M., Barber, P. A., Petoe, M. A., & Ackerley, S. J. (2015). Proportional recovery after stroke depends on corticomotor integrity: Proportional Recovery After Stroke. *Annals of Neurology*, 78(6), 848–859. <https://doi.org/10.1002/ana.24472>
- Calamante, F., Tournier, J.-D., Jackson, G. D., & Connelly, A. (2010). Track-density imaging (TDI): Super-resolution white matter imaging using whole-brain track-density mapping. *NeuroImage*, 53(4), 1233–1243. <https://doi.org/10.1016/j.neuroimage.2010.07.024>
- Campbell, K. L., Grady, C. L., Ng, C., & Hasher, L. (2012). Age differences in the frontoparietal cognitive control network: Implications for distractibility. *Neuropsychologia*, 50(9), 2212–2223. <https://doi.org/10.1016/j.neuropsychologia.2012.05.025>

References

- Canales-Rodríguez, E. J., Daducci, A., Sotiropoulos, S. N., Caruyer, E., Aja-Fernández, S., Radua, J., Mendizabal, J. M. Y., Iturria-Medina, Y., Melie-García, L., Alemán-Gómez, Y., Thiran, J. P., Sarró, S., Pomarol-Clotet, E., & Salvador, R. (2015). Spherical deconvolution of multichannel diffusion MRI data with non-Gaussian noise models and spatial regularization. *PLoS ONE*, 10(10), 1–29. <https://doi.org/10.1371/journal.pone.0138910>
- Canales-Rodríguez, E. J., Legarreta, J. H., Pizzolato, M., Rensonnet, G., Girard, G., Patino, J. R., Barakovic, M., Romascano, D., Alemán-Gómez, Y., Radua, J., Pomarol-Clotet, E., Salvador, R., Thiran, J. P., & Daducci, A. (2019). Sparse wars: A survey and comparative study of spherical deconvolution algorithms for diffusion MRI. *NeuroImage*, 184, 140–160. <https://doi.org/10.1016/j.neuroimage.2018.08.071>
- Carmichael, S. T. (2003). Plasticity of Cortical Projections after Stroke. *The Neuroscientist*, 9(1), 64–75. <https://doi.org/10.1177/1073858402239592>
- Carmichael, S. T. (2012). Brain Excitability in Stroke: The Yin and Yang of Stroke Progression. *Archives of Neurology*, 69(2), 161. <https://doi.org/10.1001/archneurol.2011.1175>
- Carmichael, S. T., & Chesselet, M.-F. (2002). Synchronous Neuronal Activity Is a Signal for Axonal Sprouting after Cortical Lesions in the Adult. *The Journal of Neuroscience*, 22(14), 6062–6070. <https://doi.org/10.1523/JNEUROSCI.22-14-06062.2002>
- Carmichael, S. T., Tatsukawa, K., Katsman, D., Tsuyuguchi, N., & Kornblum, H. I. (2004). Evolution of Diaschisis in a Focal Stroke Model. *Stroke*, 35(3), 758–763. <https://doi.org/10.1161/01.STR.0000117235.11156.55>
- Carmichael, S. T., Wei, L., Rovainen, C. M., & Woolsey, T. A. (2001). New Patterns of Intracortical Projections after Focal Cortical Stroke. *Neurobiology of Disease*, 8(5), 910–922. <https://doi.org/10.1006/nbdi.2001.0425>
- Carneiro, A. A. O., Vilela, G. R., Araujo, D. B. de, & Baffa, O. (2006). MRI relaxometry: Methods and applications. *Brazilian Journal of Physics*, 36(1a). <https://doi.org/10.1590/S0103-97332006000100005>
- Carrera, E., & Tononi, G. (2014). Diaschisis: Past, present, future. *Brain*, 137(9), 2408–2422. <https://doi.org/10.1093/brain/awu101>
- Carter, A. R., Astafiev, S. V., Lang, C. E., Connor, L. T., Rengachary, J., Strube, M. J., Pope, D. L. W., Shulman, G. L., & Corbetta, M. (2010). Resting interhemispheric functional magnetic resonance imaging connectivity predicts performance after stroke. *Annals of Neurology*, 67(3), 365–375. <https://doi.org/10.1002/ana.21905>
- Chen, J. L., & Schlaug, G. (2013). Resting State Interhemispheric Motor Connectivity and White Matter Integrity Correlate with Motor Impairment in Chronic Stroke. *Frontiers in Neurology*, 4, 178. <https://doi.org/10.3389/fneur.2013.00178>
- Chen, S., Zeng, L., & Hu, Z. (2014). Progressing haemorrhagic stroke: Categories, causes, mechanisms and managements. *Journal of Neurology*, 261(11), 2061–2078. <https://doi.org/10.1007/s00415-014-7291-1>
- Choi, I.-Y., & Jezard, P. (2021). *ADVANCED NEURO MR TECHNIQUES AND APPLICATIONS*. ELSEVIER ACADEMIC PRESS.

References

- Chopp, M., Zhang, Z. G., & Jiang, Q. (2007). Neurogenesis, Angiogenesis, and MRI Indices of Functional Recovery From Stroke. *Stroke*, 38(2), 827–831. <https://doi.org/10.1161/01.STR.0000250235.80253.e9>
- Chu, C.-Y., Huang, J.-P., Sun, C.-Y., Zhang, Y.-L., Liu, W.-Y., & Zhu, Y.-M. (2015). *Estimating intravoxel fiber architecture using constrained compressed sensing combined with multitensor adaptive smoothing*. 12.
- Ciesla, N., Dinglas, V., Fan, E., Kho, M., Kuramoto, J., & Needham, D. (2011). Manual Muscle Testing: A Method of Measuring Extremity Muscle Strength Applied to Critically Ill Patients. *Journal of Visualized Experiments : JoVE*, 50, 2632. <https://doi.org/10.3791/2632>
- Cioli, C., Abdi, H., Beaton, D., Burnod, Y., & Mesmoudi, S. (2014). Differences in Human Cortical Gene Expression Match the Temporal Properties of Large-Scale Functional Networks. *PLoS ONE*, 9(12), e115913. <https://doi.org/10.1371/journal.pone.0115913>
- Clarkson, A. N., Huang, B. S., MacIsaac, S. E., Mody, I., & Carmichael, S. T. (2010). Reducing excessive GABA-mediated tonic inhibition promotes functional recovery after stroke. *Nature*, 468(7321), 305–309. <https://doi.org/10.1038/nature09511>
- Colon-Perez, L. M., Couret, M., Triplett, W., Price, C. C., & Mareci, T. H. (2016). Small Worldness in Dense and Weighted Connectomes. *Frontiers in Physics*, 4(MAY). <https://doi.org/10.3389/FPHY.2016.00014>
- Connell, L. A., Chesworth, B., Ackerley, S., Smith, M.-C., & Stinear, C. M. (2021). Implementing the PREP2 Algorithm to Predict Upper Limb Recovery Potential After Stroke in Clinical Practice: A Qualitative Study. *Physical Therapy*, 101(5), pzab040. <https://doi.org/10.1093/ptj/pzab040>
- Corbetta, M., Ramsey, L., Callejas, A., Baldassarre, A., Hacker, C. D., Siegel, J. S., Astafiev, S. V., Rengachary, J., Zinn, K., Lang, C. E., Connor, L. T., Fucetola, R., Strube, M., Carter, A. R., & Shulman, G. L. (2015). Common Behavioral Clusters and Subcortical Anatomy in Stroke. *Neuron*, 85(5), 927–941. <https://doi.org/10.1016/j.neuron.2015.02.027>
- Cramer, S. C., Koroshetz, W. J., & Finklestein, S. P. (2007). *The Case for Modality-Specific Outcome Measures in Clinical Trials of Stroke Recovery-Promoting Agents*. 3.
- CRediT author statement. (2022). <https://www.elsevier.com/authors/policies-and-guidelines/credit-author-statement>
- Crofts, A., Kelly, M. E., & Gibson, C. L. (2020). Imaging Functional Recovery Following Ischemic Stroke: Clinical and Preclinical fMRI Studies. *Journal of Neuroimaging*, 30(1), 5–14. <https://doi.org/10.1111/jon.12668>
- Daducci, A., Canales-Rodriguez, E. J., Descoteaux, M., Garyfallidis, E., Gur, Y., Lin, Y. C., Mani, M., Merlet, S., Paquette, M., Ramirez-Manzanares, A., Reisert, M., Rodrigues, P. R., Seppehrband, F., Caruyer, E., Choupan, J., Deriche, R., Jacob, M., Menegaz, G., Prckovska, V., ... Thiran, J. P. (2014). Quantitative comparison of reconstruction methods for intra-voxel fiber recovery from diffusion MRI. *IEEE Transactions on Medical Imaging*, 33(2), 384–399. <https://doi.org/10.1109/TMI.2013.2285500>
- Daducci, A., Dal Palu, A., Lemkaddem, A., & Thiran, J.-P. (2013). A convex optimization framework for global tractography. *IEEE International Symposium on Biomedical Imaging*, 524–527. <https://doi.org/10.1109/ISBI.2013.6556527>

References

- Daducci, A., Dal Palu, A., Lemkaddem, A., & Thiran, J.-P. (2015). COMMIT: Convex Optimization Modeling for Microstructure Informed Tractography. *IEEE Transactions on Medical Imaging*, 34(1), 246–257. <https://doi.org/10.1109/TMI.2014.2352414>
- Damoiseaux, J. S. (2017). Effects of aging on functional and structural brain connectivity. *NeuroImage*, 160, 32–40. <https://doi.org/10.1016/j.neuroimage.2017.01.077>
- Dayan, M., Kreutzer, S., & Clark, C. A. (2015). Tractography of the optic radiation: A repeatability and reproducibility study. *NMR in Biomedicine*, 28(4), 423–431. <https://doi.org/10.1002/NBM.3266>
- Deco, G., Jirsa, V. K., & McIntosh, A. R. (2011). Emerging concepts for the dynamical organization of resting-state activity in the brain. *Nature Reviews Neuroscience*, 12(1), 43–56. <https://doi.org/10.1038/nrn2961>
- Deco, G., Jirsa, V., McIntosh, A. R., Sporns, O., & Kotter, R. (2009). Key role of coupling, delay, and noise in resting brain fluctuations. *Proceedings of the National Academy of Sciences*, 106(25), 10302–10307. <https://doi.org/10.1073/pnas.0901831106>
- Deco, G., Senden, M., & Jirsa, V. (2012). How anatomy shapes dynamics: A semi-analytical study of the brain at rest by a simple spin model. *Frontiers in Computational Neuroscience*, 6. <https://doi.org/10.3389/fncom.2012.00068>
- D’Elia, L. F., Satz, P., Uchiyama, C., & White, T. (1996). Color Trails Test Professional Manual. *Psychological Assessment Resources*.
- Descoteaux, M., Deriche, R., Knosche, T. R., & Anwander, A. (2009). Deterministic and Probabilistic Tractography Based on Complex Fibre Orientation Distributions. *IEEE Transactions on Medical Imaging*, 28(2), 269–286. <https://doi.org/10.1109/TMI.2008.2004424>
- Destrieux, C., Fischl, B., Dale, A., & Halgren, E. (2010). Automatic parcellation of human cortical gyri and sulci using standard anatomical nomenclature. *NeuroImage*, 53(1), 1–15. <https://doi.org/10.1016/j.neuroimage.2010.06.010>
- Dhanis, H., Blondiaux, E., Bolton, T., Faivre, N., Rognini, G., Van De Ville, D., & Blanke, O. (2022). Robotically-induced hallucination triggers subtle changes in brain network transitions. *NeuroImage*, 248, 118862. <https://doi.org/10.1016/j.neuroimage.2021.118862>
- DMRIPrep. (2022). [Python]. NeuroImaging PREProcessing toolS. <https://github.com/nipreps/dmriprep> (Original work published 2019)
- Dolivo, C., & Assal, G. (1985). Tests neuropsychologiques rapides pour la recherche d’une détérioration intellectuelle. *Psychologie Médicale*, 17(14), 2093–2095.
- Doughty, C., Wang, J., Feng, W., Hackney, D., Pani, E., & Schlaug, G. (2016). Detection and Predictive Value of Fractional Anisotropy Changes of the Corticospinal Tract in the Acute Phase of a Stroke. *Stroke*, 47(6), 1520–1526. <https://doi.org/10.1161/STROKEAHA.115.012088>
- Dum, R. P., & Strick, P. L. (1996). Spinal Cord Terminations of the Medial Wall Motor Areas in Macaque Monkeys. *Journal of Neuroscience*, 16(20), 6513–6525. <https://doi.org/10.1523/JNEUROSCI.16-20-06513.1996>
- Duncan, P. W., Min Lai, S., & Keighley, J. (2000). Defining post-stroke recovery: Implications for design and interpretation of drug trials. *Neuropharmacology*, 39(5), 835–841. [https://doi.org/10.1016/S0028-3908\(00\)00003-4](https://doi.org/10.1016/S0028-3908(00)00003-4)

References

- Efron, B., & Tibshirani, R. (1986). Bootstrap Methods for Standard Errors, Confidence Intervals, and Other Measures of Statistical Accuracy. *Statistical Science*, 1(1), 54–75. <https://doi.org/10.1214/ss/1177013815>
- Egger, P., Evangelista, G. G., Koch, P. J., Park, C.-H., Levin-Gleba, L., Girard, G., Beanato, E., Lee, J., Choirat, C., Guggisberg, A. G., Kim, Y.-H., & Hummel, F. C. (2021). Disconnectomics of the Rich Club Impacts Motor Recovery After Stroke. *Stroke*, 52(6), 2115–2124. <https://doi.org/10.1161/STROKEAHA.120.031541>
- Esteban, O., Markiewicz, C. J., Blair, R. W., Moodie, C. A., Isik, A. I., Erramuzpe, A., Kent, J. D., Goncalves, M., DuPre, E., Snyder, M., Oya, H., Ghosh, S. S., Wright, J., Durnez, J., Poldrack, R. A., & Gorgolewski, K. J. (2019). fMRIPrep: A robust preprocessing pipeline for functional MRI. *Nature Methods*, 16(1), 111–116. <https://doi.org/10.1038/s41592-018-0235-4>
- Evangelista, G. G., Egger, P., Brügger, J., Beanato, E., Koch, P. J., Ceroni, M., Fleury, L., Cadic-Melchior, A., Meyer, N., de León Rodríguez, D., Girard, G., Léger, B., Turlan, J.-L., Mühl, A., Vuadens, P., Adolphsen, J., Jagella, C., Constantin, C., Alvarez, V., ... Hummel, F. C. (under revision, see Appendix). *Differential impact of brain network efficiency on post-stroke motor and attentional deficits*.
- Fan, Y., Wu, C., Liu, H., Lin, K., Wai, Y., & Chen, Y. (2015). Neuroplastic changes in resting-state functional connectivity after stroke rehabilitation. *Frontiers in Human Neuroscience*, 9, 546. <https://doi.org/10.3389/fnhum.2015.00546>
- Favre, I., Zeffiro, T. A., Detante, O., Krainik, A., Hommel, M., & Jaillard, A. (2014). Upper Limb Recovery After Stroke Is Associated With Ipsilesional Primary Motor Cortical Activity. *Stroke*, 45(4), 1077–1083. <https://doi.org/10.1161/STROKEAHA.113.003168>
- Felling, R. J., & Song, H. (2015). Epigenetic mechanisms of neuroplasticity and the implications for stroke recovery. *Experimental Neurology*, 268, 37–45. <https://doi.org/10.1016/j.expneurol.2014.09.017>
- Feng, W., Wang, J., Chhatbar, P. Y., Doughty, C., Landsittel, D., Lioutas, V.-A., Kautz, S. A., & Schlaug, G. (2015). Corticospinal tract lesion load: An imaging biomarker for stroke motor outcomes: CST Lesion Load Predicts Stroke Motor Outcomes. *Annals of Neurology*, 78(6), 860–870. <https://doi.org/10.1002/ana.24510>
- Fethney, J. (2010). Statistical and clinical significance, and how to use confidence intervals to help interpret both. *Australian Critical Care*, 23(2), 93–97. <https://doi.org/10.1016/j.aucc.2010.03.001>
- Filippi, M. (2015). *Oxford textbook of neuroimaging*. Oxford University Press.
- Finn, E. S., Shen, X., Scheinost, D., Rosenberg, M. D., Huang, J., Chun, M. M., Papademetris, X., & Constable, R. T. (2015). Functional connectome fingerprinting: Identifying individuals based on patterns of brain connectivity. *Nature Neuroscience*, 18(11), 1664. <https://doi.org/10.1038/NN.4135>
- Fischl, B. (2004). Automatically Parcellating the Human Cerebral Cortex. *Cerebral Cortex*, 14(1), 11–22. <https://doi.org/10.1093/cercor/bhg087>
- Fischl, B. (2012). FreeSurfer. *NeuroImage*, 62(2), 774–781. <https://doi.org/10.1016/j.neuroimage.2012.01.021>
- Fischl, B., Salat, D. H., Busa, E., Albert, M., Dieterich, M., Haselgrove, C., van der Kouwe, A., Killiany, R., Kennedy, D., Klaveness, S., Montillo, A., Makris, N., Rosen, B., & Dale, A. M. (2002). Whole brain segmentation: Automated labeling of neuroanatomical structures in the human brain. *Neuron*, 33(3), 341–355.

References

- Fischl, B., van der Kouwe, A., Destrieux, C., Halgren, E., Ségonne, F., Salat, D. H., Busa, E., Seidman, L. J., Goldstein, J., Kennedy, D., Caviness, V., Makris, N., Rosen, B., & Dale, A. M. (2004). Automatically Parcellating the Human Cerebral Cortex. *Cerebral Cortex*, 14(1), 11–22. <https://doi.org/10.1093/cercor/bhg087>
- Fornito, A., Zalesky, A., & Breakspear, M. (2013). Graph analysis of the human connectome: Promise, progress, and pitfalls. *NeuroImage*, 80, 426–444. <https://doi.org/10.1016/j.neuroimage.2013.04.087>
- Fox, M. D. (2018). Mapping Symptoms to Brain Networks with the Human Connectome. *New England Journal of Medicine*, 379(23), 2237–2245. <https://doi.org/10.1056/NEJMra1706158>
- Frässle, S., Lomakina, E. I., Razi, A., Friston, K. J., Buhmann, J. M., & Stephan, K. E. (2017). Regression DCM for fMRI. *NeuroImage*, 155, 406–421. <https://doi.org/10.1016/j.neuroimage.2017.02.090>
- Fries, P. (2005). A mechanism for cognitive dynamics: Neuronal communication through neuronal coherence. *Trends in Cognitive Sciences*, 9(10), 474–480. <https://doi.org/10.1016/j.tics.2005.08.011>
- Frigo, M., Deslauriers-Gauthier, S., Parker, D., Aziz Ould Ismail, A., John Kim, J., Verma, R., & Deriche, R. (2020). Diffusion MRI tractography filtering techniques change the topology of structural connectomes. *Journal of Neural Engineering*, 17(6), 065002. <https://doi.org/10.1088/1741-2552/abc29b>
- Friston, K. J. (1994). Functional and effective connectivity in neuroimaging: A synthesis. *Human Brain Mapping*, 2(1–2), 56–78. <https://doi.org/10.1002/hbm.460020107>
- Friston, K. J., Harrison, L., & Penny, W. (2003). Dynamic causal modelling. *NeuroImage*, 19(4), 1273–1302. [https://doi.org/10.1016/S1053-8119\(03\)00202-7](https://doi.org/10.1016/S1053-8119(03)00202-7)
- Fritsch, G., & Hitzig, E. (1870). Über die elektrische Erregbarkeit des Grosshirns. *Arch Anat Physiol Wissen* 1870; 37: 300–332. Reprinted in 2009: Electric Excitability of the cerebrum. *Epilepsy and Behavior*, 15, 123–130.
- Fugl-Meyer, A. R. (1980). Post-stroke hemiplegia assessment of physical properties. *Scandinavian Journal of Rehabilitation Medicine. Supplement*, 7, 85–93.
- Fulton, J. F., & Sheehan, D. (1935). The uncrossed lateral pyramidal tract in higher primates. *Journal of Anatomy*, 69(Pt 2), 181.
- Gandolla, M., Niero, L., Molteni, F., Guanziroli, E., Ward, N. S., & Pedrocchi, A. (2021). Brain Plasticity Mechanisms Underlying Motor Control Reorganization: Pilot Longitudinal Study on Post-Stroke Subjects. *Brain Sciences*, 11(3), 329. <https://doi.org/10.3390/brainsci11030329>
- Garyfallidis, E., Brett, M., Amirbekian, B., Rokem, A., van der Walt, S., Descoteaux, M., Nimmo-Smith, I., & Dipy Contributors. (2014). Dipy, a library for the analysis of diffusion MRI data. *Frontiers in Neuroinformatics*, 8. <https://doi.org/10.3389/fninf.2014.00008>
- Gauthier, L., Dehaut, F., & Joannette, Y. (1989). The bells test: A quantitative and qualitative test for visual neglect. *International Journal of Clinical Neuropsychology*, 11(2), 49–54.
- Ghosh, A., Rho, Y., McIntosh, A. R., Kötter, R., & Jirsa, V. K. (2008). Noise during Rest Enables the Exploration of the Brain's Dynamic Repertoire. *PLoS Computational Biology*, 4(10), e1000196. <https://doi.org/10.1371/journal.pcbi.1000196>
- Gigandet, X., Griffa, A., Kober, T., Daducci, A., Gilbert, G., Connelly, A., Hagmann, P., Meuli, R., Thiran, J. P., & Krueger, G. (2013). A Connectome-Based Comparison of Diffusion MRI Schemes. *PLoS ONE*, 8(9). <https://doi.org/10.1371/journal.pone.0075061>

References

- Girard, G., Caminiti, R., Battaglia-Mayer, A., St-Onge, E., Ambrosen, K. S., Eskildsen, S. F., Krug, K., Dyrby, T. B., Descoteaux, M., Thiran, J. P., & Innocenti, G. M. (2020). On the cortical connectivity in the macaque brain: A comparison of diffusion tractography and histological tracing data. *NeuroImage*, 221, 117201. <https://doi.org/10.1016/J.NEUROIMAGE.2020.117201>
- Glasser, M. F., Coalson, T. S., Robinson, E. C., Hacker, C. D., Harwell, J., Yacoub, E., Ugurbil, K., Andersson, J., Beckmann, C. F., Jenkinson, M., Smith, S. M., & Van Essen, D. C. (2016). A multi-modal parcellation of human cerebral cortex. *Nature*, 536(7615), 171–178. <https://doi.org/10.1038/nature18933>
- Godefroy, O., Leclercq, C., Roussel, M., Moroni, C., Quaglino, V., Beaunieux, H., Tallia, H., Nédélec-Ciceri, C., Bonnin, C., Thomas-Anterion, C., Varvat, J., Aboulafia-Brakha, T., Assal, F., & GRECOG-VASC Neuropsychological Committee. (2012). French adaptation of the vascular cognitive impairment harmonization standards: The GRECOG-VASC study. *International Journal of Stroke: Official Journal of the International Stroke Society*, 7(4), 362–363. <https://doi.org/10.1111/j.1747-4949.2012.00794.x>
- Golestani, A.-M., Tymchuk, S., Demchuk, A., & Goodyear, B. G. (2013). Longitudinal Evaluation of Resting-State fMRI After Acute Stroke With Hemiparesis. *Neurorehabilitation and Neural Repair*, 27(2), 153–163. <https://doi.org/10.1177/1545968312457827>
- Grefkes, C., & Fink, G. R. (2014). Connectivity-based approaches in stroke and recovery of function. *The Lancet Neurology*, 13(2), 206–216. [https://doi.org/10.1016/S1474-4422\(13\)70264-3](https://doi.org/10.1016/S1474-4422(13)70264-3)
- Grefkes, C., & Fink, G. R. (2020). Recovery from stroke: Current concepts and future perspectives. *Neurological Research and Practice*, 2(1), 17. <https://doi.org/10.1186/s42466-020-00060-6>
- Grefkes, C., Nowak, D. A., Eickhoff, S. B., Dafotakis, M., Küst, J., Karbe, H., & Fink, G. R. (2008). Cortical connectivity after subcortical stroke assessed with functional magnetic resonance imaging. *Annals of Neurology*, 63(2), 236–246. <https://doi.org/10.1002/ana.21228>
- Grefkes, C., Nowak, D. A., Wang, L. E., Dafotakis, M., Eickhoff, S. B., & Fink, G. R. (2010). Modulating cortical connectivity in stroke patients by rTMS assessed with fMRI and dynamic causal modeling. *NeuroImage*, 50(1), 233–242. <https://doi.org/10.1016/j.neuroimage.2009.12.029>
- Grefkes, C., & Ward, N. S. (2014). Cortical Reorganization After Stroke: How Much and How Functional? *The Neuroscientist*, 20(1), 56–70. <https://doi.org/10.1177/1073858413491147>
- Griffa, A., Amico, E., Liégeois, R., Van De Ville, D., & Preti, M. G. (2022). Brain structure-function coupling provides signatures for task decoding and individual fingerprinting. *NeuroImage*, 250, 118970. <https://doi.org/10.1016/j.neuroimage.2022.118970>
- Gu, S., Pasqualetti, F., Cieslak, M., Telesford, Q. K., Yu, A. B., Kahn, A. E., Medaglia, J. D., Vettel, J. M., Miller, M. B., Grafton, S. T., & Bassett, D. S. (2015). Controllability of structural brain networks. *Nature Communications*, 6(1), 8414. <https://doi.org/10.1038/ncomms9414>
- Gu, Z., Jamison, K. W., Sabuncu, M. R., & Kuceyeski, A. (2021). Heritability and interindividual variability of regional structure-function coupling. *Nature Communications*, 12(1), 4894. <https://doi.org/10.1038/s41467-021-25184-4>
- Guggisberg, A. G., Koch, P. J., Hummel, F. C., & Buetefisch, C. M. (2019). Brain networks and their relevance for stroke rehabilitation. *Clinical Neurophysiology*, 130(7), 1098–1124. <https://doi.org/10.1016/j.clinph.2019.04.004>

References

- Guggisberg, A. G., Nicolo, P., Cohen, L. G., Schnider, A., & Buch, E. R. (2017). Longitudinal Structural and Functional Differences Between Proportional and Poor Motor Recovery After Stroke. *Neurorehabilitation and Neural Repair*, 31(12), 1029–1041. <https://doi.org/10.1177/1545968317740634>
- Hagemann, G., Redecker, C., Neumann-Haefelin, T., Freund, H.-J., & Witte, O. W. (1998). Increased long-term potentiation in the surround of experimentally induced focal cortical infarction. *Annals of Neurology*, 44(2), 255–258. <https://doi.org/10.1002/ana.410440217>
- Hagmann, P., Cammoun, L., Gigandet, X., Meuli, R., Honey, C. J., Wedeen, V. J., & Sporns, O. (2008). Mapping the Structural Core of Human Cerebral Cortex. *PLoS Biology*, 6(7), e159. <https://doi.org/10.1371/journal.pbio.0060159>
- Hagmann, P., Kuran, M., Gigandet, X., Thiran, P., Wedeen, V. J., Meuli, R., & Thiran, J.-P. (2007). Mapping Human Whole-Brain Structural Networks with Diffusion MRI. *PLoS ONE*, 2(7), e597. <https://doi.org/10.1371/journal.pone.0000597>
- Hannanu, F. F., Zeffiro, T. A., Lamalle, L., Heck, O., Renard, F., Thuriot, A., Krainik, A., Hommel, M., Detante, O., & Jaillard, A. (2017). Parietal operculum and motor cortex activities predict motor recovery in moderate to severe stroke. *NeuroImage : Clinical*, 14, 518–529. <https://doi.org/10.1016/j.nicl.2017.01.023>
- Hawe, R. L., Scott, S. H., & Dukelow, S. P. (2019). Taking Proportional Out of Stroke Recovery. *Stroke*, 50(1), 204–211. <https://doi.org/10.1161/STROKEAHA.118.023006>
- Hawrylycz, M. J., Lein, E. S., Guillozet-Bongaarts, A. L., Shen, E. H., Ng, L., Miller, J. A., van de Lagemaat, L. N., Smith, K. A., Ebbert, A., Riley, Z. L., Abajian, C., Beckmann, C. F., Bernard, A., Bertagnolli, D., Boe, A. F., Cartagena, P. M., Chakravarty, M. M., Chapin, M., Chong, J., ... Jones, A. R. (2012). An anatomically comprehensive atlas of the adult human brain transcriptome. *Nature*, 489(7416), 391–399. <https://doi.org/10.1038/nature11405>
- He, S.-Q., Dum, R. P., & Strick, P. L. (1993). Topographic organization of corticospinal projections from the frontal lobe: Motor areas on the lateral surface of the hemisphere. *Journal of Neuroscience*, 13(3), 952–980.
- Hendricks, H. T., van Limbeek, J., Geurts, A. C., & Zwarts, M. J. (2002). Motor recovery after stroke: A systematic review of the literature. *Archives of Physical Medicine and Rehabilitation*, 83(11), 1629–1637. <https://doi.org/10.1053/apmr.2002.35473>
- Honey, C. J., Kotter, R., Breakspear, M., & Sporns, O. (2007). Network structure of cerebral cortex shapes functional connectivity on multiple time scales. *Proceedings of the National Academy of Sciences*, 104(24), 10240–10245. <https://doi.org/10.1073/pnas.0701519104>
- Honey, C. J., & Sporns, O. (2008). Dynamical consequences of lesions in cortical networks. *Human Brain Mapping*, 29(7), 802–809. <https://doi.org/10.1002/hbm.20579>
- Honey, C. J., Sporns, O., Cammoun, L., Gigandet, X., Thiran, J. P., Meuli, R., & Hagmann, P. (2009). Predicting human resting-state functional connectivity from structural connectivity. *Proceedings of the National Academy of Sciences*, 106(6), 2035–2040. <https://doi.org/10.1073/pnas.0811168106>
- Hope, T. M. H., Friston, K., Price, C. J., Leff, A. P., Rotshtein, P., & Bowman, H. (2019). Recovery after stroke: Not so proportional after all? *Brain*, 142(1), 15–22. <https://doi.org/10.1093/brain/awy302>

References

- Hoshi, E., & Tanji, J. (2007). Distinctions between dorsal and ventral premotor areas: Anatomical connectivity and functional properties. *Current Opinion in Neurobiology*, 17(2), 234–242. <https://doi.org/10.1016/j.conb.2007.02.003>
- Hossmann, K.-A. (2006). Pathophysiology and Therapy of Experimental Stroke. *Cellular and Molecular Neurobiology*, 26(7–8), 1055–1081. <https://doi.org/10.1007/s10571-006-9008-1>
- Hummel, F. C., Celnik, P., Pascual-Leone, A., Fregni, F., Byblow, W. D., Buetefisch, C. M., Rothwell, J., Cohen, L. G., & Gerloff, C. (2008). Controversy: Noninvasive and invasive cortical stimulation show efficacy in treating stroke patients. *Brain Stimulation*, 1(4), 370–382. <https://doi.org/10.1016/j.brs.2008.09.003>
- Huntenburg, J. M., Bazin, P.-L., Goulas, A., Tardif, C. L., Villringer, A., & Margulies, D. S. (2017). A Systematic Relationship Between Functional Connectivity and Intracortical Myelin in the Human Cerebral Cortex. *Cerebral Cortex*, 27(2), 981–997. <https://doi.org/10.1093/cercor/bhx030>
- Iglesias, J. E., Van Leemput, K., Bhatt, P., Casillas, C., Dutt, S., Schuff, N., Truran-Sacrey, D., Boxer, A., & Fischl, B. (2015). Bayesian segmentation of brainstem structures in MRI. *NeuroImage*, 113, 184–195. <https://doi.org/10.1016/J.NEUROIMAGE.2015.02.065>
- Jamieson, A. J., Davey, C. G., & Harrison, B. J. (2021). Differential Modulation of Effective Connectivity in the Brain's Extended Face Processing System by Fearful and Sad Facial Expressions. *Eneuro*, 8(2), ENEURO.0380-20.2021. <https://doi.org/10.1523/ENEURO.0380-20.2021>
- Jang, S. H., Chang, C. H., Lee, J., Kim, C. S., Seo, J. P., & Yeo, S. S. (2013). Functional Role of the Corticoreticular Pathway in Chronic Stroke Patients. *Stroke*, 44(4), 1099–1104. <https://doi.org/10.1161/STROKEAHA.111.000269>
- Jenkinson, M., Bannister, P., Brady, M., & Smith, S. (2002). Improved optimization for the robust and accurate linear registration and motion correction of brain images. *NeuroImage*, 17(2), 825–841.
- Jenkinson, M., & Smith, S. (2001). A global optimisation method for robust affine registration of brain images. *Medical Image Analysis*, 5(2), 143–156. [https://doi.org/10.1016/S1361-8415\(01\)00036-6](https://doi.org/10.1016/S1361-8415(01)00036-6)
- Jensen, J. H., Helpert, J. A., Ramani, A., Lu, H., & Kaczynski, K. (2005). Diffusional kurtosis imaging: The quantification of non-gaussian water diffusion by means of magnetic resonance imaging. *Magnetic Resonance in Medicine*, 53(6), 1432–1440. <https://doi.org/10.1002/mrm.20508>
- Jeurissen, B., Descoteaux, M., Mori, S., & Leemans, A. (2017). Diffusion MRI fiber tractography of the brain. *NMR in Biomedicine*, 32(4). <https://doi.org/10.1002/nbm.3785>
- Jeurissen, B., Descoteaux, M., Mori, S., & Leemans, A. (2019). Diffusion MRI fiber tractography of the brain. *NMR in Biomedicine*, 32(4), e3785. <https://doi.org/10.1002/nbm.3785>
- Jeurissen, B., Tournier, J.-D., Dhollander, T., Connelly, A., & Sijbers, J. (2014). Multi-tissue constrained spherical deconvolution for improved analysis of multi-shell diffusion MRI data. *NeuroImage*, 103, 411–426. <https://doi.org/10.1016/j.neuroimage.2014.07.061>
- Jolkkonen, J. (2016). *Translational Hurdles in Stroke Recovery Studies*. 12.
- Jung, T., Kim, J., Seo, J., Jin, S., Lee, H., Lee, S., Lee, Y., & Chang, Y. (2013). Combined information from resting-state functional connectivity and passive movements with functional magnetic resonance imaging differentiates fast late-onset motor recovery from progressive recovery in hemiplegic stroke patients: A pilot study. *Journal of Rehabilitation Medicine*, 45(6), 546–552. <https://doi.org/10.2340/16501977-1165>

References

- Karahanoğlu, F. I., & Van De Ville, D. (2015). Transient brain activity disentangles fMRI resting-state dynamics in terms of spatially and temporally overlapping networks. *Nature Communications*, 6(1), 7751. <https://doi.org/10.1038/ncomms8751>
- Katan, M., & Luft, A. (2018). Global Burden of Stroke. *Seminars in Neurology*, 38(02), 208–211. <https://doi.org/10.1055/s-0038-1649503>
- Kellner, E., Dhital, B., Kiselev, V. G., & Reisert, M. (2016). Gibbs-ringing artifact removal based on local subvoxel-shifts: Gibbs-Ringing Artifact Removal. *Magnetic Resonance in Medicine*, 76(5), 1574–1581. <https://doi.org/10.1002/mrm.26054>
- Kessels, R. P. C., van Zandvoort, M. J. E., Postma, A., Kappelle, L. J., & de Haan, E. H. F. (2000). The Corsi Block-Tapping Task: Standardization and Normative Data. *Applied Neuropsychology*, 7(4), 252–258. https://doi.org/10.1207/S15324826AN0704_8
- Kim, K. H., Kim, Y.-H., Kim, M. S., Park, C., Lee, A., & Chang, W. H. (2015). Prediction of Motor Recovery Using Diffusion Tensor Tractography in Supratentorial Stroke Patients With Severe Motor Involvement. *Annals of Rehabilitation Medicine*, 39(4), 570. <https://doi.org/10.5535/arm.2015.39.4.570>
- Koch, P. J., & Hummel, F. C. (2017). Toward precision medicine: Tailoring interventional strategies based on noninvasive brain stimulation for motor recovery after stroke. *Current Opinion in Neurology*, 30(4), 388–397. <https://doi.org/10.1097/WCO.0000000000000462>
- Koch, P. J., Park, C.-H., Girard, G., Beanato, E., Egger, P., Evangelista, G. G., Lee, J., Wessel, M. J., Morishita, T., Koch, G., Thiran, J.-P., Guggisberg, A. G., Rosso, C., Kim, Y.-H., & Hummel, F. C. (2021). The structural connectome and motor recovery after stroke: Predicting natural recovery. *Brain*, 144(7), 2107–2119. <https://doi.org/10.1093/brain/awab082>
- Koch, P., Schulz, R., & Hummel, F. C. (2016). Structural connectivity analyses in motor recovery research after stroke. *Annals of Clinical and Translational Neurology*, 3(3), 233–244. <https://doi.org/10.1002/acn3.278>
- Koeppen, A. H. (2004). Wallerian degeneration: History and clinical significance. *Journal of the Neurological Sciences*, 220(1), 115–117. <https://doi.org/10.1016/j.jns.2004.03.008>
- Konopleva, L., Il'yasov, K. A., Teo, S. J., Coenen, V. A., Kaller, C. P., & Reisert, M. (2020). Robust Intra-Individual Estimation of Structural Connectivity by Principal Component Analysis. *NeuroImage*, 226(December 2020), 117483. <https://doi.org/10.1016/j.neuroimage.2020.117483>
- Krakauer, J. W., Carmichael, S. T., Corbett, D., & Wittenberg, G. F. (2012). Getting Neurorehabilitation Right: What Can Be Learned From Animal Models? *Neurorehabilitation and Neural Repair*, 26(8), 923–931. <https://doi.org/10.1177/1545968312440745>
- Krishnan, A., Williams, L. J., McIntosh, A. R., & Abdi, H. (2011). Partial Least Squares (PLS) methods for neuroimaging: A tutorial and review. *NeuroImage*, 56(2), 455–475. <https://doi.org/10.1016/j.neuroimage.2010.07.034>
- Kurokawa, R., Kamiya, K., Koike, S., Nakaya, M., Uematsu, A., Tanaka, S. C., Kamagata, K., Okada, N., Morita, K., Kasai, K., & Abe, O. (2021). Cross-scanner reproducibility and harmonization of a diffusion MRI structural brain network: A traveling subject study of multi-b acquisition. *NeuroImage*, 245(September), 118675. <https://doi.org/10.1016/j.neuroimage.2021.118675>

References

- Kwakkel, G., Kollen, B. J., van der Grond, J., & Prevo, A. J. H. (2003). Probability of Regaining Dexterity in the Flaccid Upper Limb: Impact of Severity of Paresis and Time Since Onset in Acute Stroke. *Stroke*, 34(9), 2181–2186. <https://doi.org/10.1161/01.STR.0000087172.16305.CD>
- Lai, T. W., Zhang, S., & Wang, Y. T. (2014). Excitotoxicity and stroke: Identifying novel targets for neuroprotection. *Progress in Neurobiology*, 115, 157–188. <https://doi.org/10.1016/j.pneurobio.2013.11.006>
- Lawrence, E. S., Coshall, C., Dundas, R., Stewart, J., Rudd, A. G., Howard, R., & Wolfe, C. D. A. (2001). Estimates of the Prevalence of Acute Stroke Impairments and Disability in a Multiethnic Population. *Stroke*, 32(6), 1279–1284. <https://doi.org/10.1161/01.STR.32.6.1279>
- Lazar, R. M., Minzer, B., Antoniello, D., Festa, J. R., Krakauer, J. W., & Marshall, R. S. (2010). Improvement in Aphasia Scores After Stroke Is Well Predicted by Initial Severity. *Stroke*, 41(7), 1485–1488. <https://doi.org/10.1161/STROKEAHA.109.577338>
- Lee, B.-C., Choi, J., & Martin, B. J. (2020). Roles of the prefrontal cortex in learning to time the onset of pre-existing motor programs. *PLOS ONE*, 15(11), e0241562. <https://doi.org/10.1371/journal.pone.0241562>
- Lee, J., Lee, M., Kim, D.-S., & Kim, Y.-H. (2015). Functional reorganization and prediction of motor recovery after a stroke: A graph theoretical analysis of functional networks. *Restorative Neurology and Neuroscience*, 33(6), 785–793. <https://doi.org/10.3233/RNN-140467>
- Lee, J.-K. (2004). Nogo Receptor Antagonism Promotes Stroke Recovery by Enhancing Axonal Plasticity. *Journal of Neuroscience*, 24(27), 6209–6217. <https://doi.org/10.1523/JNEUROSCI.1643-04.2004>
- LeFort, S. M. (1993). The Statistical versus Clinical Significance Debate. *Image: The Journal of Nursing Scholarship*, 25(1), 57–62. <https://doi.org/10.1111/j.1547-5069.1993.tb00754.x>
- Leyton, A. S., & Sherrington, C. S. (1917). Observations on the excitable cortex of the chimpanzee, orang-utan, and gorilla. *Quarterly Journal of Experimental Physiology: Translation and Integration*, 11(2), 135–222.
- Liew, S., Zavaliangos-Petropulu, A., Jahanshad, N., Lang, C. E., Hayward, K. S., Lohse, K. R., Juliano, J. M., Assogna, F., Baugh, L. A., Bhattacharya, A. K., Bigjahan, B., Borich, M. R., Boyd, L. A., Brodtmann, A., Buetefisch, C. M., Byblow, W. D., Cassidy, J. M., Conforto, A. B., Craddock, R. C., ... Thompson, P. M. (2020). The ENIGMA Stroke Recovery Working Group: Big data neuroimaging to study brain–behavior relationships after stroke. *Human Brain Mapping*, 43(1), 129–148. <https://doi.org/10.1002/hbm.25015>
- Lim, J. Y., Oh, M.-K., Park, J., & Paik, N.-J. (2020). Does Measurement of Corticospinal Tract Involvement Add Value to Clinical Behavioral Biomarkers in Predicting Motor Recovery after Stroke? *Neural Plasticity*, 10.
- Liu, X., & Duyn, J. H. (2013). Time-varying functional network information extracted from brief instances of spontaneous brain activity. *Proceedings of the National Academy of Sciences*, 110(11), 4392–4397. <https://doi.org/10.1073/pnas.1216856110>
- Liuzzi, G., Hörniß, V., Lechner, P., Hoppe, J., Heise, K., Zimerman, M., Gerloff, C., & Hummel, F. C. (2014). Development of movement-related intracortical inhibition in acute to chronic subcortical stroke. *Neurology*, 82(3), 198–205. <https://doi.org/10.1212/WNL.0000000000000028>

References

- Lubben, N., Ensink, E., Coetzee, G. A., & Labrie, V. (2021). The enigma and implications of brain hemispheric asymmetry in neurodegenerative diseases. *Brain Communications*, 3(3), fcab211. <https://doi.org/10.1093/braincomms/fcab211>
- Lunven, M., & Bartolomeo, P. (2017). Attention and spatial cognition: Neural and anatomical substrates of visual neglect. *Annals of Physical and Rehabilitation Medicine*, 60(3), 124–129. <https://doi.org/10.1016/j.rehab.2016.01.004>
- Luppino, G., Matelli, M., Camarda, R., & Rizzolatti, G. (1993). Corticocortical connections of area F3 (SMA-proper) and area F6 (pre-SMA) in the macaque monkey. *Journal of Comparative Neurology*, 338(1), 114–140.
- Maier, O., Schröder, C., Forkert, N. D., Martinetz, T., & Handels, H. (2015). Classifiers for Ischemic Stroke Lesion Segmentation: A Comparison Study. *PLOS ONE*, 10(12), e0145118. <https://doi.org/10.1371/journal.pone.0145118>
- Maier-Hein, K. H., Neher, P. F., Houde, J.-C., Côté, M.-A., Garyfallidis, E., Zhong, J., Chamberland, M., Yeh, F.-C., Lin, Y.-C., Ji, Q., Reddick, W. E., Glass, J. O., Chen, D. Q., Feng, Y., Gao, C., Wu, Y., Ma, J., He, R., Li, Q., ... Descoteaux, M. (2017). The challenge of mapping the human connectome based on diffusion tractography. *Nature Communications*, 8(1), 1349. <https://doi.org/10.1038/s41467-017-01285-x>
- Malagurski, B., Liem, F., Oschwald, J., Mérillat, S., & Jäncke, L. (2020). Longitudinal functional brain network reconfiguration in healthy aging. *Human Brain Mapping*, 41(17), 4829–4845. <https://doi.org/10.1002/hbm.25161>
- Malcolm, J. G., Shenton, M. E., & Rathi, Y. (2010). Filtered Multitensor Tractography. *IEEE Transactions on Medical Imaging*, 29(9), 1664–1675. <https://doi.org/10.1109/TMI.2010.2048121>
- Marchi, N. A., Ptak, R., Di Pietro, M., Schnider, A., & Guggisberg, A. G. (2017). Principles of proportional recovery after stroke generalize to neglect and aphasia. *European Journal of Neurology*, 24(8), 1084–1087. <https://doi.org/10.1111/ene.13296>
- Margulies, D. S., Ghosh, S. S., Goulas, A., Falkiewicz, M., Huntenburg, J. M., Langs, G., Bezgin, G., Eickhoff, S. B., Castellanos, F. X., Petrides, M., Jefferies, E., & Smallwood, J. (2016). Situating the default-mode network along a principal gradient of macroscale cortical organization. *Proceedings of the National Academy of Sciences*, 113(44), 12574–12579. <https://doi.org/10.1073/pnas.1608282113>
- Mathiowetz, V., Weber, K., Kashman, N., & Volland, G. (1985). Adult Norms for the Nine Hole Peg Test of Finger Dexterity. *The Occupational Therapy Journal of Research*, 5(1), 24–38. <https://doi.org/10.1177/153944928500500102>
- Mathiowetz, V., Weber, K., Volland, G., & Kashman, N. (1984). Reliability and validity of grip and pinch strength evaluations. *The Journal of Hand Surgery*, 9(2), 222–226. [https://doi.org/10.1016/s0363-5023\(84\)80146-x](https://doi.org/10.1016/s0363-5023(84)80146-x)
- MathWorks—MATLAB and Simulink Conferences. (v2019b). <https://ch.mathworks.com/>
- McIntosh, A. R., Bookstein, F. L., Haxby, J. V., & Grady, C. L. (1996). Spatial Pattern Analysis of Functional Brain Images Using Partial Least Squares. *NeuroImage*, 3(3), 143–157. <https://doi.org/10.1006/nimg.1996.0016>
- McIntosh, A. R., Chau, W. K., & Protzner, A. B. (2004). Spatiotemporal analysis of event-related fMRI data using partial least squares. *NeuroImage*, 23(2), 764–775. <https://doi.org/10.1016/j.neuroimage.2004.05.018>

References

- McIntosh, A. R., & Lobaugh, N. J. (2004). Partial least squares analysis of neuroimaging data: Applications and advances. *NeuroImage*, 23, S250–S263. <https://doi.org/10.1016/j.neuroimage.2004.07.020>
- Medaglia, J. D., Huang, W., Karuza, E. A., Kelkar, A., Thompson-Schill, S. L., Ribeiro, A., & Bassett, D. S. (2018). Functional alignment with anatomical networks is associated with cognitive flexibility. *Nature Human Behaviour*, 2(2), 156–164. <https://doi.org/10.1038/s41562-017-0260-9>
- Miall, R. C. (2016). Cortical Motor Control. In D. W. Pfaff & N. D. Volkow (Eds.), *Neuroscience in the 21st Century: From Basic to Clinical* (pp. 1315–1336). Springer. https://doi.org/10.1007/978-1-4939-3474-4_128
- Min, Y.-S., Park, J. W., Park, E., Kim, A.-R., Cha, H., Gwak, D.-W., Jung, S.-H., Chang, Y., & Jung, T.-D. (2020). Interhemispheric Functional Connectivity in the Primary Motor Cortex Assessed by Resting-State Functional Magnetic Resonance Imaging Aids Long-Term Recovery Prediction among Subacute Stroke Patients with Severe Hand Weakness. *Journal of Clinical Medicine*, 9(4), 975. <https://doi.org/10.3390/jcm9040975>
- Montgomery, J., Hislop, H., & Connelly, B. (2007). *Daniels and Worthingham's Muscle Testing: Techniques of Manual Examination*. Maryland Heights, MO: Saunders. Elsevier.
- Morris, J. C., Heyman, A., Mohs, R. C., Hughes, J. P., van Belle, G., Fillenbaum, G., Mellits, E. D., & Clark, C. (1989). The consortium to establish a registry for Alzheimer's disease (CERAD): I. Clinical and neuropsychological assessment of Alzheimer's disease. *Neurology*.
- Moura, L. M., & Conforto, A. B. (2019). Diffusion Tensor Imaging Biomarkers to Predict Motor Outcomes in Stroke: A Narrative Review. *Frontiers in Neurology*, 10, 17.
- Murphy, T. H., & Corbett, D. (2009). Plasticity during stroke recovery: From synapse to behaviour. *Nature Reviews Neuroscience*, 10(12), 861–872. <https://doi.org/10.1038/nrn2735>
- Murphy, T. H., Li, P., Betts, K., & Liu, R. (2008). Two-Photon Imaging of Stroke Onset In Vivo Reveals That NMDA-Receptor Independent Ischemic Depolarization Is the Major Cause of Rapid Reversible Damage to Dendrites and Spines. *Journal of Neuroscience*, 28(7), 1756–1772. <https://doi.org/10.1523/JNEUROSCI.5128-07.2008>
- Nachev, P., Kennard, C., & Husain, M. (2008). Functional role of the supplementary and pre-supplementary motor areas. *Nature Reviews Neuroscience*, 9(11), 856–869. <https://doi.org/10.1038/nrn2478>
- Nasreddine, Z. S., Phillips, N. A., Bédirian, V., Charbonneau, S., Whitehead, V., Collin, I., Cummings, J. L., & Chertkow, H. (2005). The Montreal Cognitive Assessment, MoCA: A Brief Screening Tool For Mild Cognitive Impairment. *Journal of the American Geriatrics Society*, 53(4), 695–699. <https://doi.org/10.1111/j.1532-5415.2005.53221.x>
- Nielsen, J. A., Zielinski, B. A., Ferguson, M. A., Lainhart, J. E., & Anderson, J. S. (2013). An Evaluation of the Left-Brain vs. Right-Brain Hypothesis with Resting State Functional Connectivity Magnetic Resonance Imaging. *PLoS ONE*, 8(8), e71275. <https://doi.org/10.1371/journal.pone.0071275>
- Nouri, S., & Cramer, S. C. (2011). Anatomy and physiology predict response to motor cortex stimulation after stroke. *Neurology*, 77(11), 1076–1083. <https://doi.org/10.1212/WNL.0b013e31822e1482>
- Nozais, V., Forkel, S. J., Foulon, C., Petit, L., & Thiebaut de Schotten, M. (2021). Functionnectome as a framework to analyse the contribution of brain circuits to fMRI. *Communications Biology*, 4(1), 1035. <https://doi.org/10.1038/s42003-021-02530-2>

References

- Nys, G. M. S., van Zandvoort, M. J. E., de Kort, P. L. M., Jansen, B. P. W., de Haan, E. H. F., & Kappelle, L. J. (2007). Cognitive Disorders in Acute Stroke: Prevalence and Clinical Determinants. *Cerebrovascular Diseases*, 23(5–6), 408–416. <https://doi.org/10.1159/000101464>
- Ocampo-Pineda, M., Schiavi, S., Rheault, F., Girard, G., Petit, L., Descoteaux, M., & Daducci, A. (2021). Hierarchical Microstructure Informed Tractography. *Brain Connectivity*, brain.2020.0907. <https://doi.org/10.1089/brain.2020.0907>
- O'Donnell, L. J., Daducci, A., Wassermann, D., & Lenglet, C. (2017). *Advances in computational and statistical diffusion MRI*. 14.
- Ogawa, S., Lee, T. M., Kay, A. R., & Tank, D. W. (1990). Brain magnetic resonance imaging with contrast dependent on blood oxygenation. *Proceedings of the National Academy of Sciences*, 87(24), 9868–9872. <https://doi.org/10.1073/pnas.87.24.9868>
- Olafson, E. R., Jamison, K. W., Sweeney, E. M., Liu, H., Wang, D., Bruss, J. E., Boes, A. D., & Kuceyeski, A. (2021). Functional connectome reorganization relates to post-stroke motor recovery and structural and functional disconnection. *NeuroImage*, 245, 118642. <https://doi.org/10.1016/j.neuroimage.2021.118642>
- Overman, J. J., & Carmichael, S. T. (2014). Plasticity in the Injured Brain: More than Molecules Matter. *The Neuroscientist*, 20(1), 15–28. <https://doi.org/10.1177/1073858413491146>
- Park, C., Chang, W. H., Ohn, S. H., Kim, S. T., Bang, O. Y., Pascual-Leone, A., & Kim, Y.-H. (2011). Longitudinal Changes of Resting-State Functional Connectivity During Motor Recovery After Stroke. *Stroke*, 42(5), 1357–1362. <https://doi.org/10.1161/STROKEAHA.110.596155>
- Paus, T., Petrides, M., Evans, A. C., & Meyer, E. (1993). Role of the human anterior cingulate cortex in the control of oculomotor, manual, and speech responses: A positron emission tomography study. *Journal of Neurophysiology*, 70(2), 453–469.
- Penfield, W., & Welch, K. (1951). The supplementary motor area of the cerebral cortex: A clinical and experimental study. *AMA Archives of Neurology & Psychiatry*, 66(3), 289–317.
- Pennati, G. V., Plantin, J., Carment, L., Roca, P., Baron, J.-C., Pavlova, E., Borg, J., & Lindberg, P. G. (2020). Recovery and Prediction of Dynamic Precision Grip Force Control After Stroke. *Stroke*, 51(3), 944–951. <https://doi.org/10.1161/STROKEAHA.119.026205>
- Pessoa, L. (2014). Understanding brain networks and brain organization. *Physics of Life Reviews*, 11(3), 400–435. <https://doi.org/10.1016/j.plrev.2014.03.005>
- Peters, D. M., Fridriksson, J., Stewart, J. C., Richardson, J. D., Rorden, C., Bonilha, L., Middleton, A., Gleichgerrcht, E., & Fritz, S. L. (2018). Cortical disconnection of the ipsilesional primary motor cortex is associated with gait speed and upper extremity motor impairment in chronic left hemispheric stroke: Movement and Cortical Disconnection in Stroke. *Human Brain Mapping*, 39(1), 120–132. <https://doi.org/10.1002/hbm.23829>
- Picard, N., & Strick, P. L. (1996). Motor Areas of the Medial Wall: A Review of Their Location and Functional Activation. *Cerebral Cortex*, 6(3), 342–353. <https://doi.org/10.1093/cercor/6.3.342>
- Picard, N., & Strick, P. L. (2001). Imaging the premotor areas. *Current Opinion in Neurobiology*, 11(6), 663–672. [https://doi.org/10.1016/S0959-4388\(01\)00266-5](https://doi.org/10.1016/S0959-4388(01)00266-5)
- Pinter, D., Gattringer, T., Fandler-Höfler, S., Kneihsl, M., Eppinger, S., Deutschmann, H., Pichler, A., Poltrum, B., Reishofer, G., Ropele, S., Schmidt, R., & Enzinger, C. (2020). Early Progressive Changes in White

References

- Matter Integrity Are Associated with Stroke Recovery. *Translational Stroke Research*, 11(6), 1264–1272. <https://doi.org/10.1007/s12975-020-00797-x>
- Porter, R., & Lemon, R. (1993). *Corticospinal function and voluntary movement*. Oxford University Press, USA.
- Prabhakaran, S., Zarah, E., Riley, C., Speizer, A., Chong, J. Y., Lazar, R. M., Marshall, R. S., & Krakauer, J. W. (2008). Inter-individual Variability in the Capacity for Motor Recovery After Ischemic Stroke. *Neurorehabilitation and Neural Repair*, 22(1), 64–71. <https://doi.org/10.1177/1545968307305302>
- Prčkovska, V., Rodrigues, P., Puigdel·livol Sanchez, A., Ramos, M., Andorra, M., Martinez-Heras, E., Falcon, C., Prats-Galino, A., & Villoslada, P. (2016). Reproducibility of the Structural Connectome Reconstruction across Diffusion Methods. *Journal of Neuroimaging*, 26(1), 46–57. <https://doi.org/10.1111/JON.12298>
- Preti, M. G., & Van De Ville, D. (2019). Decoupling of brain function from structure reveals regional behavioral specialization in humans. *Nature Communications*, 10(1), 4747. <https://doi.org/10.1038/s41467-019-12765-7>
- Puig, J., Blasco, G., Daunis-I-Estadella, J., Thomalla, G., Castellanos, M., Figueras, J., Remollo, S., van Eendenburg, C., Sánchez-González, J., Serena, J., & Pedraza, S. (2013). Decreased Corticospinal Tract Fractional Anisotropy Predicts Long-term Motor Outcome After Stroke. *Stroke*, 44(7), 2016–2018. <https://doi.org/10.1161/STROKEAHA.111.000382>
- Puig, J., Blasco, G., Schlaug, G., Stinear, C. M., Daunis-i-Estadella, P., Biarnes, C., Figueras, J., Serena, J., Hernández-Pérez, M., Alberich-Bayarri, A., Castellanos, M., Liebeskind, D. S., Demchuk, A. M., Menon, B. K., Thomalla, G., Nael, K., Wintermark, M., & Pedraza, S. (2017). Diffusion tensor imaging as a prognostic biomarker for motor recovery and rehabilitation after stroke. *Neuroradiology*, 59(4), 343–351. <https://doi.org/10.1007/s00234-017-1816-0>
- Puig, J., Pedraza, S., Blasco, G., Daunis-i-Estadella, J., Prados, F., Remollo, S., Prats-Galino, A., Soria, G., Boada, I., Castellanos, M., & Serena, J. (2011). Acute Damage to the Posterior Limb of the Internal Capsule on Diffusion Tensor Tractography as an Early Imaging Predictor of Motor Outcome after Stroke. *American Journal of Neuroradiology*, 32(5), 857–863. <https://doi.org/10.3174/ajnr.A2400>
- Quandt, F., Bönstrup, M., Schulz, R., Timmermann, J. E., Mund, M., Wessel, M. J., & Hummel, F. C. (2019). The functional role of beta-oscillations in the supplementary motor area during reaching and grasping after stroke: A question of structural damage to the corticospinal tract. *Human Brain Mapping*, 40(10), 3091–3101. <https://doi.org/10.1002/hbm.24582>
- Que, M., Witte, O. W., Neumann-Haefelin, T., Schiene, K., Schroeter, M., & Zilles, K. (1999). Changes in GABAA and GABAB receptor binding following cortical photothrombosis: A quantitative receptor autoradiographic study. *Neuroscience*, 93(4), 1233–1240. [https://doi.org/10.1016/S0306-4522\(99\)00197-9](https://doi.org/10.1016/S0306-4522(99)00197-9)
- R Core Team. (2017). *R: The R Project for Statistical Computing*. <https://www.r-project.org/>
- Ramsey, L. E., Siegel, J. S., Lang, C. E., Strube, M., Shulman, G. L., & Corbetta, M. (2017). Behavioural clusters and predictors of performance during recovery from stroke. *Nature Human Behaviour*, 1(3), 0038. <https://doi.org/10.1038/s41562-016-0038>
- Ranganathan, P., Pramesh, C. S., & Buyse, M. (2015). Common pitfalls in statistical analysis: Clinical versus statistical significance. *Perspectives in Clinical Research*, 6(3), 169–170. <https://doi.org/10.4103/2229-3485.159943>

References

- Rathore, S. S., Hinn, A. R., Cooper, L. S., Tyroler, H. A., & Rosamond, W. D. (2002). Characterization of Incident Stroke Signs and Symptoms: Findings From the Atherosclerosis Risk in Communities Study. *Stroke*, 33(11), 2718–2721. <https://doi.org/10.1161/01.STR.0000035286.87503.31>
- Rehme, A. K., Eickhoff, S. B., Rottschy, C., Fink, G. R., & Grefkes, C. (2012). Activation likelihood estimation meta-analysis of motor-related neural activity after stroke. *Neuroimage*, 59(3), 2771–2782.
- Rehme, A. K., Eickhoff, S. B., Wang, L. E., Fink, G. R., & Grefkes, C. (2011). Dynamic causal modeling of cortical activity from the acute to the chronic stage after stroke. *NeuroImage*, 55(3), 1147–1158. <https://doi.org/10.1016/j.neuroimage.2011.01.014>
- Rehme, A. K., Volz, L. J., Feis, D.-L., Eickhoff, S. B., Fink, G. R., & Grefkes, C. (2015). Individual prediction of chronic motor outcome in the acute post-stroke stage: Behavioral parameters versus functional imaging. *Human Brain Mapping*, 36(11), 4553–4565. <https://doi.org/10.1002/hbm.22936>
- Ringman, J. M., Saver, J. L., Woolson, R. F., Clarke, W. R., & Adams, H. P. (2004). Frequency, risk factors, anatomy, and course of unilateral neglect in an acute stroke cohort. *Neurology*, 63(3), 468–474. <https://doi.org/10.1212/01.WNL.0000133011.10689.CE>
- Ritter, P., Schirner, M., McIntosh, A. R., & Jirsa, V. K. (2013). The Virtual Brain Integrates Computational Modeling and Multimodal Neuroimaging. *Brain Connectivity*, 3(2), 121–145. <https://doi.org/10.1089/brain.2012.0120>
- Rode, G., Pagliari, C., Huchon, L., Rossetti, Y., & Pisella, L. (2017). Semiology of neglect: An update. *Annals of Physical and Rehabilitation Medicine*, 60(3), 177–185. <https://doi.org/10.1016/j.rehab.2016.03.003>
- Roine, T., Jeurissen, B., Perrone, D., Aelterman, J., Philips, W., Sijbers, J., & Leemans, A. (2019). Reproducibility and intercorrelation of graph theoretical measures in structural brain connectivity networks. *Medical Image Analysis*, 52, 56–67. <https://doi.org/10.1016/J.MEDIA.2018.10.009>
- Roland, P. E., Skinhoj, E., Lassen, N. A., & Larsen, B. (1980). Different cortical areas in man in organization of voluntary movements in extrapersonal space. *Journal of Neurophysiology*, 43(1), 137–150.
- Rouiller, E. M., Babalian, A., Kazennikov, O., Moret, V., Yu, X.-H., & Wiesendanger, M. (1994). Transcallosal connections of the distal forelimb representations of the primary and supplementary motor cortical areas in macaque monkeys. *Experimental Brain Research*, 102(2), 227–243.
- Sacco, R. L., Kasner, S. E., Broderick, J. P., Caplan, L. R., Connors, J. J. (Buddy), Culebras, A., Elkind, M. S. V., George, M. G., Hamdan, A. D., Higashida, R. T., Hoh, B. L., Janis, L. S., Kase, C. S., Kleindorfer, D. O., Lee, J.-M., Moseley, M. E., Peterson, E. D., Turan, T. N., Valderrama, A. L., & Vinters, H. V. (2013). An Updated Definition of Stroke for the 21st Century: A Statement for Healthcare Professionals From the American Heart Association/American Stroke Association. *Stroke*, 44(7), 2064–2089. <https://doi.org/10.1161/STR.0b013e318296aeca>
- Sagi, Y., Tavor, I., Hofstetter, S., Tzur-Moryosef, S., Blumenfeld-Katzir, T., & Assaf, Y. (2012). Learning in the Fast Lane: New Insights into Neuroplasticity. *Neuron*, 73(6), 1195–1203. <https://doi.org/10.1016/j.neuron.2012.01.025>
- Sandi, C. (2013). Stress and cognition. *WIREs Cognitive Science*, 4(3), 245–261. <https://doi.org/10.1002/wcs.1222>
- Sarwar, T., Tian, Y., Yeo, B. T. T., Ramamohanarao, K., & Zalesky, A. (2021). Structure-function coupling in the human connectome: A machine learning approach. *NeuroImage*, 226, 117609. <https://doi.org/10.1016/j.neuroimage.2020.117609>

References

- Saver, J. L. (2006). Time Is Brain—Quantified. *Stroke*, 37(1), 263–266. <https://doi.org/10.1161/01.STR.0000196957.55928.ab>
- Schiavi, S., Ocampo-Pineda, M., Barakovic, M., Petit, L., Descoteaux, M., Thiran, J.-P., & Daducci, A. (2020). A new method for accurate in vivo mapping of human brain connections using microstructural and anatomical information. *Science Advances*, 6(31), eaba8245. <https://doi.org/10.1126/sciadv.aba8245>
- Schilling, K. G., Gao, Y., Stepniewska, I., Janve, V., Landman, B. A., & Anderson, A. W. (2019). Anatomical accuracy of standard-practice tractography algorithms in the motor system—A histological validation in the squirrel monkey brain. *Magnetic Resonance Imaging*, 55(June 2018), 7–25. <https://doi.org/10.1016/j.mri.2018.09.004>
- Scholz, J., Klein, M. C., Behrens, T. E. J., & Johansen-Berg, H. (2009). Training induces changes in white-matter architecture. *Nature Neuroscience*, 12(11), 1370–1371. <https://doi.org/10.1038/nn.2412>
- Schulz, R., Braass, H., Liuzzi, G., Hoerniss, V., Lechner, P., Gerloff, C., & Hummel, F. C. (2015). White matter integrity of premotor–motor connections is associated with motor output in chronic stroke patients. *NeuroImage: Clinical*, 7, 82–86. <https://doi.org/10.1016/j.nicl.2014.11.006>
- Schulz, R., Koch, P., Zimmerman, M., Wessel, M., Bönstrup, M., Thomalla, G., Cheng, B., Gerloff, C., & Hummel, F. C. (2015). Parietofrontal motor pathways and their association with motor function after stroke. *Brain*, 138(7), 1949–1960. <https://doi.org/10.1093/brain/awv100>
- Schulz, R., Park, E., Lee, J., Chang, W. H., Lee, A., Kim, Y.-H., & Hummel, F. C. (2017). Interactions Between the Corticospinal Tract and Premotor–Motor Pathways for Residual Motor Output After Stroke. *Stroke*, 48(10), 2805–2811. <https://doi.org/10.1161/STROKEAHA.117.016834>
- Schumacher, L. V., Reisert, M., Nitschke, K., Egger, K., Urbach, H., Hennig, J., Weiller, C., & Kaller, C. P. (2018). Probing the reproducibility of quantitative estimates of structural connectivity derived from global tractography. *NeuroImage*, 175, 215–229. <https://doi.org/10.1016/j.neuroimage.2018.01.086>
- Seunarine, K. K., & Alexander, D. C. (2014). Multiple Fibers. In *Diffusion MRI* (pp. 105–123). Elsevier. <https://doi.org/10.1016/B978-0-12-396460-1.00006-8>
- Sheppard, S. M., Keator, L. M., Breining, B. L., Wright, A. E., Saxena, S., Tippet, D. C., & Hillis, A. E. (2020). Right hemisphere ventral stream for emotional prosody identification: Evidence from acute stroke. *Neurology*, 94(10), e1013–e1020. <https://doi.org/10.1212/WNL.00000000000008870>
- Sherbondy, A. J., Rowe, M. C., & Alexander, D. C. (2010). MicroTrack: An Algorithm for Concurrent Projectome and Microstructure Estimation. In T. Jiang, N. Navab, J. P. W. Pluim, & M. A. Viergever (Eds.), *Medical Image Computing and Computer-Assisted Intervention—MICCAI 2010* (pp. 183–190). Springer Berlin Heidelberg.
- Siegel, J. S., Ramsey, L. E., Snyder, A. Z., Metcalf, N. V., Chacko, R. V., Weinberger, K., Baldassarre, A., Hacker, C. D., Shulman, G. L., & Corbetta, M. (2016). Disruptions of network connectivity predict impairment in multiple behavioral domains after stroke. *Proceedings of the National Academy of Sciences*, 113(30), E4367–E4376. <https://doi.org/10.1073/pnas.1521083113>
- Silasi, G., & Murphy, T. H. (2014). Stroke and the Connectome: How Connectivity Guides Therapeutic Intervention. *Neuron*, 83(6), 1354–1368. <https://doi.org/10.1016/j.neuron.2014.08.052>

References

- Smets, E. M. A., Garssen, B., Bonke, B., & De Haes, J. C. J. M. (1995). The multidimensional Fatigue Inventory (MFI) psychometric qualities of an instrument to assess fatigue. *Journal of Psychosomatic Research*, 39(3), 315–325. [https://doi.org/10.1016/0022-3999\(94\)00125-O](https://doi.org/10.1016/0022-3999(94)00125-O)
- Smith, M.-C., Byblow, W. D., Barber, P. A., & Stinear, C. M. (2017). Proportional Recovery From Lower Limb Motor Impairment After Stroke. *Stroke*, 48(5), 1400–1403. <https://doi.org/10.1161/STROKEAHA.116.016478>
- Smith, R. E., Tournier, J. D., Calamante, F., & Connelly, A. (2015a). The effects of SIFT on the reproducibility and biological accuracy of the structural connectome. *NeuroImage*, 104, 253–265. <https://doi.org/10.1016/J.NEUROIMAGE.2014.10.004>
- Smith, R. E., Tournier, J.-D., Calamante, F., & Connelly, A. (2013). SIFT: Spherical-deconvolution informed filtering of tractograms. *NeuroImage*, 67, 298–312. <https://doi.org/10.1016/j.neuroimage.2012.11.049>
- Smith, R. E., Tournier, J.-D., Calamante, F., & Connelly, A. (2015b). SIFT2: Enabling dense quantitative assessment of brain white matter connectivity using streamlines tractography. *NeuroImage*, 119, 338–351. <https://doi.org/10.1016/j.neuroimage.2015.06.092>
- Smith, S. M. (2002). Fast robust automated brain extraction. *Human Brain Mapping*, 17(3), 143–155. <https://doi.org/10.1002/hbm.10062>
- Smith, S. M., Fox, P. T., Miller, K. L., Glahn, D. C., Fox, P. M., Mackay, C. E., Filippini, N., Watkins, K. E., Toro, R., & Laird, A. R. (2009). Correspondence of the brain's functional architecture during activation and rest. *Proceedings of the National Academy of Sciences*, 106(31), 13040–13045.
- Smith, S. M., Jenkinson, M., Woolrich, M. W., Beckmann, C. F., Behrens, T. E. J., Johansen-Berg, H., Bannister, P. R., De Luca, M., Drobnjak, I., Flitney, D. E., Niazy, R. K., Saunders, J., Vickers, J., Zhang, Y., De Stefano, N., Brady, J. M., & Matthews, P. M. (2004). Advances in functional and structural MR image analysis and implementation as FSL. *NeuroImage*, 23, S208–S219. <https://doi.org/10.1016/j.neuroimage.2004.07.051>
- Snaith, R. P. (2003). The Hospital Anxiety And Depression Scale. *Health and Quality of Life Outcomes*, 1(1), 29. <https://doi.org/10.1186/1477-7525-1-29>
- Spielberger, C. D. (1983). *State-trait anxiety inventory for adults*.
- Spielberger, C. D. (2010). State-Trait Anxiety Inventory. In *The Corsini Encyclopedia of Psychology* (pp. 1–1). John Wiley & Sons, Ltd. <https://doi.org/10.1002/9780470479216.corpsy0943>
- SPM - Statistical Parametric Mapping. (SPM12). <https://www.fil.ion.ucl.ac.uk/spm/>
- Sporns, O. (2010). *Networks of the Brain: Quantitative Analysis and Modeling*. 8.
- Sporns, O. (2011). *Networks of the brain*. MIT Press.
- Sporns, O. (2018). Graph theory methods: Applications in brain networks. *Translational Research*, 20(2), 11.
- Sporns, O., Tononi, G., & Kötter, R. (2005). The Human Connectome: A Structural Description of the Human Brain. *PLoS Computational Biology*, 1(4), e42. <https://doi.org/10.1371/journal.pcbi.0010042>
- Stejskal, E. O., & Tanner, J. E. (1965). Spin Diffusion Measurements: Spin Echoes in the Presence of a Time-Dependent Field Gradient. *The Journal of Chemical Physics*, 42(1), 288–292. <https://doi.org/10.1063/1.1695690>

References

- Stephan, K. E., Tittgemeyer, M., Knösche, T. R., Moran, R. J., & Friston, K. J. (2009). Tractography-based priors for dynamic causal models. *NeuroImage*, 47(4), 1628–1638. <https://doi.org/10.1016/j.neuroimage.2009.05.096>
- Stinear, C. M. (2017). Prediction of motor recovery after stroke: Advances in biomarkers. *The Lancet Neurology*, 16(10), 826–836. [https://doi.org/10.1016/S1474-4422\(17\)30283-1](https://doi.org/10.1016/S1474-4422(17)30283-1)
- Stinear, C. M., Ackerley, S., & Byblow, W. (2013). Rehabilitation is Initiated Early After Stroke, but Most Motor Rehabilitation Trials Are Not: A Systematic Review. *Stroke*, 44(7), 2039–2045. <https://doi.org/10.1161/STROKEAHA.113.000968>
- Stinear, C. M., Barber, P. A., Smale, P. R., Coxon, J. P., Fleming, M. K., & Byblow, W. D. (2007). Functional potential in chronic stroke patients depends on corticospinal tract integrity. *Brain*, 130(1), 170–180. <https://doi.org/10.1093/brain/awl333>
- Stinear, C. M., Byblow, W. D., Ackerley, S. J., Smith, M.-C., Borges, V. M., & Barber, P. A. (2017). PREP2: A biomarker-based algorithm for predicting upper limb function after stroke. *Annals of Clinical and Translational Neurology*, 4(11), 811–820. <https://doi.org/10.1002/acn3.488>
- Stinear, C. M., Lang, C. E., Zeiler, S., & Byblow, W. D. (2020). Advances and challenges in stroke rehabilitation. *The Lancet Neurology*, 19(4), 348–360. [https://doi.org/10.1016/S1474-4422\(19\)30415-6](https://doi.org/10.1016/S1474-4422(19)30415-6)
- Stiso, J., & Bassett, D. S. (2018). Spatial Embedding Imposes Constraints on Neuronal Network Architectures. *Trends in Cognitive Sciences*, 22(12), 1127–1142. <https://doi.org/10.1016/j.tics.2018.09.007>
- Suárez, L. E., Markello, R. D., Betzel, R. F., & Misic, B. (2020). Linking Structure and Function in Macroscale Brain Networks. *Trends in Cognitive Sciences*, 24(4), 302–315. <https://doi.org/10.1016/j.tics.2020.01.008>
- Takatsuru, Y., Fukumoto, D., Yoshitomo, M., Nemoto, T., Tsukada, H., & Nabekura, J. (2009). Neuronal Circuit Remodeling in the Contralateral Cortical Hemisphere during Functional Recovery from Cerebral Infarction. *Journal of Neuroscience*, 29(32), 10081–10086. <https://doi.org/10.1523/JNEUROSCI.1638-09.2009>
- Tax, C. M. W., Bastiani, M., Veraart, J., Garyfallidis, E., & Okan Irfanoglu, M. (2022). What's new and what's next in diffusion MRI preprocessing. *NeuroImage*, 249, 118830. <https://doi.org/10.1016/j.neuroimage.2021.118830>
- Thiel, A., & Vahdat, S. (2015). Structural and Resting-State Brain Connectivity of Motor Networks After Stroke. *Stroke*, 46(1), 296–301. <https://doi.org/10.1161/STROKEAHA.114.006307>
- Thomas, C., Ye, F. Q., Irfanoglu, M. O., Modi, P., Saleem, K. S., Leopold, D. A., & Pierpaoli, C. (2014). Anatomical accuracy of brain connections derived from diffusion MRI tractography is inherently limited. *Proceedings of the National Academy of Sciences*, 111(46), 16574–16579. <https://doi.org/10.1073/PNAS.1405672111>
- Thomas Yeo, B. T., Krienen, F. M., Sepulcre, J., Sabuncu, M. R., Lashkari, D., Hollinshead, M., Roffman, J. L., Smoller, J. W., Zöllei, L., Polimeni, J. R., Fischl, B., Liu, H., & Buckner, R. L. (2011). The organization of the human cerebral cortex estimated by intrinsic functional connectivity. *Journal of Neurophysiology*, 106(3), 1125–1165. <https://doi.org/10.1152/jn.00338.2011>
- Tippett, D., Godin, B., Oishi, K., Oishi, K., Davis, C., Gomez, Y., Trupe, L., Kim, E., & Hillis, A. (2018). Impaired Recognition of Emotional Faces after Stroke Involving Right Amygdala or Insula. *Seminars in Speech and Language*, 39(01), 087–100. <https://doi.org/10.1055/s-0037-1608859>

References

- Tournier, J. D., Calamante, F., & Connelly, A. (2007). Robust determination of the fibre orientation distribution in diffusion MRI: Non-negativity constrained super-resolved spherical deconvolution. *NeuroImage*. <https://doi.org/10.1016/j.neuroimage.2007.02.016>
- Tournier, J.-D., Calamante, F., Gadian, D. G., & Connelly, A. (2004). Direct estimation of the fiber orientation density function from diffusion-weighted MRI data using spherical deconvolution. *NeuroImage*, 23(3), 1176–1185. <https://doi.org/10.1016/j.neuroimage.2004.07.037>
- Tournier, J.-D., Smith, R., Raffelt, D., Tabbara, R., Dhollander, T., Pietsch, M., Christiaens, D., Jeurissen, B., Yeh, C.-H., & Connelly, A. (2019). MRtrix3: A fast, flexible and open software framework for medical image processing and visualisation. *NeuroImage*, 202, 116137. <https://doi.org/10.1016/j.neuroimage.2019.116137>
- Triggs, W. J., Calvanio, R., & Levine, M. (1997). Transcranial magnetic stimulation reveals a hemispheric asymmetry correlate of intermanual differences in motor performance. *Neuropsychologia*, 35(10), 1355–1363. [https://doi.org/10.1016/S0028-3932\(97\)00077-8](https://doi.org/10.1016/S0028-3932(97)00077-8)
- Turrigiano, G. G., & Nelson, S. B. (2004). Homeostatic plasticity in the developing nervous system. *Nature Reviews Neuroscience*, 5(2), 97–107. <https://doi.org/10.1038/nrn1327>
- Uddin, L. Q., Yeo, B. T. T., & Spreng, R. N. (2019). Towards a universal taxonomy of macro-scale functional human brain networks. *Brain Topography*, 32(6), 926–942. <https://doi.org/10.1007/s10548-019-00744-6>
- Urbin, M. A., Hong, X., Lang, C. E., & Carter, A. R. (2014). Resting-State Functional Connectivity and Its Association With Multiple Domains of Upper-Extremity Function in Chronic Stroke. *Neurorehabilitation and Neural Repair*, 28(8), 761–769. <https://doi.org/10.1177/1545968314522349>
- Van De Ville, D., Farouj, Y., Preti, M. G., Liégeois, R., & Amico, E. (2021). When makes you unique: Temporality of the human brain fingerprint. *Science Advances*, 7(42), 751–766. https://doi.org/10.1126/SCIADV.ABJ0751/SUPPL_FILE/SCIADV.ABJ0751_SM.PDF
- van Meer, M. P. A., van der Marel, K., Wang, K., Otte, W. M., el Bouazati, S., Roeling, T. A. P., Viergever, M. A., Berkelbach van der Sprenkel, J. W., & Dijkhuizen, R. M. (2010). Recovery of Sensorimotor Function after Experimental Stroke Correlates with Restoration of Resting-State Interhemispheric Functional Connectivity. *The Journal of Neuroscience*, 30(11), 3964–3972. <https://doi.org/10.1523/JNEUROSCI.5709-09.2010>
- Varela, F., Lachaux, J.-P., Rodriguez, E., & Martinerie, J. (2001). The brainweb: Phase synchronization and large-scale integration. *Nature Reviews Neuroscience*, 2(4), 229–239. <https://doi.org/10.1038/35067550>
- Veerbeek, J. M., Winters, C., van Wegen, E. E. H., & Kwakkel, G. (2018). Is the proportional recovery rule applicable to the lower limb after a first-ever ischemic stroke? *PLOS ONE*, 13(1), e0189279. <https://doi.org/10.1371/journal.pone.0189279>
- Virani, S. S., Alonso, A., Aparicio, H. J., Benjamin, E. J., Bittencourt, M. S., Callaway, C. W., Carson, A. P., Chamberlain, A. M., Cheng, S., Delling, F. N., Elkind, M. S. V., Evenson, K. R., Ferguson, J. F., Gupta, D. K., Khan, S. S., Kissela, B. M., Knutson, K. L., Lee, C. D., Lewis, T. T., ... On behalf of the American Heart Association Council on Epidemiology and Prevention Statistics Committee and Stroke Statistics Subcommittee. (2021). Heart Disease and Stroke Statistics—2021 Update: A Report From the American Heart Association. *Circulation*, 143(8). <https://doi.org/10.1161/CIR.0000000000000950>

References

- Vliet, R., Selles, R. W., Andrinopoulou, E., Nijland, R., Ribbers, G. M., Frens, M. A., Meskers, C., & Kwakkel, G. (2020). Predicting Upper Limb Motor Impairment Recovery after Stroke: A Mixture Model. *Annals of Neurology*, 87(3), 383–393. <https://doi.org/10.1002/ana.25679>
- Wang, C., Qin, W., Zhang, J., Tian, T., Li, Y., Meng, L., Zhang, X., & Yu, C. (2014). Altered Functional Organization within and between Resting-State Networks in Chronic Subcortical Infarction. *Journal of Cerebral Blood Flow & Metabolism*, 34(4), 597–605. <https://doi.org/10.1038/jcbfm.2013.238>
- Wang, L., Yu, C., Chen, H., Qin, W., He, Y., Fan, F., Zhang, Y., Wang, M., Li, K., Zang, Y., Woodward, T. S., & Zhu, C. (2010). Dynamic functional reorganization of the motor execution network after stroke. *Brain*, 133(4), 1224–1238. <https://doi.org/10.1093/brain/awq043>
- Ward, N. S. (2017). Restoring brain function after stroke—Bridging the gap between animals and humans. *Nature Reviews Neurology*, 13(4), 244–255. <https://doi.org/10.1038/nrneurol.2017.34>
- Ward, N. S., Newton, J. M., Swayne, O. B. C., Lee, L., Thompson, A. J., Greenwood, R. J., Rothwell, J. C., & Frackowiak, R. S. J. (2006). Motor system activation after subcortical stroke depends on corticospinal system integrity. *Brain*, 129(3), 809–819. <https://doi.org/10.1093/brain/awl002>
- Wassermann, D., Makris, N., Rath, Y., Shenton, M., Kikinis, R., Kubicki, M., & Westin, C.-F. (2016). The white matter query language: A novel approach for describing human white matter anatomy. *Brain Structure & Function*, 221(9), 4705. <https://doi.org/10.1007/S00429-015-1179-4>
- Wechsler, D. (2008). Wechsler adult intelligence scale—Fourth Edition (WAIS-IV). *San Antonio, TX: NCS Pearson*, 22(498), 816–827.
- Whitfield-Gabrieli, S., & Nieto-Castanon, A. (2012). Conn: A Functional Connectivity Toolbox for Correlated and Anticorrelated Brain Networks. *Brain Connectivity*, 2(3), 125–141. <https://doi.org/10.1089/brain.2012.0073>
- Whitlock, J. R. (2017). Posterior parietal cortex. *Current Biology*, 27(14), R691–R695. <https://doi.org/10.1016/j.cub.2017.06.007>
- Wieloch, T., & Nikolich, K. (2006). Mechanisms of neural plasticity following brain injury. *Current Opinion in Neurobiology*, 16(3), 258–264. <https://doi.org/10.1016/j.conb.2006.05.011>
- Winship, I. R., & Murphy, T. H. (2008). In Vivo Calcium Imaging Reveals Functional Rewiring of Single Somatosensory Neurons after Stroke. *Journal of Neuroscience*, 28(26), 6592–6606. <https://doi.org/10.1523/JNEUROSCI.0622-08.2008>
- Winstein, C. J., Stein, J., Arena, R., Bates, B., Cherney, L. R., Cramer, S. C., Deruyter, F., Eng, J. J., Fisher, B., Harvey, R. L., Lang, C. E., MacKay-Lyons, M., Ottenbacher, K. J., Pugh, S., Reeves, M. J., Richards, L. G., Stiers, W., & Zorowitz, R. D. (2016). Guidelines for Adult Stroke Rehabilitation and Recovery: A Guideline for Healthcare Professionals From the American Heart Association/American Stroke Association. *Stroke*, 47(6). <https://doi.org/10.1161/STR.0000000000000098>
- Winters, C., van Wegen, E. E. H., Daffertshofer, A., & Kwakkel, G. (2015). Generalizability of the Proportional Recovery Model for the Upper Extremity After an Ischemic Stroke. *Neurorehabilitation and Neural Repair*, 29(7), 614–622. <https://doi.org/10.1177/1545968314562115>
- Winters, C., van Wegen, E. E. H., Daffertshofer, A., & Kwakkel, G. (2017). Generalizability of the Maximum Proportional Recovery Rule to Visuospatial Neglect Early Poststroke. *Neurorehabilitation and Neural Repair*, 31(4), 334–342. <https://doi.org/10.1177/1545968316680492>

References

- Witt, S. T., van Ettinger-Veenstra, H., Salo, T., Riedel, M. C., & Laird, A. R. (2021). What Executive Function Network is that? An Image-Based Meta-Analysis of Network Labels. *Brain Topography*, 34(5), 598–607. <https://doi.org/10.1007/s10548-021-00847-z>
- Xu, H., Qin, W., Chen, H., Jiang, L., Li, K., & Yu, C. (2014). Contribution of the Resting-State Functional Connectivity of the Contralesional Primary Sensorimotor Cortex to Motor Recovery after Subcortical Stroke. *PLoS ONE*, 9(1), e84729. <https://doi.org/10.1371/journal.pone.0084729>
- Yeh, C. H., Smith, R. E., Liang, X., Calamante, F., & Connelly, A. (2016). Correction for diffusion MRI fibre tracking biases: The consequences for structural connectomic metrics. *NeuroImage*, 142, 150–162. <https://doi.org/10.1016/j.neuroimage.2016.05.047>
- Zanchi, D., Montandon, M.-L., Sinanaj, I., Rodriguez, C., Depoorter, A., Herrmann, F. R., Borgwardt, S., Giannakopoulos, P., & Haller, S. (2017). Decreased Fronto-Parietal and Increased Default Mode Network Activation is Associated with Subtle Cognitive Deficits in Elderly Controls. *Neurosignals*, 25(1), 127–138. <https://doi.org/10.1159/000486152>
- Zeiler, S. R., Hubbard, R., Gibson, E. M., Zheng, T., Ng, K., O'Brien, R., & Krakauer, J. W. (2016). Paradoxical Motor Recovery From a First Stroke After Induction of a Second Stroke: Reopening a Postischemic Sensitive Period. *Neurorehabilitation and Neural Repair*, 30(8), 794–800. <https://doi.org/10.1177/1545968315624783>
- Zeiler, S. R., & Krakauer, J. W. (2013). The interaction between training and plasticity in the poststroke brain: *Current Opinion in Neurology*, 26(6), 609–616. <https://doi.org/10.1097/WCO.0000000000000025>
- Zhang, F., Wu, Y., Norton, I., Rath, Y., Golby, A. J., & O'Donnell, L. J. (2019). Test–retest reproducibility of white matter parcellation using diffusion MRI tractography fiber clustering. *Human Brain Mapping*, 40(10), 3041–3057. <https://doi.org/10.1002/HBM.24579>
- Zhang, S., & Murphy, T. H. (2007). Imaging the Impact of Cortical Microcirculation on Synaptic Structure and Sensory-Evoked Hemodynamic Responses In Vivo. *PLoS Biology*, 5(5), e119. <https://doi.org/10.1371/journal.pbio.0050119>
- Zhang, Y., Brady, M., & Smith, S. (2001). Segmentation of brain MR images through a hidden Markov random field model and the expectation-maximization algorithm. *IEEE Transactions on Medical Imaging*, 20(1), 45–57. <https://doi.org/10.1109/42.906424>
- Zhao, T., Duan, F., Liao, X., Dai, Z., Cao, M., He, Y., & Shu, N. (2015). Test-retest reliability of white matter structural brain networks: A multiband diffusion MRI study. *Frontiers in Human Neuroscience*, 0(FEB), 59. <https://doi.org/10.3389/FNHUM.2015.00059>
- Zimmermann, P., & Fimm, B. (2002). A test battery for attentional performance. *Applied Neuropsychology of Attention. Theory, Diagnosis and Rehabilitation*, 110–151.

Appendix

5.1 Supplementary Study 1: Towards individualized Medicine in Stroke – the TiMeS project: protocol of longitudinal, multi-modal, multi-domain study in stroke

Fleury L^{1,2*}, Koch PJ^{1,2,3*}, Wessel MJ^{1,2,4*}, Bonvin C⁵, San Millan D⁵, Ghika J⁵, Constantin C⁵, Vuadens P⁶, Adolphsen J⁷, Cadic-Melchior AG^{1,2}, Brügger J^{1,2}, Beanato E^{1,2}, Ceroni M^{1,2}, Menoud P^{1,2}, de Leon Rodriguez D², Zufferey V², Meyer N⁸, Egger P^{1,2}, Harquel S^{1,2}, Popa T^{1,2}, Raffin E^{1,2}, Girard G.^{9, 10}, Thiran JP^{7, 9, 10}, Vaney C⁷, Alvarez V⁵, Turlan J-P⁶, Mühl A⁶, Leger B⁶, Morishita T^{1,2}, Micera S^{11, 12}, Blanke O^{8, 13}, Van de Ville D^{10, 14, 15}, Hummel FC^{1,2, 16}

¹ Defitech Chair for Clinical Neuroengineering, Center for Neuroprosthetics (CNP) and Brain Mind Institute (BMI), École polytechnique fédérale de Lausanne (EPFL), Geneva, Switzerland

² Defitech Chair for Clinical Neuroengineering, CNP and BMI, EPFL Valais, Clinique Romande de Réadaptation, Sion, Switzerland

Swiss Federal Institute of Technology (EPFL Valais), Sion, Switzerland

³ Department of Neurology, University of Lübeck, Lübeck, Germany

⁴ Department of Neurology, Julius-Maximilians-University Würzburg, Würzburg, Germany

⁵ Hôpital du Valais, Sion, Switzerland

⁶ Clinique Romande de Réadaptation, Sion, Switzerland

⁷ Berner Klinik, Crans-Montana, Switzerland

⁸ Laboratory of Cognitive Neuroscience, Brain Mind Institute & Center for Neuroprosthetics, Ecole Polytechnique Fédérale de Lausanne (EPFL), Campus Biotech, Geneva, Switzerland

Radiology Department, Centre Hospitalier Universitaire Vaudois and University of Lausanne, Lausanne, Switzerland

⁹ Signal Processing Laboratory (LTS5), Ecole Polytechnique Fédérale de Lausanne (EPFL), Switzerland

¹⁰ CIBM Center for Biomedical Imaging, Switzerland

¹¹ The Biorobotics Institute and Department of Excellence in Robotics & AI, Scuola Superiore Sant'Anna, Pisa, Italy

¹² Bertarelli Foundation Chair in Translational Neuroengineering, Centre for Neuroprosthetics and Institute of Bioengineering, School of Engineering, Ecole Polytechnique Fédérale de Lausanne (EPFL), Lausanne, Switzerland

¹³ Department of Neurology, University of Geneva (UNIGE), Geneva, Switzerland;

¹⁴ Medical Image Processing Lab, Institute of Bioengineering, Center for Neuroprosthetics, Ecole Polytechnique Fédérale de Lausanne, Lausanne, VD, Switzerland.

¹⁵ Department of Radiology and Medical Informatics, University of Geneva (UNIGE), Geneva, Switzerland

¹⁶ Clinical Neuroscience, Geneva University Hospital, Geneva, Switzerland

* Share first authorship

Correspondence: Friedhelm Hummel, Defitech Chair for Clinical Neuroengineering, Center for Neuroprosthetics (CNP) and Brain Mind Institute (BMI), École polytechnique fédérale de Lausanne (EPFL), Campus Biotech, Room H4.3.132.084, Chemin des Mines 9, 1202 Geneva, Switzerland. Email: friedhelm.hummel@epfl.ch

Abstract

Despite recent improvements, complete motor recovery occurs in less than 15% of stroke patients. To improve the therapeutic outcomes, there is a strong need to tailor treatments to each individual patient. However, there is a lack of knowledge concerning the precise neuronal mechanisms underlying the degree and course of motor recovery and its individual differences, especially in the view of network properties despite the fact that it became more and more clear that stroke is a network disorder. The TiMeS project is a longitudinal exploratory study aiming at characterizing stroke phenotypes of a large, representative stroke cohort through an extensive, multi-modal and multi-domain evaluation. The ultimate goal of the study is to identify prognostic biomarkers allowing to predict the individual degree and course of motor recovery and its underlying neuronal mechanisms paving the way for novel interventions and treatment stratification for the individual patients. A total of up to 100 patients will be assessed at 4 timepoints over the first year after the stroke: during the first (T1) and third (T2) week, then three (T3) and twelve (T4) months after stroke onset. To assess underlying mechanisms of recovery with a focus on network analyses and brain connectivity, we will apply synergistic state-of-the-art systems neuroscience methods including functional and structural magnetic resonance imaging (MRI), and electrophysiological evaluation based on transcranial magnetic stimulation (TMS) coupled with electroencephalography (EEG) and electromyography (EMG). In addition, an extensive, multi-domain neuropsychological evaluation will be performed at each timepoint, covering all sensorimotor and cognitive domains. This project will significantly add to the understanding of underlying mechanisms of motor recovery with a strong focus on the interactions between the motor and other cognitive domains and multimodal network analyses. The population-based, multi-dimensional dataset will serve as a basis to develop biomarkers to predict outcome and promote personalized stratification towards individually tailored treatment concepts using neuro-technologies, thus paving the way towards personalized precision medicine approaches in stroke rehabilitation.

Introduction and rationale

With 80 million survivors in 2016, stroke is the second most common cause of acquired disabilities in the world (GBD 2019 Diseases and Injuries Collaborators, 2020; Gorelick, 2019). This number is still increasing due to the population growth and ageing (Feigin et al., 2015). Better acute stroke management results in an improved stroke survival on the one hand, but a higher prevalence of chronic stroke on the other hand (Gorelick, 2019). Yet, complete motor recovery still occurs in less than 15% of patients (Hendricks et al., 2002). Although motor deficits are the most debilitating and investigated (Kwakkel et al., 2003; Lai et al., 2002; Langhorne et al., 2009), patients also show consistent long-lasting cognitive deficits (Barker-Collo, Feigin, Parag, et al., 2010; Nys et al., 2007), with a relevant proportion of patients having multiple domains affected. These long-term impairing behavioral deficits have a strong impact on patients' reintegration, on patients and their relatives' daily life, but also on socioeconomics and health care systems (Barker-Collo & Feigin, 2006; GBD 2016 Stroke Collaborators, 2019). Therefore, the call for effective strategies of neurorehabilitation in order to maximize the rate of recovery is recognized as an important priority to substantially reduce the burden of stroke survivors (Feigin et al., 2014; Gorelick, 2019). However, the heterogeneity in stroke outcome and in individual recovery potential is an important challenge to address to provide optimal rehabilitative therapies. A crucial aspect to take up this challenge is to deepen our understanding of individual courses of recovery and the underlying neuronal mechanisms through the identification of associated biomarkers (Stinear, 2017).

On the behavioral level, stroke is known to yield multiple deficits. The most reported and debilitating ones are the motor impairments, present in 50% to 80% of stroke survivors (Langhorne et al., 2009). In particular, damages to the upper extremity function are common and significantly impact the patients' capacity to retrieve independence, as well as to reintegrate to professional life (Coupar et al., 2012; Lang et al., 2013). Besides motor deficits, cognitive impairment is common in stroke survivors although initially less obvious, half of stroke survivors reporting to suffer problems in at least one cognitive domain, an area much less studied than the motor domain (Barker-Collo, Feigin, Parag, et al., 2010; Dennis et al., 2000). Cognitive impairment could be found in multiple domains most frequently in, e.g., executive functions, attentional functions or memory. Such deficits are significantly persistent after one to several years after the stroke (Barker-Collo, Feigin, Parag, et al., 2010; Ramsey et al., 2017). Cognitive deficits also represent an obstacle for patients to go back into a normal daily life (Barker-Collo & Feigin, 2006; Hochstenbach et al., 2001; Patel et al., 2002). Furthermore, these dysfunctions might also strongly impact, slow or prevent proper motor recovery and response to treatment (Mullick et al., 2015).

For example, it is known that executive functions, such as information processing and motor planning are essential in the processes of motor (re)learning (Elliott, 2003), which is crucial in motor rehabilitation following stroke. However, despite few investigations of the relationships between these domains (e.g. Ramsey et al., 2017; Verstraeten et al., 2020), research mainly focused so far on deficits in only one domain, e.g. motor (Koch et al., 2016), language (Hartwigsen, 2016) or attentional (Barker-Collo, Feigin, Lawes, et al., 2010), domain and neglected largely the interaction between them. Thus, there is a strong lack of knowledge about how deficits in different domains depend on and influence each other in regard of impairment, residual functions and the process of regaining lost functions after a stroke.

Recovery is often incomplete among stroke survivors, and the potential of restoring lost functions is crucially highly heterogeneous between patients (Byblow et al., 2015; P. J. Koch & Hummel, 2017). For example, spontaneous natural recovery in motor domain occurs in roughly 2/3 of patients (Stinear, 2017) who recover about ~70% in average of their maximum recovery potential given their initial impairment (Prabhakaran et al., 2008). On the other side, roughly 1/3 presents altered or insufficient intrinsic plasticity after stroke leading to a poor natural recovery (Stinear, 2017). Such heterogeneity has also been reported in other cognitive deficits e.g., neglect and aphasia (Marchi et al., 2017). In addition, stroke survivors act highly heterogeneous in the view of the response towards specific treatment strategies, resulting in the distinction between responders and non-responders (Coscia et al., 2019; Micera et al., 2020; Morishita & Hummel, 2017). For instance, patients with cortical lesions specifically demonstrated lower responsiveness to repetitive Transcranial Magnetic Stimulation (TMS) protocols (Lefaucheur et al., 2020). Therefore, a key challenging aspect for enhancing neuro-rehabilitation efficacy might be to shed light on the heterogeneity of stroke patients and leverage this information to determine and predict the degree of impairment and potential for individual functional recovery (Bonkhoff & Grefkes, 2021; Koch et al., 2021). This heterogeneity in stroke ranges from brain reorganization to behavioral outcomes and needs to be accounted for when planning rehabilitation strategies (Bonkhoff & Grefkes, 2021; Morishita & Hummel, 2017).

The identification of specific individual patterns of recovery through a multi-domain perspective during the first weeks/months post-stroke, and crucially the uncovering of the underlying brain reorganization mechanisms would be a massive step towards the optimization of treatment strategies for each patient. However, there is a lack of understanding concerning the detailed neuronal mechanisms following a stroke lesion and during the course of recovery. Accumulating evidence suggests that stroke is not a focal disorder, but a network disorder (Guggisberg et al.,

2019; Rehme & Grefkes, 2013). In addition to local brain tissue damage, stroke also impacts the functioning of connected areas (close or remote from the lesion) as a result of alterations in brain networks (Carrera & Tononi, 2014). In addition, functional reorganization associated with recovery is also not restricted to a focal area. For instance, cortical plasticity associated with motor recovery is not restricted to the primary motor cortex (M1), but rather embraces the complete motor network, including primary and secondary motor cortical areas in both hemispheres, subcortical areas like the basal ganglia and the cerebellum (Grefkes & Fink, 2014; Grefkes & Ward, 2014; Koch et al., 2021). Factors such as lesion size and location (REF), as well as structural and functional prerequisites and dynamics (Egger et al., 2021) might relevantly influence recovery-associated plasticity processes in the brain leading to heterogeneous, widespread and time-dependent changes of brain reorganization and connectivity between patients. To improve rehabilitative strategies, it is therefore crucial to take this heterogeneity into account and understand how it relates to the pattern of network reorganization and the range of behavioral outcomes following a stroke.

On the basis of this reasoning, there is a strong need for an exact phenotyping of patients considering stroke heterogeneity to predict outcome, course of recovery leading to improve stroke recovery and treatment outcomes. Such challenge requires to gain a detailed and fundamental knowledge about the precise neuronal mechanisms associated with behavioral recovery, with a particular emphasis on brain networks changes. In addition, is essential to investigate the different domains impacted by the stroke and not just focusing on one behavioral outcome. As network and behavioral alterations following stroke are dynamic and not linear, a longitudinal investigation is of great importance. Such phenotyping will allow to distinguish distinct profiles of patients with associated dynamics of brain reorganization over the course of recovery. Enhancing the fundamental knowledge of stroke diversity through a multimodal and multidomain approach would serve as a basis to pave the way for personalized precision medicine in the field of stroke recovery to achieve maximal treatment effects.

To take up this challenge, the TiMeS project aims at characterizing in details phenotypes of stroke patients allowing to determine the individual course and degree of recovery following stroke and to identify relevant biomarkers associated with recovery. To that purpose, the goal is to collect a large multidimensional dataset that would be representative for the stroke population. Measurements will come from synergistic state-of-the-art systems neuroscience methods including magnetic resonance imaging (MRI), transcranial magnetic stimulation (TMS) coupled with electroencephalography (EEG), in a longitudinal assessment from acute to chronic stage in

the first year after the stroke. As stroke is not a focal disorder, subsequent analyses will focus on networks properties within the whole brain and their changes over time, in combination with stroke behavioral outcomes. To provide detailed knowledge about the behavioral patterns and relationships between domains, the procedure will contain an extensive evaluation of behavioral outcomes in multiple domains, including a multi-cognitive assessment not only looking on the motor domain. The multidimensional dataset acquired through this research will enable to assess for the first time the complex interactions of structural and functional brain connectivity parameters within certain domain-specific networks as well as within the whole brain, and to associate them with stroke behavioral outcomes and functional recovery.

Methods

Study design

The present project is an on-going longitudinal observational study. We follow-up a total of up to 100 stroke patients at four timepoints over a year (T1: 1st week, T2: three weeks, T3: three months, T4: twelve months) from the acute to the chronic phase of recovery after the ictal event. At each timepoint, we investigate the neural correlates of recovery and the underlying plasticity through a multi-modal and multi-domain set of evaluations including structural and functional neuroimaging (MRI), electrophysiology (resting-state EEG, and TMS coupled with EEG) and an extensive battery of tests assessing the multi-domain functional and behavioral outcomes of the patients.

Objectives

The main goal of the study is to assess the inter-individual variance and different phenotypes of patients after an ischemic or hemorrhagic stroke. The main goal is divided into three related objectives: 1) to evaluate the neuro-imaging and neurophysiological factors that determine the course and degree of recovery with a focus on connectomics, 2) to determine the interactions between multiple cognitive, visual, sensory, and motor functions and their impact on impairment, residual functions and recovery, and 3) to associate the changes in connectomics parameters with the clinical-behavioral outcomes.

To complete these objectives, we apply a multimodal assessment of neuro-imaging and neurophysiological parameters to leverage the advantages of each methods and account for their specific limitations to achieve an as much detailed picture as possible, especially in the view of the importance of network analyses. In addition, we use an extensive battery of behavioral tests to

get detailed information concerning the patients' motor and cognitive profiles as well as their dynamics. The overall goal of this research will be to integrate and combine the multimodal data (i.e. neuroimaging, electrophysiology, and behavioral) together to obtain detailed and complete phenotypes of stroke patients.

Primary outcome

As upper extremity function and impairment are the main reason for long-term disability and predictors of reintegration in normal life and functional independence after stroke, longitudinal recovery of the upper limb function and its underlying mechanisms are the primary interest of this study. Upper limb motor function includes multiple aspects, fine and gross dexterity, gross motor function, strength, spasticity, etc (Santisteban et al., 2016). These aspects are assessed longitudinally using the same set of reliable and validated clinical tests at each timepoint (see *Appendix 1* for details). We are especially interested in how other cognitive domains and their alterations after a stroke impact on motor recovery.

Secondary outcomes

Secondary outcomes are specific readouts based on the multi-domain cognitive evaluation and the multi-modal data from system neurosciences techniques, i.e. neuro-imaging and electrophysiological methods.

Magnetic Resonance Imaging (MRI)

Structural, diffusion-weighted and resting-state functional MRI are used to obtain individual structural and functional network properties to evaluate lesion-related neuronal alterations as well as their dynamics throughout the recovery phase, i.e. neuronal plasticity, reorganization and degeneration. Analyses will mainly focus on brain network alterations and changes over time through disconnectomics (Veldsman & Brodtmann, 2019) and by applying computational approaches such as graph theory methods (Sporns, 2018), e.g the *Rich-Club* approach (van den Heuvel & Sporns, 2011). In addition, integrated analyses of brain structure and function will be emphasized, e.g. by using the Structural Decoupling Index (SDI), a metric that allows to quantify the coupling strength between structure and function (Preti & Van De Ville, 2019). MRI methods and sequences are detailed in *Appendix n°2*.

Electrophysiological recordings

Functional measurements of the cortical excitability are provided by means of Transcranial Magnetic Stimulation (TMS). We use single pulses delivered to the primary motor cortex (M1) to generate motor evoked potential (MEPs) and to screen for cortico-spinal tract integrity. We also apply paired-pulses to assess the short-interval intracortical inhibition (SICI; [Kujirai et al., 1993](#)). This is thought to reflect GABA_A-mediated inhibition in the motor cortex (Chen, 2004). Electroencephalography (EEG) allows to assess the resting state brain connectivity (Babiloni et al., 2020), but more importantly, in combination with TMS, EEG is used to assess interregional connectivity in the brain and to characterize the TMS-evoked potential and its evolution during the course of recovery. Therefore, TMS-EEG represents a unique method to study brain dynamics and their changes over time as it allows to record directly and non-invasively various neurophysiological processes across motor and non-motor areas e.g. cortical responsiveness, cortico-cortical interactions, local excitation and inhibition, oscillatory activity etc (see Tremblay et al., 2019 for a recent review). Electrophysiological methods are detailed in *Appendix n°3*.

Behavioral outcomes

To assess precisely the motor and cognitive profiles of the patients, an extensive battery of 40 tests is performed at each timepoint by a trained neuropsychologist. The battery covers sensory-motor domains as well as each neuro-cognitive domain as defined in the DSM-V, i.e. executive functions, language, complex attention, learning and memory, social cognition, perceptual-motor domains (Sachdev et al., 2014). Multiple questionnaires complete this battery to evaluate additional aspects such as fatigue, mood, functional independence and recovery. See appendix n°3 for details.

Study organization

Ethical considerations

The study was designed and is conducted according to the guidelines of the Declaration of Helsinki. All the procedures were approved by the cantonal ethics committee (Project ID 2018-01355).

Eligibility

We look for stroke patients presenting some upper limb motor impairment in the acute stage. In order to get a heterogeneous cohort, we screen patients with first-ever as well as recurrent stroke, either ischemic or hemorrhagic. Detailed inclusion and exclusion criteria are following:

- Inclusion criteria
 - o Age > 18 years old
 - o First-ever or recurrent stroke
 - o Ischemic or hemorrhagic stroke
 - o Stroke incident < 7 days at consent
 - o Motor impairment in the acute stage, objectified by a clinical assessment
 - o Absence of contraindication for NIBS and MRI
- Exclusion criteria
 - o Severe neuropsychiatric (e.g. major depression, severe dementia) or medical disease
 - o Not able to consent
 - o Severe sensory or cognitive impairment or musculoskeletal dysfunctions prohibiting to understand instructions or the perform the experimental tasks
 - o Implanted medical electronic devices or ferromagnetic metal implants, which are not MRI and TMS compatible
 - o History of seizures
 - o Medication that significantly interacts with NIBS being benzodiazepines, tricyclic antidepressant and antipsychotics
 - o Pregnancy
 - o Regular use of narcotic drugs
 - o Request of not being informed in case of incidental findings

Recruitment and screening

Stroke patients are recruited at the *Hôpital du Valais* (HVS), at the stroke unit. The member of staff in charge of the recruitment checks the list of new entries at the hospital daily. When a new patient is eligible (see Inclusion and Exclusion criteria), the medical staff is consulted and a first screening visit is organized with the patient. The study is presented in detail to the patient, and eligibility is further evaluated. Patients are provided with 24-hours for reflection in regard of participation before signing the consent to participate. If the patient consents, the first visit (T1) is organized during the first week after the stroke, while the patient is most of the time still hospitalized. The procedures are performed in accordance with the ethical approval.

Data acquisition and follow-up

The 1st behavioral evaluation and the MRI acquisition are performed at the HVS. The electrophysiological measurements are performed in the laboratory, located in the *Clinique*

Romande de Réadaptation (CRR) physically connected to the HVS. The total measurement time is of around 10 hours, distributed in several sessions.

The patients enrolled in the study are then transferred for rehabilitation from the HVS to one of the two rehabilitation clinics collaborating within the present study, that is the CRR and the Berner Klinik (BK; Crans-Montana) or to home. The 3 weeks (T2) behavioral evaluation is performed during the in-patient stay, or in the laboratory if the patient was sent back home after the acute phase. For the 3 months (T3) and 12 months follow-ups (T4), patients are invited to our laboratory on the HVS/CRR campus for behavioral, MRI and electrophysiological recordings.

Data management and statistical considerations

Based on previous comparable project (e.g. Corbetta et al., 2015; N=132 patients) and given the estimated feasibility of our extensive multi-modal and multi-domain evaluations, we aimed to recruit up to 100 patients, with a recruitment rate of up to 40 patients a year. As drop-outs are common for this type of longitudinal study, we expect some missing datapoints and will use statistical approaches that are robust to missing values such as linear mixed models.

As the study is mainly explorative in its nature, we do not use a classical power calculation. We will analyze the different behavioral domains individually but we also aim to integrate the multimodal data together in statistical models and computational approaches, in order to determine interactions between the different parameters. Statistics will be performed using either R software (2017, R Core Team, Vienna, <https://www.R-project.org/>), the SPSS software (2017, IBM SPSS Statistics for Windows, IBM Corp, Armonk, New York), the JASP software, Matlab (v2020b, Mathworks, The MathWorks, Massachusetts, <http://www.mathworks.ch>) and/or Python (2009, CreateSpace, Scotts Valley, California). We will use a broad spectrum of statistical tools designed for high-dimensional datasets, like general linear model analyses. Besides, we will also use machine learning tools as classifiers, supervised and unsupervised and deep learning algorithms as they provide the opportunity to derive insights from imaging and electrophysiological data coupled with behavior to produce predictive models and to discovering phenotypes of patients (Tozlu et al., 2020; Wessel et al., 2021). Specific factors included in statistical modeling will be either hypothesis-driven or mainly exploratory.

Discussion

As depicted in the introduction, stroke results in multi-domain behavioral deficits in survivors. Although motor deficits (in particular in the upper extremity) are the most impairing, the prevalence of cognitive deficits is also highly important and concerns multiple domains. In addition, they were demonstrated to likely impact the functional recovery and the reintegration in life following stroke, as well as the outcomes of motor rehabilitation (Mullick et al., 2015). Yet, little attention has been paid so far to how cognitive and motor domains are related and influence each other following stroke and there is a lack of detailed phenotyping of behavioral outcomes and their evolution though it would be of high interest to improve rehabilitation tailoring (Corbetta et al., 2015; Duncan et al., 2005)

Some studies have investigated the relationships between cognitive and motor outcomes (Corbetta et al., 2015; Einstad et al., 2021; Fong et al., 2001; Ramsey et al., 2017; Sagnier et al., 2017; Verstraeten et al., 2020) and showed that cognitive impairments were common even in patients with mild strokes, and that relationships exist between motor and cognitive domains. This highlights the relevance of such multi-domain approaches, emphasizing that motricity and cognition should not be investigated separately. For instance, Einstad and colleagues (2021) have recently demonstrated that poor motor performances are associated with impaired global cognition scores and executive dysfunctions. However, such studies made use of a limited battery of tests and/or focused on one particular timeframe during stroke recovery without any longitudinal assessment (i.e. acute, sub-acute, chronic). Ramsey and colleagues (2017) employed a battery of motor and cognitive tests to evaluate the patients over the course of recovery during the first year; at 1-2 weeks, three months and one year after the stroke. They reported that across multiple domains, sub-acute scores were strong predictors of the performance in the chronic stage and that the magnitude and time course of recovery were comparable between cognitive and motor domains. Specific behavioral clusters were identified (e.g., a strong relationship between motor impairment and attention) and shown as being stable over the three timepoints. In addition, the authors described relationships of interest between domains over the course of recovery (e.g. language deficits influenced the recovery of verbal memory). Interestingly, the authors studied how lesion topography could explain behavior, as it was done in another study from the same group (Corbetta et al., 2015) and pointed out that white matter damage could be a key feature in explaining behavioral recovery. Other studies from the same cohort independently investigated the relationships between resting-state fMRI data and behavior by showing that altered functional connectivity correlated with behavioral deficits in the motor and attention domains (Siegel, Snyder, et al., 2016) and in hemi-spatial neglect (Ramsey et al., 2016). In addition,

the authors demonstrated that memory deficits are better predicted by functional connectivity than by lesion topography while the motor and visual deficits might be better predicted by lesion location than functional connectivity (Siegel, Ramsey, et al., 2016). Altogether, these studies emphasized the importance of multi-domain behavioral assessments and the interest of investigating brain-behavior relationships both through structural and functional measures as they provide complementary insights. However, patients enrolled in this cohort were substantially younger than the natural population of stroke survivors (average age 54 ± 11 years old, range 19-83, benchmark 69.2 years in 2005 Greater Cincinnati/Northern Kentucky cohort; [Kissela et al., 2012](#)) and executive functions were not assessed in the battery. Plus, the authors focused on one modality (MRI) to assess brain features which provides rich but limited insights about the neuronal mechanisms underlying post-stroke recovery. To date, no study provided any extensive behavioral evaluation (with an approach centered on the individuals rather than the whole cohort) and during the course of recovery following stroke while combining data with multimodal assessments of brain network plasticity.

A common factor in many of these studies is the interplay between structural and functional connectivity. Structure influences function in the obvious way, while function influences structure in the long term. However, there is strong evidence that the strength of the link between structure and function is domain-dependent. The findings of Siegel, Ramsey and colleagues suggest that function is tightly coupled to structure in the motor and visual domains, while the two are more decoupled for “higher order” domains such as memory. These findings have been echoed in Preti & Van De Ville’s work ([2019](#)), which found that brain regions responsible for “low level sensory function” tend to exhibit strong structural-functional coupling, and vice versa.

The present study aspires to bolster our understanding of mechanics underlying multiple-domain deficits by providing a multi-modal and multi-domain evaluation of stroke patients longitudinally during the first year after the stroke. This research intends to investigate the different behavioral profiles and their dynamics in stroke patients, not only looking at the motor domain but undergoing a holistic approach coupled with neuro-imaging and electrophysiological parameters. Therefore, the originality of the project lies in the multiplicity of the approaches undertaken that will allow to provide a very detailed picture of the recovery and the reorganization in the brain following stroke. Structural, diffusion-weighted and functional MRI will provide the opportunity to study network dysfunctions as well as the complex interactions between brain function and structure. In addition, simultaneous EEG recording during TMS is a promising approach that will enable to explore brain connectivity and recovery pattern for functional networks after stroke by

providing a direct measure of the cortical activity induced by TMS. By combining modalities with different advantages (such as either excellent spatial or temporal resolution, structural versus functional information) and by following patients along the first year, we will provide a complete dataset allowing to integrate multimodal information in statistical and computational models. The overall goal is to determine interactions between the different parameters and to determine factors usable as biomarkers for phenotyping patients in regard of the course and the degree of recovery.

Identifying such biomarkers might help (1) to predict the course of recovery, i.e. to early detect patients that will spontaneously recover and those who will not and, consequently, (2) to personalize the therapeutic strategies in order to meet the individual needs of each patient and to maximize the treatment benefits. Therefore, this work will serve as a basis for improving existing treatments or developing novel and innovative ones tailored to the individual patients' characteristics by providing a better understanding of neural mechanisms underlying successful recovery. For instance, non-invasive brain stimulation (NIBS) are neuro-technologies that are more and more used in stroke rehabilitation to promote motor recovery (Hummel & Cohen, 2006; Morishita & Hummel, 2017; Raffin & Hummel, 2018) due to their noninvasiveness, relatively low cost and limited side effects. However, there is a high heterogeneity in the outcomes (Alia et al., 2017; Coscia et al., 2019; Micera et al., 2020; Nicolo et al., 2015; Wessel et al., 2021): effects of NIBS are still limited, which can be partly explained by the use of non-personalized approaches (Grefkes & Fink, 2016; Morishita & Hummel, 2017). Some biomarkers have already been identified to stratify patients in order to assess the individual recovery potential, for instance the cortico-spinal tract integrity as measured by presence or absence of MEP (Lindenberg et al., 2012). However there is still a lack of fundamental knowledge on the topic especially considering the longitudinal changes in brain dynamics following stroke (Koch et al., 2016). The detailed phenotyping based on the dataset from the present study might further help to provide extra layers of stratifications allowing more precise predictions about treatment outcomes in order to reduce the number of non-responders (Wessel et al., 2021). Therefore, some potential perspectives are to further design interventional studies to analyze the efficacy of neurotechnologies-based treatment personalized thanks to clustering and stratifying algorithms arising from this research.

Since this work involves plural and extensive multi-modal assessments, it is worthwhile to emphasize that the patients need to be physically and mentally capable of undergoing such multiple recordings. Plus, as the patients need to understand what the project entails, severe

language deficits prevent possible participants to be enrolled because they do not have the ability to consent while being transparently informed. Furthermore, the presence of TMS recordings is associated with a consistent list of exclusion criteria related to medication, epilepsy or metal implants that could interact with the stimulation. These aspects might cause a bias in the recruitment of patients that we need to consider when interpreting the results. Still, we look for cohort as heterogeneous as possible to cluster patients and identify specific patterns of recovery and brain reorganization.

Summary and conclusions

A better understanding of the neuronal mechanisms associated with recovery-related plasticity and reorganization of the brain networks after a stroke is needed to enhance the understanding of the recovery process, and to predict the outcome and course of recovery. This knowledge will enable to develop and apply interventional strategies in a personalized way to enhance the effects of the treatments for each individual patient. The TiMeS project is a longitudinal, multimodal, and multidomain study of a large, representative cohort of patients during the first year after the stroke, including neuro-imaging, electrophysiological and extensive behavioral evaluations. This exploratory research will provide the opportunity to integrate and combine multidimensional data from neuroscience systems methods together with detailed behavioral outcomes to identify specific biomarkers of recovery. This phenotyping will serve as a basis to tailor current rehabilitation strategies according to each patient's individual needs and to develop innovative personalized neuro-technologies based treatment like NIBS, beyond a one-fits-all approach. Overall, the knowledge gained from this study will pave the way for establishing a close link between basic neuroscience and the development of novel treatments into clinical routine towards precision medicine in stroke, which is highly promising to reduce the burden of the disease.

References

- Alia, C., Spalletti, C., Lai, S., Panarese, A., Lamola, G., Bertolucci, F., Vallone, F., Di Garbo, A., Chisari, C., Micera, S., & Caleo, M. (2017). Neuroplastic Changes Following Brain Ischemia and their Contribution to Stroke Recovery : Novel Approaches in Neurorehabilitation. *Frontiers in Cellular Neuroscience*, 11, 76. <https://doi.org/10.3389/fncel.2017.00076>
- Babiloni, C., Barry, R. J., Başar, E., Blinowska, K. J., Cichocki, A., Drinkenburg, W. H. I. M., Klimesch, W., Knight, R. T., Lopes da Silva, F., Nunez, P., Oostenveld, R., Jeong, J., Pascual-Marqui, R., Valdes-Sosa, P., & Hallett, M. (2020). International Federation of Clinical Neurophysiology (IFCN) – EEG research workgroup : Recommendations on frequency and topographic analysis of resting state EEG rhythms. Part 1: Applications in clinical research studies. *Clinical Neurophysiology*, 131(1), 285-307. <https://doi.org/10.1016/j.clinph.2019.06.234>
- Barker-Collo, S., & Feigin, V. (2006). The impact of neuropsychological deficits on functional stroke outcomes. *Neuropsychology Review*, 16(2), 53-64. <https://doi.org/10.1007/s11065-006-9007-5>
- Barker-Collo, S., Feigin, V. L., Parag, V., Lawes, C. M. M., & Senior, H. (2010). Auckland Stroke Outcomes Study : Part 2: Cognition and functional outcomes 5 years poststroke. *Neurology*, 75(18), 1608-1616. <https://doi.org/10.1212/WNL.0b013e3181fb44c8>
- Barker-Collo, S., Feigin, V., Lawes, C., Senior, H., & Parag, V. (2010). Natural history of attention deficits and their influence on functional recovery from acute stages to 6 months after stroke. *Neuroepidemiology*, 35(4), 255-262. <https://doi.org/10.1159/000319894>
- Bonkhoff, A. K., & Grefkes, C. (2021). Precision medicine in stroke : Towards personalized outcome predictions using artificial intelligence. *Brain*, awab439. <https://doi.org/10.1093/brain/awab439>
- Byblow, W. D., Stinear, C. M., Barber, P. A., Petoe, M. A., & Ackerley, S. J. (2015). Proportional recovery after stroke depends on corticomotor integrity. *Annals of Neurology*, 78(6), 848-859. <https://doi.org/10.1002/ana.24472>
- Carrera, E., & Tononi, G. (2014). Diaschisis: Past, present, future. *Brain*, 137(9), 2408-2422. <https://doi.org/10.1093/brain/awu101>
- Chen, R. (2004). Interactions between inhibitory and excitatory circuits in the human motor cortex. *Experimental Brain Research*, 154(1), 1-10. <https://doi.org/10.1007/s00221-003-1684-1>
- Corbetta, M., Ramsey, L., Callejas, A., Baldassarre, A., Hacker, C. D., Siegel, J. S., Astafiev, S. V., Rengachary, J., Zinn, K., Lang, C. E., Connor, L. T., Fucetola, R., Strube, M., Carter, A. R., & Shulman, G. L. (2015). Common behavioral clusters and subcortical anatomy in stroke. *Neuron*, 85(5), 927-941. <https://doi.org/10.1016/j.neuron.2015.02.027>
- Coscia, M., Wessel, M. J., Chaudary, U., Millán, J. D. R., Micera, S., Guggisberg, A., Vuadens, P., Donoghue, J., Birbaumer, N., & Hummel, F. C. (2019). Neurotechnology-aided interventions for upper limb motor rehabilitation in severe chronic stroke. *Brain: A Journal of Neurology*, 142(8), 2182-2197. <https://doi.org/10.1093/brain/awz181>
- Coupar, F., Pollock, A., Rowe, P., Weir, C., & Langhorne, P. (2012). Predictors of upper limb recovery after stroke : A systematic review and meta-analysis. *Clinical Rehabilitation*, 26(4), 291-313. <https://doi.org/10.1177/0269215511420305>
- Daducci, A., Dal Palu, A., Lemkaddem, A., & Thiran, J.-P. (2015). COMMIT: Convex Optimization Modeling for Microstructure Informed Tractography. *IEEE Transactions on Medical Imaging*, 34(1), 246-257. <https://doi.org/10.1109/TMI.2014.2352414>
- Dennis, M., O'Rourke, S., Lewis, S., Sharpe, M., & Warlow, C. (2000). Emotional outcomes after stroke : Factors associated with poor outcome. *Journal of Neurology, Neurosurgery, and Psychiatry*, 68(1), 47-52. <https://doi.org/10.1136/jnnp.68.1.47>
- Duncan, P. W., Zorowitz, R., Bates, B., Choi, J. Y., Glasberg, J. J., Graham, G. D., Katz, R. C., Lamberty, K., & Reker, D. (2005). Management of Adult Stroke Rehabilitation Care : A clinical practice guideline. *Stroke*, 36(9), e100-143. <https://doi.org/10.1161/01.STR.0000180861.54180.FF>

- Egger, P., Evangelista, G. G., Koch, P. J., Park, C.-H., Levin-Gleba, L., Girard, G., Beanato, E., Lee, J., Choirat, C., Guggisberg, A. G., Kim, Y.-H., & Hummel, F. C. (2021). Disconnectomics of the Rich Club Impacts Motor Recovery After Stroke. *Stroke*, 52(6), 2115-2124. <https://doi.org/10.1161/STROKEAHA.120.031541>
- Einstad, M. S., Saltvedt, I., Lydersen, S., Ursin, M. H., Munthe-Kaas, R., Ihle-Hansen, H., Knapskog, A.-B., Askim, T., Beyer, M. K., Næss, H., Seljeseth, Y. M., Ellekjær, H., & Thingstad, P. (2021). Associations between post-stroke motor and cognitive function : A cross-sectional study. *BMC Geriatrics*, 21(1), 103. <https://doi.org/10.1186/s12877-021-02055-7>
- Elliott, R. (2003). Executive functions and their disorders. *British Medical Bulletin*, 65, 49-59. <https://doi.org/10.1093/bmb/65.1.49>
- Feigin, V. L., Forouzanfar, M. H., Krishnamurthi, R., & Mensah, G. A. (2014). Global burden of stroke : An underestimate - Authors' reply. *Lancet (London, England)*, 383(9924), 1205-1206. [https://doi.org/10.1016/S0140-6736\(14\)60596-1](https://doi.org/10.1016/S0140-6736(14)60596-1)
- Feigin, V. L., Krishnamurthi, R. V., Parmar, P., Norrving, B., Mensah, G. A., Bennett, D. A., Barker-Collo, S., Moran, A. E., Sacco, R. L., Truelsen, T., Davis, S., Pandian, J. D., Naghavi, M., Forouzanfar, M. H., Nguyen, G., Johnson, C. O., Vos, T., Meretoja, A., Murray, C. J. L., ... GBD 2013 Stroke Panel Experts Group. (2015). Update on the Global Burden of Ischemic and Hemorrhagic Stroke in 1990-2013 : The GBD 2013 Study. *Neuroepidemiology*, 45(3), 161-176. <https://doi.org/10.1159/000441085>
- Fong, K. N., Chan, C. C., & Au, D. K. (2001). Relationship of motor and cognitive abilities to functional performance in stroke rehabilitation. *Brain Injury*, 15(5), 443-453. <https://doi.org/10.1080/02699050010005940>
- GBD 2016 Stroke Collaborators. (2019). Global, regional, and national burden of stroke, 1990-2016 : A systematic analysis for the Global Burden of Disease Study 2016. *The Lancet. Neurology*, 18(5), 439-458. [https://doi.org/10.1016/S1474-4422\(19\)30034-1](https://doi.org/10.1016/S1474-4422(19)30034-1)
- GBD 2019 Diseases and Injuries Collaborators. (2020). Global burden of 369 diseases and injuries in 204 countries and territories, 1990-2019 : A systematic analysis for the Global Burden of Disease Study 2019. *Lancet (London, England)*, 396(10258), 1204-1222. [https://doi.org/10.1016/S0140-6736\(20\)30925-9](https://doi.org/10.1016/S0140-6736(20)30925-9)
- Gorelick, P. B. (2019). The global burden of stroke : Persistent and disabling. *The Lancet Neurology*, 18(5), 417-418. [https://doi.org/10.1016/S1474-4422\(19\)30030-4](https://doi.org/10.1016/S1474-4422(19)30030-4)
- Grefkes, C., & Fink, G. R. (2014). Connectivity-based approaches in stroke and recovery of function. *The Lancet Neurology*, 13(2), 206-216. [https://doi.org/10.1016/S1474-4422\(13\)70264-3](https://doi.org/10.1016/S1474-4422(13)70264-3)
- Grefkes, C., & Fink, G. R. (2016). Noninvasive brain stimulation after stroke : It is time for large randomized controlled trials! *Current Opinion in Neurology*, 29(6), 714-720. <https://doi.org/10.1097/WCO.0000000000000395>
- Grefkes, C., & Ward, N. S. (2014). Cortical Reorganization After Stroke : How Much and How Functional? *The Neuroscientist*, 20(1), 56-70. <https://doi.org/10.1177/1073858413491147>
- Guggisberg, A. G., Koch, P. J., Hummel, F. C., & Buetefisch, C. M. (2019). Brain networks and their relevance for stroke rehabilitation. *Clinical Neurophysiology: Official Journal of the International Federation of Clinical Neurophysiology*, 130(7), 1098-1124. <https://doi.org/10.1016/j.clinph.2019.04.004>
- Hartwigsen, G. (2016). Adaptive Plasticity in the Healthy Language Network : Implications for Language Recovery after Stroke. *Neural Plasticity*, 2016, 9674790. <https://doi.org/10.1155/2016/9674790>
- Hendricks, H. T., van Limbeek, J., Geurts, A. C., & Zwarts, M. J. (2002). Motor recovery after stroke : A systematic review of the literature. *Archives of Physical Medicine and Rehabilitation*, 83(11), 1629-1637. <https://doi.org/10.1053/apmr.2002.35473>
- Hochstenbach, J. B., Anderson, P. G., van Limbeek, J., & Mulder, T. T. (2001). Is there a relation between neuropsychologic variables and quality of life after stroke? *Archives of Physical Medicine and Rehabilitation*, 82(10), 1360-1366. <https://doi.org/10.1053/apmr.2001.25970>

- Hummel, F. C., & Cohen, L. G. (2006). Non-invasive brain stimulation : A new strategy to improve neurorehabilitation after stroke? *The Lancet Neurology*, 5(8), 708-712. [https://doi.org/10.1016/S1474-4422\(06\)70525-7](https://doi.org/10.1016/S1474-4422(06)70525-7)
- Kissela, B. M., Khoury, J. C., Alwell, K., Moomaw, C. J., Woo, D., Adeoye, O., Flaherty, M. L., Khatri, P., Ferioli, S., De Los Rios La Rosa, F., Broderick, J. P., & Kleindorfer, D. O. (2012). Age at stroke : Temporal trends in stroke incidence in a large, biracial population. *Neurology*, 79(17), 1781-1787. <https://doi.org/10.1212/WNL.0b013e318270401d>
- Koch, P. J., & Hummel, F. C. (2017). Toward precision medicine : Tailoring interventional strategies based on noninvasive brain stimulation for motor recovery after stroke. *Current Opinion in Neurology*, 30(4), 388-397. <https://doi.org/10.1097/WCO.0000000000000462>
- Koch, P. J., Park, C.-H., Girard, G., Beanato, E., Egger, P., Evangelista, G. G., Lee, J., Wessel, M. J., Morishita, T., Koch, G., Thiran, J.-P., Guggisberg, A. G., Rosso, C., Kim, Y.-H., & Hummel, F. C. (2021). The structural connectome and motor recovery after stroke : Predicting natural recovery. *Brain: A Journal of Neurology*, 144(7), 2107-2119. <https://doi.org/10.1093/brain/awab082>
- Koch, P., Schulz, R., & Hummel, F. C. (2016). Structural connectivity analyses in motor recovery research after stroke. *Annals of Clinical and Translational Neurology*, 3(3), 233-244. <https://doi.org/10.1002/acn3.278>
- Kujirai, T., Caramia, M. D., Rothwell, J. C., Day, B. L., Thompson, P. D., Ferbert, A., Wroe, S., Asselman, P., & Marsden, C. D. (1993). Corticocortical inhibition in human motor cortex. *The Journal of Physiology*, 471, 501-519. <https://doi.org/10.1113/jphysiol.1993.sp019912>
- Kwakkel, G., Kollen, B. J., van der Grond, J., & Prevo, A. J. H. (2003). Probability of regaining dexterity in the flaccid upper limb : Impact of severity of paresis and time since onset in acute stroke. *Stroke*, 34(9), 2181-2186. <https://doi.org/10.1161/01.STR.0000087172.16305.CD>
- Lai, S.-M., Studenski, S., Duncan, P. W., & Perera, S. (2002). Persisting consequences of stroke measured by the Stroke Impact Scale. *Stroke*, 33(7), 1840-1844. <https://doi.org/10.1161/01.str.0000019289.15440.f2>
- Lang, C. E., Bland, M. D., Bailey, R. R., Schaefer, S. Y., & Birkenmeier, R. L. (2013). Assessment of upper extremity impairment, function, and activity after stroke : Foundations for clinical decision making. *Journal of Hand Therapy: Official Journal of the American Society of Hand Therapists*, 26(2), 104-114;quiz 115. <https://doi.org/10.1016/j.jht.2012.06.005>
- Langhorne, P., Coupar, F., & Pollock, A. (2009). Motor recovery after stroke : A systematic review. *The Lancet Neurology*, 8(8), 741-754. [https://doi.org/10.1016/S1474-4422\(09\)70150-4](https://doi.org/10.1016/S1474-4422(09)70150-4)
- Lefaucheur, J.-P., Aleman, A., Baeken, C., Benninger, D. H., Brunelin, J., Di Lazzaro, V., Filipović, S. R., Grefkes, C., Hasan, A., Hummel, F. C., Jääskeläinen, S. K., Langguth, B., Leocani, L., Londero, A., Nardone, R., Nguyen, J.-P., Nyffeler, T., Oliveira-Maia, A. J., Oliviero, A., ... Ziemann, U. (2020). Evidence-based guidelines on the therapeutic use of repetitive transcranial magnetic stimulation (rTMS) : An update (2014–2018). *Clinical Neurophysiology*, 131(2), 474-528. <https://doi.org/10.1016/j.clinph.2019.11.002>
- Lindenberg, R., Zhu, L. L., Rüber, T., & Schlaug, G. (2012). Predicting functional motor potential in chronic stroke patients using diffusion tensor imaging. *Human Brain Mapping*, 33(5), 1040-1051. <https://doi.org/10.1002/hbm.21266>
- Marchi, N. A., Ptak, R., Di Pietro, M., Schnider, A., & Guggisberg, A. G. (2017). Principles of proportional recovery after stroke generalize to neglect and aphasia. *European Journal of Neurology*, 24(8), 1084-1087. <https://doi.org/10.1111/ene.13296>
- Micera, S., Caleo, M., Chisari, C., Hummel, F. C., & Pedrocchi, A. (2020). Advanced Neurotechnologies for the Restoration of Motor Function. *Neuron*, 105(4), 604-620. <https://doi.org/10.1016/j.neuron.2020.01.039>

- Morishita, T., & Hummel, F. C. (2017). Non-invasive Brain Stimulation (NIBS) in Motor Recovery After Stroke : Concepts to Increase Efficacy. *Current Behavioral Neuroscience Reports*, 4(3), 280-289. <https://doi.org/10.1007/s40473-017-0121-x>
- Mullick, A. A., Subramanian, S. K., & Levin, M. F. (2015). Emerging evidence of the association between cognitive deficits and arm motor recovery after stroke : A meta-analysis. *Restorative Neurology and Neuroscience*, 33(3), 389-403. <https://doi.org/10.3233/RNN-150510>
- Nicolo, P., Ptak, R., & Guggisberg, A. G. (2015). Variability of behavioural responses to transcranial magnetic stimulation : Origins and predictors. *Neuropsychologia*, 74, 137-144. <https://doi.org/10.1016/j.neuropsychologia.2015.01.033>
- Nys, G. M. S., van Zandvoort, M. J. E., de Kort, P. L. M., Jansen, B. P. W., de Haan, E. H. F., & Kappelle, L. J. (2007). Cognitive disorders in acute stroke : Prevalence and clinical determinants. *Cerebrovascular Diseases (Basel, Switzerland)*, 23(5-6), 408-416. <https://doi.org/10.1159/000101464>
- Patel, M. D., Coshall, C., Rudd, A. G., & Wolfe, C. D. A. (2002). Cognitive impairment after stroke : Clinical determinants and its associations with long-term stroke outcomes. *Journal of the American Geriatrics Society*, 50(4), 700-706. <https://doi.org/10.1046/j.1532-5415.2002.50165.x>
- Prabhakaran, S., Zarahn, E., Riley, C., Speizer, A., Chong, J. Y., Lazar, R. M., Marshall, R. S., & Krakauer, J. W. (2008). Inter-individual variability in the capacity for motor recovery after ischemic stroke. *Neurorehabilitation and Neural Repair*, 22(1), 64-71. <https://doi.org/10.1177/1545968307305302>
- Preti, M. G., & Van De Ville, D. (2019). Decoupling of brain function from structure reveals regional behavioral specialization in humans. *Nature Communications*, 10(1), 4747. <https://doi.org/10.1038/s41467-019-12765-7>
- Raffin, E., & Hummel, F. C. (2018). Restoring Motor Functions After Stroke : Multiple Approaches and Opportunities. *The Neuroscientist: A Review Journal Bringing Neurobiology, Neurology and Psychiatry*, 24(4), 400-416. <https://doi.org/10.1177/1073858417737486>
- Ramsey, L. E., Siegel, J. S., Baldassarre, A., Metcalf, N. V., Zinn, K., Shulman, G. L., & Corbetta, M. (2016). Normalization of network connectivity in hemi-spatial neglect recovery. *Annals of neurology*, 80(1), 127-141. <https://doi.org/10.1002/ana.24690>
- Ramsey, L. E., Siegel, J. S., Lang, C. E., Strube, M., Shulman, G. L., & Corbetta, M. (2017). Behavioural clusters and predictors of performance during recovery from stroke. *Nature Human Behaviour*, 1(3), 1-10. <https://doi.org/10.1038/s41562-016-0038>
- Rehme, A. K., & Grefkes, C. (2013). Cerebral network disorders after stroke : Evidence from imaging-based connectivity analyses of active and resting brain states in humans. *The Journal of Physiology*, 591(Pt 1), 17-31. <https://doi.org/10.1113/jphysiol.2012.243469>
- Sachdev, P. S., Blacker, D., Blazer, D. G., Ganguli, M., Jeste, D. V., Paulsen, J. S., & Petersen, R. C. (2014). Classifying neurocognitive disorders : The DSM-5 approach. *Nature Reviews. Neurology*, 10(11), 634-642. <https://doi.org/10.1038/nrneurol.2014.181>
- Sagnier, S., Renou, P., Olindo, S., Debruxelles, S., Poli, M., Rouanet, F., Munsch, F., Tourdias, T., & Sibon, I. (2017). Gait Change Is Associated with Cognitive Outcome after an Acute Ischemic Stroke. *Frontiers in Aging Neuroscience*, 9. <https://www.frontiersin.org/article/10.3389/fnagi.2017.00153>
- Santisteban, L., Térémetz, M., Bleton, J.-P., Baron, J.-C., Maier, M. A., & Lindberg, P. G. (2016). Upper Limb Outcome Measures Used in Stroke Rehabilitation Studies : A Systematic Literature Review. *PLOS ONE*, 11(5), e0154792. <https://doi.org/10.1371/journal.pone.0154792>
- Siegel, J. S., Ramsey, L. E., Snyder, A. Z., Metcalf, N. V., Chacko, R. V., Weinberger, K., Baldassarre, A., Hacker, C. D., Shulman, G. L., & Corbetta, M. (2016). Disruptions of network connectivity predict impairment in multiple behavioral domains after stroke. *Proceedings of the National Academy of Sciences of the United States of America*, 113(30), E4367-4376. <https://doi.org/10.1073/pnas.1521083113>
- Siegel, J. S., Snyder, A. Z., Ramsey, L., Shulman, G. L., & Corbetta, M. (2016). The effects of hemodynamic lag on functional connectivity and behavior after stroke. *Journal of Cerebral Blood Flow and*

- Metabolism: Official Journal of the International Society of Cerebral Blood Flow and Metabolism*, 36(12), 2162-2176. <https://doi.org/10.1177/0271678X15614846>
- Sporns, O. (2018). Graph theory methods: Applications in brain networks. *Dialogues in Clinical Neuroscience*, 20(2), 111-121.
- Stinear, C. M. (2017). Prediction of motor recovery after stroke: Advances in biomarkers. *The Lancet. Neurology*, 16(10), 826-836. [https://doi.org/10.1016/S1474-4422\(17\)30283-1](https://doi.org/10.1016/S1474-4422(17)30283-1)
- Tournier, J.-D., Smith, R., Raffelt, D., Tabbara, R., Dhollander, T., Pietsch, M., Christiaens, D., Jeurissen, B., Yeh, C.-H., & Connelly, A. (2019). MRtrix3: A fast, flexible and open software framework for medical image processing and visualisation. *NeuroImage*, 202, 116137. <https://doi.org/10.1016/j.neuroimage.2019.116137>
- Tozlu, C., Edwards, D., Boes, A., Labar, D., Tsagaris, K. Z., Silverstein, J., Lane, H. P., Sabuncu, M. R., Liu, C., & Kuceyeski, A. (2020). Machine Learning methods predict individual upper limb motor impairment following therapy in chronic stroke. *Neurorehabilitation and neural repair*, 34(5), 428-439. <https://doi.org/10.1177/1545968320909796>
- Tremblay, S., Rogasch, N. C., Premoli, I., Blumberger, D. M., Casarotto, S., Chen, R., Di Lazzaro, V., Farzan, F., Ferrarelli, F., Fitzgerald, P. B., Hui, J., Ilmoniemi, R. J., Kimiskidis, V. K., Kugiumtzis, D., Lioumis, P., Pascual-Leone, A., Pellicciari, M. C., Rajji, T., Thut, G., ... Daskalakis, Z. J. (2019). Clinical utility and prospective of TMS-EEG. *Clinical Neurophysiology: Official Journal of the International Federation of Clinical Neurophysiology*, 130(5), 802-844. <https://doi.org/10.1016/j.clinph.2019.01.001>
- van den Heuvel, M. P., & Sporns, O. (2011). Rich-Club Organization of the Human Connectome. *The Journal of Neuroscience*, 31(44), 15775-15786. <https://doi.org/10.1523/JNEUROSCI.3539-11.2011>
- Veldsman, M., & Brodtmann, A. (2019). Disconnectomics: Stroke-related disconnection and dysfunction in distributed brain networks. *International Journal of Stroke*, 14(1), 6-8. <https://doi.org/10.1177/1747493018806166>
- Verstraeten, S., Mark, R. E., Dieleman, J., van Rijsbergen, M., de Kort, P., & Sitskoorn, M. M. (2020). Motor Impairment Three Months Post Stroke Implies A Corresponding Cognitive Deficit. *Journal of Stroke and Cerebrovascular Diseases*, 29(10), 105119. <https://doi.org/10.1016/j.jstrokecerebrovasdis.2020.105119>
- Wessel, M. J., Egger, P., & Hummel, F. C. (2021). Predictive models for response to non-invasive brain stimulation in stroke: A critical review of opportunities and pitfalls. *Brain Stimulation*, 14(6), 1456-1466. <https://doi.org/10.1016/j.brs.2021.09.006>

Appendix

1. Behavioral testing battery details
2. MRI sequence details
3. TMS-EEG detailed protocol

Supplement 1 – Neuropsychological evaluation

Motor and cognitive tests

The battery of tests includes 14 tests assessing the sensory and motor functions, and 26 tests assessing the cognitive functions (see Table 1). It covers the neurocognitive domains described in the DSM-V (Sachdev et al., 2014), i.e. complex attention, language, learning and memory, executive functions, social cognition, perceptual-motor functions, with the latter divided into perceptual and motor functions.

The DSM-V does not name any proprietary tests to objectively assess these functions. Therefore, we selected the tests and questionnaires on the basis of their validity and reproducibility as well as the existence of normative data in the literature. We chose several tests per neurocognitive domain to have an extensive and detailed evaluation, and also to have data that are representative of the several subdomains for each neurocognitive domain.

We use the same battery for each timepoint, excluding a few tests that are skipped during the first timepoint in order to reduce the total time of the evaluation as patients are in general highly fatigable during the first week after the stroke. If possible, versioning was used to reduce learning effects.

The entire evaluation is divided into at least two sessions of 2 to 3 hours per timepoint, depending on the patients' state and availability. Breaks are imposed to the patients during the session to maintain their attention and concentration, but they are also able to take some rest at any time. The order of the tests is pre-defined to reduce the possible interferences between the different tests but the neuropsychologist keeps to possibility to adjust if this is needed regarding the patients' state. In any case, the final tests' order for each evaluation is recorded on the patient's file.

Specific materials and license were acquired for each test. The evaluation is conducted by a neuropsychologist with a relevant clinical experience who follows rigorously the instructions provided by the authors of each test. The instructions of the tests are given, in French, Italian, or German, depending on the patients' first language. When possible, the version of the tests is adapted to the language used, especially for memory tests for which we have French, Italian, English, and Portuguese versions.

Questionnaires

In addition, we use 16 questionnaires assessing daily life aspects of patients, including physical and mental activity, functional level of dependance and level of reintegration, mental state, fatigue, sleep; etc (see Table 1). The questionnaires are filled by the patients themselves when they are able to, and checked by the neuropsychologist. If needed, the neuropsychologist helps the patients by reading and filling the questionnaires for them. These questionnaires are used at each timepoint plus an additional time between the third and the fourth time points.

Appendix

Test	Function assessed	Reference
<i>Clinical evaluation</i>		
NIHSS	Neurological examination	Brott et al., 1989
<i>General cognitive screening</i>		
Montreal Cognitive Assessment	All cognitive functions – general screening	Nasreddine et al., 2005
<i>Attention</i>		
Test of Attention Performance – Phasic alert test	Alertness, intensity of attention	Zimmermann & Fimm, 2016
Test of Attention Performance – Divided attention test	Attentional selectivity, focused attention	Zimmermann & Fimm, 2016
D2-R	Sustained and focused attention	Brickenkamp, 2015
<i>Social cognition</i>		
Geneva Emotions Recognition Test – Short*	Emotion recognition ability	Schlegel et al., 2016
<i>Executive functions</i>		
Frontal Assessment Battery	Executive functions	Dubois et al., 2000
Stroop Victoria	Flexibility, inhibition, processing speed	Spreen & Strauss, 1991; Bayard et al., 2007
Bimanual coordination	Planification, programming	Dolivo & Assal, , 1985
Apraxia Screen of Test for Upper-Limb Apraxia	Planification, programming	Vanbellingen et al., 2010

Appendix

CERAD Constructional Praxis	Planification, programmation	Morris et al., 1989; Roussel & Godefroy, 2016 – GRECOGVASC battery
Color Trail Test	Planification, programmation, information processing speed	D'Elia et al., 1996
Bisiach anosognosia scale	Self-awareness	Bisiach et al., 1986
Somatoparaphrenia test	Self-awareness	Ronchi et al., adapted
5-points tests*	Flexibility	Strauss & Knapp, 1982
Language		
LAST	Repetition, comprehension	Flamand-Roze et al., 2011; Koenig-Bruhin et al., 2016
Ardila's language test*	Denomination	Ardila, 2007
Token Test*	Comprehension	De Renzi & Vignolo, 1962
Phonological verbal fluency	Fluency	Roussel & Godefroy, 2016 - GRECOGVASC battery
Semantic verbal fluency	Fluency	Roussel & Godefroy, 2016 - GRECOGVASC battery
Learning and Memory		
Hopkins Verbal Learning Test – revised*	Verbal episodic memory	Brandt, 1990
Doors test*	Visual episodic memory	Roussel & Godefroy, 2016 - GRECOGVASC battery
Digit span	Verbal short-term memory	Wechsler, 2008 - Wechsler Adult Intelligence Scale
Corsi-Kessels	Visual short-term memory	Kessels et al., 2000
Motor functioning		
Fugl-Meyer	Upper limb function	Fugl-Meyer, 1980
Pinch&Grip	Hand strength	Mathiowetz et al., 1984

Appendix

Medical Research Council strength testing	muscle	Upper limb strength	Ciesla et al., 2011, Hislop & Montgomery, 2007
Nine-Hole Peg Test		Fine manual dexterity	Mathiowetz et al., 1985
Box and Blocks test		Gross manual dexterity	Mathiowetz et al., 1985
Purdue Pegboard Test		Fine manual dexterity, coordination	Tiffin & Asher, 1948
Action Research Arm Test*		Upper limb function	Lyle, 1981
Modified Ashworth Scale		Spasticities	Bohannon & Smith, 1987
2 minutes walk test*		Gait	Butland et al., 1982
10 meters walk test*		Gait	van Hedel et al., 2005
Time Up and Go test*		Gait, balance, functional ability	Podsiadlo & Richardson, 1991
Berg Balance Scale		Balance	Berg, 1992
Sensory			
Rivermead Assessment of performance	Sensory	Face, hands, feet sensitivity	Winward & Halligan, 2002
Perceptual function			
Overlapping figures test		Gnosis, neglect	Unilateral neglect assessment battery of the GEREN, 2002
Bisection line test		Neglect	Unilateral neglect assessment battery of the GEREN, 2002
Bells cancellation test		Neglect	Unilateral neglect assessment battery of the GEREN, 2002
Questionnaires			
Stroke Impact Scale (SIS)		General recovery	Duncan et al., 2003
Hospital Anxiety and Depression Scale (HADS)		Anxiety and depression	Zigmond & Snaith, 1983

Appendix

State/Trait Anxiety Inventory for adults (STAI)		Spielberger, 1983
Fear and stress scale	Fear and stress	Carmen Sandi's version
Medical Outcome Study Short Form 12		Ware & Sherbourne, 1992; Hurst et al., 1998
Modified Reintegration to Normal Living Index	Reintegration	Wood-Dauphinee et al., 1988
Social Comparison Scale	Social comparison	Allan & Gilbert, 1995
Generalized Self Efficacy Scale	Efficacy	Scharzer & Jerusalem, 1995
Pittsburgh Sleep Quality Index		Buyssse et al., 1989
Multidimensional Fatigue Inventory	Sleep and Fatigue	Smets et al., 1995
Feeling of foreignness questionnaire		
Neurobehavioral questionnaire	Disembodiment	
Barthel index		Mahoney & Barthel, 1965
mRS modified Rankin Scale		van Swieten et al., 1988
FAC functional ambulation category	Functional indexes	Holden et al., 1984
FIM functional independence		Kidd et al., 1995
Edinburgh handedness inventory	Handedness	Oldfield, 1971

Table legend - The table 1. lists all the tests and questionnaires used in TiMeS, with the main function(s) assessed by the tool. The latter information is not exhaustive as some tests could assess functions in multiple neurocognitive domains (for instance, the Color Trail Test mainly assesses some executive functions but could also give information about the sustained attention capacity). The third column indicates the authors / owners of the tests.

References

- Allan, S., & Gilbert, P. (1995). A social comparison scale: Psychometric properties and relationship to psychopathology. *Personality and Individual Differences*, 19(3), 293-299. [https://doi.org/10.1016/0191-8869\(95\)00086-L](https://doi.org/10.1016/0191-8869(95)00086-L)
- Ardila, A. (2007). Toward the development of a cross-linguistic naming test. *Archives of Clinical Neuropsychology*, 22(3), 297-307. <https://doi.org/10.1016/j.acn.2007.01.016>
- Azouvi, P., Samuel, C., Louis-Dreyfus, A., Bernati, T., Bartolomeo, P., Beis, J.-M., Chokron, S., Leclercq, M., Marchal, F., Martin, Y., De Montety, G., Olivier, S., Perennou, D., Pradat-Diehl, P., Praxial, C., Rode, G., Siéoff, E., Wiart, L., Rousseaux, M., & French Collaborative Study Group on Assessment of Unilateral Neglect (GEREN/GRECO). (2002). Sensitivity of clinical and behavioural tests of spatial neglect after right hemisphere stroke. *Journal of Neurology, Neurosurgery, and Psychiatry*, 73(2), 160-166. <https://doi.org/10.1136/jnnp.73.2.160>
- Bayard, S., Erkes, J., Moroni, C., & Collège des Psychologues Cliniciens spécialisés en Neuropsychologie du Languedoc Roussillon (CPCN Languedoc Roussillon). (2011). Victoria Stroop Test: Normative data in a sample group of older people and the study of their clinical applications in the assessment of inhibition in Alzheimer's disease. *Archives of Clinical Neuropsychology: The Official Journal of the National Academy of Neuropsychologists*, 26(7), 653-661. <https://doi.org/10.1093/arclin/acr053>
- Berg, K. O., Maki, B. E., Williams, J. I., Holliday, P. J., & Wood-Dauphinee, S. L. (1992). Clinical and laboratory measures of postural balance in an elderly population. *Archives of Physical Medicine and Rehabilitation*, 73(11), 1073-1080.
- Bisiach, E., Vallar, G., Perani, D., Papagno, C., & Berti, A. (1986). Unawareness of disease following lesions of the right hemisphere: Anosognosia for hemiplegia and anosognosia for hemianopia. *Neuropsychologia*, 24(4), 471-482. [https://doi.org/10.1016/0028-3932\(86\)90092-8](https://doi.org/10.1016/0028-3932(86)90092-8)
- Brickenkamp, R. & Zillmer, E. (1998). *The d2 Test of Attention*. Seattle, Washington: Hogrefe & Huber Publishers
- Bohannon, R. W., & Smith, M. B. (1987). Interrater reliability of a modified Ashworth scale of muscle spasticity. *Physical Therapy*, 67(2), 206-207. <https://doi.org/10.1093/ptj/67.2.206>
- Brandt, J. (1991). The hopkins verbal learning test: Development of a new memory test with six equivalent forms. *Clinical Neuropsychologist*, 5(2), 125-142. <https://doi.org/10.1080/13854049108403297>
- Brott, T., Adams, H. P., Olinger, C. P., Marler, J. R., Barsan, W. G., Biller, J., Spilker, J., Holleran, R., Eberle, R., & Hertzberg, V. (1989). Measurements of acute cerebral infarction: A clinical examination scale. *Stroke*, 20(7), 864-870. <https://doi.org/10.1161/01.str.20.7.864>
- Butland, R. J., Pang, J., Gross, E. R., Woodcock, A. A., & Geddes, D. M. (1982). Two-, six-, and 12-minute walking tests in respiratory disease. *British Medical Journal (Clinical research ed.)*, 284(6329), 1607-1608.
- Buyse, D. J., Reynolds, C. F., Monk, T. H., Berman, S. R., & Kupfer, D. J. (1989). The Pittsburgh sleep quality index: A new instrument for psychiatric practice and research. *Psychiatry Research*, 28(2), 193-213. [https://doi.org/10.1016/0165-1781\(89\)90047-4](https://doi.org/10.1016/0165-1781(89)90047-4)
- Ciesla, N., Dinglas, V., Fan, E., Kho, M., Kuramoto, J., & Needham, D. (2011). Manual Muscle Testing: A Method of Measuring Extremity Muscle Strength Applied to Critically Ill Patients. *Journal of Visualized Experiments: JoVE*, 50, 2632. <https://doi.org/10.3791/2632>
- De Renzi, A., & Vignolo, L. A. (1962). Token test: A sensitive test to detect receptive disturbances in aphasics. *Brain: A Journal of Neurology*, 85, 665-678. <https://doi.org/10.1093/brain/85.4.665>
- De Renzi, A., & Vignolo, L. A. (1962). Token test: A sensitive test to detect receptive disturbances in aphasics. *Brain: a journal of neurology*.
- D'Elia, L., & Satz, P. (1989). *Color Trails I and 2*. Odessa, FL: Psychological Assessment Resources.

- Dolivo, C., & Assal, G. (1985). Tests neuropsychologiques rapides pour la recherche d'une détérioration intellectuelle. *Psychologie médicale*, 17(14), 2093-2095.
- Dubois, B., Slachevsky, A., Litvan, I., & Pillon, B. (2000). The FAB : A frontal assessment battery at bedside. *Neurology*, 55(11), 1621-1626. <https://doi.org/10.1212/WNL.55.11.1621>
- Duncan, P. W., Lai, S. M., Bode, R. K., Perera, S., & DeRosa, J. (2003). Stroke Impact Scale-16 : A brief assessment of physical function. *Neurology*, 60(2), 291-296. <https://doi.org/10.1212/01.wnl.0000041493.65665.d6>
- Flamand-Roze, C., Falissard, B., Roze, E., Maintigneux, L., Beziz, J., Chacon, A., Join-Lambert, C., Adams, D., & Denier, C. (2011). Validation of a new language screening tool for patients with acute stroke : The Language Screening Test (LAST). *Stroke*, 42(5), 1224-1229. <https://doi.org/10.1161/STROKEAHA.110.609503>
- Förderreuther, S., Sailer, U., & Straube, A. (2004). Impaired self-perception of the hand in complex regional pain syndrome (CRPS). *Pain*, 110(3), 756-761. <https://doi.org/10.1016/j.pain.2004.05.019>
- Fugl-Meyer, A. R. (1980). Post-stroke hemiplegia assessment of physical properties. *Scandinavian Journal of Rehabilitation Medicine*. Supplement, 7, 85-93.
- Galer, B. S., & Jensen, M. (1999). Neglect-like symptoms in complex regional pain syndrome : Results of a self-administered survey. *Journal of Pain and Symptom Management*, 18(3), 213-217. [https://doi.org/10.1016/s0885-3924\(99\)00076-7](https://doi.org/10.1016/s0885-3924(99)00076-7)
- Godefroy, O., Leclercq, C., Roussel, M., Moroni, C., Quaglino, V., Beaunieux, H., Tallia, H., Nédélec-Ciceri, C., Bonnin, C., Thomas-Anterion, C., Varvat, J., Aboulafia-Brakha, T., Assal, F., & GRECOG-VASC Neuropsychological Committee. (2012). French adaptation of the vascular cognitive impairment harmonization standards : The GRECOG-VASC study. *International Journal of Stroke: Official Journal of the International Stroke Society*, 7(4), 362-363. <https://doi.org/10.1111/j.1747-4949.2012.00794.x>
- Holden, M. K., Gill, K. M., Magliozzi, M. R., Nathan, J., & Piehl-Baker, L. (1984). Clinical gait assessment in the neurologically impaired. Reliability and meaningfulness. *Physical Therapy*, 64(1), 35-40. <https://doi.org/10.1093/ptj/64.1.35>
- Hurst, N. P., Ruta, D. A., & Kind, P. (1998). Comparison of the MOS short form-12 (SF12) health status questionnaire with the SF36 in patients with rheumatoid arthritis. *British Journal of Rheumatology*, 37(8), 862-869. <https://doi.org/10.1093/rheumatology/37.8.862>
- Hislop, H. J., & Montgomery, J. (2007). Daniels and Worthingham's Muscle Testing Techniques of Manual Examination, Eight Edition. Missouri: Saunders Elsevier, 95-98.
- Jerusalem, M., & Schwarzer, R. (1995). General Self-Efficacy Scale--Revised--English Version. APA PsycTests.
- Kessels, R. P. C., van Zandvoort, M. J. E., Postma, A., Kappelle, L. J., & de Haan, E. H. F. (2000). The Corsi Block-Tapping Task : Standardization and Normative Data. *Applied Neuropsychology*, 7(4), 252-258. https://doi.org/10.1207/S15324826AN0704_8
- Kidd, D., Stewart, G., Baldry, J., Johnson, J., Rossiter, D., Petruckevitch, A., & Thompson, A. J. (1995). The Functional Independence Measure : A comparative validity and reliability study. *Disability and Rehabilitation*, 17(1), 10-14. <https://doi.org/10.3109/09638289509166622>
- Koenig-Bruhin, M., Vanbellingen, T., Schumacher, R., Pflugshaupt, T., Annoni, J. M., Müri, R. M., Bohlhalter, S., & Nyffeler, T. (2016). Screening for Language Disorders in Stroke : German Validation of the Language Screening Test (LAST). *Cerebrovascular Diseases Extra*, 6(1), 27-31. <https://doi.org/10.1159/000445778>
- Luszczynska, A., Scholz, U., & Schwarzer, R. (2005). The general self-efficacy scale : Multicultural validation studies. *The Journal of Psychology*, 139(5), 439-457. <https://doi.org/10.3200/JRLP.139.5.439-457>

- Lyle, R. C. (1981). A performance test for assessment of upper limb function in physical rehabilitation treatment and research. *International Journal of Rehabilitation Research*, 4(4), 483-492.
- Mahoney, F. I., & Barthel, D. W. (1965). FUNCTIONAL EVALUATION : THE BARTHEL INDEX. *Maryland State Medical Journal*, 14, 61-65.
- Mathiowetz, V., Volland, G., Kashman, N., & Weber, K. (1985). Adult norms for the Box and Block Test of manual dexterity. *The American Journal of Occupational Therapy: Official Publication of the American Occupational Therapy Association*, 39(6), 386-391. <https://doi.org/10.5014/ajot.39.6.386>
- Mathiowetz, V., Weber, K., Kashman, N., & Volland, G. (1985). Adult Norms for the Nine Hole Peg Test of Finger Dexterity. *The Occupational Therapy Journal of Research*, 5(1), 24-38. <https://doi.org/10.1177/153944928500500102>
- Mathiowetz, V., Weber, K., Volland, G., & Kashman, N. (1984). Reliability and validity of grip and pinch strength evaluations. *The Journal of Hand Surgery*, 9(2), 222-226. [https://doi.org/10.1016/s0363-5023\(84\)80146-x](https://doi.org/10.1016/s0363-5023(84)80146-x)
- Morris, J. C., Heyman, A., Mohs, R. C., Hughes, J. P., van Belle, G., Fillenbaum, G. D. M. E., ... & Clark, C. (1989). The consortium to establish a registry for Alzheimer's disease (CERAD): I. Clinical and neuropsychological assessment of Alzheimer's disease. *Neurology*.
- Nasreddine, Z. S., Phillips, N. A., Bédirian, V., Charbonneau, S., Whitehead, V., Collin, I., Cummings, J. L., & Chertkow, H. (2005). The Montreal Cognitive Assessment, MoCA : A Brief Screening Tool For Mild Cognitive Impairment. *Journal of the American Geriatrics Society*, 53(4), 695-699. <https://doi.org/10.1111/j.1532-5415.2005.53221.x>
- Oldfield, R. C. (1971). The assessment and analysis of handedness : The Edinburgh inventory. *Neuropsychologia*, 9(1), 97-113. [https://doi.org/10.1016/0028-3932\(71\)90067-4](https://doi.org/10.1016/0028-3932(71)90067-4)
- Podsiadlo, D., & Richardson, S. (1991). The timed « Up & Go » : A test of basic functional mobility for frail elderly persons. *Journal of the American Geriatrics Society*, 39(2), 142-148. <https://doi.org/10.1111/j.1532-5415.1991.tb01616.x>
- Regard, M., Strauss, E., & Knapp, P. (1982). Children's Production on Verbal and Non-Verbal Fluency Tasks. *Perceptual and Motor Skills*, 55(3), 839-844. <https://doi.org/10.2466/pms.1982.55.3.839>
- Roussel, M., & Godefroy, O. (2016). La batterie GRECOGVASC: Evaluation et diagnostic des troubles neurocognitifs vasculaires avec ou sans contexte d'accident vasculaire cérébral. *De Boeck Supérieur*.
- Sandi, C. (2013). Stress and cognition. *WIREs Cognitive Science*, 4(3), 245-261. <https://doi.org/10.1002/wcs.1222>
- Schlegel, K., Grandjean, D., & Scherer, K. R. (2014). Introducing the Geneva emotion recognition test : An example of Rasch-based test development. *Psychological Assessment*, 26(2), 666-672. <https://doi.org/10.1037/a0035246>
- Smets, E. M. A., Garssen, B., Bonke, B., & De Haes, J. C. J. M. (1995). The multidimensional Fatigue Inventory (MFI) psychometric qualities of an instrument to assess fatigue. *Journal of Psychosomatic Research*, 39(3), 315-325. [https://doi.org/10.1016/0022-3999\(94\)00125-0](https://doi.org/10.1016/0022-3999(94)00125-0)
- Snaith, R. P. (2003). The Hospital Anxiety And Depression Scale. *Health and Quality of Life Outcomes*, 1(1), 29. <https://doi.org/10.1186/1477-7525-1-29>
- Spielberger, C. D. (1983). State-trait anxiety inventory for adults (STAI-AD). *APA PsycTests*.
- Spielberger, C. D. (2010). State-Trait Anxiety Inventory. In *The Corsini Encyclopedia of Psychology* (p. 1-1). John Wiley & Sons, Ltd. <https://doi.org/10.1002/9780470479216.corpsy0943>

Strauss, E., Strauss, P. of P. E., Sherman, N. and A. A. P. D. of P. and C. N. E. M. S., Sherman, E. M. S., Spreen, O., & Spreen, B. P. of P. O. (2006). *A Compendium of Neuropsychological Tests: Administration, Norms, and Commentary*. Oxford University Press.

Tiffin, J., & Asher, E. J. (1948). The Purdue Pegboard : Norms and studies of reliability and validity. *Journal of Applied Psychology*, 32(3), 234-247. <https://doi.org/10.1037/h0061266>

Vallar, G., & Ronchi, R. (2009). Somatoparaphrenia : A body delusion. A review of the neuropsychological literature. *Experimental Brain Research*, 192(3), 533-551. <https://doi.org/10.1007/s00221-008-1562-y>

Vanbellinghen, T., Kersten, B., Winckel, A. V. de, Bellion, M., Baronti, F., Müri, R., & Bohlhalter, S. (2011). A new bedside test of gestures in stroke : The apraxia screen of TULIA (AST). *Journal of Neurology, Neurosurgery & Psychiatry*, 82(4), 389-392. <https://doi.org/10.1136/jnnp.2010.213371>

van Hedel, H. J., Wirz, M., & Dietz, V. (2005). Assessing walking ability in subjects with spinal cord injury : Validity and reliability of 3 walking tests. *Archives of Physical Medicine and Rehabilitation*, 86(2), 190-196. <https://doi.org/10.1016/j.apmr.2004.02.010>

van Swieten, J. C., Koudstaal, P. J., Visser, M. C., Schouten, H. J., & van Gijn, J. (1988). Interobserver agreement for the assessment of handicap in stroke patients. *Stroke*, 19(5), 604-607. <https://doi.org/10.1161/01.str.19.5.604>

Wechsler, D. (1955). Wechsler adult intelligence scale--. *Archives of Clinical Neuropsychology*.

Ware, J. E., & Sherbourne, C. D. (1992). The MOS 36-Item Short-Form Health Survey (SF-36) : I. Conceptual Framework and Item Selection. *Medical Care*, 30(6), 473-483.

Winward, C. E., Halligan, P. W., & Wade, D. T. (2002). The Rivermead Assessment of Somatosensory Performance (RASP) : Standardization and reliability data. *Clinical Rehabilitation*, 16(5), 523-533. <https://doi.org/10.1191/0269215502cr522oa>

Wood-Dauphinee, S. L., Opzoomer, M. A., Williams, J. I., Marchand, B., & Spitzer, W. O. (1988). Assessment of global function : The reintegration to normal living index. *Archives of Physical Medicine and Rehabilitation*, 69(8), 583-590. Scopus.

Zimmermann, P., & Fimm, B. (2002). A test battery for attentional performance. *Applied neuropsychology of attention. Theory, diagnosis and rehabilitation*, 110-151.

Supplement 2 – Neuro-imaging recordings

Data acquisition

Structural, functional, diffusion-weighted and susceptibility-weighted imaging data are acquired using a 3T Magnetom Prisma scanner (Siemens, Erlangen, Germany) with a 64-channel head and neck coil.

Diffusion-weighted imaging (DWI)

Diffusion-weighted images are acquired using pulsed gradient spin echo technique (TR = 5000 ms; TE = 77 ms; slices = 84; FOV = 234 mm; voxel resolution = $1.6 \times 1.6 \times 1.6$ mm; readout bandwidth = 1630 Hz/pixels; SENSE acceleration factor = 3). Seven T2-weighted images without diffusion weighting ($b = 0$ s/mm²) are acquired, including one in opposite phase encoded direction. Further, 101 images with noncollinear diffusion gradient directions distributed equally over the half-sphere covering 5 diffusion gradient strengths are obtained (b -values = [300.0, 700.0, 1000.0, 2000.0, 3000.0] s/mm²; shell-samples = [3, 7, 16, 29, 46]). Total acquisition time is 11:06 min.

T1-weighted image

A T1-weighted image is acquired using a 3D Magnetization-Prepared Rapid Gradient-Echo sequence (MPRAGE, TR = 2300 ms; TE = 2.96 ms; flip angle = 9°; slices = 192; voxel size = $1 \times 1 \times 1$ mm, FOV 256 × 256 mm, acquisition time = 5:12min).

multi-echo GRASE

A multi-echo GRASE sequence supporting CAIPIRINHA parallel imaging is used for myelin water imaging. Therefore multi-echo T₂ imaging are acquired. (in-plane resolution 1.6mm x 1.6mm; slice thickness 1.6mm; 84 slices; acquisition time = 10:30min) (Piredda et al., 2021).

Blood oxygenation-level dependent (BOLD) MRI / functional MRI (fMRI)

Resting-state BOLD data (with fixation cross) is acquired using a multi-band echo-planar imaging (EPI) sequence. In total, 385 functional volumes are acquired and every volume comprises 75 axial slices covering the whole brain (in-plane resolution = 2mm x 2mm; slice thickness 2mm; no gap, FOV = 256mm, TE = 32ms, TR=1250ms, flip angle = 58°, Accel. Factor slice = 5, acquisition time = 8:13min).

GRE field mapping

GRE field mapping is acquired covering the whole brain (75 axial slices), using the following imaging parameters: in-plane resolution = 2mm x 2mm; slice thickness = 2mm; FOV = 224mm, TR = 704mm TE1 = 4.92ms, TE2 = 7.38ms, flip angle = 60°, acquisition time = 2:41min.

mp2rage

3D T1-weighted Magnetization-Prepared 2 Rapid Gradient-Echo (MP2RAGE) sequence (INV1 or TI1 = 700 ms, flip angle = 4° and INV2 or TI2 = 2500 ms, flip angle = 5°, TE = 2.98 ms, TR = 5000 ms, acquisition time = 8:22min) with an isotropic resolution of 1 mm³.

Susceptibility-weighted imaging (SWI)

We are using a susceptibility-weighted imaging sequence with a TR of 28ms, a TE of 20ms, FOV = 230mm, FOV phase = 78.1%, in-plane resolution of 0.6mm x 0.6mm, slice thickness = 1.2mm, flip angle = 15°, acquisition time = 4:07min.

Image Analysis

Lesion segmentation

All the lesion masks were hand-drawn using mrview from MRtrix3 (Tournier et al., 2019) and subsequently verified by a neurologist.

Diffusion-weighted imaging

The diffusion-weighted images are preprocessed using, MRtrix3, FSL topup and eddy (Andersson et al., 2003; Andersson and Sotiropoulos, 2016; Smith et al., 2004; Tournier et al., 2019). First, Gibbs ringing artefacts are removed from the data (E et al., 2016; Tournier et al., 2019), then motion artefact reduction, as well as field inhomogeneity, susceptibility-induced off-resonance field and eddy currents correction are performed. Multi-shell multi-tissue constrained spherical deconvolution (B et al., 2014) is used to estimate the fibre orientation distributions within each voxel. Whole-brain probabilistic tractography is performed using the second-order integration over fibre orientation distribution (iFOD2(Tournier et al., 2019), initiating streamlines in all voxels of the white matter. For each dataset, 1 million streamlines are selected with both endpoints in the individual cortical or subcortical mask using the Dipy software package (Garyfallidis et al., 2014). The obtained tractograms are weighted fitting the underlying diffusion compartment model using a Stick-Ball-Zeppelin model based on COMMIT (Daducci et al., 2015). The stick compartment models the intra-axonal water with parallel diffusivity of 1.7E-3 mm²/s and no perpendicular diffusivity. The Ball compartment models the extra-axonal water with isotropic diffusivity of 1.7E-3 mm²/s and free water with diffusivity of 3.0E-3 mm²/s. The Zeppelin compartment models the extra-axonal water with parallel diffusivity of 1.7E-3 mm²/s and perpendicular diffusivity of 0.51E-3 mm²/s. Tissue partial volume estimates are obtained from the T1-weighted image using the FSL Fast (Zhang et al., 2000) and BET (Smith 2002) methods. The T1-weighted image is registered to

the average b0 image using FSL FLIRT (Jenkinson and Smith, 2001) and FNIRT (Andersson et al., 2007; Jenkinson et al., 2012) methods.

For the cortical parcellation, we choose either the Destrieux (74 areas per hemisphere) (Destrieux et al., 2010) or the Glasser atlas (180 areas per hemisphere) (Glasser et al., 2016) using FreeSurfer (Fischl et al., 2004; Fischl, 2012). To the Destrieux parcellation, we add subcortical areas (6 areas per hemisphere) and a subdivision of the brainstem (3 areas), totalizing 163 cortical and subcortical areas for the “Destrieux parcellation”. The parcellations are performed on the T1 mprage image. For stroke patients, the voxels corresponding to the lesion are stamped out and replaced by the mirrored voxels of the contralateral side. For each participant, a structural connectome (SC) is built with 163 (Destrieux atlas), respectively 360 (Glasser atlas), pairs of areas obtained through the parcellation.

Functional (BOLD) Imaging

All preprocessing and statistical analyses are conducted using the SPM12 package (Wellcome Department of Cognitive Neurology, London, UK; www.fil.ion.ucl.ac.uk/spm) running on MATLAB (v2020b, Mathworks, The MathWorks, Massachusetts, <http://www.mathworks.ch>). Functional images are realigned to the mean functional image. Then, the anatomical image is co-registered to the mean functional image. The anatomical image is segmented into tissue maps based on tissue probability maps of SPM12 (for patients, voxels corresponding to the lesion are not considered). The resulting forward deformation field is used to warp both the anatomical and functional images into MNI space. Finally, the functional images are smoothed using a Gaussian kernel (FWHM = 6mm). The first 10 volumes are discarded so that the fMRI signal achieves steady-state magnetization, resulting in 375 functional volumes.

Using the conn toolbox (Whitfield-Gabrieli & Nieto-Castanon, 2012), voxel fMRI time courses are detrended and nuisance variables are regressed out (6 head motion parameters, average cerebrospinal fluid and white matter signal). Finally, a band-pass filter is applied (0.01-0.15Hz) to improve signal-to-noise ratio. The average timeseries is then extracted for every ROI of the Glasser parcellation and a functional connectome is obtained by computing the Pearson correlation between timeseries.

References

- Andersson, J. L., Skare, S., & Ashburner, J. (2003). How to correct susceptibility distortions in spin-echo echo-planar images: application to diffusion tensor imaging. *Neuroimage*, 20(2), 870-888.
- Andersson, J. L., Jenkinson, M., & Smith, S. (2007). Non-linear registration, aka Spatial normalisation FMRIB technical report TR07JA2. *FMRIB Analysis Group of the University of Oxford*, 2(1), e21.
- Andersson, J. L., & Sotiropoulos, S. N. (2016). An integrated approach to correction for off-resonance effects and subject movement in diffusion MR imaging. *Neuroimage*, 125, 1063-1078.

Ashburner, J., Barnes, G., Chen, C. C., Daunizeau, J., Flandin, G., Friston, K., ... & Penny, W. (2014). SPM12 manual. *Wellcome Trust Centre for Neuroimaging, London, UK*, 2464.

Daducci, A., Dal Palù, A., Lemkaddem, A., & Thiran, J. P. (2014). COMMIT: Convex optimization modeling for microstructure informed tractography. *IEEE transactions on medical imaging*, 34(1), 246-257.

Destrieux, C., Fischl, B., Dale, A., & Halgren, E. (2010). Automatic parcellation of human cortical gyri and sulci using standard anatomical nomenclature. *Neuroimage*, 53(1), 1-15.

Fischl, B., Van Der Kouwe, A., Destrieux, C., Halgren, E., Ségonne, F., Salat, D. H., ... & Dale, A. M. (2004). Automatically parcellating the human cerebral cortex. *Cerebral cortex*, 14(1), 11-22.

Fischl, B. (2012). FreeSurfer. *Neuroimage*, 62(2), 774-781.

Garyfallidis, E., Brett, M., Amirbekian, B., Rokem, A., Van Der Walt, S., Descoteaux, M., & Nimmo-Smith, I. (2014). Dipy, a library for the analysis of diffusion MRI data. *Frontiers in neuroinformatics*, 8, 8.

Glasser, M. F., Coalson, T. S., Robinson, E. C., Hacker, C. D., Harwell, J., Yacoub, E., ... & Van Essen, D. C. (2016). A multi-modal parcellation of human cerebral cortex. *Nature*, 536(7615), 171-178.

Jenkinson, M., & Smith, S. (2001). A global optimisation method for robust affine registration of brain images. *Medical image analysis*, 5(2), 143-156.

Jenkinson, M., Beckmann, C. F., Behrens, T. E., Woolrich, M. W., & Smith, S. M. (2012). Fsl. *Neuroimage*, 62(2), 782-790.

Supplement 3 – Electrophysiological recordings

Electrophysiological recordings (resting-state EEG and TMS-EEG coupling) are performed at each time point post stroke: within a week, three weeks, three months, and one year after the ictal event; not for all patients the 4 timepoints are available.

Electroencephalography (EEG)

EEG recordings are acquired using a 64 passive electrodes EEG BrainCap-MR (Brain Vision LLC, North Carolina, USA) with the reference electrode at FCz and the ground at AFz. The data is recorded with the help of BrainVision Recorder (Brain Vision LLC, North Carolina, USA). The experiment is performed in a faraday cage (IAC Acoustics, Illinois, USA) to limit power line interference. Each electrode is brought to an impedance below 5 kOhm or as low as possible. Impedance levels are recorded at the beginning and end of the session. Data are recorded using DC mode, a resolution of 0.5 μ V and a low-pass filter (cutoff frequency of 1 kHz) at a sampling rate of 5 kHz.

Electromyography (EMG)

The EMG activity is recorded using pairs of disposable Ag-AgCl electrodes on 7 muscles in the affected side (First Dorsal Interossei, FDI; Abductor Digiti Minimi, ADM; Abductor Pollicis Brevis, APB; Flexor Carpi Ulnaris, FCU; Flexor Carpi Radialis, FCR; Extensor Carpi Radialis, ECR; Extensor Carpi Ulnaris, ECU) and 1 muscle on the non-affected one (FDI). The signal is amplified and sampled at 3 kHz using a Noraxon DTS Receiver (Scottsdale, Arizona, United States) using a band-pass filter from 10 Hz to 1000 Hz, and digitized at 5 kHz using Signal software (Cambridge Electronic Design Limited, Cambridge, UK) for further processing on a laptop.

Transcranial Magnetic Stimulation

Neuronavigated TMS is applied using a MagPro X100 stimulator connected to an MC-B70 coil (Magventure, Farum, Denmark). A neuronavigation system (Localite GmbH, Bonn, Germany) is used throughout the experiment to track and record the position of the stimulation coil in respect to the patient's individual anatomy, using T1-weighted images (see supp. 2). EEG channel coordinates are also recorded using the neuronavigation system. Biphasic pulses inducing a posterior to anterior current direction are delivered over the first dorsal intraosseous (FDI) hotspot of the affected arm. The stimulation intensity is adjusted to produce MEPs presenting a peak-to-peak amplitude between 0.5 to 1 mV. If no visible MEP (50 μ V) can be elicited at maximal stimulator output, the intensity is set similarly on the unaffected hemisphere. The resting motor threshold (rMT) is defined as the lowest intensity necessary to evoke MEPs higher than 50 μ V in at least 5 out of 10 trials. Two types of stimulation are applied: a single pulse at the supra-motor threshold intensity fixed earlier or a double pulse (Short-

interval Cortical Inhibition; SICI) comprised of a condition pulse at 80% rMT followed by a test pulse at the supra-motor threshold intensity, with an inter-stimulus interval of 3 ms.

In order to reduce electromagnetic and acoustic interference resulting from the TMS, electrodes wires are oriented perpendicular to the magnetic field and a thin layer of foam is applied between the coil and the scalp (Veniero et al., 2009; Braack et al., 2015).

Data preprocessing

EMG: EMG data are exported to Matlab files to be used with a custom graphical interface for pre-processing. Rejection criteria are as follows: trials with muscle pre-activation exceeding $\pm 25 \mu\text{V}$ from baseline less than 100 ms before TMS onset (Delorme & Makeig, 2004) and/or $\pm 100 \mu\text{V}$ from baseline 500–100 ms before the pulse are rejected. Trials containing artefacts or with documented suboptimal coil placement are rejected from further analysis.

EEG: EEG data are analyzed on Matlab (MathWorks, Massachusetts, USA) using the Fieldtrip (Oostenveld et al., 2011), Brainstorm (Tadel et al., 2011), EEGLAB (Delorme A & Makeig S, 2004) and TESA (Rogasch et al., 2017) toolboxes. Resting-state EEG recording are preprocessed following international standards (Babiloni et al., 2020) that were successfully used in previous studies on stroke patients (Snyder et al. 2021). First, the continuous data are epoched in non-overlapping 2 s time windows. After removing bad channels and trials, an ICA is performed in order to filter out any remaining ocular, muscular or electrical artifacts. Data are finally re-referenced (average reference), and time-frequency maps are drawn from them by means of multitaper frequency transformation within the 1-50 Hz frequency bandwidth. Regarding TMS-EEG recordings, the preprocessing pipeline is similar to the one defined by Rogasch et al. (2017) and consists of: epoching, removing data corrupted by the TMS pulse [-5,+20ms], removing bad trials and channels after a visual inspection, removing the remaining TMS artefact and others artefacts such as eye blinks or large muscle artefacts using two rounds of ICA, and finally re-referencing to the average reference.

References

Delorme A & Makeig S (2004) EEGLAB: an open-source toolbox for analysis of single-trial EEG dynamics, *Journal of Neuroscience Methods* 134:9-21

Nigel C. Rogasch, Caley Sullivan, Richard H. Thomson, Nathan S. Rose, Neil W. Bailey, Paul B. Fitzgerald, Faranak Farzan, Julio C. Hernandez-Pavon, Analysing concurrent transcranial magnetic stimulation and electroencephalographic data: A review and introduction to the open-source TESA software. *NeuroImage*. 2017, 147 : 934-951

Babiloni, C., Barry, R.J., Başar, E., Blinowska, K.J., Cichocki, A., Drinkenburg, W.H.I.M., Klimesch, W., Knight, R.T., Lopes da Silva, F., Nunez, P., Oostenveld, R., Jeong, J., Pascual-Marqui, R., Valdes-Sosa, P., Hallett, M., 2020. International Federation of Clinical Neurophysiology (IFCN) – EEG research workgroup: Recommendations on

frequency and topographic analysis of resting state EEG rhythms. Part 1: Applications in clinical research studies. *Clinical Neurophysiology* 131, 285–307. <https://doi.org/10.1016/j.clinph.2019.06.234>

Snyder, D.B., Schmit, B.D., Hyngstrom, A.S., Beardsley, S.A., 2021. Electroencephalography resting-state networks in people with Stroke. *Brain and Behavior* 11, e02097. <https://doi.org/10.1002/brb3.2097>

Oostenveld, R., Fries, P., Maris, E., Schoffelen, J.-M., 2011. FieldTrip: Open Source Software for Advanced Analysis of MEG, EEG, and Invasive Electrophysiological Data. *Computational Intelligence and Neuroscience* 2011, 1–9. <https://doi.org/10.1155/2011/156869>

Tadel, F., Baillet, S., Mosher, J.C., Pantazis, D., Leahy, R.M., 2011. Brainstorm: A User-Friendly Application for MEG/EEG Analysis. *Computational Intelligence and Neuroscience* 2011. <https://doi.org/10.1155/2011/879716>

5.2 Supplementary Study 2: Differential impact of brain network efficiency on post-stroke motor and attentional deficits

Giorgia G. Evangelista^{1,2,†} Philip Egger^{1,2,†} Julia Brügger^{1,2} Elena Beanato^{1,2} Philipp J. Koch^{3,4} Martino Ceroni^{1,2} Lisa Fleury^{1,2} Andéol Cadic-Melchior^{1,2} Nathalie Meyer⁵ Diego de León Rodríguez^{5,6} Gabriel Girard^{7,8,9} Bertrand Léger¹⁰ Jean-Luc Turlan¹⁰ Andreas Mühl¹⁰ Philippe Vuadens¹⁰ Jan Adolphsen¹¹ Caroline Jagella¹² Christophe Constantin¹³ Vincent Alvarez¹³ Joseph-André Ghika¹³ Diego San Millán¹³ Christophe Bonvin¹³ Takuya Morishita^{1,2} Maximilian J. Wessel^{1,2,14} Dimitri Van de Ville^{15,16} and Friedhelm C. Hummel^{1,2,17}

† both authors contributed equally

Abstract

Most studies on stroke have been designed to examine one deficit in isolation, yet survivors often have multiple deficits in different domains. While the mechanisms underlying multiple-domain deficits remain poorly understood, network-theoretical methods may open new avenues of understanding.

50 subacute stroke patients (7±3days post-stroke) underwent diffusion-weighted magnetic resonance imaging and a battery of clinical tests of motor and cognitive functions.

We defined indices of impairment in strength, dexterity, and attention. We also computed imaging-based probabilistic tractography and whole brain connectomes. Overlaying individual lesion masks onto the tractograms enabled us to split the connectomes into their affected and unaffected parts and associate them to impairment.

To efficiently integrate inputs from different sources, brain networks rely on a “rich-club” of a few hub nodes. Lesions harm efficiency, particularly when they target the rich-club. We computed efficiency of the unaffected connectome, and found it was more strongly correlated to impairment in strength, dexterity and attention than efficiency of the total connectome. The magnitude of the correlation between efficiency and impairment followed the order attention > dexterity ≈ strength. Network weights associated with the rich-club were more strongly correlated to efficiency than non-rich-club weights.

Attentional impairment is more sensitive to disruption of coordinated network activity between brain regions than motor impairment, which is sensitive to disruption of localized network activity. Providing more accurate reflections of actually functioning parts of the network enables the incorporation of information about the impact of brain lesions on connectomics contributing to a better understanding of underlying stroke mechanisms.

Author affiliations:

1. Defitech Chair of Clinical Neuroengineering, Center for Neuroprosthetics (CNP) and Brain Mind Institute (BMI), École polytechnique fédérale de Lausanne (EPFL), 1202 Geneva, Switzerland
2. Defitech Chair of Clinical Neuroengineering, CNP and BMI, EPFL Valais, Clinique Romande de Réadaptation, 1950 Sion, Switzerland
3. Department of Neurology, University of Lübeck, 23569 Lübeck, Germany
4. Center of Brain, Behavior and Metabolism, University of Lübeck, 23569 Lübeck, Germany
5. Laboratory of Cognitive Neuroscience, CNP and BMI, EPFL, 1202 Geneva, Switzerland
6. Lausanne University Hospital (CHUV), 1011 Lausanne, Switzerland
7. Signal Processing Laboratory (LTS5), School of Engineering, EPFL, 1015 Lausanne, Switzerland
8. Center for Biomedical Imaging (CIBM), 1015 Lausanne, Switzerland
9. Department of Radiology, CHUV, 1011 Lausanne, Switzerland
10. Clinique Romande de Réadaptation, 1950 Sion, Switzerland
11. Mediclin Reha-Zentrum Plau am See, 19395 Plau am See, Germany
12. Berner Klinik Montana, 3963 Crans-Montana, Switzerland
13. Department of Neurology, Hôpital du Valais, 1950 Sion, Switzerland
14. Department of Neurology, University Hospital Würzburg, 97080 Würzburg, Germany
15. Medical Image Processing Laboratory, Institute of Bioengineering, EPFL, 1202 Geneva, Switzerland
16. Department of Radiology and Medical Informatics, University of Geneva (UNIGE), 1205 Geneva, Switzerland
17. Department of Neurology, Geneva University Hospital (HUG), 1205 Geneva, Switzerland

Correspondence to: Prof. Dr. Friedhelm C. Hummel

Campus Biotech

Chemin des Mines 9

1202 Geneva, Switzerland

Email: friedhelm.hummel@epfl.ch

Running title: Global efficiency and poststroke deficit

Keywords: stroke; motor; attention; structural; connectivity

Abbreviations: DWI = Diffusion-Weighted Imaging; GE = Global Efficiency; NIBS = Non-Invasive Brain Stimulation; NMF = Nonnegative Matrix Factorization; RC = Rich-Club; TAP = Test of Attentional Performance; CTT = Color Trail Test; VAF = Variance Accounted For

Introduction

It has long been acknowledged that different regions of the brain are linked with each other in complex patterns, making networks a natural mathematical model for the brain, with regions of the brain serving as nodes and edges being weighted according to structural characteristics.¹⁻⁴ Furthermore, neuroimaging evidence in humans suggests that stroke is a network disease, indicating that using network theory as the basis of a model for stroke⁵⁻⁷ might significantly enhance the understanding of stroke, its deficits and the recovery from them.

It is useful to think of networks on a spectrum between regularity and randomness. Connectivity in regular networks tends to feature well-defined local communities, while in random networks it tends to feature one global community with costly long-distance connections;⁸ brain networks occupy the zone on the spectrum in which the tradeoff between global integration and local segregation is optimal.¹ They optimize the tradeoff with an architecture featuring a small set of hub nodes called a “rich-club” (RC).^{1,9} These hubs are “rich” because they are strongly connected to nearby nodes, and form a “club” because they are strongly connected to each other. The RC can be thought of as a backbone for global connectivity, and therefore “attacks” (e.g., stroke lesions) against it will have a greater impact on global connectivity than random attacks of similar magnitude.⁹

When brain networks are “attacked” by a stroke, the effect on global integration can be considerable, particularly when the attack focuses on the RC.¹⁰ Likewise, the effect on behavioral function can be significant, particularly on cognitive functions, such as attention, that rely heavily on global integration as opposed to those functions whose neurological substrate is more localized, such as sensory-motor functions.¹¹

Structural connectomics relies on models of white matter tractography computed from diffusion-weighted imaging (DWI). In areas with high axon density, water molecule diffusion has a strong preference for the direction of the axons, i.e., high anisotropy. By chaining together high-anisotropy voxels in the relevant directions, one can extract a model for white matter tracts. Typically, stroke-lesioned tissue in the brain undergoes significant changes including liquefactive necrosis reducing the anisotropy impacting on the modelled white matter tracts. Nonetheless, many paths pass through lesioned tissue, even though they might not correspond to a functioning axon bundle.

We set out to answer two questions. First, is the understanding of connectomics significantly enhanced by the lesion structure information derived from DWI? To answer this question, we defined the structural connectome with and without explicit lesion information, respectively, and compared the data to behavioral metrics.

Second, how strongly are network-theoretic notions of global connectivity or RC integrity associated with stroke-induced impairment in different behavioral domains? We hypothesized that global connectivity and RC integrity will be associated with these behavioral functions, but that this association will be stronger in the “less-localized” attentional domain than in the “more-localized” motor domain. To test this hypothesis, we defined indices of impairment in motor and attentional functioning, and correlated them with a mathematically-defined notion of global efficiency (GE).

Materials and methods

Patients

We recruited eighty-five stroke patients admitted between 2018 and 2021 to the stroke unit of the Hospital of Valais in Sion, Switzerland, of which $N = 50$ completed both imaging sessions and behavioral tests and were therefore included in the study (Fig 1B). The inclusion criteria included being older than eighteen years, presence of a motor deficit, and absence of contraindications for MRI or noninvasive brain stimulation (NIBS). Exclusion criteria included requests not to be informed in case of incidental findings, inability to provide informed consent, severe neuropsychiatric or medical disease, history of seizures, pregnancy, regular use of narcotic drugs, presence of implanted devices incompatible with MRI or transcranial magnetic stimulation, use of medication that interacts with NIBS, severe sensory, musculoskeletal or cognitive deficit incompatible with understanding instructions or performing experiments. For detailed patient characteristics please see Table 1. The lesion locations were representative of the overall stroke patient population as shown in the lesion heatmap (Fig 1A), and were not used as a selection criterion. All patients gave written informed consent at the time of enrolment. The current data was acquired in the framework of a larger project (TiMeS project work package 1) and all research was approved by the local ethical committee swissethics (approval number 2018-01355).

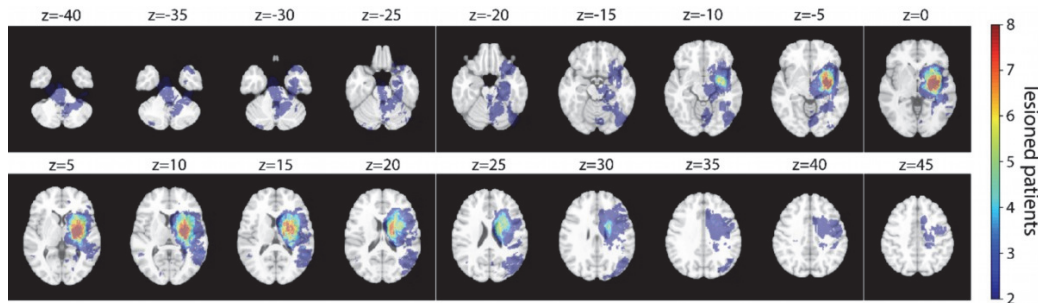


Figure 1. Cohort characteristics. (A) Lesion heatmap where all patients' lesions are co-registered to the MNI template brain and flipped onto the right hemisphere. Titles refer to z coordinates in the MNI space, i.e. mm superior to the anterior commissure. **(B)** Patient flowchart. Please note that of the recruited patients, only those who underwent MRI and all behavioral tests were included in the study.

Table 1. Patient characteristics

	Value ^a	Unit
Sex	38 male / 12 female	Patients
Age	65.2 ± 13.7	Years
Time of MRI	4 ± 2	Days post-stroke
Time of behavioral tests	7 ± 3	Days post-stroke
Paretic side	28 left / 22 right	Patients
Thrombolysis	17 yes / 33 no	Patients
NIHSS	5.8 ± 5	Points
FMUE	53.6 ± 18.1	Points
Fist grip strength	28.1 ± 15.8	Kg force
Pinch grip strength	3.6 ± 2.2	Kg force
Key grip strength	5.8 ± 3.3	Kg force

Appendix

Box & Block test	34.6 ± 18.6	Blocks
Purdue pegboard test	6.7 ± 4.4	Pegs
CTT part A	77 ± 56	Seconds
CTT part B	143 ± 78	Seconds
RT on alertness test of TAP	342 ± 130	Milliseconds
RT on divided attention test (single condition) of TAP	1012 ± 205	Milliseconds

^aCategorical values are given as breakdowns by level of the category, separated by forward slashes. Numeric values are given with mean and standard deviation, separated by \pm .

NIHSS = National Institutes of Health Stroke Scale.

FMUE = Fugl-Meyer Upper Extremity score

RT = Reaction Time

Clinical Assessment

Each patient underwent MRI at the subacute stage in addition to a battery of clinical tests of motor and cognitive function. The focus of the present work was on motor and attentional functions. Motor strength was measured by performing the fist, grip and pinch strength tests¹² on both hands, motor dexterity by performing the Box&Block¹³ and Purdue¹⁴ tests. Attentional functions were measured using the Test of Attentional Performance (TAP),¹⁵ the Color Trail Test (CTT) parts A and B,^{16,17} and the Bells test.¹⁸ These tests were selected for fitting in the Sohlberg-Mateer model, which involves the use of five types of attention of increasing difficulty.¹⁹

MRI Data Acquisition

All images were acquired using a 3T MAGNETOM Prisma (Siemens Healthcare, Erlangen, Germany) with a 64-channel head and neck coil. T1-weighted anatomic images were acquired using 3D magnetization-prepared, rapid acquisition gradient-echo sequence (MPRAGE) with the following parameters: 192 axial slices, response time = 2300ms, echo time = 2.96ms, flip angle = 9°, voxel size = 1×1×1mm, field of view = 256×256mm. For the DWI, diffusion gradients with five different gradient strengths (b-values = [300,700,1000,2000,3000]s/mm²; shell-samples = [3,7,16,29,46]) were obtained in 101 non-collinear directions distributed equally over the brain in 84 axial slices. The images were acquired using the pulsed gradient spin echo technique with the following parameters: repetition time = 5000ms, echo time = 77ms, field of view = 234×234mm, voxel resolution=1.6×1.6×1.6mm, readout bandwidth = 1630Hz/pixel, GRAPPA acceleration factor = 3. Seven T2-weighted images without diffusion weighting (b=0s/mm²) were acquired, including one in opposite phase encoded direction.

Lesion Segmentation

All the lesion masks were hand-drawn using MRview from MRtrix3²⁰ and subsequently verified by a neurologist. This enabled us to also compute, for each streamline, the binary value indicating whether or not the streamline passed through the lesion as described in previous work.¹⁰

Image Analysis

Tissue partial volume maps were estimates from the T1-weighted image and registered to the average b0 image using FSL.²¹ FreeSurfer was used to obtain a brain parcellation including 74 cortical areas per hemisphere (Destrieux atlas), subcortical areas (thalamus, caudate, putamen, hippocampus, amygdala),

the cerebellum, and a subdivision of the brainstem (midbrain, pons, medulla), yielding 163 brain areas.²² The voxels corresponding to the lesion were stamped out and replaced by the mirrored voxels of the contralateral side.

The DWI were preprocessed using MRtrix3,²⁰ and FSL²¹(Gibbs ringing, motion, field inhomogeneity, susceptibility-induced off-resonance field, eddy currents and bias-field correction). Multi-shell multi-tissue constrained spherical deconvolution²³ was used to estimate the fiber orientation distributions within each voxel. Whole-brain probabilistic tractography was performed using the MRtrix3 second-order integration over fibre orientation distribution method,²⁰ initiating streamlines in all voxels of the white matter. For each dataset, 1 million streamlines were selected with both endpoints in the individual cortical or subcortical mask using the Dipy software package.²⁴ Every streamline in the obtained tractograms was weighted fitting the underlying diffusion compartment model using a Stick-Ball-Zeppelin²⁵ model using COMMIT.²⁶

For each patient, a structural connectome was built with 13,202 pairs of areas obtained through the parcellation.^{10,27}

Total and Unaffected Connectome

In our previous work,¹⁰ we computed whole brain connectomes as follows: for each pair of regions of interest, we compute the sum of the COMMIT weights of the streamlines that are in between the two regions. Then we use the binary map indicating whether or not the streamline passed through the lesion to split the full connectome C_{total} into the sum

$$C_{total} = C_{unaffected} + D \quad (1)$$

$$C_{total}[i, j] = \sum_{\text{streamline } k \text{ goes from } i \text{ to } j} w_k \quad (2)$$

$$C_{unaffected}[i, j] = \sum_{\substack{\text{streamline } k \text{ goes from } i \text{ to } j \\ \text{and does not pass through the lesion}}} w_k \quad (3)$$

$$D[i, j] = \sum_{\substack{\text{streamline } k \text{ goes from } i \text{ to } j \\ \text{and passes through the lesion}}} w_k \quad (4)$$

In this way, we are able to incorporate the lesion more explicitly and we get a normalized way of treating the affected and unaffected streamlines on the same footing. This novel construction of disconnectomes provides a network-theoretic lesion profile, which quantifies the difference between the traditional notion of connectome and our new notion of unaffected connectome.

Rich-club, Edge Weight, and Node Weight

We considered the same set of nodes as found by van den Heuvel and Sporns to form the RC, namely the bilateral precuneus, superior frontal cortex, superior parietal cortex, hippocampus, putamen, and

thalamus.⁹ Finally, we split the edges into three groups (Fig 2): pure RC connections (between RC nodes); feeder connections (between a RC node and a non-RC node); and local connections (between non-RC nodes).

Each edge has a weight; each node has a weight, defined to be the sum of the weights of all edges linked to that node.

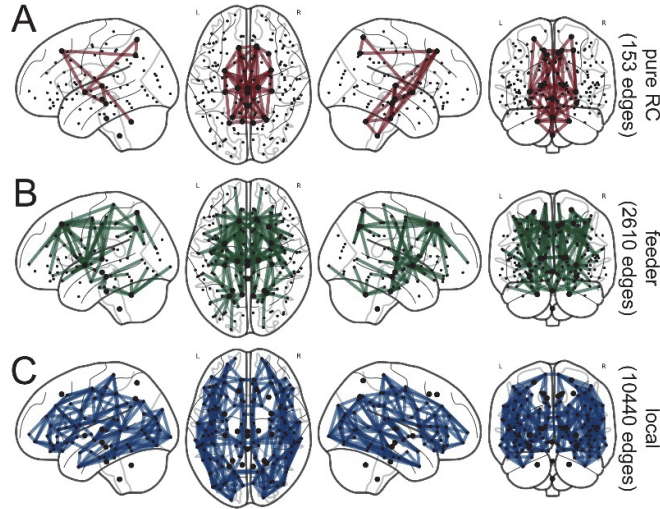


Figure 2. Connectome nodes and edges on glass brain. Our parcellation contains 163 nodes, depicted as dots on the brain. 18 of these nodes, shown as enlarged dots, are the RC nodes. The edges are partitioned into pure RC (A, red), feeder (B, green), and local (C, blue) types.

Dimensionality Reduction

The behavioral metrics of the present project were combined for the 2 domains. There are numerous methods to reduce the dimensionality of features. Popular methods include principal component analysis²⁸ and nonnegative matrix factorization (NMF);²⁹ because the present data are nonnegative by nature and distance from zero impairment has a relevant meaning, we chose NMF. The amount of information that is lost by reducing features is captured by calculating the proportion of variance accounted for (VAF) by the low-dimensional representation.²⁹

Behavioral Metrics

To measure strength impairment, we consider the average force in three trials exerted by the patients on both hands, and calculate a normalized impairment metric as follows:

$$F_{norm} = \frac{F_{nonparetic} - F_{paretic}}{F_{nonparetic} + F_{paretic}} \quad (5)$$

in a fist grip, a pinch grip and a key grip,¹² giving the three features $FIST_{norm}$, $PINCH_{norm}$, and KEY_{norm} . These features are bounded between -1 and 1, where -1 means only the paretic hand exerts force, 0 means both hands exert equal force, and 1 means only the nonparetic hand exerts force. While mildly negative values are possible, they are unlikely to be clinically meaningful, so we set negative values to zero in order for the features to be nonnegative. Patients missing all three of $FIST_{norm}$, $PINCH_{norm}$ and KEY_{norm} were excluded; those who were missing some but not all were replaced by the mean of all non-

missing data in the respective field. Finally, we used NMF ($VAF = 97\%$) to reduce the three features into one strength impairment index $strength = 1.39 \times FIST_{norm} + 1.43 \times PINCH_{norm} + 1.53 \times KEY_{norm}$.

(6)

To measure dexterity impairment, we consider the number of fine motor tasks performed by the patient with both hands in a given time limit. As before, we calculate the normalized functional metric

$$N_{norm} = \frac{N_{nonparetic} - N_{paretic}}{N_{nonparetic} + N_{paretic}} \quad (7)$$

in the box-and-block test³⁰ and the Purdue pegboard test,¹⁴ set negative values to zero, impute missing data, and use NMF ($VAF = 97\%$) to reduce the two features into one dexterity impairment index

$$dexterity = 1.43 \times B\&B_{norm} + 1.53 \times Purdue_{norm}. \quad (8)$$

To measure functional deficits in attention, we began with the widely-used model of Sohlberg-Mateer,¹⁹ which suggests measuring five tasks of increasing difficulty, as described in Table 2:

Table 2. Sohlberg-Mateer attention model

Component	Type of Task	Metric	Unit
Focused	Response to discrete stimuli	Mean RT on alertness test (no warning) of TAP	Milliseconds
Sustained	Ability to work in a quiet environment	Completion time of CTT part A	Seconds
Selective	Ability to ignore distractors	Completion time of Bells test ^a	Seconds
Alternating	Shifting attention between tasks	Completion time of CTT part B	Seconds
Divided	Response to multiple stimuli	Mean RT on divided attention test of TAP	Milliseconds

^aA penalty of 0.7 seconds was added for every omission in the Bells test

RT = Reaction Time

We normalize each of these features to have maximal value 1, impute missing values, and use NMF ($VAF = 94\%$) to reduce the five normalized features to one attention impairment index

$$attention = 1.34 \times focused + 0.98 \times sustained + 1.40 \times selective + 1.32 \times alternating + 2.35 \times divided. \quad (9)$$

Global Efficiency

Most networks lie on a spectrum from regularity to randomness, or equivalently from local segregation to global integration. Many biological networks are “small-world” networks, which have both the clustered nature of locally segregated networks and the short path length of globally integrated networks.^{31,32} The GE of a network with n nodes is defined by Rubinov and Sporns³² as

$$GE = \frac{1}{n(n-1)} \sum_{i \neq j} \frac{1}{d_{ij}}, \quad (10)$$

where d_{ij} is the length of the shortest path between nodes i and j in the network. The quantity d_{ij} is defined to be the smallest sum of reciprocal edge weights in any path from i to j . GE of the brain networks were computed using the Brain Connectivity Toolbox, a MATLAB toolbox developed by Rubinov and Sporns.³²

Data availability

Data will be made available upon reasonable request.

Results

We used the Brain Connectivity Toolbox³² to compute the weighted GE of each patient's total connectome C_{total} and unaffected connectome $C_{unaffected}$; and then correlated these with strength, dexterity and attention impairment.

All correlations were estimated using bootstrap resampling³³ with 10,000 iterations, i.e., at each iteration we drew 50 patients from our sample of 50 (with replacement) and computed the respective correlations on the subsample. We computed the Pearson correlation between GE_{total} and impairment (Fig 3, blue; strength: $r = -.20, P = .07$, dexterity: $r = -.11, P = .25$, attention: $r = -.41, P = .0001$); and between $GE_{unaffected}$ and impairment (Fig 3, green; strength: $r = -.30, P = .02$, dexterity: $r = -.30, P = .05$, attention: $r = -.55, P = .0001$). The negative correlations are expected, given that GE is known to contribute to better functional outcomes;^{11,34} p-values are proportions of bootstrap correlations that were non-negative.

We computed effect sizes for the difference between $r(GE_{unaffected}, impairment)$ and $r(GE_{total}, impairment)$ across bootstrap iterations using Cohen's d statistic rather than Student's t due to the latter showing inflated effect sizes with large datasets;³⁵ p-values were computed by probability of superiority.³⁶ $GE_{unaffected}$ was more strongly correlated with impairment than GE_{total} (strength: $d = -0.73, P = .07$, dexterity: $d = -1.1, P = .006$, attention: $d = -1.5, P = .004$). We did not control for age, as age was found not to be a meaningful covariate in previous studies of older healthy subjects.¹¹

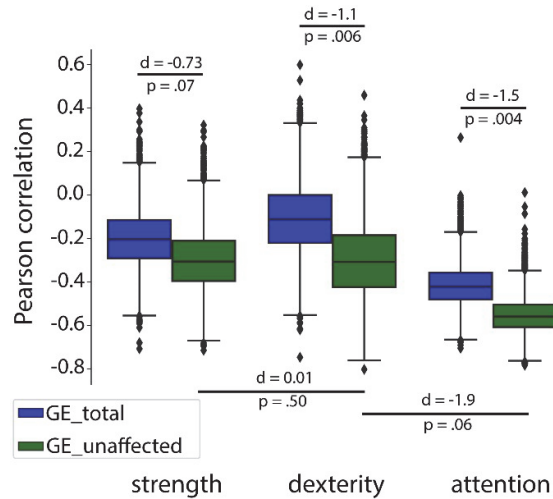


Figure 3. Bootstrapped correlations between connectome GE and impairment. Boxplots show bootstrapped Pearson correlations on the ordinata between GE and the three types of impairment on the abscissa. Blue plots refer to GE_{total} , while green plots refer to $GE_{unaffected}$. Note that all correlations tend to be negative and that correlations with $GE_{unaffected}$ tend to be stronger (i.e. more negative) than those with GE_{total} . Note also that GE tends to be more strongly correlated to attention impairment than to strength or dexterity impairment, while it seems to be equally strongly correlated to strength and dexterity impairment.

It is known from work of van den Heuvel and Sporns⁹ that attacks on pure RC edges result in more loss of GE than attacks of similar magnitude on feeder or local edges. Conversely, we expected that greater integrity of pure RC edges should correspond to greater GE in the network, and this is the case (Fig 4A,

left: one-way ANOVA $F = 82.1, P \approx 0$). Greater integrity of RC nodes also corresponds to greater GE in the network (Fig 4B, left: two-sample t test $T = 2.6, P = .009$).

It has been shown that among healthy older subjects, when considering correlations to attention, which requires integration of inputs from across the brain, pure RC edges are strongest, then feeder, then local; however, no such order exists for correlations to visual processing, which is more localized.¹¹ The same holds when considering RC nodes as opposed to non-RC nodes.

We have found analogous results to those reported by Baggio and colleagues¹¹ in healthy older adults. Pure RC edge weights have more negative (i.e. stronger) correlations to behavior than feeder and local edges, and that this gap is smallest for strength and largest for attention (Fig 4A, right: one-way ANOVA. Strength: $F = 6.5, P = .001$; dexterity: $F = 19.7, P = 10^{-9}$; attention: $F = 89.4, P = 10^{-39}$). Similarly, RC node weights have stronger correlations to behavior than non-RC node weights, and this gap is smallest for strength and largest for attention (Fig 4B, right: two-sample t test. Strength: $T = 0.7, P = .474$; dexterity: $T = 2.0, P = .048$; attention: $T = 3.0, P = .003$).

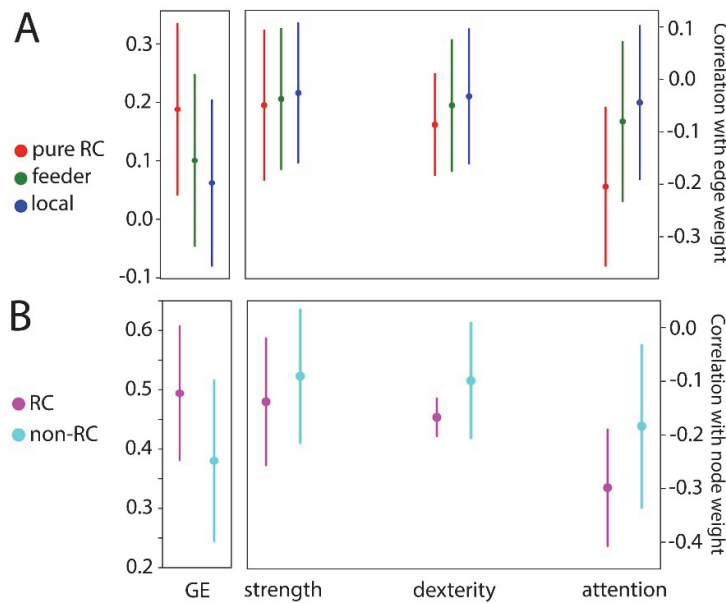


Figure 4. Correlations between connectome GE, graph weights, and impairment. Plots show mean and standard deviation. (A, left) Correlations between edge weight and $GE_{unaffected}$. Please note that the order pure RC > feeder > local holds. (A, right) Correlations between edge weight and impairment. Please note that the order pure RC < feeder < local holds in all domains, and that the gap is largest in the attentional domain. (B, left) Correlations between node weight and $GE_{unaffected}$. Please note that RC nodes have stronger correlation to $GE_{unaffected}$ than non-RC nodes. (B, right) Correlations between node weight and impairment. Please note that RC nodes have stronger correlations to behavior than non-RC nodes and that the gap increases between strength, dexterity, and attention.

Discussion

Given the complex pattern of interactions between different parts of the brain, mathematical tools for complex network analyses offer an exciting opportunity to better understand underlying mechanisms of neurological disorders, especially when current findings strongly support the maxim that many neurological disorders, including stroke, are network disorders.^{5,37} Therefore, connectomics has great potential to yield important insights into post-stroke impairment, recovery mechanisms and advance our understanding by evaluation of the specific patient's pattern of brain connectivity.

Our data point toward the existence of considerable differences in the mechanisms underlying deficits in the motor and attentional domains. These differences provide reason for optimism that while treatments designed to promote more globally efficient brain networks are likely to have benefits in treating many deficits, this is particularly true of attentional deficits.

While the stroke patients in the present study were selected for their motor deficit, a considerable share of the patients also showed cognitive/attentional deficits (e.g., 39/50 pathological on MOCA). It has been suggested from studies of older healthy subjects¹¹ and stroke patients^{38,39} that cognitive functions, such as attention, memory or language functions, are more heavily reliant on integration of inputs from different parts of the brain than functions such as motor and visual ones, which reside in “more specialized” local brain networks. This important assumption has been confirmed by the present findings that $GE_{unaffected}$ is more strongly correlated to attention than to motor strength or dexterity, highlighting the reliance of the attentional domain on larger-scale emergent dynamics. It is of note that the correlation between $GE_{unaffected}$ and strength does not seem to differ significantly from that between $GE_{unaffected}$ and dexterity, highlighting the fact that the motor domain, whether for pure strength production or for more fine motor skills, is less reliant on emergent (larger-scale) dynamics than attention is. Mathematical modeling conducted by Sporns and van den Heuvel has found that the resilience of brain networks to “attack” varies depending on the place of attack, indicating that attacks on pure RC edges result in greater drops in GE than other (non-RC) attacks of similar magnitude.⁹ Accordingly, we found that RC node weight and pure RC edge weight were more strongly correlated to attention than to motor functions, suggesting that the importance of the RC is derived from its disproportionate impact on network efficiency.

The presented approach adds a layer of personalization to traditional connectomics by separating fibers according to whether or not they are impacted by the patient’s particular lesion. This approach has borne fruit, as the unaffected connectome is more strongly associated with behavior than the traditional total connectome. From a hypothesis-driven perspective, the importance of including a lesion profile in the measurement of brain networks is obvious as white matter tracts can be detected by DWI-derived tractography, though probably with more diffusivity inhomogeneities, even if they are interrupted by a lesion (particularly in the early post-stroke period). Such tractography by itself fails to acknowledge that if tracts are interrupted by the lesion, their ability to transmit information is compromised and they will not contribute to the normal functioning of the network. From a data-driven perspective, it has been found that GE_{total} does not differ significantly either over time, or even between stroke patients and healthy controls,³⁸ casting doubt on the value of GE_{total} as a biomarker. By contrast, we provide evidence that $GE_{unaffected}$ differs significantly from GE_{total} , and that in stroke patients $GE_{unaffected}$ is more strongly correlated to behavior than GE_{total} is.

Consequently, we find that explicitly discarding tracts that pass through the lesion as inoperative ensures that the unaffected connectome is a more accurate reflection of true patterns of connectivity than the traditional structural connectome, and thus a better candidate as a stroke-related biomarker.

Limitations

The primary drawback of the present approach is that splitting the total connectome into its affected and unaffected parts requires that one draw lesion masks and overlay them onto the tractography. This imposes considerable additional work, yet we are convinced that the benefits in terms of relevance to behavior and understanding of mechanisms are worth the cost. In addition to being time-consuming and labor intensive, they require substantial anatomical expertise, which might introduce a considerable source of variability; both on an inter-rater and (to a lesser extent) test-retest basis.⁴⁰ While the use of machine learning algorithms to delineate lesions holds some promise, it is a sufficiently

difficult task that at the time of writing, human-drawn lesions remain the gold standard, with even the best available algorithms failing to come close to inter-rater levels of agreement with humans.⁴¹

Future Work

The present study was conducted cross-sectionally, however longitudinal evaluation of parameters of network efficiency in the affected and unaffected parts of the network will open novel opportunities to study the mechanisms underlying recovery of multi-domain (e.g., motor and attention) post-stroke deficits. It will provide novel insights into the reorganization of structural brain networks, how these reorganizational patterns relate to recovery of behavioral functions, and whether they allow prediction of outcome or treatment stratification. In particular, it would be worth investigating whether among our cohort, patients' increase in GE over time was associated with recovery from their impairment, particularly attentional impairment.

There are biological reasons to expect that this might occur. Reparative axonal sprouting is characterized by growth of long-distance connections,⁴² the precise type of connections that contribute most to GE. It has also been found to be clearly associated with post-stroke behavioral recovery.⁴²

Conclusions

While the patients in the present cohort were selected for motor deficits, most of them also had an attention deficit, which can have an additional impact on the recovery process. This considerable overlap between motor and attentional deficits implies the need for finer-grained discriminators between multidomain deficits and their underlying mechanisms.

Here, we suggest structural connectivity analyses of RC properties with a focus on affected and unaffected parts of the network to better characterize these multi-domain deficits in the subacute stage after stroke. These analyses allow the following conclusions: First, current approaches of structural connectomics use DWI to trace axon fiber bundles and simply rely on lesion-induced tract inhomogeneities. However, this implicit taking into account of the lesion is suboptimal, particularly in the acute and subacute phase as it might lead to the tractography finding tracts that are no longer functional. Therefore, the present results support the importance of explicitly overlaying lesion masks onto the tractography to be able to split the structural connectome into its unaffected (well-functioning) and affected (disconnectome, non-functional) parts to determine which parts of the brain network are actually relevant to residual functions and impairment. Secondly, based on this approach, the present results suggest that in stroke patients, attention is more sensitive to non-integrity of the connectome (especially the RC) and the resulting deficiency of GE than motor functions, strongly underscoring the differential importance of RC network properties for different behavioral functions. The present results further confirm and are consistent with reports in healthy subjects that the neural substrate underlying motor functions is rather localized, while that underlying attention is based on a more global representation in terms of RC organization.

Acknowledgements

We thank S. Avanzi for the excellent support during the recruitment and data acquisition process.

Funding

Partially supported by #2017-205 'Personalized Health and Related Technologies (PHRT-205)' of the ETH Domain, Defitech Foundation (Strike-the-Stroke project, Morges, Switzerland), Bertarelli Foundation (Catalyst Deep-MCI-T project), FreeNovation Program of the Novartis Research Foundation and the Wyss Center for Bio and Neuroengineering. We acknowledge access to the facilities and expertise of the CIBM, a Swiss research center of excellence founded and supported by CHUV, University of Lausanne, EPFL, UNIGE and HUG and of the MRI facilities of the Human Neuroscience Platform of the Fondation Campus Biotech Geneva founded and supported by the UNIGE, HUG and EPFL.

References

1. Bassett DS, Bullmore E. Small-world brain networks. *Neuroscientist*. 2006;12(6):512-523. doi:10.1177/1073858406293182
2. Bullmore E, Sporns O. Complex Brain Networks: Graph Theoretical Analysis of Structural and Functional Systems. *Nature Reviews Neuroscience*. 2009;10:186-198.
3. Sporns O. *Networks of the Brain*. MIT Press; 2011:xi, 412.
4. Sporns O. *Discovering the Human Connectome*. MIT Press; 2012.
5. Guggisberg AG, Koch PJ, Hummel FC, Buetefisch CM. Brain networks and their relevance for stroke rehabilitation. *Clin Neurophysiol*. 2019;130(7):1098-1124. doi:10.1016/j.clinph.2019.04.004
6. Aben HP, Biessels GJ, Weaver NA, et al. Extent to Which Network Hubs Are Affected by Ischemic Stroke Predicts Cognitive Recovery. *Stroke*. 2019;50(10):2768-2774. doi:10.1161/STROKEAHA.119.025637
7. Ktena SI, Schirmer MD, Etherton MR, et al. Brain Connectivity Measures Improve Modeling of Functional Outcome after Acute Ischemic Stroke. *Stroke*. 2019;50(10):2761-2767. doi:10.1101/590497
8. Watts DJ, Strogatz SH. Collective dynamics of 'small-world' networks. 1998;393:3.
9. van den Heuvel MP, Sporns O. Rich-Club Organization of the Human Connectome. *J Neurosci*. 2011;31(44):15775-15786. doi:10.1523/JNEUROSCI.3539-11.2011
10. Egger P, Evangelista GG, Koch PJ, et al. Disconnectomics of the Rich Club Impacts Motor Recovery After Stroke. *Stroke*. 2021;52(6):2115-2124. doi:10.1161/STROKEAHA.120.031541
11. Baggio HC, Segura B, Junque C, de Reus MA, Sala-Llloch R, van den Heuvel MP. Rich Club Organization and Cognitive Performance in Healthy Older Participants. *J Cogn Neurosci*. 2015;27(9):1801-1810. doi:10.1162/jocn_a_00821
12. Choi YM. Comparison of Grip and Pinch Strength in Adults with Dexterity Limitations to Normative Values. *Procedia Manufacturing*. 2015;3:5326-5333. doi:10.1016/j.promfg.2015.07.637

13. Mathiowetz V, Weber K, Volland G, Kashman N. Reliability and validity of grip and pinch strength evaluations. *J Hand Surg Am.* 1984;9(2):222-226. doi:10.1016/s0363-5023(84)80146-x
14. Tiffin J, Asher EJ. The Purdue pegboard; norms and studies of reliability and validity. *J Appl Psychol.* 1948;32(3):234-247. doi:10.1037/h0061266
15. Zimmermann P, Fimm B. *Test of Attentional Performance Manual (Version 2.3)*. 3rd ed. Psytest; 2016.
16. Reitan RM. The relation of the trail making test to organic brain damage. *J Consult Psychol.* 1955;19(5):393-394. doi:10.1037/h0044509
17. Messinis L, Malegiannaki AC, Christodoulou T, Panagiotopoulos V, Papathanasopoulos P. Color Trails Test: Normative Data and Criterion Validity for the Greek Adult Population. *Archives of Clinical Neuropsychology.* 2011;26(4):322-330. doi:10.1093/arclin/acr027
18. Gauthier L, Dehaut F, Joanette Y. The Bells Test: A quantitative and qualitative test for visual neglect. *International Journal of Clinical Neuropsychology.* 1989;11(2):49-54.
19. Sohlberg MM, Mateer CA. Cognitive rehabilitation: An integrative neuropsychological approach. *Cognitive rehabilitation: An integrative neuropsychological approach*. Published online 2001:xix, 492-xix, 492.
20. Tournier JD, Smith R, Raffelt D, et al. MRtrix3: A fast, flexible and open software framework for medical image processing and visualisation. *NeuroImage.* 2019;202:116137. doi:10.1016/j.neuroimage.2019.116137
21. Smith SM, Jenkinson M, Woolrich MW, et al. Advances in functional and structural MR image analysis and implementation as FSL. *Neuroimage.* 2004;23 Suppl 1:S208-219. doi:10.1016/j.neuroimage.2004.07.051
22. Destrieux C, Fischl B, Dale A, Halgren E. Automatic parcellation of human cortical gyri and sulci using standard anatomical nomenclature. *Neuroimage.* 2010;53(1):1-15. doi:10.1016/j.neuroimage.2010.06.010
23. Jeurissen B, Tournier JD, Dhollander T, Connelly A, Sijbers J. Multi-tissue constrained spherical deconvolution for improved analysis of multi-shell diffusion MRI data. *Neuroimage.* 2014;103:411-426. doi:10.1016/j.neuroimage.2014.07.061
24. Garyfallidis E, Brett M, Amirbekian B, et al. Dipy, a library for the analysis of diffusion MRI data. *Front Neuroinform.* 2014;8:8. doi:10.3389/fninf.2014.00008
25. Alexander DC. A general framework for experiment design in diffusion MRI and its application in measuring direct tissue-microstructure features. *Magnetic Resonance in Medicine.* 2008;60(2):439-448. doi:10.1002/mrm.21646

26. Daducci A, Dal Palu A, Lemkaddem A, Thiran JP. COMMIT: Convex Optimization Modeling for Microstructure Informed Tractography. *IEEE Transactions on Medical Imaging*. 2015;34(1):246-257. doi:10.1109/TMI.2014.2352414
27. Koch PJ, Park CH, Girard G, et al. The structural connectome and motor recovery after stroke: predicting natural recovery. *Brain*. 2021;144(7):2107-2119. doi:10.1093/brain/awab082
28. Hotelling H. Analysis of a complex of statistical variables into principal components. *Journal of Educational Psychology*. 1933;24(6):417-441. doi:10.1037/h0071325
29. Lee DD, Seung HS. Learning the parts of objects by non-negative matrix factorization. *Nature*. 1999;401(6755):788-791. doi:10.1038/44565
30. Mathiowetz V, Volland G, Kashman N, Weber K. Adult Norms for the Box and Block Test of Manual Dexterity. *The American Journal of Occupational Therapy*. 1985;39(6):386-391. doi:10.5014/ajot.39.6.386
31. Latora V, Marchiori M. Efficient Behavior of Small-World Networks. *Phys Rev Lett*. 2001;87(19):198701. doi:10.1103/PhysRevLett.87.198701
32. Rubinov M, Sporns O. Complex network measures of brain connectivity: Uses and interpretations. *NeuroImage*. 2010;52(3):1059-1069. doi:10.1016/j.neuroimage.2009.10.003
33. Efron B. Bootstrap Methods: Another Look at the Jackknife. *Ann Statist*. 1979;7(1):1-26. doi:10.1214/aos/1176344552
34. van den Heuvel MP, Sporns O. An anatomical substrate for integration among functional networks in human cortex. *J Neurosci*. 2013;33(36):14489-14500. doi:10.1523/JNEUROSCI.2128-13.2013
35. Cohen J. *Statistical Power Analysis for the Behavioral Sciences*. Routledge; 2013.
36. Ruscio J. A probability-based measure of effect size: robustness to base rates and other factors. *Psychol Methods*. 2008;13(1):19-30. doi:10.1037/1082-989X.13.1.19
37. Grefkes C, Fink GR. Connectivity-based approaches in stroke and recovery of function. *The Lancet Neurology*. 2014;13(2):206-216. doi:10.1016/S1474-4422(13)70264-3
38. Siegel JS, Seitzman BA, Ramsey LE, et al. Re-emergence of modular brain networks in stroke recovery. *Cortex*. 2018;101:44-59. doi:10.1016/j.cortex.2017.12.019
39. Salvalaggio A, De Filippo De Grazia M, Zorzi M, Thiebaut de Schotten M, Corbetta M. Post-stroke deficit prediction from lesion and indirect structural and functional disconnection. *Brain*. 2020;143(7):2173-2188. doi:10.1093/brain/awaa156
40. Liew SL, Anglin JM, Banks NW, et al. A large, open source dataset of stroke anatomical brain images and manual lesion segmentations. *Scientific Data*. 2018;5(1):180011. doi:10.1038/sdata.2018.11

Appendix

41. Maier O, Schröder C, Forkert ND, Martinetz T, Handels H. Classifiers for Ischemic Stroke Lesion Segmentation: A Comparison Study. *PLoS One*. 2015;10(12):e0145118. doi:10.1371/journal.pone.0145118
42. Carmichael ST, Kathirvelu B, Schweppe CA, Nie EH. Molecular, Cellular and Functional Events in Axonal Sprouting after Stroke. *Exp Neurol*. 2017;287(Pt 3):384-394. doi:10.1016/j.expneurol.2016.02.007

Curriculum Vitae

First name Julia
Last name Brügger
Address Dorfweg Jeizinen 2
3945 Gampel
E-Mail bruegger.julia@bluewin.ch
Mobile number +41 79 595 56 24
Date of birth February 5th 1992
Nationality Swiss



Education

06/2018 – 05/2022

Swiss Federal Institute of Technology Lausanne (EPFL)

PhD in Neuroscience in the Lab of Prof. Hummel

Title: Determining patterns of motor recovery after stroke by longitudinal multimodal MRI: A step towards patient stratification

Methods: resting-state fMRI and diffusion MRI

Project: Towards individualized Medicine in Stroke (TiMeS)

Longitudinal, multimodal study aiming at a better understanding of post-stroke recovery with the goal to define new predictive biomarkers for the degree and course of recovery as well as for response to treatment

08/2015 – 08/2017

University of Amsterdam, The Netherlands

Master of Science in Biomedical Sciences

Cluster: Neurobiology

Track: Cognitive Neurobiology and Clinical Neurophysiology

Overall GPA: 8.7 / 10 (A+, Excellent)

First internship (six months): Grade 8.5 / 10

Institution: University of Amsterdam, The Netherlands

Group: Prof. dr. Cyriel M.A. Pennartz

Methods: Optogenetics, recordings with tetrodes in rats

Title: *"Non-REM sleep associated LFPs and their role in orbitofrontal cell ensemble reactivation"*

Curriculum Vitae

Second internship (eight months): Grade 9.0 / 10
Institution: Swiss Federal Institute of Technology Lausanne, Switzerland
Group: Prof. dr. Olaf Blanke
Methods: fMRI, Virtual Reality
Title: *"Investigations into the neural and behavioural mechanisms of the spontaneous and imagined subjective first-person perspective"*

Literature Review (two months): Grade 8.5 / 10
Institution: Netherlands Institute for Neuroscience, The Netherlands
Group: Prof. dr. Dick F. Swaab
Title: *"Transsexualism: structural and functional sex differences in the human brain and potential hormonal causes"*

09/2012 – 07/2015

University of Fribourg, Switzerland

Bachelor of Science in Biomedical Sciences

Overall GPA: Grade 5.1 / 6

Bachelor thesis: Grade 5.5 / 6
Institution: University of Fribourg, Switzerland
Group: Prof. Eric Rouiller
Topic: *"EEG study in alert macaque monkey performing a sensory-motor task"*

09/2007 - 06/2012

Lycée-Collège des Creusets in Sion, Switzerland

High School

GPA: 5.5 / 6

Main (optional) subject: Spanish

Award for the best GPA in Mathematics: Grade 6 / 6

Award for the best diploma thesis: Grade 6 / 6

Topic: *"Der Röstigraben – trennt uns wirklich so viel?"*

08/2009 – 11/2009

St Augustine's High School in Edinburgh, Great Britain

Three-month exchange in Scotland

Work experience

08/2017 – 01/2018

École polytechnique fédérale de Lausanne (EPFL)

Campus Biotech, Geneva, Switzerland

Scientific collaborator in the Laboratory of Cognitive Neuroscience (LNCO)

Leading a project investigating the neural mechanisms underlying the first-person perspective by means of fMRI.

02/2015 – 07/2015

University of Fribourg

Fribourg, Switzerland

Tutor (teaching assistant) for practical histology and anatomy courses

09/2013 – 07/2015

University of Fribourg

Fribourg, Switzerland

Student representative at the Faculty Council (Faculty of Science)

Student representative at the Department Council (Department of Medicine)

Curriculum Vitae

09/2010 - 06/2012

Lycée-Collège des Creusets

Sion, Switzerland

Tutor for High School students

Mathematics, English, German, Physics, Spanish and French

Professional qualifications

04/2020

IMD Leadership Essentials Program

Honors and Awards

08/2017

Graduation with distinction (*Cum Laude*)

Master of Science in Biomedical Sciences

University of Amsterdam, The Netherlands

GPA 8.7 / 10 (A+, Excellent)

07/2012

Award for the best diploma thesis

Lycée-Collège des Creusets, Sion, Switzerland

07/2012

Award for the best GPA in Mathematics

Lycée-Collège des Creusets, Sion, Switzerland

Languages

German

First language

French

Level C2, bilingual written and spoken

English

Level C2 written and spoken

Spanish

Level B2 written and spoken

Dutch

Level B1 passive understanding

Italian

Level A2 passive understanding

Programming

MATLAB

Advanced

R

Advanced

Python

Good skills

Bash

Good skills

Conference Posters

05/2019

Lemanic Neuroscience Annual Meeting (LNAM)

Validation of a tractography and structural connectome pipeline for a prospective longitudinal study in stroke patients

05/2022

European Stroke Organization Conference (ESOC)

Acute changes in the coupling between brain structure and function following a stroke